This file is part of the following work:

Kerans, Andrew J. (2011) *Characterisation of electromagnetic propagation inside the maritime evaporation duct at x-band and findings on the meteorology of duct formation.* **PhD Thesis, James Cook University.**

Access to this file is available from:

https://doi.org/10.25903/02qq%2D8108

ResearchOnline@JCU

This file is part of the following reference:

Kerans, Andrew J. (2011) *Characterisation of electromagnetic propagation inside the maritime evaporation duct at X-Band and findings on the meteorology of duct formation.* **PhD thesis, James Cook University.**

Access to this file is available from:

http://researchonline.jcu.edu.au/18425/

JAMES COOK
UNIVERSITY
AUSTRALIA

Characterisation of electromagnetic propagation inside the maritime evaporation duct at X-Band and findings on the meteorology of duct formation

Thesis submitted by

Andrew J. Kerans SMIEEE

B.Eng (Electrical and Electronics) NTU

M.Eng.Sci. (Communications) UNSW ADFA

Grad.Dip.Eng (Civil and Environmental) UNSW

in January 2011

for the degree of Doctor of Philosophy

in the School of Electrical and Computer Engineering

James Cook University

Declaration

I declare that this Thesis is my own work and has not been submitted in any form for another degree or diploma at any university or other institute of tertiary education. Information derived from the published and unpublished work of others has been acknowledged in the text, and a list of references is given.

Andrew Kerans

January 2011

Statement on Access to this Thesis

I, the under-signed, the author of this work, understand that James Cook University will make this work available for use within the University Library, and via the Australian Digital Thesis Network, for use elsewhere.

I understand that as an unpublished work, a Thesis has significant protection under the Copyright Act. I do not wish to place any restriction on access to this Thesis. However, any use of its content must be acknowledged and could potentially be restricted by future patents.

_____

Andrew Kerans

January 2011

Acknowledgements

Abstract

Radio wave propagation over the ocean at frequencies above about 1 GHz differs from that over land due to the effect of a stratified layer just above the sea's surface known as the evaporation duct. The height and strength of this duct are the main factors affecting propagation.

Bulk parameters have been developed to define duct height mainly in temperate zones; their applicability to the tropical region is as yet ambiguous as is the effect of wind speed on duct effective height in these regions.

Significant previous work has been carried out on identifying duct height from atmospheric parameters, and thus behaviour by Babin et al [28]. The author contacted Dr Babin who made available his entire Thesis [39] which was most useful in our early research on duct height.

In this work, measurements from sensor buoys are presented along with wind speed measurements and an equation for duct height postulated by Kulessa and Hermann is examined. The developmental algorithm appears to reasonably fit a series of wind speeds taken in the Gulf St. Vincent, South Australia, in a temperate climate and Southern Ocean. Data is presented and the equation discussed for the tropical zone, from this some duct height predictions are made. These duct heights are compared with those calculated using bulk parameters and conclusions are drawn for the tropical littoral zone.

Radio wave propagation inside the duct is therefore considered to be anomalous with over the horizon paths producing near line of sight loss values.

In this research the phenomenon is demonstrated in the results from one long distance experiment conducted over a one week period. Results from a 24 hour period are fully analysed along with analysis of another period in the campaign when the results were different from those expected. Other experiments over shorter paths using a ten-element receiver array are presented and the results used to make conclusions on the accuracy of the Parabolic Equation Models (PEM) in the tropical littoral zone.

A design for a sixteen element array capable of resolving angle of arrival in a duct and the theory of its operation is also discussed along with information on the construction, installation and testing of this array concept. The mathematics which is can be used to extract angle of arrival from the array is also presented.

Table of Contents

List of Tables

List of Figures

List of Refereed Publications from this work

Kerans, A.J., Kulessa, A.S., Hermann, J. and Woods, G. S., "Evaporation Duct Statistics Around Australia and the West Pacific", AP2000 Millennium Conference on Antennas & Propagation, Davos – Switzerland, 9-14 April 2000.

Kerans, A.J., Kulessa, A.S., Woods, G.S., French, G. and Lensson, E., "Remote Sensing of Radio Refractive Atmospheric Effects in Northern Australia", Workshop on Applications of Radio Science (WARS'02), University of Technology, Sydney, 21-22 February 2002.

Kerans, A.J. and Woods, G.S., "Comparison of Microwave Propagation Models and Evaporation duct Height Estimation Techniques with Actual Near Water Atmospheric and Radio Data Taken in North Queensland, Australia in May, 2001", 2nd Student Conference on Research and Development (SCOReD 2002), Shah Alam, Malaysia, 16-17 July 2002.

Kerans, A.J., Kulessa, A.S., Woods, G.S., French, G. and Lensson, E., "Remote sensing of radio refractive atmospheric effects in Northern Australia", Antennas and Propagation Society International Symposium, 2002, IEEE, Volume: 3, pp. 692- 695, August 2002, ISBN: 0-7803-7330-8.

Kerans, A.J., Kulessa, A.S., and Woods, G.S., "Estimation of angle of arrival using amplitude measurements across an array", Eighth Australian Symposium on Antennas Sydney, 12-13 February 2003, Session 6.

Kerans, A.J., Kulessa, A.S., Woods, G.S., French, G. and Hermann, J., "Implication of Anomalous Propagation in the Evaporation Duct for Radars at X and Ku Band", Journal of Battlefield Technology, Volume 6, Number 3, pp. 25-29, November 2003.

Kerans, A.J., Woods, G.S. and Kulessa, A.S., "Microwave Propagation within a Tropical Maritime Evaporation Duct, a Comparison of Measured Data and Simulations" ClimDiff, Fortaleza, 17-19 November 2003.

Kerans, A.J. and Woods, G.S., "Observations of anomalous over the horizon microwave radio propagation inside the tropical maritime evaporation duct in North Queensland, Australia. Part One: normal ducting events", URSI Commission F, Triennium Open Symposium, Cairns, Queensland, Australia, 1-4 June 2004.

Kerans, A.J. and Woods, G.S., "Observations of anomalous over the horizon microwave radio propagation inside the tropical maritime evaporation duct in North Queensland, Australia. Part Two: some anomalous and as yet unexplained events", URSI Commission F, Triennium Open Symposium, Cairns, Queensland, Australia, 1-4 June 2004.

Woods, G. S., **Kerans, A.J.** and Maskell, D.L., "Simulated Angle of arrival Measurements for an Over Ocean Microwave Radio Link", URSI Commission F, Triennium Open Symposium, Cairns, Queensland, Australia, 1-4 June 2004.

Woods, G.S., Maskell, D.L. and **Kerans, A.J.**, "New angle of arrival measurement technique for over ocean propagation studies", Ninth International Conference on Communication Systems, ICCS 2004, Singapore, 6-9 September 2004.

Maskell, D.L., Woods, G.S. and **Kerans, A.J.**, "A Hardware Efficient Implementation of an Adaptive Subsample Delay Estimator", ISCAS 2004, Vancouver, Canada, May 2004.

Woods, G.S., **Kerans, A.J.** and Maskell, D.L., "Measuring Angle of arrival in Over Ocean Propagation Experiments", Workshop on Applications of Radio Science (WARS'04), Hobart, Australia, 18–19 February 2004.

Kerans, A.J., Kulessa, A.S., Woods, G.S. and Clark, A.J., "A theoretical design for long range over ocean microwave links using the tropical evaporation duct", IEEE Oceans'10, Sydney, Australia, 24–27 May 2010.

Chapter 1
Introduction and Thesis format

The most common mode of propagation for microwave communications is at relatively low angles over the Earth's surface. For communications, other than satellite communications, the World radio regulatory body, the International Telecommunication Union, Radio Communication sector (ITU-R), rarely studies antenna elevations above ten degrees. The majority of systems operate at or very close to zero degrees, especially on over water paths.

This low angle mode of radio propagation is also evident in radar systems, especially those used for navigation and close in defence of naval warships. A thorough understanding of radio wave propagation at low angles is therefore essential to understanding any anomalies or system failures resulting from propagation anomalies.

The first few hundred metres of the atmosphere above the surface of the Earth and sea are in a state of constant change affected by the interaction of the atmosphere with the ground and bodies of water of varying temperatures and depths. In order to understand the mechanisms of propagation in this region one needs to be able to forecast the weather in the area of interest. For large scale and meso-scale forecasting this is reasonably straight forward, however in the micro-scale, such as immediately above the surface of the sea, area wide forecasting, or even hind-casting, is extremely difficult and expensive. Unfortunately, it is in these areas that much of our interest lies, close to the surface of the sea the complex boundary conditions can lead to anomalous refractive index mechanisms leading to unstable and unusual radio wave propagation. One such effect of abnormal refractive index is the oceanic evaporation duct.

The evaporation duct is a rapid change in refractive index, which occurs above oceans in the presence of wind and has the effect of trapping radio waves above Ultra High Frequency (UHF, i.e. 300 MHz – 3 GHz). This process is known as ducting and the duct height is the effective height at which a wave would reflect from a reflecting surface. Such propagation traps the wave causing propagation over longer distances at

lower levels, higher path loss at higher levels and 'radar black holes' inside the duct where a target or object may not be detected. All of these effects have application to radar navigation and target detection as well as implications for communications radio path design and link budget calculations. One dramatic effect may be the inability of ship defence systems, such as the Phalanx close in defence system, to detect incoming sea-skimming missiles, a problem dear to the hearts of operational naval commanders.

Characterisation of propagation inside the evaporation duct is a subject that has received significant attention over the last twenty years and is well reported in the literature as discussed below. Since refractivity (N) is temperature and humidity dependent, duct formation is expected to be more prevalent in areas of high temperature and humidity. However, while significant research has been carried out in the Atlantic and Eastern Pacific, such as that by K Anderson in [1], where effects on RADAR are discussed, by Fairall et al in [2] where a comprehensive series of duct height measurements for the Atlantic are provided and as early as 1953 where, in 'Nature' [3] L Anderson discusses the effect of the duct on microwave propagation, there is no in depth reporting of the effect in the tropical waters of Northern Australia. Propagation mechanisms and actual duct formation in the tropical littoral zone similar to that in Northern Australia are less well reported with only some Mediterranean measurements available to the author [4] [5]. Mediterranean climates are sub-tropical (around 40 degrees north) not tropical. In our region of interest anomalous propagation was previously demonstrated in our region by Kulessa et al in [6]. This work builds significantly on that to provide guidance on duct formation and propagation within the duct in the Australian tropical littoral environment.

A popular method of estimating radio path loss inside the duct is the Parabolic Equation Method (PEM) and this has been developed into computer based packages, the most well known being Advanced Refractive Effects Prediction System (AREPS) and TERPEM. These packages produce a loss versus distance display over a given altitude but are reliant on calculating the duct height from 'bulk parameters', sea surface temperatures, air temperatures and relative humidity. By comparing these programs with an actual vertical 'slice' of the rays impinging on an array an estimate of the duct height can be made. Conversely, if the duct height is known from meteorological measurements then the accuracy of these simulations can be estimated for this particular

environment. We wish to explore the accuracy of these models and associated duct height estimation techniques contained in the programs for the potentially unstable marine boundary later over the Australian tropical littoral so as to assess their suitability for use to guide designers and operators of radio equipment used in these areas.

Information on the height of the duct can also be obtained from the PEM simulations and from ray tracing. If the angles of arrival of a complex wave-front were known ray tracing could be used to simply define the duct height in the absence of meteorological measurements, a PEM model could then be used to identify problematic propagation phenomena.

A problem encountered in attempting to establish the effects of the ducts is the meteorological detection of the duct itself. This is difficult and requires specialised equipment, similar to that outlined later in this Thesis, to obtain an accurate estimate of duct height. Another method of estimating duct height is via calculations of 'bulk parameters', measurements of sea surface temperature, air temperature and humidity. These estimations are less accurate but simpler and more readily carried out on board a moving ship.

The maritime oceanic duct is a refractive layer within the first 40 or so metres above the sea caused by a rapidly varying temperature and humidity gradient immediately above the ocean, which causes the refractive index, or M profile, to decrease initially with height up to a given altitude, causing a localised region of sub-refractivity and thus a duct which is called the evaporation duct.

In the tropical littoral zone north of Townsville, Queensland, Australia, the formation of the duct is controlled by the tropical weather prevalent in that area and by very warm sea surface temperatures, which can lead on occasion to an unstable lower atmosphere. This is referred to in this Thesis as the tropical evaporation duct which has implications for all designers and users of radiocommunication systems with over water paths.

The main goal of this Thesis was to study the behaviour of radio waves propagated inside the tropical evaporation duct at 11.7 GHz. Firstly the theory associated with propagation in stratified media was investigated; in Chapter 2 a theoretical study of

propagation within a stratified air mass is presented. Chapter 3 looks at the meteorology and subsequent chapters outline our research and implications drawn from it.

In the past few decades, researchers in both electromagnetic wave propagation and acoustics have studied the PEM model in an attempt to characterise both forms of propagation in stratified layers, either sound or radio in water or air. In both cases the problem is target detection, stratified layers refract or reflect the impinging wave, sometimes trapping the energy and transmitting it over abnormally long distances, on other occasions a detector may be on the opposite side of the layer and be unable to detect the target. A number of simulation packages have been developed using the PEM, their accuracy in the tropical littoral zone were at the time of commencement of this research, unverified. The various PEM based simulation models are explored in Chapter 5. We compare these models to actual measurements so as to gain an understanding of their applicability to path design and operation of radio communications equipment in the tropical littoral.

The weather is dominant in the formation of ducts and on other factors that affect propagation, such as wave heights. The weather in the region around Lucinda is dominant in the formation of ducts in the area. This topic, as well as the formation of waves, winds and sea state is explored in depth in Chapter 3.

To measure the radio waves propagating in the duct we first developed a very simple ten-element array so as to sample the received signal at various heights and then compare these results with the models. This array was used to successfully verify propagation in the duct and the accuracy of certain PEM models, AREPS and TERPEM.

The existence of a duct over a large area with sustained high signal levels relative to 'over Earth bulge' suggested the ability to communicate over very long distances at microwave frequencies using the duct as a transport mechanism. This was verified in an experiment using the ten-element array and the results, including some surprising ones, are presented in Chapter 6. This leads to certain conclusions for microwave system design and even for the collection of signals intelligence.

Expanding on our study of the weather around Lucinda, we deployed a floating 'Spar-Buoy' system that samples the atmosphere and records the data. From these samples, we are able to draw conclusions on duct formation in particular weather conditions. Measurements of wind speed and atmospheric bulk parameters from two weather platforms located at Lucinda (18° 13' 31", 146° 23' 10") and on Orpheus Island (18° 36' 48", 146° 29' 24") are presented. Weather information from other sources is also used extensively. From this information we are able to present and verify an equation relating duct height to wind speed in the tropical littoral.

Finally, I present a design for a sixteen-element array installed on Orpheus Island. This array uses novel techniques to enable the use of cheap components and processes and yet provides enough information to enable significant further research.

1.1   History of the research

In 1998 after finishing a masters' Degree at the Australian Defence Forces Academy I was attracted to this project during a presentation on a cold Canberra winter day by Dr Andrew (Andy) Kulessa of the Defence Science and Technology Organisation.

Andy was looking for a student and I was looking for a project. I listened to a number of presentations involving indoor propagation, however with all due apologies to the researchers studying that vital and interesting field, as a person who grew up in the tropics a short snapshot of Andy's words grabbed my attention:

"………*over warm tropical oceans……*"

I was hooked. And the journey has been as rewarding as the destination.

However the project had a beginning before me, Andy's previous student, Brian Piper and he, together with old colleagues friends Mal Heron and Graham Woods first discussed the embryonic findings of initial experiments in "A line of sight EM propagation experiment at 10.25 GHz in the tropical evaporation duct" published in IEE Proceedings online (19981474) in 1998, although the work was conducted in 1995 and 1996.

The spar buoys described in this work were designed by Dr. Kulessa and his team at DSTO. Beyond that however the design of each experiment, including radio systems, outlined in this Thesis and the interpretation of data from those and for the duct prevalence in the tropical littoral is the work of the author.

This is the genesis of my involvement in this research.

I have also often used the collective 'we' throughout this work where appropriate as it truly was a team effort, deploying the heavy buoys took many helpers as did erecting and taking down the various radio systems used.

1.2   Rationale

The evaporation duct, especially in tropical regions where it can be very strong, can enhance propagation enabling microwave signals to travel very long distances with path losses equal to or less than in free space. This anomalous propagation can have detrimental effects on radar coverage and can lead to intersystem interference in communications links. However the ability to use the duct to support propagation would have obvious advantages, particularly for store and forward communications systems fitted to platforms such as oil rigs moored up to one hundred kilometres from land.

In the tropical zone wether is different from that in temperate zones where the majority of pervious work has been undertaken. While it is similar in some ways to the Mediterranean as previously discussed, sea surface temperatures tend to be higher in the tropical littoral and are often higher than the air above. This research examines duct formation in this zone in particular and provides information on events in that zone.

The literature discussed in the introduction to this chapter investigates duct formation and some propagation experiments in temperate and sub tropical climates. Other than the early work by Kulessa et al [6] there is no other substantive work on duct formation and propagation within it in the Australian tropical littoral.

There are also very few references discussing comparisons of actual propagation with PEM models for this area except in [6]. Babin in his Thesis [16] compared duct height prediction models with actual measurements, but did not go on the conduct radio measurements. The author has not been able to find any work where duct heights were verified against both atmospheric models and radio data and where the accuracy of the Parabolic Equation Models (PEM) models used was also verified. Thus there is a need to study these topics for the Australian tropical littoral zone.

1.3   Research objectives

The objectives of this research are to study the formation and prevalence of evaporation ducts in the Australian tropical littoral and to conduct radio propagation experiments to verify the accuracy of both duct prediction models and the PEM models used to simulate propagation within the duct.

The origins of this project lie in (Australian) naval interest in the duct due to the effects they have on radar and communications. In Annex 1 I outline the problems in the context of this work. Radars do not behave predictably in the presence of a duct, there have been instances where radar targets have been visible to the naked eye yet still not detected by radar. Thus if the target is an incoming sea skimming missile or small hostile craft, the ship-borne defence systems cannot be accurately brought to bear.

In order to characterise anomalous propagation inside the tropical evaporation duct we have explored a number of facets associated with this propagation.

Initially we measured and characterised duct heights in the tropical littoral zone so as to gain an understanding of the existence and reliability of ducts in the region.

Secondly we took radio-frequency (RF) signal strength measurements inside evaporation ducts and compare these to available propagation modelling tools, AREPS and TERPEM, and from this drew conclusions on the reliability of these modelling packages and variability caused by weather events.

AREPS is a US navy publication available free from the US Navy's SPAWARSYSCOM department [7].

TERPEM is a similar commercial package available from Signal Science limited [8].

A long distance propagation experiment was conducted and from this we made suggestions for system design for long range paths using the evaporation duct to support transmission.

Finally I present a theoretical path design for a long distance microwave link using experience drawn from this research and from experience with a similar link designed using the results of this research.

Ancillary to this research is the equipment used to take the various measurements. The spar buoys were not designed by this author but were constructed at DSTO. All radio equipment used in this research was however designed by the author including a novel method for collecting angle or arrival information from a 16 element array. This array and its construction are described later in this Thesis.

Finally an explanation of the term *'tropical littoral zone'* in the context of this work is appropriate. This research was triggered by military interest in the topic. From Wikipedia [9] the 'littoral zone' is defined as:

"The littoral zone refers to that part of a sea, lake or river that is close to the shore. In coastal environments the littoral zone extends from the high water mark, which is rarely inundated, to shoreline areas that are permanently submerged. It always includes this intertidal zone and is often used to mean the same as the intertidal zone. However, the meaning of "littoral zone" can extend well beyond the intertidal zone.

There is no single definition. What is regarded as the full extent of the littoral zone, and the way the littoral zone is divided into sub-regions, varies in different contexts (lakes and rivers have their own definitions). The use of the term also varies from one part of the world to another, and between different disciplines. For example, military

commanders speak of the littoral in ways that are quite different from marine biologists."

The military definition of the littoral zone is used throughout this Thesis, that is the coastal region and in the North Queensland tropics bounded by the Great Barrier Reef and/or the continental islands inside it.

1.4   Research questions

A concise set of research questions was developed in the early stages of this project to guide the research and give predefined goals. These are outlined here and answered in the conclusions to the Thesis.

Question 1:   Are the available PEM models (AREPS and TERPEM) useful in predicting evaporation ducts in the Australian tropical littoral and if so, with what caveats?

Question 2:   With what prevalence do evaporation ducts exist in the tropical littoral?

Question 3:   Could a plot of receive signal strengths verses height from an RF system be used to determine if an evaporation duct is present?

Question 4:   What effects of evaporation ducting are important to radio designers?

Question 5:   Can the evaporation duct be used to support the transmission of useful data or for any other useful purpose?

A secondary objective is the design of the radio measuring equipment which is described in various Chapters throughout the Thesis.

1.5   Thesis organisation

This Thesis is presented as a series of chapters; the first gives a general overview of this rather unique topic. The remaining chapters represent the various stages of the research and resulting findings and are each supported by publications. The Thesis has been arranged to provide cohesion when reading each chapter in sequential order. Figure 1.1 illustrates the overall structure of the Thesis.

The Thesis is organised in the following format. **Chapter 2** introduces the fundamentals of microwave propagation, measurement and simulation as an introduction to the research.

Chapter 3 provides an overview of radio-meteorology and the tropical littoral zone under study. The chapter outlines basic coastal weather then looks at the area around Lucinda.

Chapter 4 presents the results of our work on duct formation in the tropical littoral and temperate oceans giving results from our meteorological measurements using buoys with associated sensors.

Chapter 5 investigates the PEM models AREPS and TERPEM. The chapter looks at a 'standard atmosphere' using these models, then explore propagation inside the duct and finally makes observations on accuracy based on actual measurements combined with our local knowledge of ducting in the area.

Chapter 6 presents the results of our longest and most conclusive radio-path experimental campaign. The first section examines expected propagation results over a long path using local ducting knowledge and makes observations from these results. The second section explores some unexpected anomalous propagation over a long path using the evaporation duct as a transmission media, examines these results and makes some observations on potential causes based on conditions in the area at the time. This last section forms the basis of later chapters.

Chapter 7 makes some simple observations about the duct acting as an angular filter. While I feel, with the benefit of a decade of research in the field, that these conclusions are obvious, they may not be to the designer or operator. The postulation also opens up a potential interesting field of research and some initial suggestions on method are also included.
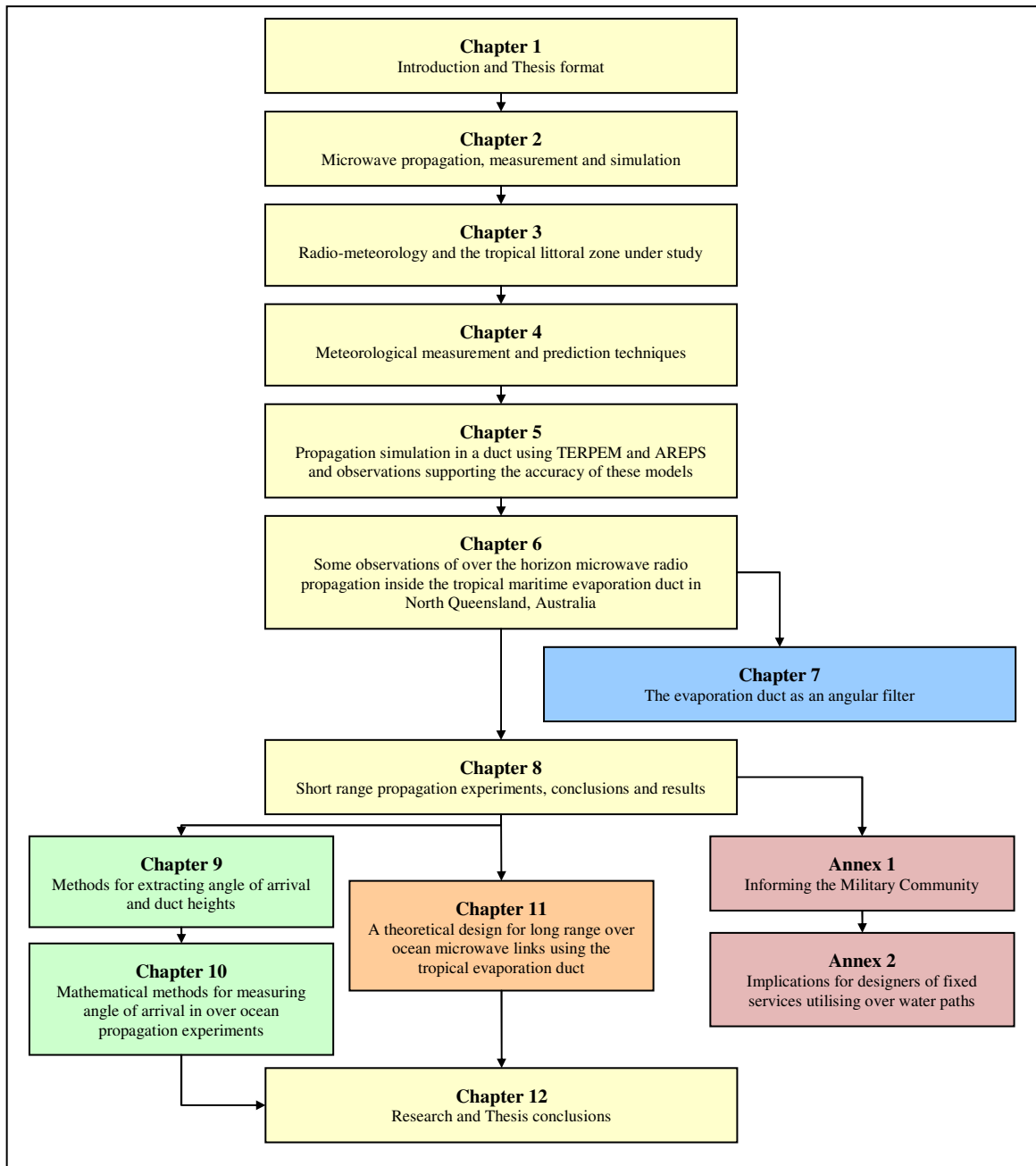
Figure 1.1: Chapter structure of this Thesis

Chapter 8 examines a series of short range propagation experiments between the jetty at Lucinda and Orpheus Island. These results are used to further validate both PEM models and our duct height estimation technique and are used to inform later chapters.

Chapter 9 discusses the design of equipment used to gather our radio propagation data and looks at a cost effective 16 element array that was designed and built by the author and installed by the team.

Chapter 10 discusses the mathematical theory behind extracting angle of arrival information from the large array.

Chapter 11 builds on the work of previous chapters and forms the basis for work presented in Annex 2.

The annexes represent some of the practical application of this research outlining issues for military commanders and providing some guidance on the use of this knowledge for the design of store and forward communications links.

Annex 1, informing the Military Community, discusses anomalous propagation within the evaporation duct from a military perspective using the information gathered during the research to give this group of mariners some insight into the effect ducting may have on their operations.

Annex 2 highlights the theory and research behind our 2010 paper in terms of its implications for fixed link designers where an over-water path is present.

1.6   Contributions from this research

This research contributes to the knowledge of microwave propagation inside the evaporation duct in three major ways.

Firstly a significant body of work on the predominance of ducts in the tropical littoral is presented along with some work on duct behaviour in strong winds.

Secondly some field measurements and comparisons with available duct and path loss prediction models is presented along with some observations on their accuracy.

Finally a the results of a long distance experiment are presented which lead to some guidance on the use of the prediction models during complex atmospheric layering and suggestions for the design of systems which may use the duct as a mechanism to support long range communications.

The work reported in this Thesis, with the exception of that previously described, is done by author and has included discussions with supervisors and experts as evident in the publications. Project supervisors Dr. Graham Woods and Dr. Andy Kulessa are included to acknowledge their contribution through input, mentoring, support, feedback and in many cases sheer physical labour.

1.7 References

[1] Andersen, K.D, "Radar Measurements at 16.5 GHz in the Oceanic Evaporation Duct", IEEE Transactions on Antennas and Propagation, Vol 37, No 1, pp. 100-106, January 1989.

[2] Fairall,C. W., Davidson,K. L., Schacher,G. E., Houlihan,T. M. "Evaporation Duct Height Measurements in the Mid-Atlantic". NAVAL OCEANOGRAPHIC OFFICE NSTL STATION MS, August 1978.

[3] Anderson, L. J. and Gossard, E.E., "Oceanic Duct and its Effect on Microwave Propagation", Nature, Vol 172, August 15 1953.

[4] Haack, T. and Burk, S.D., "Summertime Marine Refractivity Conditions along Coastal California", Journal of Applied Meteorology, Vol. 40, pp 673-687, April 2001.

[5] Haack, T., Wang, C., Garrrett, S., Glazer, A., Mailhot, J. et al., "Mesoscale Modelling of Boundary Layer Refractivity and Atmospheric Ducting", Journal of Applied Meteorology, Vol. 49, pp 2437-2457, December 2010.

[6] Kulessa, A. S., Heron, M. L. and Woods, G. S., "Refractivity variations in the tropical Australian marine environment", Australian Defence (DSTO) internal publication, 1997.

[7] http://areps.spawar.navy.mil/, last accessed 16/11/2008.

[8] http://www.signalscience.com/TERPEM.htm, last accessed 16/11/2008.

[9] Wikipedia, "Littoral zone", last accessed 31 March 2011, http://en.wikipedia.org/wiki/Littoral_zone.

Chapter 2

Microwave propagation, measurement and simulation

In this chapter, I introduce the fundamentals of microwave propagation, measurement and simulation as an introduction to the research.

Chapter 1
Introduction and Thesis format

Chapter 2
Microwave propagation, measurement and simulation

Chapter 3
Radio-meteorology and the tropical littoral zone under study

Chapter 4
Meteorological measurement and prediction techniques

Chapter 5
Propagation simulation in a duct using TERPEM and AREPS and observations supporting the accuracy of these models

Chapter 6
Some observations of over the horizon microwave radio propagation inside the tropical maritime evaporation duct in North Queensland, Australia

Chapter 7
The evaporation duct as an angular filter

Chapter 8
Short range propagation experiments, conclusions and results

Chapter 9
Methods for extracting angle of arrival and duct heights

Chapter 11
A theoretical design for long range over ocean microwave links using the tropical evaporation duct

Annex 1
Informing the Military Community

Chapter 10
Mathematical methods for measuring angle of arrival in over ocean propagation experiments

Annex 2
Implications for designers of fixed services utilising over water paths

Chapter 12
Research and Thesis conclusions

2.1 General properties of the troposphere

The troposphere is that part of the atmosphere generally considered to extend from the surface to about 10 km in altitude at northern to mid latitudes and up to 20 km at the equator.

In the troposphere the percentage of each gas does not vary with height. The only exception to this is water vapour content which while strongly dependent on local weather generally decreases rapidly with height. Another important property of the troposphere is adiabatic cooling. Temperature decreases with height at the rate of about 5 degrees per 1000 metres in the first few kilometres.

As the sun heats the surface of the earth, convective air movement contribute to the heating of the troposphere from below. Columns of rising warm air are best seen in the 'fair weather' cumulus clouds that dot the sky on warm still days. This heating is uneven across the ground and somewhat more even over the sea where temperature differences are less pronounced.

The International Standard Atmosphere (ISA) [10] defines the average pressure at the sea's surface as 1013.25 millibars (mb) and average sea level temperature as 15 degrees Celsius (C). Lapse rate is defined as 12 mb per 100 metres and 0.55 degree C per 100 metres. The ISA also assumes these lapse rates are linear and that relative humidity remains unchanged. While these figures form a basis for radio wave propagation in the troposphere they do not hold adjacent to the sea surface (or any other surface where heating and evaporation are modified from that of the ISA) and this difference forms the basis of our study into microwave radio propagation over warm tropical oceans.

2.2 Propagation of radio waves at microwave frequencies in the troposphere

The free space transmission equation provides us with the first fundamental of low angle propagation through the troposphere. Received power, p, is given by:

$$p = P_t \frac{G_t}{4\pi d^2}$$

(2.1)

Where P_t is the transmitted power delivered to the antenna, G_t is the gain of the transmit antenna and $4\pi d^2$ is the surface area of a sphere with diameter d. The path loss, that is the losses between an isotropic transmit and an isotropic receive antenna, is given by:

$$PL = -20 \, Log_{10}(\lambda/4\pi d)$$

(2.2)

From which we can derive:

$$PL = 32.4 + 20 \, Log10(DF)$$

(2.3)

Where D is distance measured in kilometres and F is frequency measured in MHz.

This equation is a very good approximation for path loss in a line of sight homogenous atmosphere. Unfortunately, the atmosphere is rarely homogenous; rather it stratifies horizontally, particularly over the tropical littoral zone resulting in many cases in a tropical evaporation duct [11].

Stratification also occurs higher in the atmosphere under the influence of large-scale meteorological events such as advection.

While the simple path loss equations serve us well in system design under most conditions, more knowledge is needed where ducts occur.

2.3   Refractive index and the atmosphere

In a homogenous atmosphere, affected only by normal adiabatic processes, the propagation of radio waves is well behaved and dependent on the refractive index of the air and the radio horizon. In a vacuum, the refractive index would be 1 everywhere and radio waves would propagate in straight lines. In a well-behaved atmosphere the refractive index is closer to 1.0003 at the Earth's surface, reducing with altitude. This

reduction with altitude causes radio waves to bend, normally towards the Earth, and thus the radio horizon is extended.

Refractive index is referred to as *n,* e.g. n=1.0003. To make the units more manageable we use N, where;

$$N = (n-1) \ 10^6 \ \text{n-units} \tag{2.4}$$

Therefore, for a 'normal' atmosphere at sea level N = 300, this value is also known as N_o. The ITU-R gives maps of N_o for the world in Recommendation P-452 [12], a sample of which is shown in Figure 2.1.

The atmosphere is not well behaved. Complex interactions between temperature pressure and humidity occur, particularly close to the surface of the sea. A standard formula for refractive index, using these parameters is given in [13].
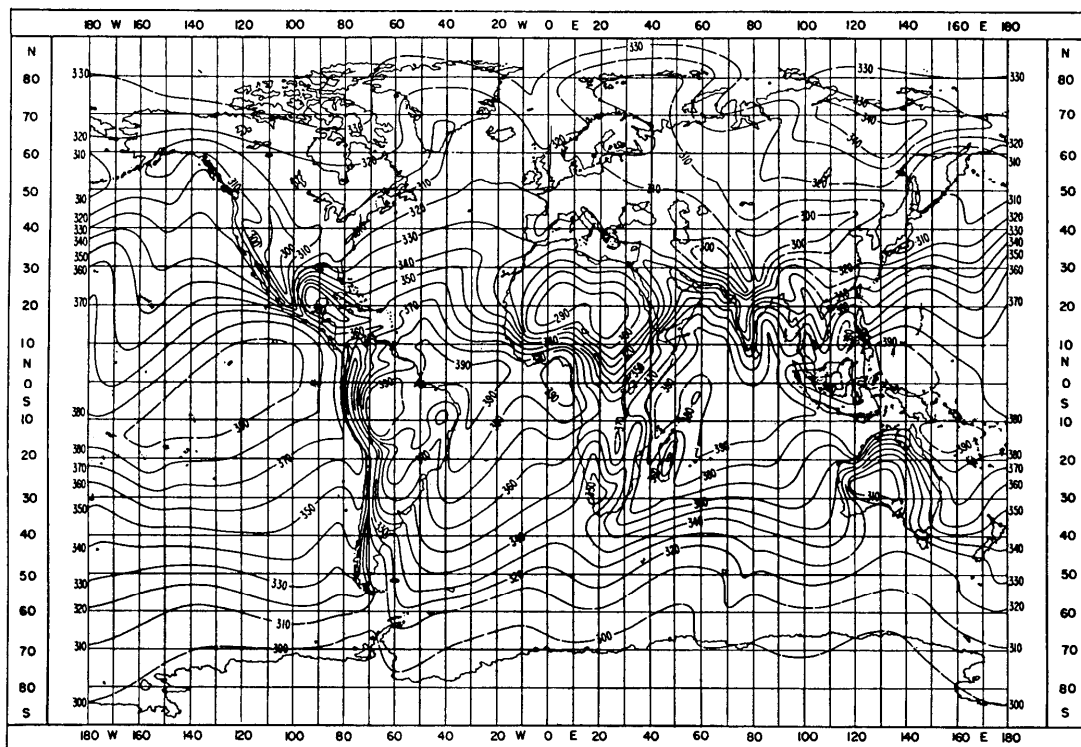
Figure 2.1: Monthly February values of N_o from ITU-R Recommendation P.452-9 [12].

A general formula for N taking into account temperature, pressure and humidity is given by:

$$N = \frac{77.6}{T}(P + 4810\frac{e}{T})$$

(2.5)

where   P is the atmospheric pressure in millibars (mb)

T is the absolute temperature in Kelvin, and

e is the partial pressure of water in millibars.

In a dry, well-mixed atmosphere the decrease in N with height can be seen to be due to the atmospheric pressure term P. Pressure falls off exponentially with height and in this atmosphere so does N. For the standard atmosphere this decrease is -39 N-units/1000 metres. As stated previously, the standard atmosphere is defined as: p = 1013.25 mb, T=288.2K, R.H= e/e_S = 70%, e = 11.9mb.

We can convert relative humidity to water vapour pressure e using:

$e = E_r r/100\ mb$

(2.6)

Where E_r is the pressure, found from charts, of water vapour, which will saturate the air at a given temperature. Figure 2.2 shows such a chart.

In a real atmosphere, departures from the normal are due to fluctuation or stratification of temperature and humidity. Looking back at equation (2.5) we can expand it:

$$N = \frac{77.6P}{T} + \frac{373256e}{T^2}$$
(2.7)

The first term can be seen to be dependent only on P and T and is called the 'dry' term. The second term has a strong dependency on humidity and is called the 'wet' term. The wet term is related to Relative Humidity, which is the amount of water the atmosphere at a given temperature can support before water becomes present as droplets (i.e. clouds). Figure 2.2 shows the saturated vapour pressure in mb as a function of temperature.
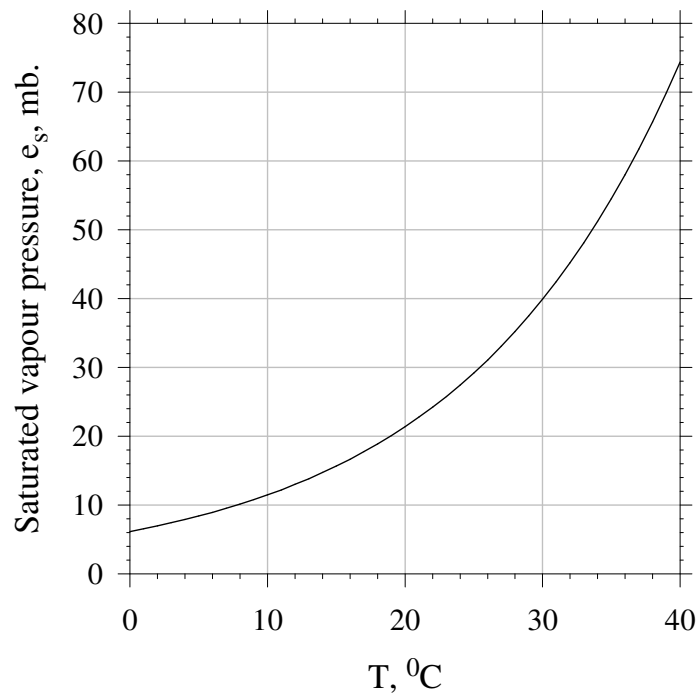
Figure 2.2: Saturated vapour pressure as a function of T and e.
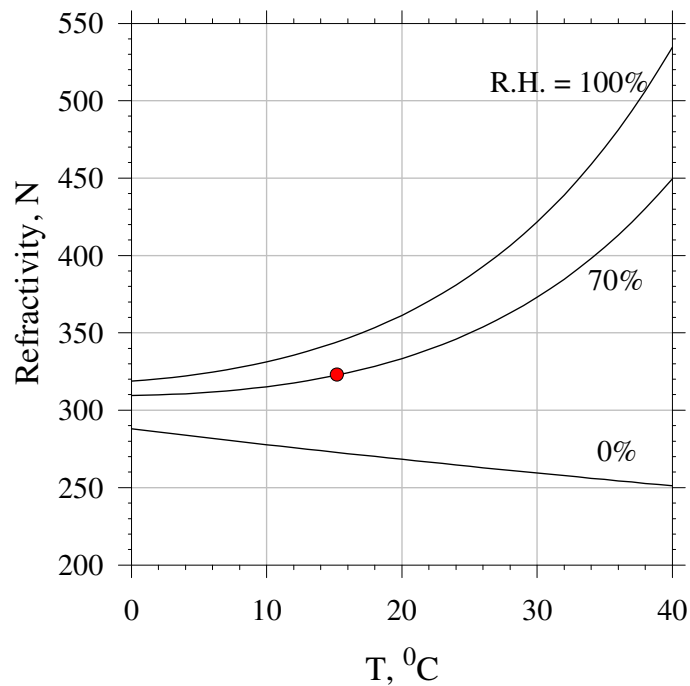
Figure 2.3: Refractivity as a function of temperature and humidity [14].

As atmospheric pressure in the standard atmosphere at sea level is 1013 mb, the dry term changes little as temperature decreases or increases. Due to the size of the multiplier in the wet term and the consequent reduction in e at those temperatures (i.e. dry cold air), the first term is dominant at lower temperatures. In tropical areas, large

changes in both T and e can occur and as a result, the wet term is dominant and large changes in N can occur, particularly close to the surface of the sea. Figure 2.3 shows graphically how refractivity increases rapidly in warm humid air over tropical waters [14]. The red dot in Figure 2.3 represents ISA conditions.

Throughout this Thesis, we shall assume that changes in N only occur vertically and that they remain the same horizontally, at least for the radio paths being tested. This assumption is made despite this being shown to not be strictly so in one set of our measurements and as depicted in Chapter Four, Figure 4.4.

Differences horizontally must be expected as the surface temperature of the ocean varies with cold up-welling. Wind speeds, relative humidity and air temperature can also be expected to vary over a long path. These differences however are small compared with the entire path and in any case, measuring them is difficult if not impossible, so the general case of horizontal homogeneity will be assumed.

The change in N with height, dN/dh, is not constant in any atmosphere over time and in particular, as will be shown, is rarely constant or ideal over warm tropical waters. In fact dN/dh can remain static (0) or even increase.

It is more convenient to draw radio-ray trajectories above a flat Earth allowing the use of flat graph paper for the plotting of rays and geographic features. To do this the radius of the Earth is made infinite and the trajectory of a ray is changed to become a factor of the normal Earth radius. This factor is called the K factor.

A ray at radius R propagating above a normal Earth of radius *a* will therefore have a modified radius over the flat Earth given by:

$$\frac{1}{R_m} = \frac{1}{R} + \frac{1}{a} \tag{2.8}$$

If we define a new variable M, the *modified radio refractivity,* where:

$$M = N + \frac{h}{a}10^{-6} \tag{2.9}$$

the new radius of the propagating wave can be accounted for:

$$\frac{1}{R_m} = \frac{dM}{dh} 10^{-6}$$

(2.10)

At sea level where h = 0 M(h) = N(h) = 300 M-units.

So M is essentially N for a flat Earth where:

$$M = (m - 1)\ 10^6, \text{ and}$$

$$m = n + \frac{h}{a}$$

(2.11)

The K factor is then derived from:

$$K = \frac{Rm}{a}$$

(2.12)

Which, from the above equations gives:

$$K = \frac{157}{\dfrac{dM}{dh}}$$

(2.13)

for an Earth radius of 6394 km.

Table 2.1, adapted from [15], categorises dN/dh and gives us an idea of the effect such refractive indices have on propagation.

K = 4/3 is also known as the standard atmosphere in our flat Earth model. In a standard atmosphere the change in pressure is the dominant factor in dN/dh.

Table 2.1: Definitions of various refractive atmospheres.

Type of atmosphere	True Earth	Flat Earth	K-factor
	Typical Refractivity Gradient dN/dh (N-units/1000m)	Typical Modified Refractivity Gradient. DM/dh (M-units/1000m)	
Sub refractive	79	236	2/3
Constant Atmospheric density	0	157	1
Normal (standard) atmosphere	-39	118	4/3
Super refractive	-157	0	≡
Ducting	-393	-236	-2/3

K = 2/3 corresponds to a sub refractive atmosphere. When this type of atmosphere exists, radio wave trajectories are bent away from the Earth. This usually occurs where very humid air is held above dry air near the ground.

Of particular interest in this study is the situation where K = -2/3, a super refractive atmosphere which leads to trapping or ducting. K = -2/3 corresponds to a negative refractivity gradient of –393 N-units/1000 metres. Refractivity gradients of this magnitude require that a layer of very humid air close to the ground or sea lie below warmer drier air above. This situation occurs regularly above oceans and as will be shown later, very regularly over warm tropical oceans. Very high humidity levels can exist in the first 5 – 40 metres above a tropical ocean and if the air above is warmer than the sea surface the system is unstable, wind can then mix the lower layer forming a gradient at around –393 N-units/1000m resulting in an evaporation duct.

It is common in the tropical littoral zone for the sea surface temperature to exceed the temperature of the air above it leading to an unstable atmospheric layer. Whether a duct forms in these situations depends then upon more complex mechanisms such as the temperature and humidity of the air flowing above the sea which depends in a large part on whether this air mass comes from over the land or over the sea and also on water vapour flux.

A graphic example of each of these situations is shown in Figure 2.4.
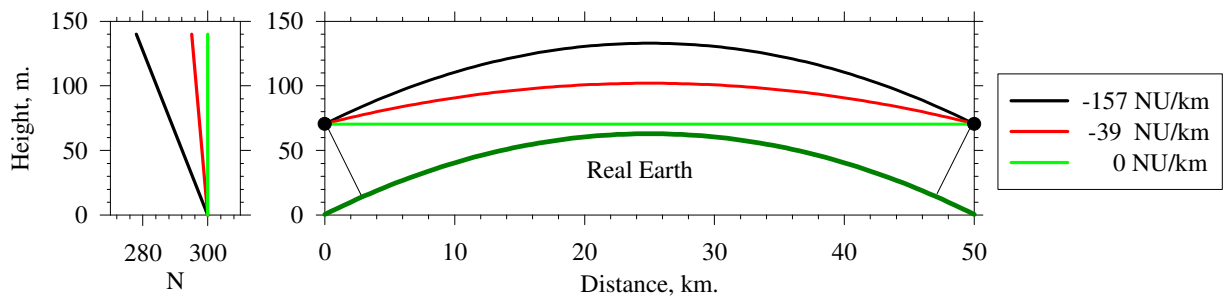
Figure 2.4: Ray paths for various refractivity [14].

2.4 Radio waves propagating inside the evaporation duct

An evaporation duct above the sea, for short paths, can support an anomalous propagation mode between a transmitter and receiver resulting in enhanced signal where both are within the duct, or interference when an unwanted signal becomes coupled in the duct. This is shown in Figure 2.5 below.

In a normal evaporation duct the gradient is initially negative corresponding to a gradient around –390 N-units/1000m. As height increases, mixing with warmer drier air changes the refractive gradient back towards the standard of –39 N-units/1000m corresponding to a 'normal' K = 4/3. This atmosphere leads to concave trajectories in the upper part of the duct leading to refraction back to the Earth.

The parameters of the duct, height and 'strength' (dM/dh) are critical to propagation inside the duct. The work of Babin in his Thesis [16] provided excellent guidance to the author of this work both on his model for defining the oceanic evaporation duct but also a comparison of other models. While there are significant differences in the climates of North Queensland and the area Babin carried out his physical research (Wallops Island Virginia USA and the Potomac River) reliance on dN/dh which relies on temperature and relative humidity remains constant. Thus we believe the conclusions from this research will hold for ours and the methods of data fitting used by Babin are applicable to the Australian tropical littoral.

While our own buoy based duct measurements were underway Babin published a paper on data collected from a mast tethered Buoy around Wallops Island Virginia [17] which

compared well with the data we had collected. Of note was the Babin buoy remained close to a ship, and thus a potential source of error. Nonetheless a comparison of the work presented in this paper confirmed our methods. Babin also published a compilation of his work in 1996 in [18] which correlated well with our work of 1998 – 2000.
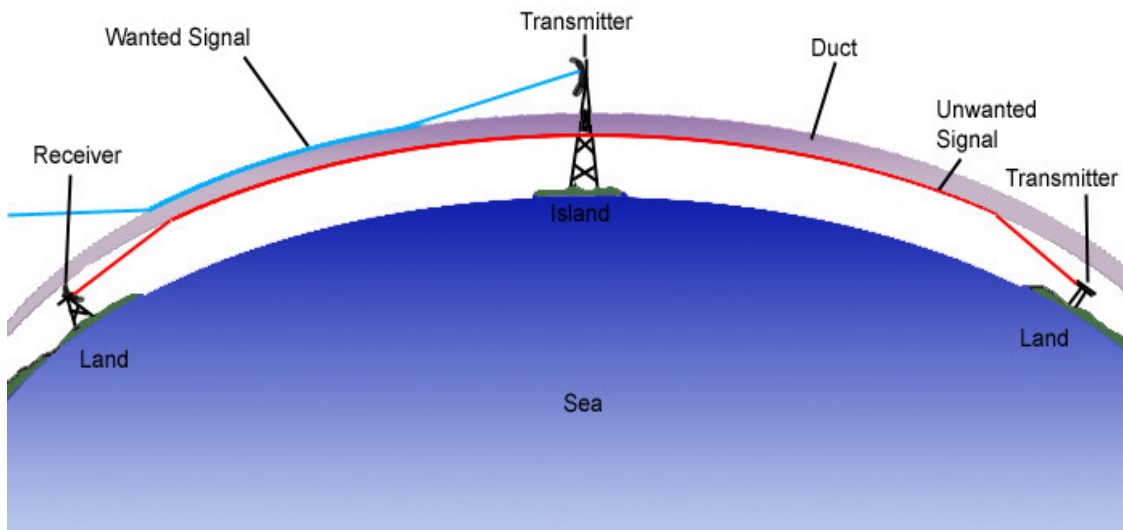
Figure 2.5: Depiction of evaporation duct and potential interference scenario.
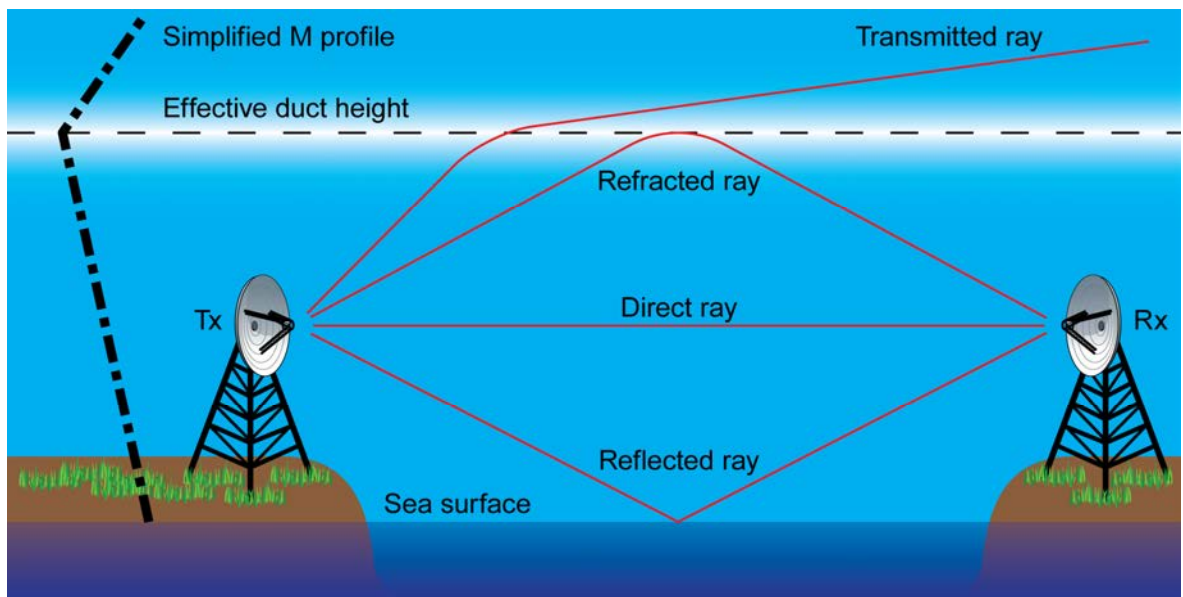
Figure 2.6: Simplified ray trace model of the evaporation duct.

Using the two refractivity regions shown in Figure 2.5, a very simple ray trace diagram shown in Figure 2.6 gives us all the information we need when discussing two rays propagating in the duct (ignoring rays reflected from the sea[1]). In this case, the transmitter is inside the duct. The transmitter can be assumed to be the source of the emissions received at the receiver. For a communications link it would be an actual transmitter, for a radar system it would be the target.

The direct ray, from transmitter to receiver below the duct height, is labelled 'Direct Ray' in Figure 2.6. The reflected ray is labelled 'Reflected Ray', the ray refracted within the duct is labelled 'Refracted Ray' and the transmitted ray is labelled 'Transmitted Ray'. If the receiver is inside the duct it will receive Direct, Reflected and Refracted rays, so depending upon the actual path and resulting phase differences the receiver may receive and enhanced or faded signal.

If the receiver is above the duct then it will receive only the transmitted signal, which may vary in strength depending on the angle of launch.

These effects have implications for system designers. These are discussed further for fixed services in Annex 2.

2.5   Conclusions

This Chapter has presented the theoretical basis of ducting. This information will be drawn on heavily in subsequent chapters to explain phenomena observed during our research.

2.6   References

[10] Manual of Aviation Meteorology, Second Edition, Australian Bureau of Meteorology, 2007, ISBN 978-0-9578991-7-9

[11] Bean, B.R. and Dutton, E.J., "Radio Meteorology", US Government Printing Office, 1966 (Extract).

---

[1] Reasonable when Earth bulge obscures the reflected path. However over very long paths there may be double (or more) reflections.

[12] ITU-R Recommendation P.452-9. Available at http://www.itu.int/rec/R-REC-
      P.452/en

[13] Shibuya, S., "A Basic Atlas of Radio-wave Propagation", Wiley Inter-science,
      1987

[14] Webster, A., Department of Physics, University of Western Ontario, London,
      Ontario, Canada, in a collaborative presentation to the team, May 2001

[15] Geiger, A.J., "Low-Angle Microwave Propagation: Physics and Modelling",
      Artech House 1991

[16] Babin. S. M. "A New Model of the Oceanic Evaporation Duct and its
      Comparison with Current Models". PhD Thesis. University of Maryland (USA)
      1996.

[17] Babin. S. M. "A Case Study of Subrefractive Conditions at Wallops Island
      Virginia" Journal of Applied Meteorology, Vol 34 May 1995.

[18] Babin. S. M. "Surface Duct Height Distributions for Wallops Island, Virginia,
      1985 – 1994." Journal of Applied Meteorology, Vol 35 January 1996.

Chapter 3

Radio-meteorology and the tropical littoral zone under study

In this chapter, I provide an overview of radio-meteorology and the tropical littoral zone under study. The chapter outlines basic coastal weather then looks at the area around Lucinda.
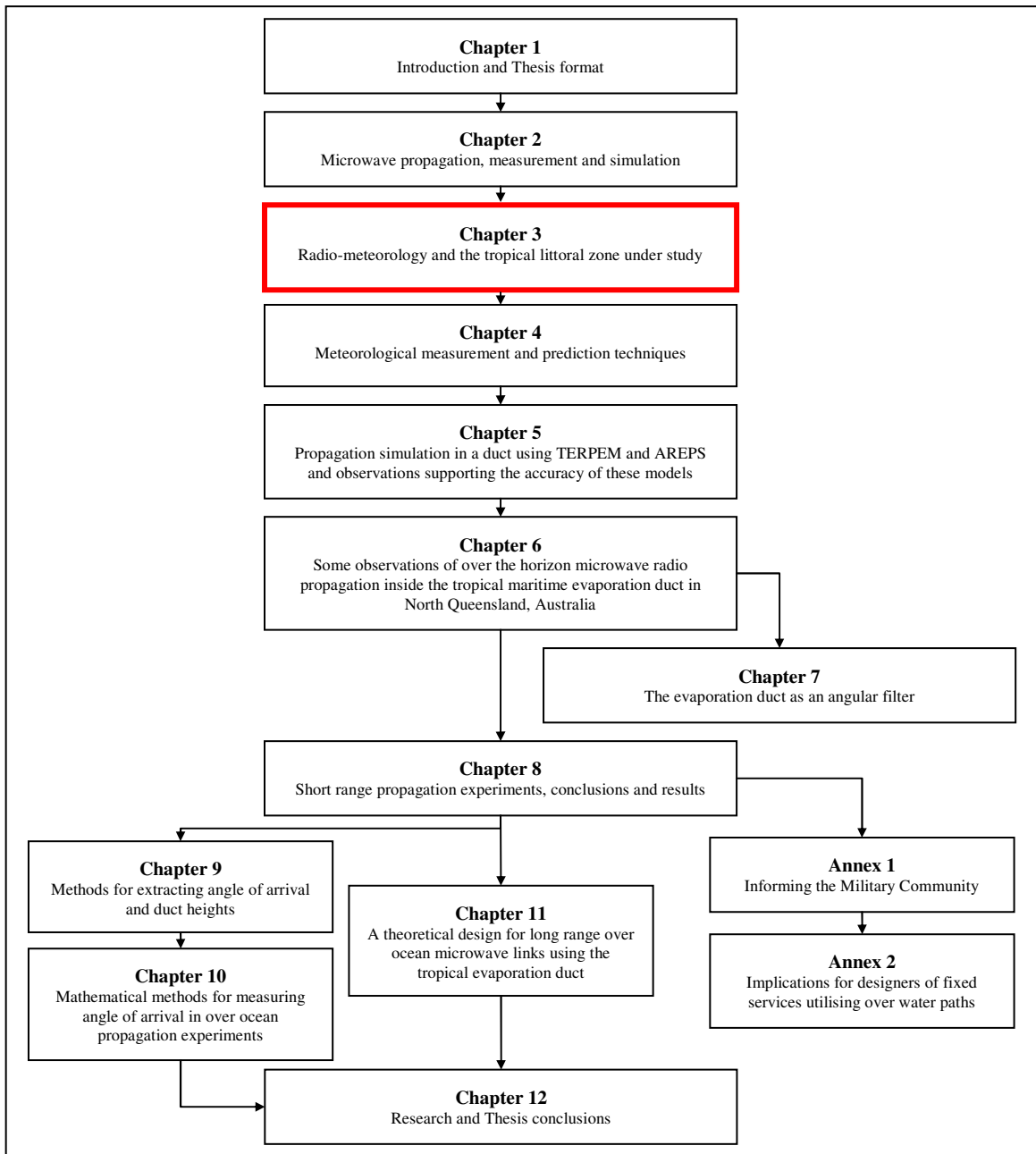
3.1   Coastal meteorology

Coastal meteorology is an important subset to general meteorology affecting how people live in and around the littoral zone. An important text relied upon heavily in this Thesis is Coastal Meteorology by Hsu [19] where the topic is explored in depth.

In the case of this project the main interest was in how the local meteorology affects the formation and life of the evaporation duct. To understand ducts a basic understanding of radiation and heat balance over the sea near the coast is required, knowledge of the way the sea breeze and land breeze are established and a little about their relative characteristics and wind and wave formation is critical.

In general the atmosphere is made up of 99% Nitrogen + Oxygen (N_2 = 78.08%, O_2 = 20.95%) however in most meteorological processes these gasses are passive [19].

Water vapour generally makes up 0 – 4% depending on local meteorology, this can reach saturation at or near the surface of the sea. In addition, water droplets are also present in large numbers near the sea's surface, especially when waves are breaking under the influence of strong winds. This is evident from observation. Water vapour and water droplets play a dominant role in the micro weather above the sea as they can change phase, particularly when mixed or moved by wind or adiabatic lifting. In the larger sense, this is evident in the formation of clouds, rain and snow. In our case, this is the basis for the formation of the evaporation duct.

Referring back to Equation 2.6, well illustrated in Figure 2.3, assuming pressure is relatively constant over the first few metres above the sea the two terms that are of most interest in duct formation are temperature and saturated (water) vapour pressure. The latter is temperature dependent. Thus vapour pressure (humidity) is the most important factor. Figure 2.3 shows that over the ranges of humidity 0% to 100% we can expect a change in refractivity (N) of 300 units.

Carbon dioxide and ozone are also important because of their effects on radiation; however these effects are beyond the scope of interest of this study.
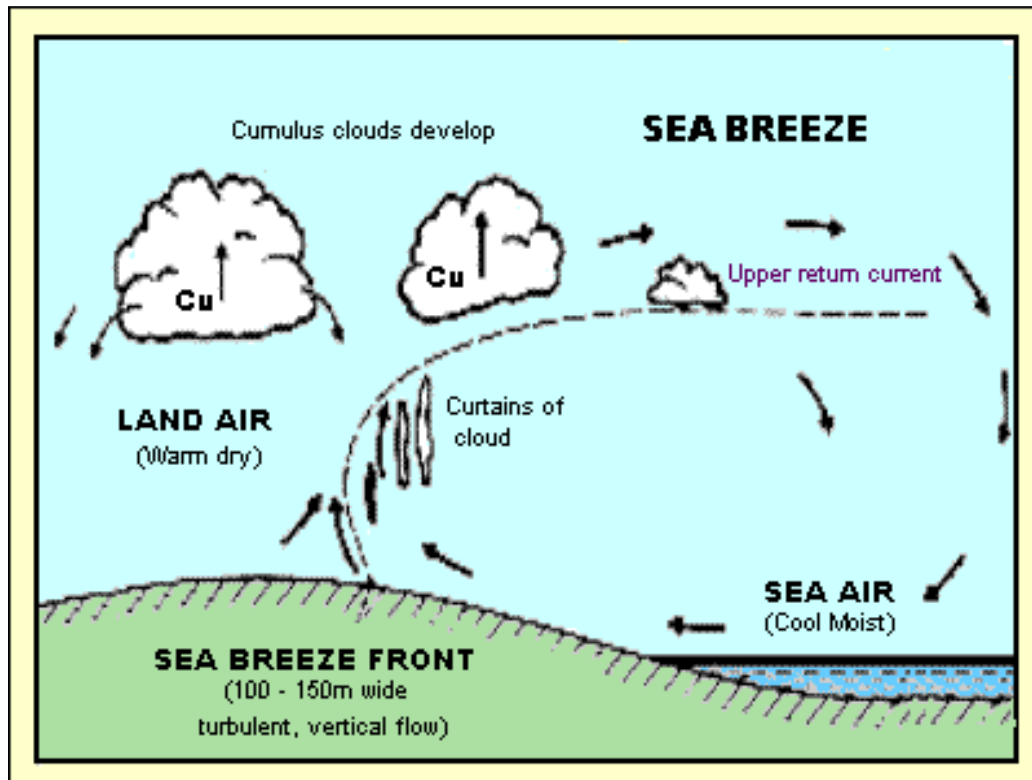
Figure 3.1: Sea Breeze Formation [20].

3.1.1 The air sea land boundary layer

Our research has shown that an upper limit for duct heights in the Australian littoral zone is around 40 metres. This is the height of the imaginary reflecting layer; to understand the formation of ducts we must study the lower atmosphere above the sea up to a height of about 100 metres. This layer is called the Surface Boundary Layer (SBL). In this layer in the littoral zone wind, surface temperature, surface friction and temperature gradient are important in the formation of surface based events such as fog, coastal fronts (bands of Cumulus cloud forming parallel with the coast) and the evaporation duct.

One important effect is that under the influence of a sea breeze, cool moist stable air is forced over land where the air is drier and has been fumigated by bush-fires, or in the north, cane fires and general human activity. Over the land, the air is warm, dry and unstable. A boundary layer forms quickly with the moist air lifting through the warmer air mass. This results in the formation of bands of cumulus clouds. From our perspective, this also causes the evaporation duct to dissipate. Depending on the

makeup of the coastal region the evaporation duct can be expected to extend inland only a few tens of metres if at all. Since we will show that wind is an important factor in the development of the duct we can expect that when the sea breeze changes over to the land breeze and in the absence of weather pattern winds, the duct will partially or completely collapse during the intervening lull in wind speed.

We could also expect a change in duct behaviour under land and sea breezes, as there are substantial temperature and humidity differences, temperature and humidity being two critical parameters in duct formation.

In general, according to Hsu [19] we can say the following about the SBL over the sea:

- Earth rotation is not important.
- Wind direction does not change with height.
- Wind speed changes appreciably with height.
- Wind speed is affected by surface stress, vertical heat flux and wave height.
- Transport of atmospheric properties is by turbulent diffusion (wind eddies).

Above the SBL under the effect of geostrophic forces wind direction, speed and temperature do change with height [21]; however this is well above the levels we are concerned about, up to about 50 metres.

As the wind blows over the surface of the sea it exerts a force on that surface. In the initial case it can be assumed that the sea surface is stationary and the air above it is moving. If both bodies were unconstrained and not viscous, the end condition would be both bodies moving together. Obviously this is not the case.

In actual fact the surface of the sea moves little compared to wind speed over it, waves form depending on wind speed and fetch, the friction at the surface boundary increases and the air speed at the boundary reduces to near that of the sea's surface. Above 100m the air blows freely, so in the intervening interval wind speed must drop under the influence of a tangential shearing stress, τ. This is illustrated in Figure 3.2 below.

The wind exerts a force F on the surface of the sea which is proportional to the area of the surface and the wind speed v. It is also proportional to the distance z which is the depth of the water. Again, at the sea bed the water speed must approach zero and so another change in speed applies between the sea bed and the sea surface. The increase in wind speed with height above the sea can also be seen in Figure 3.2 below. Figure 3.3 shows a series of measurements taken by the author to verify this theory for our experimental area in the presence of possible uncertainties caused by the Lucinda jetty.

A more mathematical approach can be found in [19], the end effect of this is wave formation, eddy formation in the winds and a change in wind speed with height. All of these effects change the micro-meteorology of the duct and explain some of the short term variations observed in our atmospheric measurements.

Simple wind speed measurements were carried out from the end of a long jetty at Lucinda in North Queensland using a hand-held device. This data is presented below for a day when the predicted wind was 20 kph and the measured wind at height from an anemometer was 19.8 kph. Note, no calibration of the different devices was carried out, measurements were made from a ladder on the jetty (which although normal to the wind direction may have produced speed changes) and that the 'zero' height above mean sea level (AMSL) was by necessity slightly above actual wave height.
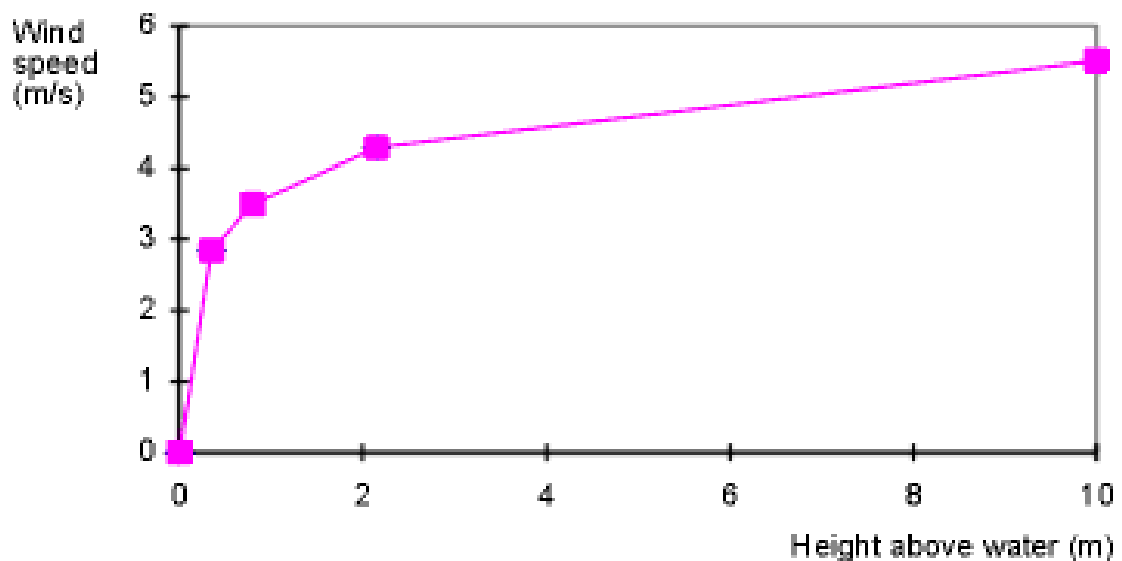
[Original data courtesy of Rod Carr]

Figure 3.2: Wind shear over the sea's surface [21].

34
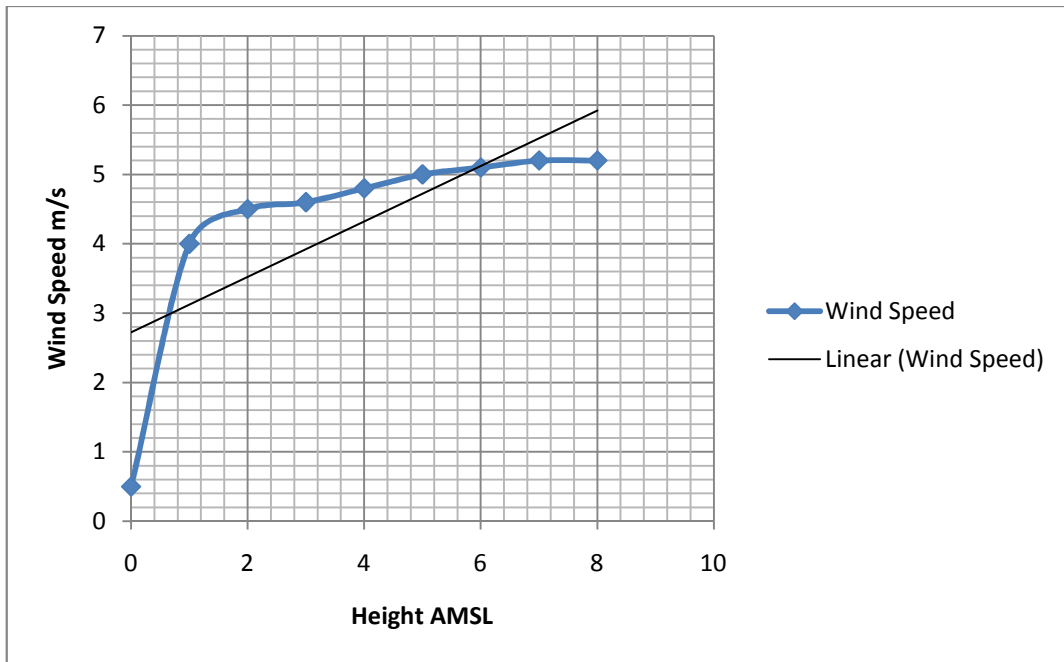
Figure 3.3: Simple wind speed measurements performed at Lucinda.

Despite these inherent errors, the curves from actual measurements described in Figure 3.3 support those from the theory shown in Figure 3.2.

3.1.2 Sea surface temperature measurements

There are a number of ways to measure sea surface temperature. The Bureau of Meteorology (BoM) has a number of free-floating buoys, which return measurements throughout Australian oceans. Unfortunately, none are operating in or around our area of interest.

The Great Barrier Reef Marine Parks Authority (GBRMPA) and the Australian Institute of Marine Science (AIMS) also monitor sea surface temperature to protect the health of the Great Barrier Reef. Unfortunately while these measurements give us some indication of sea surface temperatures they are not accurate between the Palm Island Group and the Lucinda Jetty.

The National Oceanic and Atmospheric Administration (NOAA) use satellites to take measurements of global sea surface temperatures. An example of these is shown in Figure 3.4. These are reasonably accurate for the area of interest and would be useful for large scale prediction of evaporation duct formation.
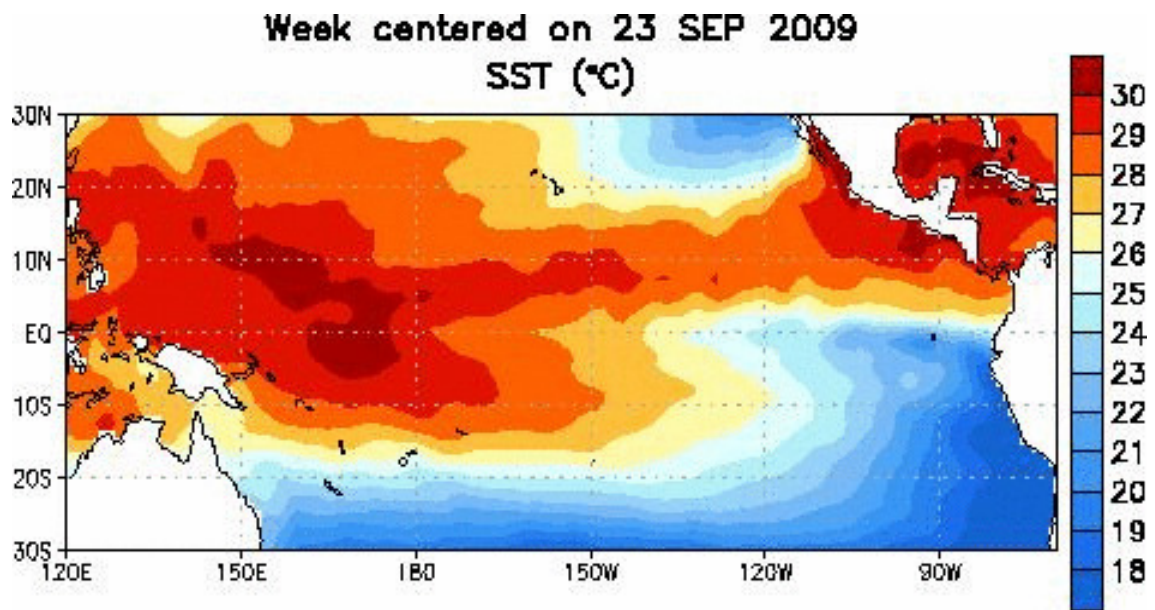
Figure 3.4: Sea Surface temperatures for the Region of Interest [22].

Finally, there is direct measurement, which we used towards the end of this project. Direct measurement is useful as it gives us a true temperature for the area of interest, but it also gives us a way to calibrate all the other sources when direct measurement is not possible. This also will be very useful if the prediction of ducts from large scale measurements is ever necessary.

Figure 3.5 shows a comparison between sea and air surface temperatures based on data collected by AIMS in Cleveland Bay near Townsville. The sea surface temperature (Red) is more stable that the air temperature (blue) which is taken at 6 metres AMSL. Where the sea surface temperature exceeds the air temperature a localised region of instability may form which causes fluctuation in the refractivity of the air immediately above it and is believed by the author to be the main cause for the variation in duct height seen, for example in Figures 5.17 and 5.19.

Different methods were used for direct measurement from either our sea-borne buoys or measurements from Lucinda Jetty. Figure 3.6 is an average for the sea surface temperature for a region seaward to about 1 kilometre from the jetty for the period of research. It should be noted that as different measurements taken at about 2:00 pm on different days during the campaign are averaged the error in this curve is in the order of

+/- 1° C over the month. Thus these figures give a general 'bulk' parameter that may be used to assist in calculating duct height, but they are not accurate.
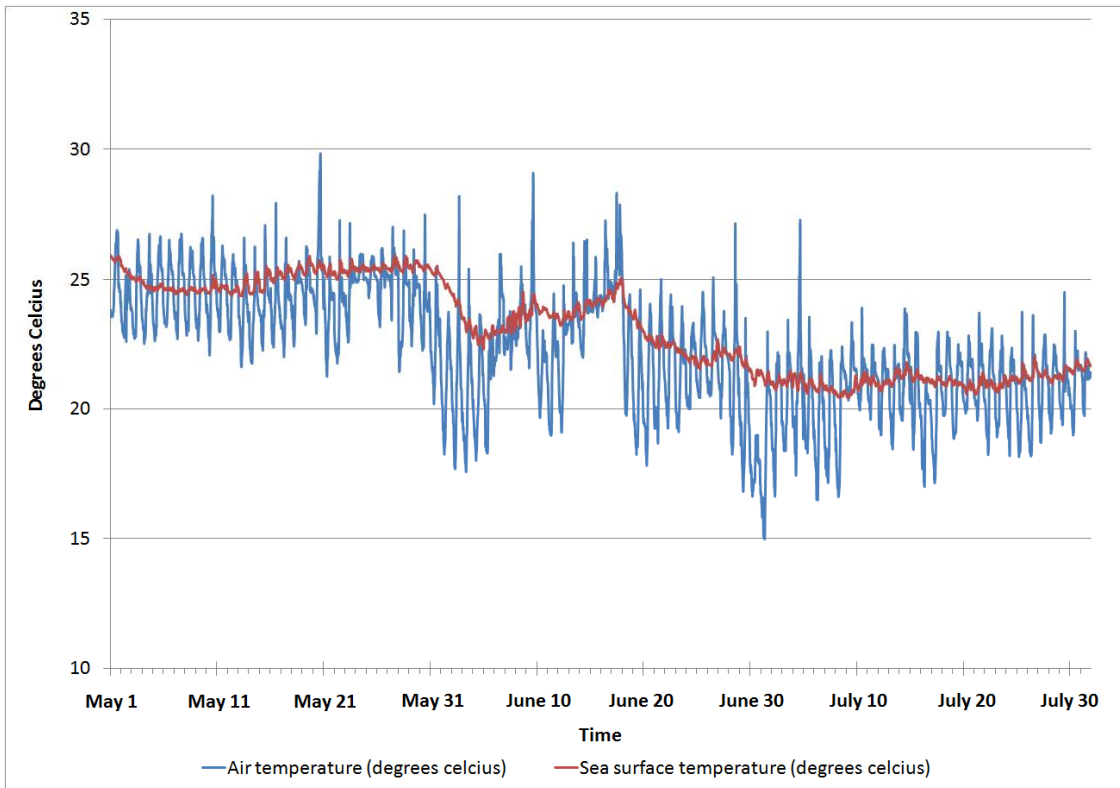
Figure 3.5: Sea surface and air temperatures for May to July 2001 [Data courtesy of Australian Institute for Marine Science]
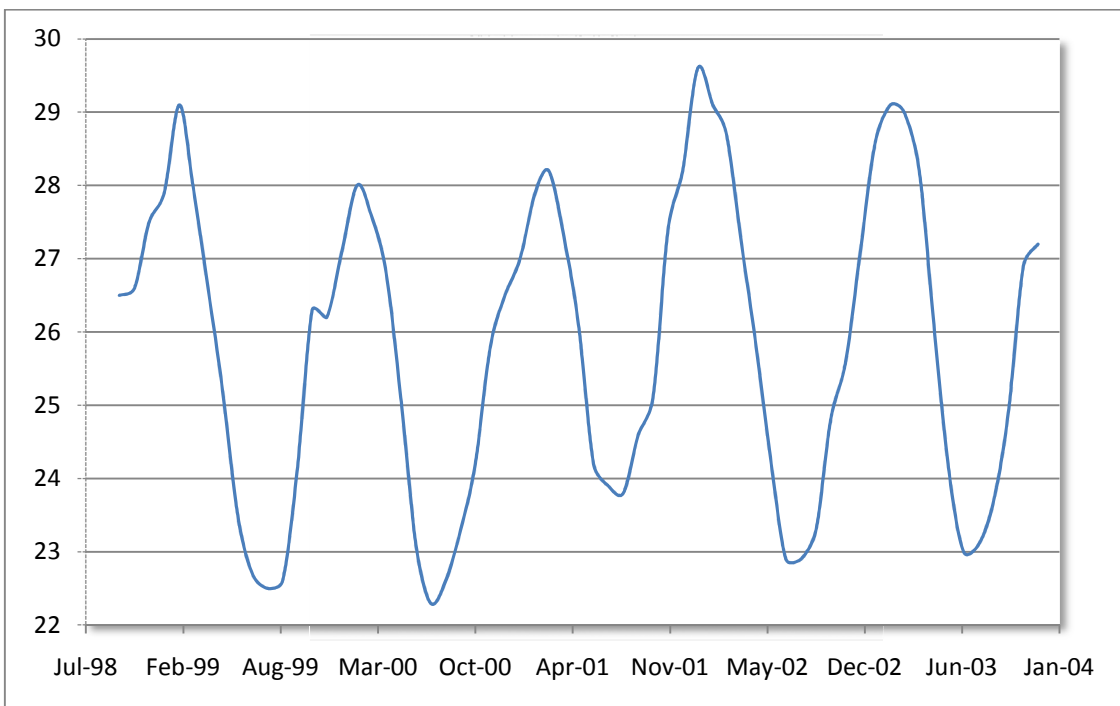
Figure 3.6: Averaged approximate sea-surface temperature for Lucinda jetty.

3.1.3 Radiation and heat balance in the littoral

The heat balance of a coastal environment is important as it is this that establishes sea and land breezes. These breezes interact with the general weather pattern and alter the wind in the coastal area. The wind combined with the heat exchange process and oceanic currents determine the sea surface temperature. The wind is vital in mixing the saturated air close to the sea's surface so that a duct can form. The wind also causes waves, which affect radio-wave reflection. Strong winds cause breaking waves which leave a significant amount of suspended sea water, in the form of sea-spray, in the duct. This also affects radio-wave propagation particularly above 15 GHz [23].

Strong winds can also affect turbulent flow in a body of water producing cold upwelling thus changing the sea surface temperature in small areas. All of these effects combine to form either a stable, a neutral or an unstable atmosphere immediately above the sea. Ducts generally form mainly in stable atmospheric conditions, i.e. the air immediately above the sea is cooler than that higher up.

Heat input and output must be in equilibrium; that is they must balance. To achieve this, the sum of all sources must equal the sum of all sinks. That is continuity must be satisfied in an adiabatic system.

In the meso-scale this is not necessarily true as large scale weather events mean that heat can be moved in or out of the system being studied, in this case the tropical littoral environment. These systems are not truly adiabatic and for a small area continuity is not satisfied.

In the general case:

$$Q_r = Q_e + Q_s + Q_v + Q_t \qquad\qquad (3.1)$$

where Q_r is the net heat gain from radiation, Q_e is the heat lost through evaporation, Q_s is the heat lost through conduction, Q_v is heat transported by ocean currents and Q_t is the storage of heat by the ocean. This is a time dependent variable.

Note that Q_r is the heat radiated into the atmosphere from a number of sources including short-wave radiation from the sun and sea (not present at night) and long-wave radiation from land and sea.

3.1.4   Land and sea breeze systems in the littoral

The presence of the coastline in the hot tropics produces a major and sudden contrast in temperature, humidity, wind, aerodynamic roughness and fumigation levels. This is further complicated in our case by the presence of several significant islands close to shore and a very large island very close to shore. We need one of these islands to mount our radio-array, so we shall forgive them for being there and ignore their effect on the local weather (The largest, Hinchinbrook Island is responsible for dramatically changing the weather towards the inland, but we are working far enough to the south and over water to avoid this phenomenon).

For sea breeze circulation to develop, a temperature difference between land and sea is needed. We shall call these T_L and T_S respectively. So a sea breeze will occur when

$T_L - T_S > 0$. So the sea breeze should continue and increase in intensity until
$T_L - T_S = 0$. This is the intuitive case and ignores friction.

However due to friction the maximum sea breeze intensity occurs somewhat before this [19]. This is because some force, derived from a positive temperature difference, is required to overcome friction.

Let us now briefly explore a generalised model for the land/sea breeze system around Lucinda, adapted from [19] using data gathered by James Cook University by this group and in [24].   The map shown in Fig 6.11 or a general map of the area would prove useful as a reference.

    a) At 6:00 am, the sea is still warmer than the land and so the land breeze is still blowing. The land breeze is altered around Hinchinbrook Island but generally stable to the south. The breeze rises near the Palm Island Group forming offshore cumulus. The land breeze is drier than the air over the sea but because

of the tropical nature of the coast and the predominance of sugar cane crops, the moisture content is still quite high.

b) By noon, the land is warmer than the sea. At the coast, the sea breeze now predominates. Further inland the land breeze is still evident and at the convergence point the sea breeze is forced aloft resulting in cumulus clouds at about 1500 feet. The sea breeze is still moderate in terms of speed and occasionally gusts due to blockage by Hinchinbrook Island resulting in the land breeze 'escaping'.

c) By 15:00 hours the sea breeze is fully developed and blows at about 10 – 15 knots. Depending on the geostrophic winds, more cumulus could form between 20 and 40 kilometres inland resulting in afternoon showers. Hinchinbrook Island causes uplifting at the coast resulting is the formation of cloud and possibly showers in the channel to the North West.

d) At around 7:00 pm the land has begun to cool but the sun still shines. Cumulus prevails over the land and the wind strength is easing to around 10 knots. Hinchinbrook still has a cloud cover.

e) By 10:00 pm the sun has set, the sea breeze predominates but is slackening.

f) At midnight the sea breeze is still evident but is now light and due to other effects, variable.

g) By around 3:00 am a lull develops where the sea breeze and land breeze cancel around the coast.

h) At 5:00 am the land breeze has developed but due to the tropical agricultural nature of the land east of the coast it is not strong rarely exceeding 10 knots unless helped by geostrophic wind.

3.2   Waves and wind

The wind causes waves to develop. For a Gaussian Rough Surface the mean power reflection coefficient is given by [15, pp 111]

$$R_S = e^{-\Delta\phi^2}$$ (3.4)

So, for a 1-metre sea with an angle of incidence of 0.2 degrees waves would be reflected with a loss of 13.4 dB. Of course the sea is complex so this figure would be highly variable in time.

The area around Lucinda is reasonably protected and thus wave heights of below 1 metre can be expected on most days. However we can expect a loss of around 10 -12 dB from reflections from a 0.5 - 1-metre high sea. Reflections from a rough surface also introduce angular changes in the propagating wave although the duct itself acts as an angular filter. We still need to understand the angular spectrum presented to the duct so we can understand what we see across the receiver array. It is important therefore to understand wave formation and shape under various wind conditions if any simulations are to be accurate.

The sea's surface is made up of a number of different wave structures mixed together. In our area these comprise mainly the oceanic swell, which is not well developed in most cases because of the nearby Great Barrier Reef, and chop caused by local winds. This chop is variable as it is affected significantly by the land-sea breeze system. When a land breeze blows the sea in our area of interest is protected.

Bottom depth is relatively constant at around 40 metres between Lucinda and Orpheus although it is very shallow at each end of the radio path. At the points where we can expect significant reflection from the sea surface the depth is constant. This is not the case for the long path experiments however we shall assume a constant sea dept here as well for simplicity.

Finally it is useful to recall the Beaufort Wind Scale shown in Table 3.1 and its observations on wave height and to compare these with our derived expectation of duct formation. It should be remembered that duct formation is only probable in stable or

neutral conditions and so the comments on duct formation in the table assume this. It is also our experience (see Figure 4.5) that in strong rain the duct also collapses. In the tropical north this is often associated with micro-bursts of rain and wind from large cumulus clouds over the sea.

Table 3.1: The Beaufort scale and comments on ducts.

Beaufort Number	Description	Wind speed ms^{-1}	Wind speed Knots	Sea state	Duct comments
0	Calm	<0.6	<1	Mirror like	No duct
1	Light air	0.7 – 2.3	1-3	Ripples	Low Unstable Duct
2	Light breeze	2.4 – 4.4	4 - 6	Small wavelets	Low Duct possible
3	Gentle breeze	4.5 – 6.6	7 - 10	Larger wavelets, some crests break	Medium height Duct forms
4	Moderate breeze	6.7 – 8.9	11 - 16	Small waves, frequent white crests	High Duct
5	Fresh breeze	9.0 – 11.3	17 - 21	Moderate waves. White crests. Some spray.	High Duct
6	Strong breeze	11.4 – 13.8	22 - 27	Large waves. Many crests. Spray.	Unstable High Duct. Height reduces.
7	Near gale	13.9 – 16.4	28 - 33	Sea heaps up. Many crests. Much spray.	Duct collapses.
8	Gale	16.5 – 19.0	34 - 40	Moderately high waves, all cresting. Much spray.	No Duct.

3.3   Conclusions

The area around Lucinda is an area strongly influenced by the land/sea breeze processes. With a tropical hinterland close to the shore, but a hot dry inland within 100 km, these interactions can be quite strong. The presence of the Palm group of islands and particularly Hinchinbrook Island has a strong influence on local weather. Localised sea surface temperatures can be high and regularly exceed the air temperature above them. Thus in the SBL the atmosphere can become locally unstable [19] which as we will discuss later and in Babin [28] can result in errors in estimating duct heights.

Our measurements in this area and in the Coral Sea, where sea surface temperatures can be higher (see Figure 3.4) are important as they are direct measurements which give an indication of duct height estimation accuracy in this region.

3.4   References

[19]   Hsu, A.S., "Coastal Meteorology", Academic Press, 1988.

[20]   "Sea Breeze Formation", Bureau of Meteorology, Australia.

[21]   Ruggles, K.W., "The vertical mean wind profile over the ocean for light to moderate winds", J Applied Meteorology, 9, 389-395, 1970.

[22]   "Sea Surface temperatures for the Region of Interest", http://www.cpc.noaa.gov/products/analysis_monitoring/enso_update/sstanim.shtml

[23]   Nathanson, "Radar Design Principles", McGraw Hill, Second Edition, 1991.

[24]   Harvey, A., "Real Time Monitoring and Short-Term Forecasting of Maritime Weather", Masters Thesis, James Cook University, March 2001.

Chapter 4
Meteorological measurement and prediction techniques

In this chapter I present an overview of research on the meteorology of duct formation and our prediction techniques for the tropical littoral. The results of research on duct formation in the tropical littoral and temperate oceans are presented in this chapter giving results from our meteorological measurements using buoys with associated sensors. As a result of this work three research conference papers have been published.

```
┌─────────────────────────────────────────────────────────────┐
│         ┌───────────────────────────────────────┐           │
│         │              Chapter 1                 │           │
│         │        Introduction and Thesis format  │           │
│         └───────────────────────────────────────┘           │
│                          │                                   │
│         ┌───────────────────────────────────────┐           │
│         │              Chapter 2                 │           │
│         │ Microwave propagation, measurement and │           │
│         │              simulation                │           │
│         └───────────────────────────────────────┘           │
│                          │                                   │
│         ┌───────────────────────────────────────┐           │
│         │              Chapter 3                 │           │
│         │ Radio-meteorology and the tropical     │           │
│         │        littoral zone under study       │           │
│         └───────────────────────────────────────┘           │
│                          │                                   │
│         ┌───────────────────────────────────────┐           │
│         │              Chapter 4                 │           │
│         │ Meteorological measurement and         │           │
│         │        prediction techniques           │           │
│         └───────────────────────────────────────┘           │
│                          │                                   │
│         ┌───────────────────────────────────────┐           │
│         │              Chapter 5                 │           │
│         │ Propagation simulation in a duct using │           │
│         │ TERPEM and AREPS and observations      │           │
│         │ supporting the accuracy of these models│           │
│         └───────────────────────────────────────┘           │
│                          │                                   │
│         ┌───────────────────────────────────────┐           │
│         │              Chapter 6                 │           │
│         │ Some observations of over the horizon  │           │
│         │ microwave radio propagation inside the │           │
│         │ tropical maritime evaporation duct in  │           │
│         │ North Queensland, Australia            │           │
│         └───────────────────────────────────────┘           │
```

Chapter 1
Introduction and Thesis format

Chapter 2
Microwave propagation, measurement and simulation

Chapter 3
Radio-meteorology and the tropical littoral zone under study

Chapter 4
Meteorological measurement and prediction techniques

Chapter 5
Propagation simulation in a duct using TERPEM and AREPS and observations supporting the accuracy of these models

Chapter 6
Some observations of over the horizon microwave radio propagation inside the tropical maritime evaporation duct in North Queensland, Australia

Chapter 7
The evaporation duct as an angular filter

Chapter 8
Short range propagation experiments, conclusions and results

Chapter 9
Methods for extracting angle of arrival and duct heights

Chapter 11
A theoretical design for long range over ocean microwave links using the tropical evaporation duct

Annex 1
Informing the Military Community

Chapter 10
Mathematical methods for measuring angle of arrival in over ocean propagation experiments

Annex 2
Implications for designers of fixed services utilising over water paths

Chapter 12
Research and Thesis conclusions

4.1 Introduction

Measurements of refractivity profiles close to the sea surface have been undertaken in several experimental campaigns around the Australian coastal waters and also in the Coral Sea and Western Pacific Ocean. The measurements were made over a wide range of climates and locations, from temperate southern regions to warm equatorial waters. This Thesis presents evaporation duct height statistics for each region showing in some cases the trends between the seasons.

The data set is representative of the climatic variations around the Australian region and shows the prominence of the evaporation duct during clear-air conditions. The effects of evaporation ducts on terrestrial or very low grazing angle Earth-space links are important because they provide a mechanism for extended propagation and for multipath, which in turn can create interference with other services. Furthermore, knowledge of the shape of refractivity profiles is important when assessing the effects of the troposphere on radio-wave propagation and is necessary in any calculation of quantities associated with ducting such as critical elevation angle and minimum trapping frequencies. The duct height is the most important parameter as it indicates the refractive strength of the duct and the refractivity profile can be inferred from this parameter. This data was submitted to the new ITU-R Study Group 3 evaporation duct data banks.

During our research around 200 hours of measurements of refractivity profiles close to the sea surface were undertaken in several experimental campaigns around the Australian coastal waters and also in the Coral Sea and Western Pacific Ocean. The measurements were made over a wide range of climates and locations, from temperate southern regions to warm equatorial waters. In this chapter we present evaporation duct height statistics for each region showing in some cases the trends between the seasons. The data set collected is representative of the climatic variations around the Australian region and shows the prominence of the evaporation duct during clear-air conditions.

4.2   A summary of duct height statistics

Several experimental campaigns aimed at monitoring the structure of the evaporation duct were jointly carried by the Defence Science and Technology Organisation (DSTO) and the James Cook University of North Queensland at a few locations along the Australian coastline and also in the Coral Sea and Pacific Ocean in 1998, 1999 and 2000. Around 200 hours of usable buoy data was collected during this period. The locations and dates of the campaigns are summarised in Table 4.1.

The purpose of these experiments was to investigate the meso-scale variations that occur in the evaporation duct structure. As a result, effort was placed in detailed measurements in a few locations rather than sparse measurements over a wider area. As the buoys were in areas of high coastal ship traffic the buoys could be left for extended periods, however some night time measurements were taken close to the jetty and at sea when we were comfortable there was no risk to boats and the buoys could be lit.

Evaporation ducts, as the name suggests and as explained in the theory, form as a result of the removal of water vapour from a wet surface. These ducts are therefore prominent in the maritime environment and knowledge of their structure is important when considering propagation links between islands or along coastlines, radar systems used for navigation or collision avoidance or even certain space-Earth links that traverse the ocean or a substantial body of water.

To determine effect on each of these systems operating inside or near the duct an accurate specification of the profile is important for obtaining good propagation predictions as propagation effects are sensitive to changes in the refractive index profile.

This is demonstrated in the two coverage diagrams in Figure 4.1, derived from the AREPS model (2001) which show signal path loss due to a 12 GHz transmitter positioned at 20 metres above ground level for two extremes in duct height, 8.5m and 28m, observed during one of the Coral Sea experiments.

Table 4.1: A summary of experimental campaigns.

Location of Experiment	Data Availability (months)	Approx Data Collected.	Distance from Land (km)
Equatorial Western Pacific	January, February		300
Coral Sea A	May	12 Hrs	
Coral Sea B	May	12 Hrs	
Coral Sea C	May	12 Hrs	
Lucinda & Palm Islands, Nth Qld	March, April, July, September, October, November	120 Hrs	6 – 10
Gulf of St Vincent, South Australia	January	12 Hrs	10

All measurements made during these campaigns were carried out using instrumented buoys which housed up to six sets of meteorological sensors up to a height of 7 metres above sea level. The refractive index at each sensor position was determined and a least squares fit was performed, assuming a log–linear refractivity model in order to estimate the duct height [25] [26]. Other models are available as outlined in [27] and [28] and these may be equally as suitable. We chose the log-linear model because it gives us good agreement with signal strength predictions that have been obtained around Australia [29]. The diversity in duct height distributions due to seasonal and geographical changes is evident from Figure 4.2 where the percentage of time that a given duct height is exceeded, is plotted as a function of duct height. Three examples are given:

1. The equatorial regions of the Western Pacific Ocean,
2. The sea around Lucinda (West Pacific),
3. The Coral Sea. All around distances centred on Cooktown. Coral Sea A, Osprey Reef 200km NE 13°55', 146° 50' Coral Sea B, Parke Reef, 100 km due north 14° 25', 145° 27' and Coral Sea C, unanchored in open sea around 150 km NE at 14° 15', 146° 15'.
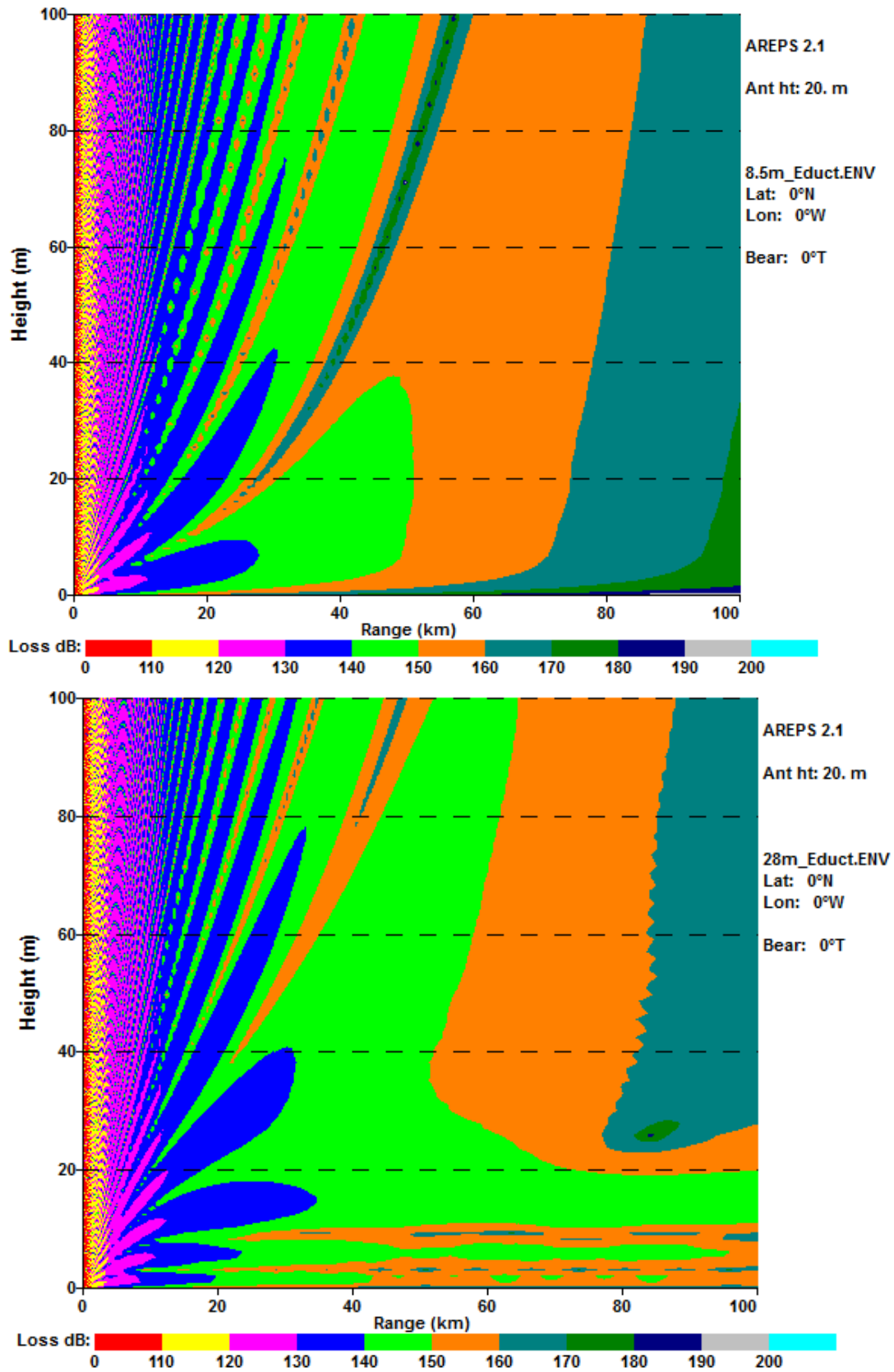
Figure 4.1: Coverage diagrams for two duct heights: 8.5 metres (top), 28 metres (bottom). Transmitter freq. 12GHz, ht = 20m.
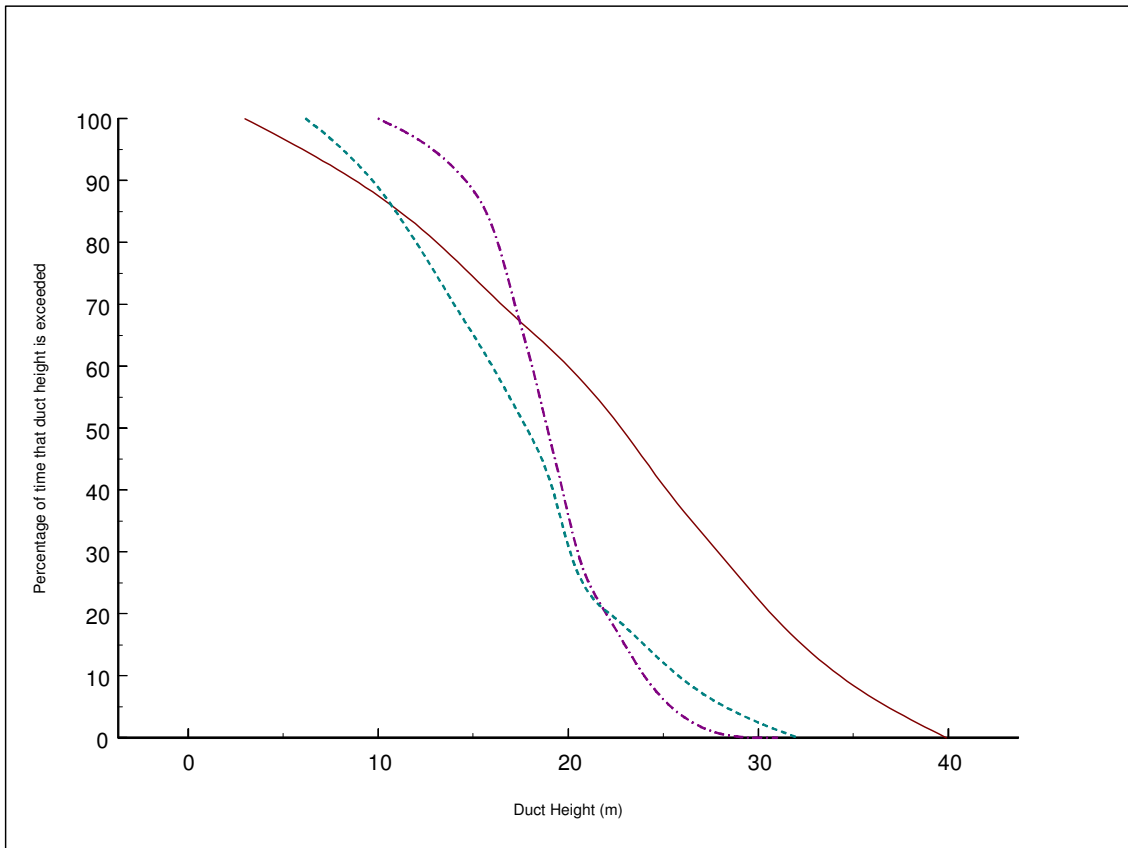
Figure 4.2: The percentage of time that a given duct height is exceeded is plotted here as a function of duct height for three different regions.

The graphs are based on 168 hours of data collection from various locations over a ten month period taken at a sampling rate of one sample per 12 seconds. The campaign dates and durations are outlined in Table 4.1 above.

The solid curve is for the equatorial West Pacific in February, the purple, dashes and dots curve is for the Coral Sea in May and the pale blue, dashed curve is for the coastal region around Lucinda, Queensland in October.

In the warm waters of the Equatorial Pacific Ocean, evaporation ducts are high. During February, sea surface temperatures can be as high as 30°C which is sufficient to cause free convection to take place. At times large ducts are formed and these are destroyed at the onset of precipitation caused by the small rain cells which are continuously forming during the day. The atmospheric conditions in the Coral Sea in May are more stable and hence the range in duct heights is less extreme. Moderate geostrophic winds caused by

the presence of high pressure cells located farther south maintain ducting conditions over large areas. Some diurnal variations in the duct height do occur. Along the coast of Australia, the sea surface temperature is slightly cooler in October than the Equatorial Western Pacific. However there is a greater variation in duct height over a diurnal cycle. This variation is due to a larger variation in the sea surface temperature as well as the formation of local sea breeze and land breeze circulations. From our measurements there is now sufficient empirical evidence to show that the development of the evaporation duct is correlated to the development of meso-scale circulations such as the sea breeze. Figure 4.3 shows an example of the growth of the evaporation duct as the sea breeze develops. This data is from an experiment carried out in the Gulf of St. Vincent, near Adelaide, South Australia, in January 1999 [30].
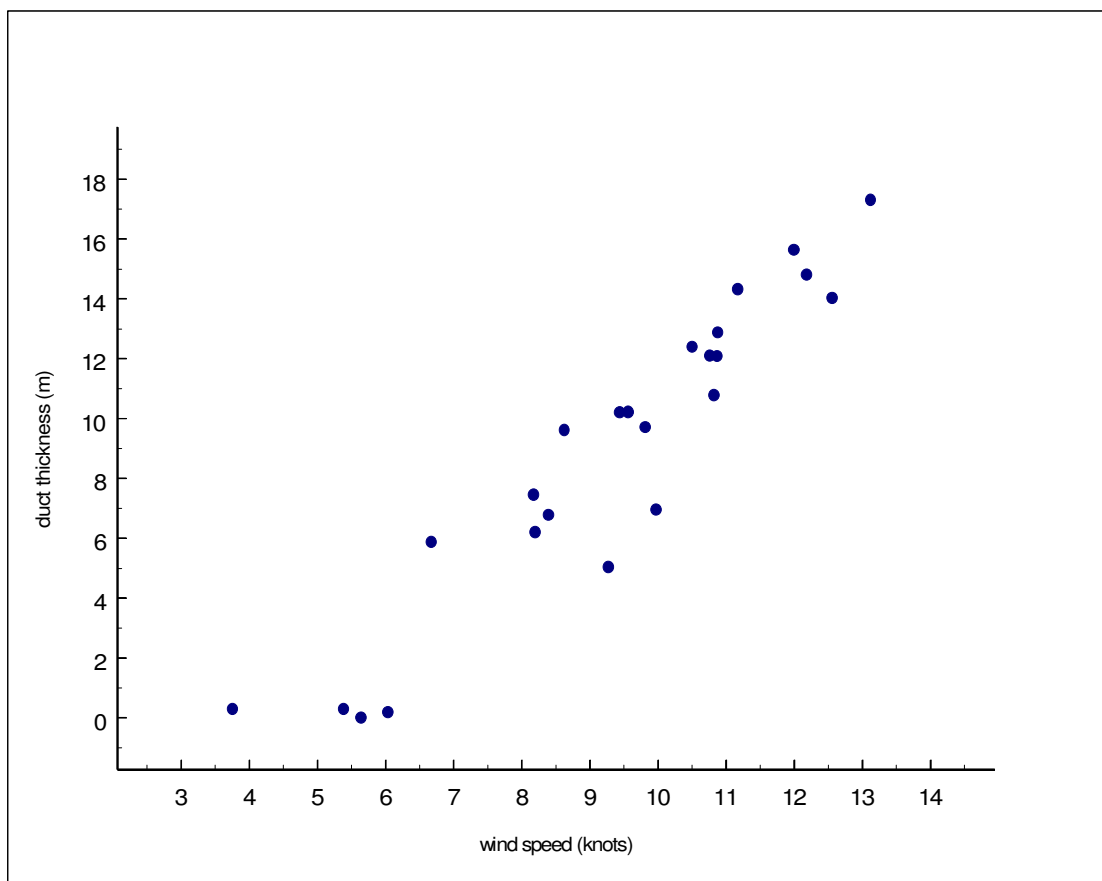
Figure 4.3: The relationship between windspeed and evaporation duct height, as measured by DSTO researchers in the Gulf of St. Vincent, South Australia [30].

Figure 4.4 shows data for stronger wind speeds showing that as the wind speed reached 20 knots the duct reached its upper limit and at higher wind speeds began to collapse.

Similar data exist for tropical regions in North Queensland [31]. This result is interesting as the altitude profile for the refractive index structure parameter depends on duct height as well [32] [33]. The relationship is given as

$$C_n^2(h) \propto d^2 h^{-\frac{2}{3}}$$
(4.1)

where h is the height above sea level, d is the duct height and C_n is the refractive index structure parameter which can be measured from an aircraft.
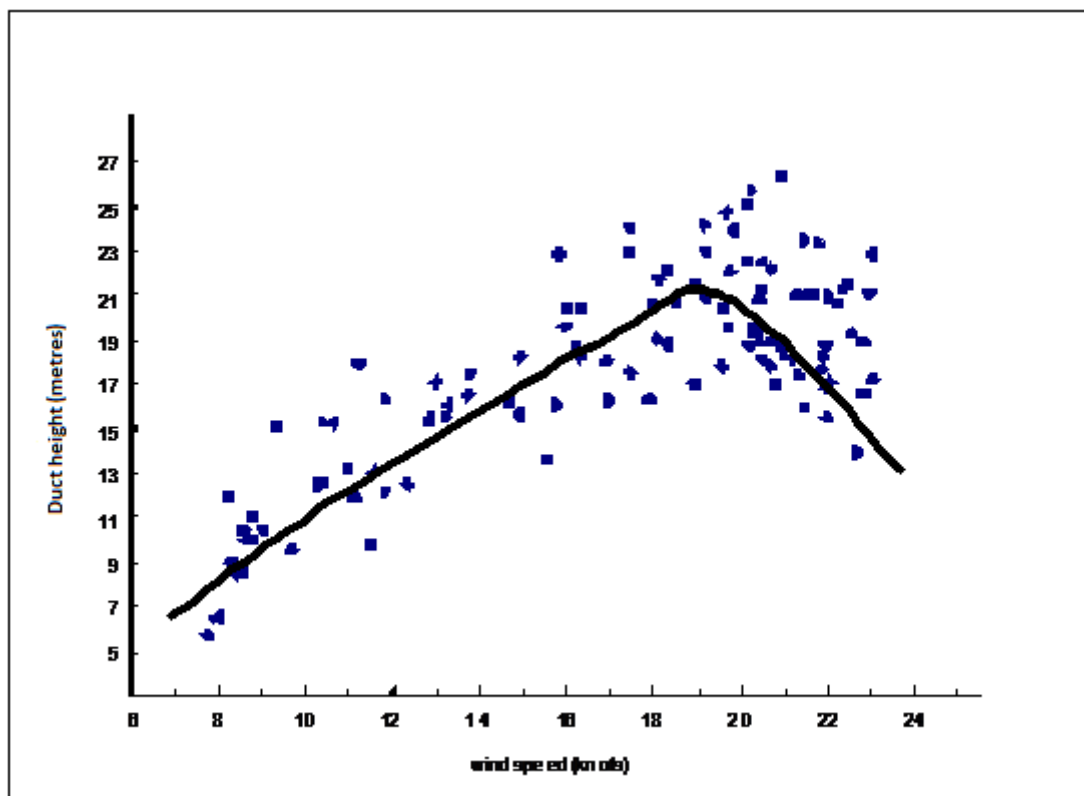
Figure 4.4: Duct height versus wind speed is plotted here from data measured in the Gulf of St Vincent on 10th January 1999 [30].

These results, taken in conjunction with Equation 4.1 suggest, in particular, a direct relationship between C_n^2, surface wind speed and duct height. This is not surprising, considering that wind shear plays a major role in generating vortices within the convective boundary layer. An analysis of data from the US Air Force Geophysics Lab [34] has indicated that C_n^2 increases with wind speed until around 5 m/s is reached, and tends to decrease with further increase in wind speed. This effect may be associated with a relationship between C_n^2 and mixing. Thus C_n^2 is less at higher wind speeds, where the ducting profile degenerates. The measurement data reported in Figure 4.3 suggests an approximately linear increase in C_n^2 with wind speed up to about 6 m/sec, (11.7 knots) which is consistent with the above findings.

4.3   Duct height changes with distance

As a result of experience gained during these measurements we postulated that duct heights would change with distance due to localised differences in wind speed, air and sea surface temperature and perhaps humidity. To determine the correlation function for this we towed two similar measuring buoys apart and compiled a graph showing the correlation function with height.

Figure 4.5 shows this correlation function. This is provided for information only as it relates to just a few measurements over one period, it does however show that a duct varied with both time, as we previously proved, and also with distance.

The reader's attention is also drawn to Figure 6.24, which shows a temporal variation of duct height at one position. This variation would not be the same in time at different locations and would lead to correlation errors.

In addition micro meteorological differences such as minute changes in temperature and humidity around a sensor would cause differences. The reader is now referred to Figure 5.12, a photograph of the two measuring devices. One is a spar buoy designed to not influence the sensors, the towed array is a raft. Heating of the raft deck and floats in sunlight is likely to cause heat eddies around the sensors leading to error.
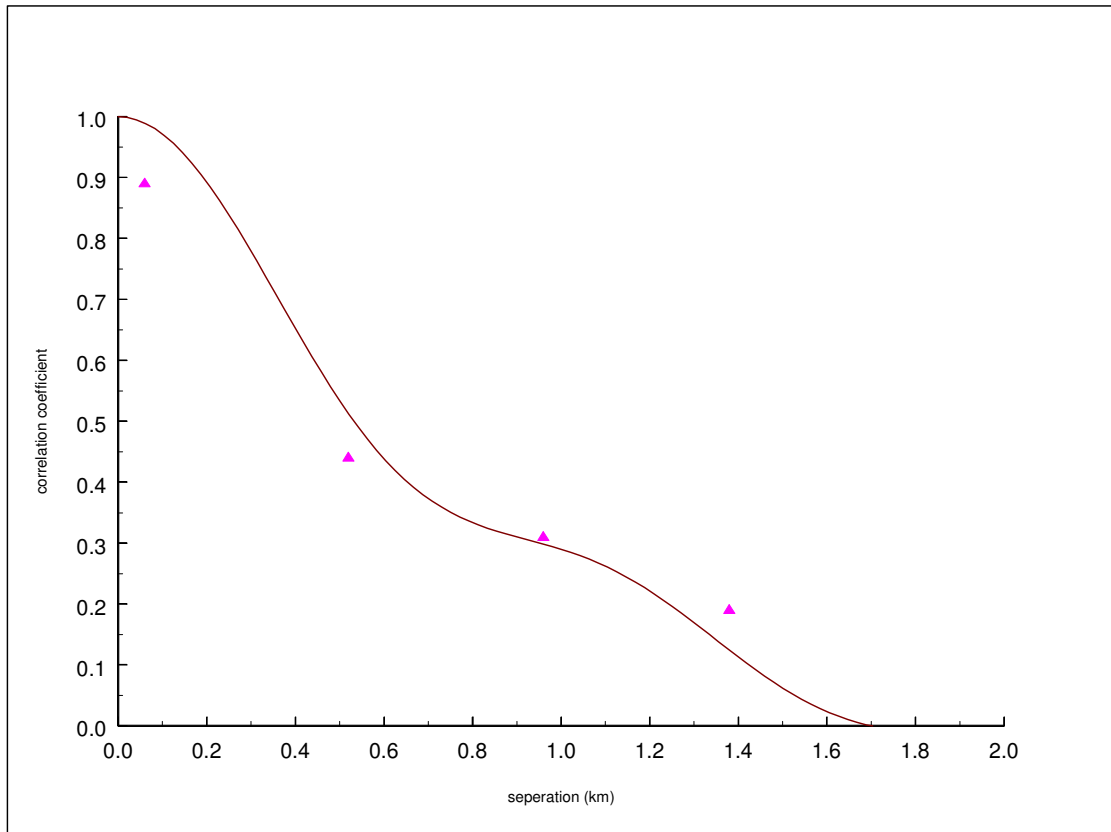
Figure 4.5: Correlation of duct height with distance.

The box drawn on Figure 8.2 demonstrates the area over which the measurements were made. The area is the feint red box drawn from the shore to the north of the sugar loading jetty, to the east the then back to shore south of the jetty. With these explanations I present the results.

4.4   Associated International Telecommunications Union (ITU) work

The International Telecommunications Union, Radiocommunications Sector (ITU-R) comprises various Study Groups which each study a particular group of topics. On it's website (www.itu.int), the ITU-R defines the role and responsibilities of each of it's Study Groups.

ITU-R Study Group 3 (SG-3) concentrates on propagation of radio waves in ionized and non-ionized media and the characteristics of radio noise, for the purpose of improving radiocommunication systems.

The following four Working Parties (WP) carry out studies on the Questions assigned to Study Group 3:

- WP 3J – Propagation fundamentals
- WP 3K – Point-to-area propagation
- WP 3L – Ionospheric propagation and radio noise
- WP 3M – Point-to-point and Earth-space propagation

The principal aim of the Working Parties is to draft Recommendations in the ITU-R P Series for subsequent adoption by Study Group 3 and approval by the Member States. The Working Parties also develop Handbooks that provide descriptive and tutorial material, especially useful for developing countries. A further task of the Working Parties is to provide, through Study Group 3, propagation information and advice to other ITU-R Study Groups in their preparation of the technical bases for Radiocommunication Conferences.

Such information typically concerns identifying relevant propagation effects and mechanisms and providing propagation prediction methods. The predictions are needed for the design and operation of radiocommunication systems and services and also for the assessment of frequency sharing between them.

The results of this work were submitted to the International Telecommunications Union Study Group Three (Propagation) WP-3J (propagation fundamentals) for inclusion in their ducting database. As this is an unusual way to report work (in the academic sense) a copy on the paper, referred to as an Input Document, is attached at the end on this chapter. This work was presented at the meeting of SG-3, WP-3J in Fortaleza, Brazil during October 2003.

4.5   Possible errors and their effect

All measurements are subject to errors, especially those in a variable radio environment. In our measurements a number of errors are possible inherent the measuring equipment and on its effect on the atmosphere in the case of our micro-meteorological measurements. Those relating to sensor error were minimised through careful

calibration of each sensor before it was assembled and launched. However humidity sensors are particularly susceptible to calibration drift when deployed. To minimise this each was recalibrated on retrieval and over the short duration missions however no discernable drift was found. In both buoy designs temperature and humidity sensors were combined in a shaded sensor package and a number of these were mounted on a mast, this configuration can be seen in Figure 5.11 where both buoys are shown.

Other errors could be caused by temperature and thus relative humidity changes in the micro-scale. These are shown as rapid fluctuations in our recorded data and are removed by smoothing over time. These would be restricted to a few metres (around two) assuming they would not have affected all sensors at once.

Of our two buoys one was built using a mesh platform and floats. This could cause temperature eddies when warmed in the sun, and from fluctuations in the recorded data these could be as much as 5 degrees Celsius in the lower sensor package. A 5 degree temperature error could produce errors in refractive index at height (dN/dh) of up to 25 units at 100% relative humidity which is significant in terms of our work.

Generally though even these errors are of short time duration and out smoothing technique would reduce their overall effect on our findings. In addition the raft buoy was only used during measurements where two buoys were needed; the majority of measurements were taken from the spar buoy to reduce error.

The spar buoy did not have any platform to heat and errors here were within the calibration of errors of 0.1C and 2% RH for a total error of around 5 N units depending on T and R.H. Pressure and sea surface temperature were also measured from the spar buoy with errors in the range of 1%. However pressure does not have a great influence on refractivity and sea surface temperature errors have only a small effect on some calculations. Thus errors inherent in the spar buoy system are much less significant.

Finally, our technique for estimating duct height relies on curve fitting. It is possible that the duct does not fit the curve exactly leading to small errors in duct height of approximately one metre. This could only be resolved via the use of larger, more expensive buoys.

4.6 References, papers and acknowledgements

4.6.1 Acknowledgements

4.6.2 Published papers

The following papers were published as a result of this research:

Kerans, A.J., Kulessa, A.S., Hermann, J. and Woods, G. S., "Evaporation Duct Statistics Around Australia and the West Pacific", AP2000 Millennium Conference on Antennas & Propagation, Davos – Switzerland, 9-14 April 2000.

Kerans, A.J., Kulessa, A.S., Woods, G.S., French, G. and Lensson, E., "Remote Sensing of Radio Refractive Atmospheric Effects in Northern Australia", Workshop on Applications of Radio Science (WARS'02), University of Technology, Sydney, 21-22 February 2002.

Kerans, A.J., Kulessa, A.S., Woods, G.S., French, G. and Lensson, E., "Remote sensing of radio refractive atmospheric effects in Northern Australia", Antennas and Propagation Society International Symposium, 2002, IEEE, Volume: 3, pp. 692- 695, August 2002, ISBN: 0-7803-7330-8.

4.6.3 References

[25] Hitney, H. V. and Vieth, R., "Statistical assessment of evaporation duct propagation," IEEE Transactions on Antennas & Propagation, vol. 38, pp. 794- 798, 1990.

[26] Früchtenicht, H. W., "Notes on duct influences on line-of-sight propagation", IEEE Transactions on Antennas & Propagation, Vol. 22, pp295-302, 1974.

[27] Christophe, F., Douchin, N., Hurtaud, Y., Dion, D., Makaruschka, R., Heemskerk, H. and Anderson, K., "Overview of NATO/AC 243/Panel 3 Activities concerning radiowave propagation in coastal environments", AGARD-CP-567, pp27-1- 27-9, 1995.

[28] Babin, S. M., Young, G.S. and Carton, J.A., "A new model of the oceanic evaporation duct", Journal of Applied Meteorology, Vol. 36, No. 3, pp 193-204, March 1997.

[29] Kulessa, A. S., Woods, G. S. and Heron, M. L., "SHF propagation in the tropical evaporation duct", unpublished, 1999.

[30] Hermann, J. A. and Kulessa, A.S., "Assessment of the role of signal fluctuations and refractive structures in microwave systems performance", DSTO Research Report, 1999, not publicly available.

[31] Kulessa, A. S., Heron, M. L. and Woods, G. S., "Temporal variations in evaporation duct heights", Proceedings of Workshop on Radio Science 1997 (WARS 97), National Committee for Radio Science, Australian Academy of Science, pp165-170, 1997.

[32] Gossard, E. E., "Clear weather meteorological effects on propagation at frequencies above 1GHz", Radio Science, vol.16, pp589-608, 1981.

[33] Levy, M. F. and Craig, K. H., "Millimetre wave propagation in the evaporation duct", Proceedings of AGARD conference no. 454: Atmospheric propagation in the UV, visible, IR and mm-wave region and related systems aspects, pp26-1 to 26-10, 1990.

[34] Ryzner, E. and Bartlo, J. A., "Dependence of C_n^2 and C_T^2 in the atmospheric boundary layer on conventional meteorological parameters", U.S. Airforce Geophysical Laboratory, Report no. AFGL-TR-86-0013, 1986.

Attached is the input to the ITU-R Study Group 3 resulting from this work. It is attached here as it is an unusual method of publishing academic work and not easily referenced or accessed.

Australia

PROPOSED DRAFT MODIFICATION OF RECOMMENDATION
ITU-R P.452

Evaporation ducting in the tropical littoral

1   Introduction

Much work has been done in Australia in recent times on the prevalence of evaporation ducts above warm tropical oceans. Australia has submitted data to the SG-3 database on ducting. We have found that an evaporation duct is generally present over a warm tropical ocean any time there is sufficient wind to mix the saturated layer at the oceans surface. Rec. P-452-10 provides a method for calculating the prevalence of a duct based on information in other references. We find that this method may underestimate duct prevalence in the tropical littoral.

2   Summary of findings

A number of experimental campaigns have been carried out over the past 5 years and the findings reported in the literature. Figure one below presents data from one group of experiments. Later data is currently being analysed and thus far supports the first set.

In Figure One the duct height statistics in the tropical littoral is shown as the centre (at the top or bottom of the graph) dotted curve. These heights were determined from instrumented buoy data. We can combine both this, measured RF and simulated RF to determine that a duct will form over tropical littoral oceans in nearly all circumstances where there is some wind.

The percentage of time that a given duct height is exceeded is plotted here as a function of duct height for three different regions. The solid curve is for the equatorial West Pacific in February (Far left at 100%), the dashes and dots, curve is for the Coral Sea in May (Far right at 100%) and the dotted, curve is for the coastal region around Lucinda, Queensland in October (Centre at 100%).
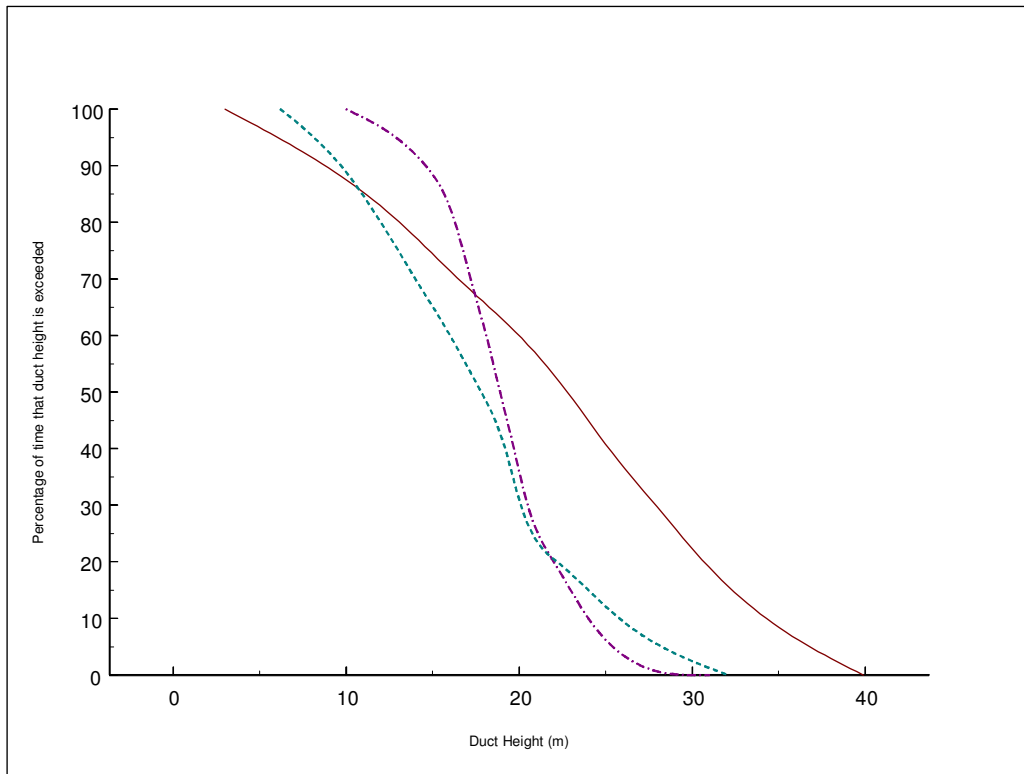
Figure One.
Duct height distribution in the Australian tropical littoral.

From these curves we can deduce that a duct will be present at a height of 10 metres or greater for about 90% of the time in the areas and times measured. The 50 percentile duct height appears to be at around 20 metres. Recent data from May 2001 is still being analysed supports these findings.

3   Proposal

Recent ITU studies resulted in a modification of footnotes 5.502 and 5.503 in the band 13.75 – 14 GHz. Studies indicated that it is possible for VSAT earth Stations to share with maritime radars in the band. Continued studies are needed to determine how

close to the coast VSATs may come in the case of 'thin' administrations such as Vietnam.

Australia is concerned the effect of evaporation ducts has not been fully taken into account in that the prevalence of ducting is underestimated.

Australia suggests the following be added to Rec. P-452. Considering X:

"That the prevalence of evaporative ducting over tropical waters is not yet fully understood.

Recommends Y. That for sharing studies over tropical waters a duct with a height of between 10 and 20 metres be considered present at all times."

4   Further work

Australia suggests further work be undertaken on duct prevalence over all oceans and that the outcome of this work be included in Rec P-452 at a later date.

Chapter 5

Propagation simulation in a duct using TERPEM and AREPS and observations supporting the accuracy of these models

The PEM models AREPS and TERPEM are investigated in this chapter. The chapter looks at a 'standard atmosphere' using these models, then explores propagation inside the duct and finally makes observations on model accuracy based on actual measurements combined with our local knowledge of ducting in the area.

```
┌─────────────────────────────────────────────────────────────┐
│                                                             │
│   ┌──────────────────────────────────────────┐             │
│   │            Chapter 1                      │             │
│   │   Introduction and Thesis format          │             │
│   └──────────────────────────────────────────┘             │
│                        │                                    │
│   ┌──────────────────────────────────────────┐             │
│   │            Chapter 2                      │             │
│   │ Microwave propagation, measurement and    │             │
│   │            simulation                     │             │
│   └──────────────────────────────────────────┘             │
│                        │                                    │
│   ┌──────────────────────────────────────────┐             │
│   │            Chapter 3                      │             │
│   │ Radio-meteorology and the tropical        │             │
│   │      littoral zone under study            │             │
│   └──────────────────────────────────────────┘             │
│                        │                                    │
│   ┌──────────────────────────────────────────┐             │
│   │            Chapter 4                      │             │
│   │ Meteorological measurement and            │             │
│   │      prediction techniques                │             │
│   └──────────────────────────────────────────┘             │
│                        │                                    │
│   ┌══════════════════════════════════════════┐             │
│   ║            Chapter 5                      ║             │
│   ║ Propagation simulation in a duct using    ║             │
│   ║ TERPEM and AREPS and observations         ║             │
│   ║ supporting the accuracy of these models   ║             │
│   └══════════════════════════════════════════┘             │
└─────────────────────────────────────────────────────────────┘
```

Chapter 6
Some observations of over the horizon microwave radio propagation inside the tropical maritime evaporation duct in North Queensland, Australia

Chapter 7
The evaporation duct as an angular filter

Chapter 8
Short range propagation experiments, conclusions and results

Chapter 9
Methods for extracting angle of arrival and duct heights

Chapter 11
A theoretical design for long range over ocean microwave links using the tropical evaporation duct

Annex 1
Informing the Military Community

Chapter 10
Mathematical methods for measuring angle of arrival in over ocean propagation experiments

Annex 2
Implications for designers of fixed services utilising over water paths

Chapter 12
Research and Thesis conclusions

In 1985, R. A. Paulus published a paper in Radio Science Vol 20 No. 4 "Practical application of an evaporation duct model" [35]. This paper represents the first of the models used to represent ducts and can be considered the forerunner of the models used in this work and the work of Babin [39]. The Paulus work is the basis for the finding by Babin that cutting ducts off at 40 metres was an erroneous way to treat them. Paulus concluded that the occurrence of ducts above 40 metres was due to stable atmospheric layers at those heights. Babin argued that this does not hold in all cases. Our work has shown that even in an unstable MBL it is very rare for ducts to occur above 40 metres (see Figure 4.2).

The Paulus model is perhaps the most widely used in early researched being incorporated into an early model called the Integrated Refractive Effects Prediction System (IREPS; the predecessor of AREPS). This model was later modified using input from Jeske [36] to correct errors at low altitudes. This modified model was used extensively in early US Navy models such as IREPS and early AREPS. A major limitation of these models is that they do not allow a duct height higher than 40m. While we and Babin find this unlikely, it is not impossible and a model should account for that probability.

Another early model is the Musson Genon Gauthier Bruth (MGB) model which was presented in 1992 [37]. A derivative of this by Battaglia [38] is used in TERPEM.

The Babin model is presented extensively in [39] which also contains a comparison of the models described above. Table 5.1 is a brief comparison derived from [39] which shows the root mean square (RMS) error for duct heights in metres for each of the three models compared to boat data. Note though that there could also be error in Babin's boat mounted sensors which contribute to the overall error. Nonetheless this gives a good measure of the accuracy of each model.

The Babin model performs best in all cases and for others not considered here. Of interest is the sensitivity range in unstable atmospheres (warm air trapped below cool) which is a possibility in the tropical littoral.

Table 5.1: A comparison of duct height RMS errors for three models, adapted from [39].

Model	RMS Error (m)
Babin	3.0
MGB	13.1
Paulus Jeske	4.3

5.1   A standard atmosphere

In Chapter 2, section 2.3 a 'standard atmosphere' was discussed. It is useful at this point to introduce an TERPEM plot for a standard atmosphere to give the reader something with which to compare future plots. Figure 5.1 represents such a plot, a TERPEM plot of the same event is similar and does not require reproduction.

This plot represents power levels at height and distance that could be expected from transmission over 20 km in a uniform standard atmosphere.

5.2   TERPEM

The TERPEM propagation package is a tool for the forecasting and analysis of refraction, ducting and terrain effects on radio links and radar systems. It is based on a hybrid model combining parabolic equation (PEM) and ray-trace techniques. TERPEM is particularly useful in our studies as it introduces a loss caused by reflection from a rough sea based on the wind speed.

The TERPEM model propagates a radiowave from one range to the next while preserving an impedance boundary condition at the air/water interface.

TERPEM uses the Dockery and Kuttler discrete mixed transform PEM [40]. This model uses a ray-trace to work out incidence angles at the sea surface. This allows the modelling of a range-dependent impedance, allowing the modelling of electrical constants and surface roughness.
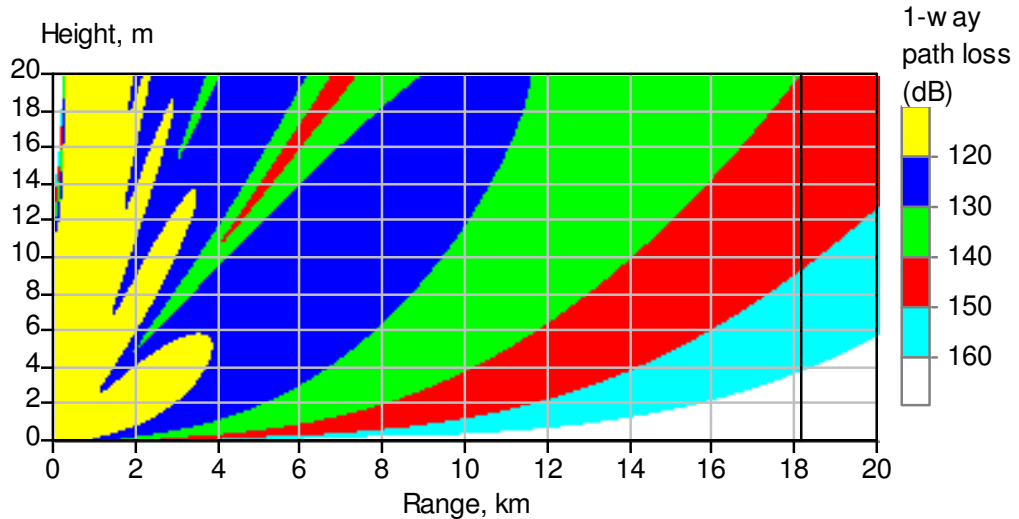
Figure 5.1: A TERPEM plot in a standard atmosphere.

For propagation over the rough sea surface, effective reflection coefficients depending on the rms wave height can be computed for a given angle of incidence. These can then be used to calibrate the mixed transform at each range. Local angles of incidence are computed using geometrical optics.

The roughness factor, which multiplies the smooth case reflection coefficient, is given by the Miller-Brown model [41].

The authors of TERPEM point out that for very rough seas, the model loses accuracy. It does provide very good results for moderate to rough seas (on the Beaufort Scale between 3 and 5. See Table 3.1), and gives a good idea of propagation performance in very rough conditions.

5.3   Using TERPEM

TERPEM uses the boundary layer model of Battaglia [38]. This model copes well with unstable conditions, when the air is cooler than the sea, and with weakly stable conditions, when the air is slightly warmer than the sea. An iterative method is used to compute the main scaling parameter, the Monin-Obukhov stability length.

The following input parameters are required to calculate the duct height:

- Sea temperature, T_{sea}
- Air temperature, T_{air}
- Relative humidity, H_{rel}
- Wind speed, V_{wind}

TERPEM allows entering these variables in a number of unit choices.

Wind speed (for duct): note that TERPEM also requires wind speed for the sea roughness calculation; different speeds can be entered for duct height calculation or roughness. Although these would normally have the same value, TERPEM allows them to be specified separately for modelling purposes, which is useful as it allows us to specify the roughness and test for each duct height.

Height of measurements: the height above the sea surface at which the air temperature, relative humidity and wind speed are measured. We have seen why this is important in Chapter 3, where we explored wind speed differences with height.

Figure 5.2 shows a plot from TERPEM over 20 km, the approximate distance from the end of the Lucinda jetty to the Orpheus Island research station. Transmitter height is five metres. The duct in this case is at 27 metres for an air temperature, T_{air} of 30°C, a sea surface temperature, T_{sea} of 26°C, relative humidity, H_{rel} of 60% and a wind speed, V_{wind} of 10 ms^{-1}.

Figure 5.3 shows a vertical slice of Figure 5.2, taken at 18.2 km. This range is significant as it is the range of the first group of experiments using the ten-element array. The interference pattern for the multi-ray propagation within the duct is evident.

This is one of the most useful outputs of TERPEM as it can be used to compare results with all of our arrays and from that determine the applicability of the package for determining propagation in the tropical evaporation duct.
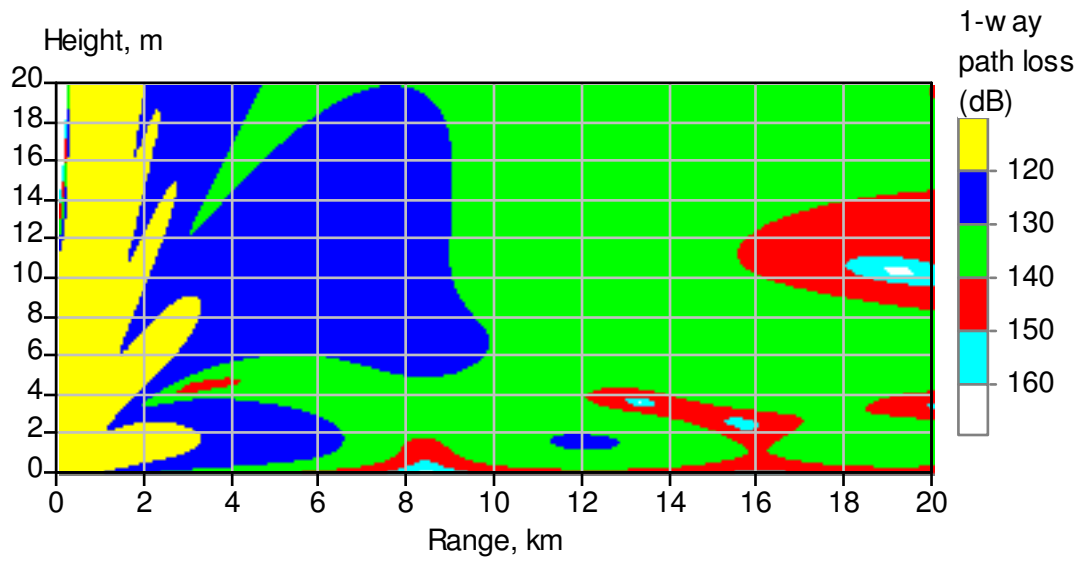
Figure 5.2: TERPEM plot of simulated path Lucinda to Orpheus.
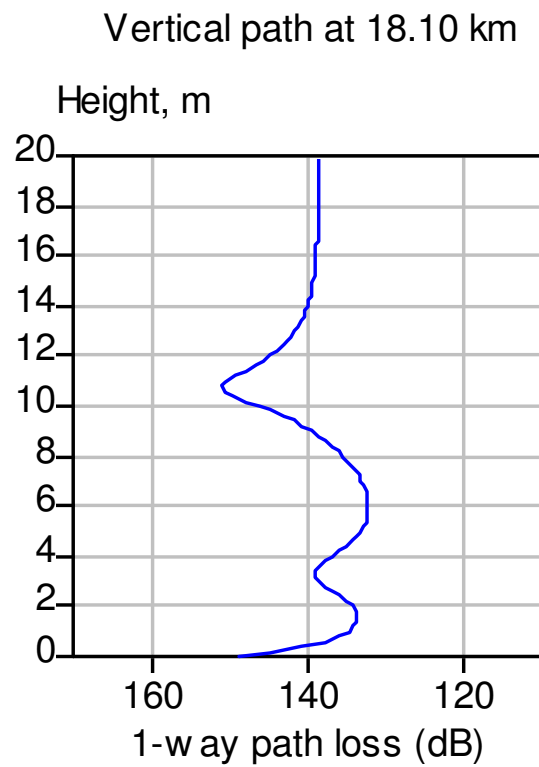
Figure 5.3: A vertical TERPEM Slice.

Another useful output from TERPEM is shown in Figure 5.4. This is the path loss for a given height. In this case, 10.4 metres has been chosen as this corresponds to a 'black hole, which is evident in Figure 5.5 at 18.5 km (It appears as a red/blue hole in that picture).

Also notable in Figure 5.4 are the interference patterns early on the path, which correspond to reflected waves from the sea surface. It can be seen that these fluctuations disappear with distance and that the overall pattern corresponds to that over a spherical path.
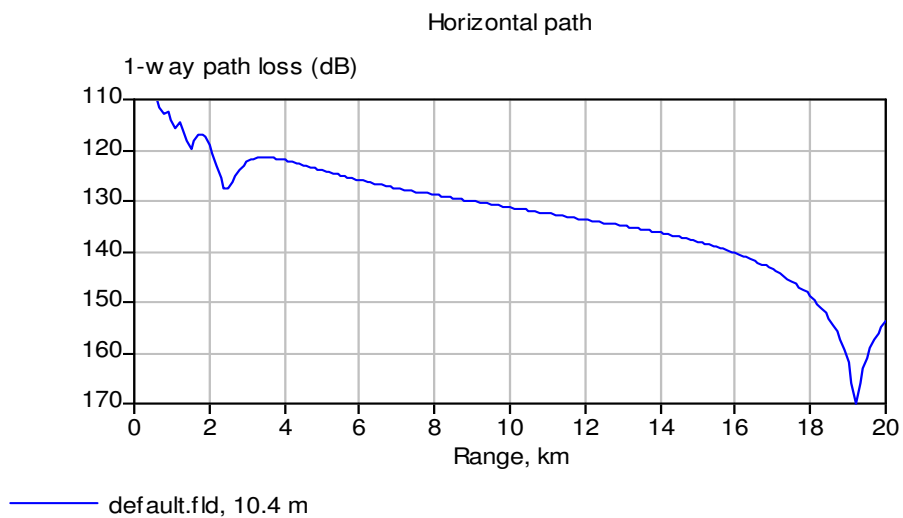
Figure 5.4: Path loss with distance from TERPEM.
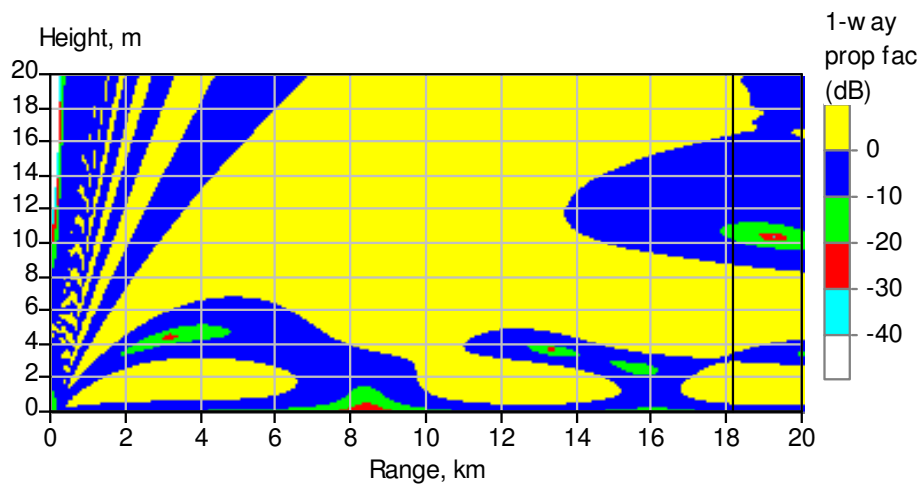
Figure 5.5: TERPEM propagation factor.

TERPEM can also produce graphs of *Propagation Factor* which is the path loss related to free space. In this diagram the yellow is path loss less than or equal to free space. Green and red are path losses exceeding free space. This is particularly useful as we can see that at 3 km range and 4.5 metres height, we have a radar black hole, no power reaches there, so no power could be reflected. At this height and range, we would normally expect successful line of sight target detection (See Figure 5.1).

Finally, to allow comparison I have included a simulation using the same parameters as before but setting the atmospheric parameters to those of a standard atmosphere in Figure 5.1. The difference in Figure 5.5 and Figure 5.1 graphically illustrate the effect on radio propagation when the evaporation duct is present.

5.4   AREPS

The Advanced Refractive Effects Prediction System (AREPS) program computes and displays a number of electromagnetic (EM) system performance tools designed to aid a tactical commander. From the perspective of this research AREPS provides a tool which predicts path loss inside ducts using a combination of the PEM and ray optics.

The most current refractive effects assessment from the US navy 'SPARWAR office' is the Advanced Refractive Environmental Prediction System (AREPS). AREPS computes basically the same refractive tactical decision aids as the previously discussed IREPS using the same refractivity models. AREPS uses a more advanced prediction model that produces more accurate predictions of ducting and propagation. The most significant advantage of AREPS is that it can produce refractive effects predictions *over land* using terrain data obtained from either the National Imagery and Mapping Agency (NIMA) or the users own sources. In addition, AREPS is able to evaluate range-dependent scenarios, and can also compute radar detection ranges for multiple bearings simultaneously. The *AREPS User's Manual,* SSC San Diego Technical Document 3028 provides a detailed description of the AREPS program.

AREPS displays path loss in two ways, as a range height diagram as shown in Figure 5.6 or as a slice as shown in Figure 5.7.
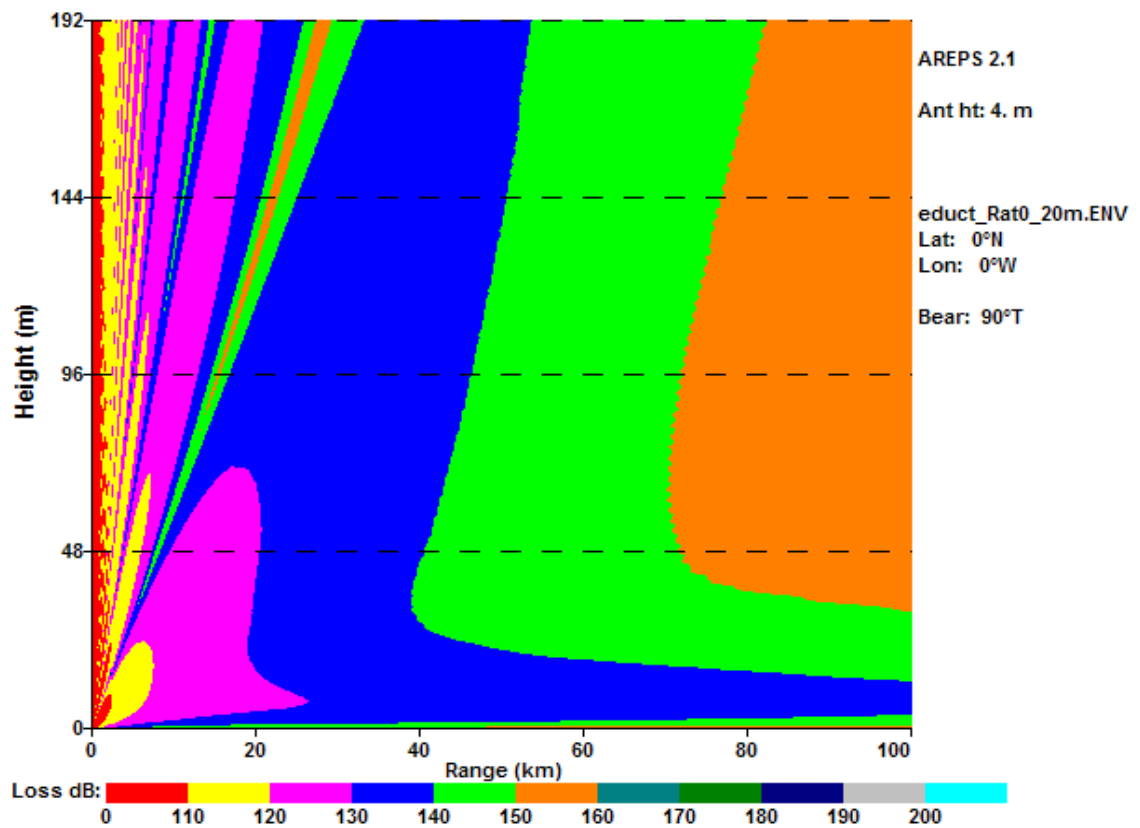
Figure 5.6: A typical AREPS range plot with duct.
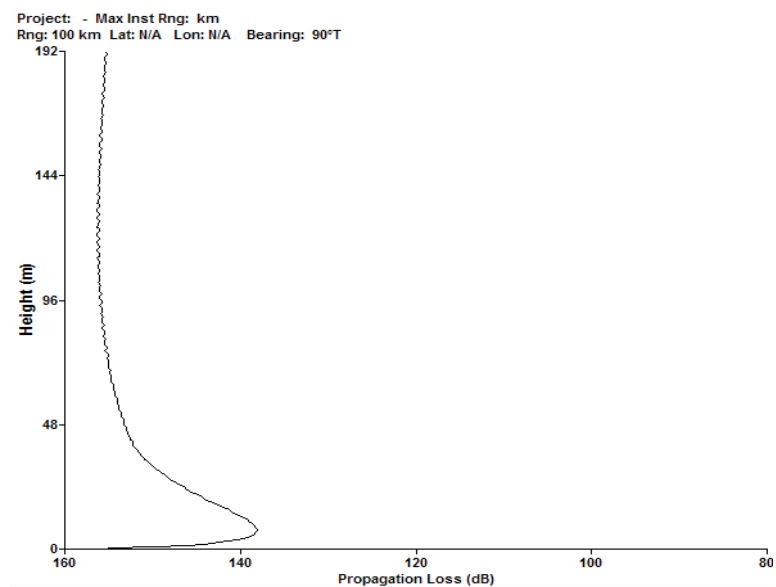
Figure 5.7: An AREPS slice plot.

Range plots are useful for determining predicted propagation loss at a given range over a specified height and give a pictorial representation of propagation due to a duct. AREPS slice plots are useful for comparing actual received signal strengths with predictions.

5.5   Comparisons between PEM models and measurements

5.5.1 Introduction

An understanding of the refractivity over oceans, which leads to the formation of the evaporation duct, is important in understanding radio wave propagation above UHF frequencies over oceans. In this section we review experimental radio propagation measurements from a tropical over-ocean link. These measurements are compared with predictions obtained from a commercially available propagation software tool using measured atmospheric parameters. The good correlation in results suggests meteorological data collected during earlier experiments can be used to draw general conclusions about microwave radio propagation in the tropical littoral environment.

The parabolic equation method (PEM) for modelling in horizontally inhomogeneous environments is well described by Barrios in [42]. These models were originally applied to acoustic modelling but the radar community, including in our research, have begun to rely on models derived from the PEM to determine anomalous propagation at radio frequencies and inside the tropical evaporation duct.

This section investigates the applicability of the two PEM packages and models under investigation to real world planning and operational scenarios. It shows that the TERPEM package is reliable for general estimation of signal strength or propagation loss in the presence of evaporation ducts and thus could be used to warn of anomalous conditions or as a tool in the design of long range overwater microwave paths.

These results thus meet one of the objectives of our research, to establish the basis upon which this modelling tool can be used to model actual propagation loss in the tropical evaporation duct.

This work also shows that given the PEM simulations can be trusted, radio-meteorology is a reasonably accurate method for the measurement of duct height.

The final part of this section explores some anomalous events, including one where we believe both an evaporation duct and an advection duct were present during our long path experiment.

The behaviour of the signal strength, whether there was an advection duct or not, reinforced our belief that the PEM based models are good tools for general modelling of propagation inside the duct, but should not (and in fact cannot) be used for real time simulations where the outcome may be critical.

Looking for a causal effect for the semi-stationary interference pattern seen in the above readings we considered a more complex trapping layer may be involved. We then noted a fire on a nearby island which was indicative of a temperature inversion.

The smoke rose to about 250 metres and then spread indicating the possibility of coastal advection and thus the formation of an advection duct. The smoke from this fire can be seen in Figure 5.8 below. In this photograph, the receiver array can be seen with Palm Island in the background. The smoke layering is obvious. Using the height of Palm Island as a reference this layer is calculated as around 250 metres.

Another AREPS environment profile was built using previously measured results for near surface atmospheric values and creating a trapping layer at around 250 metres. The results can be seen in Figures 5.9 and 5.10 below.

Comparing Figure 5.9 with its cousin, Figure 5.10, we see that the more complex, 'double trapping' atmosphere creates a more complex received signal strength in the first few metres of the atmosphere where our measurements were taken. Figure 5.9 is an approximation using the path losses above and the link budgets from the measurement system. While this is not an exact replication of the measured data, the similarity with the received levels in Figure 5.10 is obvious. Given that, in the absence of soundings, the upper air structure was 'guestimated' from visual observations. This

similarity is remarkable and points to the influence of complex atmospheric influences in such long paths.

Figure 5.8: Smoke over Palm Island.
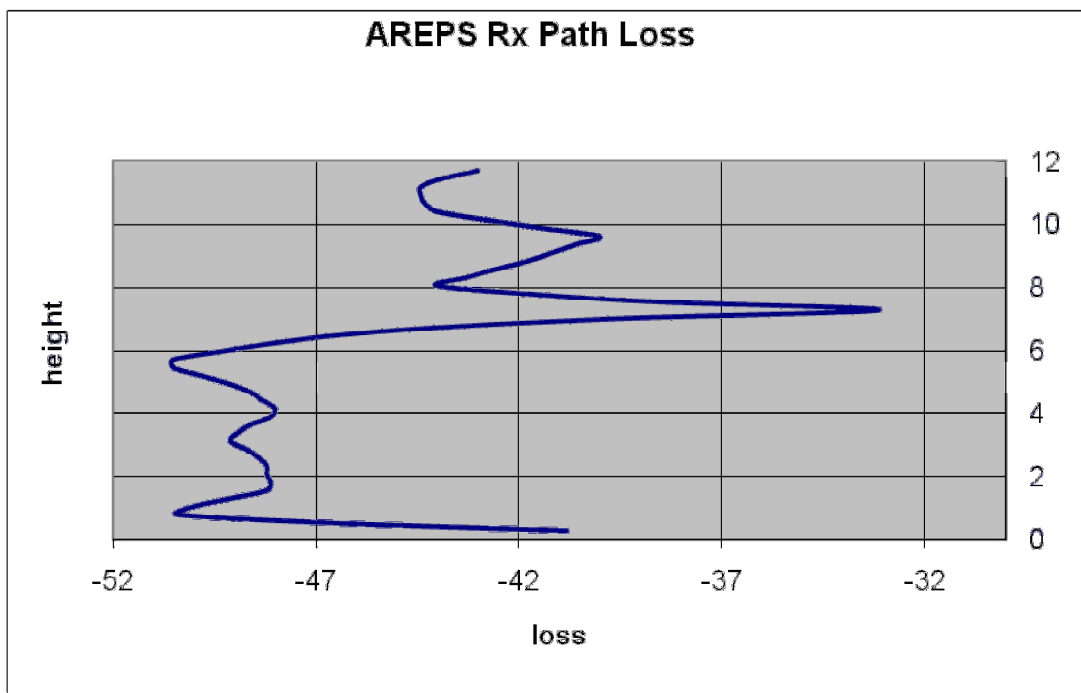
Figure 5.9: AREPS slice using a modified atmosphere.
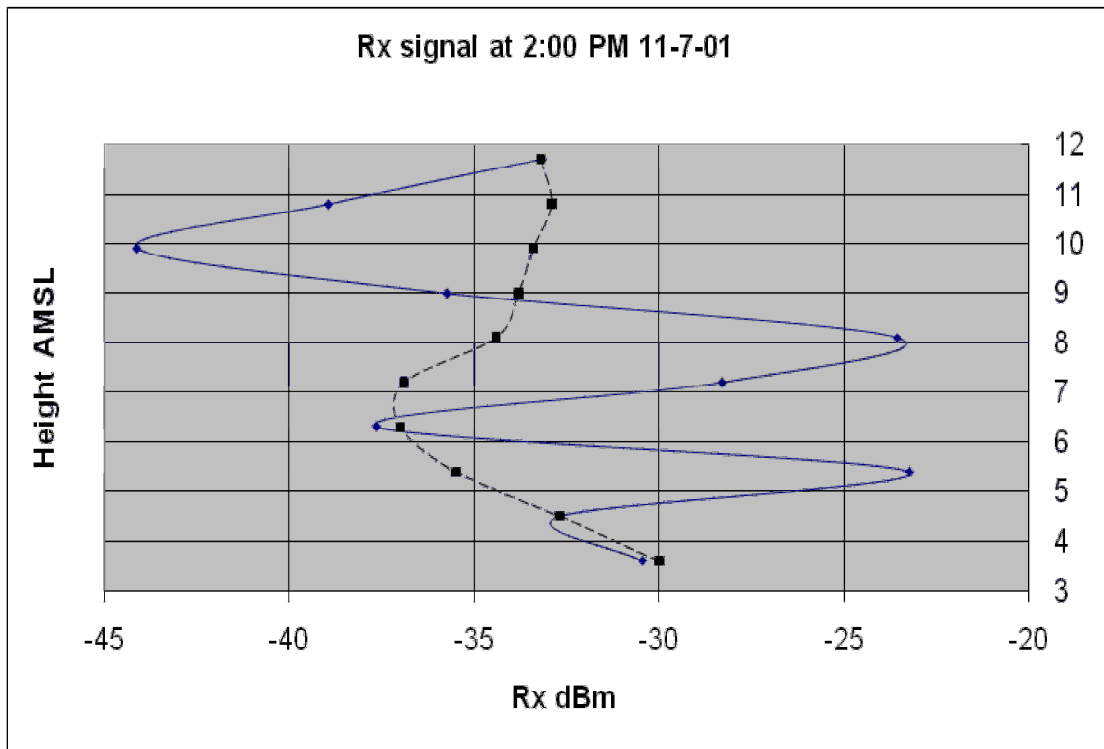
Figure 5.10: Actual RF measurements at 2:00PM (Single duct AREPS plot in black).

In order to develop a model usable for comparison, evaporation duct heights are estimated using a model based curve fit of actual data taken between 1.5 and 7 metres above the sea surface using the buoys shown in Figure 5.11. This data is plotted and compared to previous results on the probability and duration of ducting. Duct height statistics have been collected for warm tropical oceans where the boundary layer changes from stable to unstable on a diurnal basis.

At the same time, RF measurements were made at heights ranging from 3.4 to about 10 metres over an 18.2 km over water path in the same area. This data is compared to plots made from the commercial models such as TERPEM [43] and model applicability for warm tropical oceans is discussed. The use of RF data to estimate evaporation duct heights is also explored.

Figure 5.11: Buoys used to take measurements. Spar-buoy in back.

5.5.2 Why are the models important

Radio propagation above the ocean is important for radar operators, fixed link designers and ITU experts studying sharing between different systems where over water paths are present. This work examines actual radio and boundary layer meteorological measurements made in May 2001 over warm tropical waters in Far North Queensland, Australia.

5.5.3 Data collection and comparison

Both radio and meteorological data were collected during this campaign.
Meteorological data was collected using a spar buoy while radio data was collected over

an 18.2 km path using a 10.7 GHz transmitter and a ten element array comprised of slotted waveguides, commercial low-noise block converters (LNBs) and a switch box. The array is pictured in Figure 5.12.

The ten-element array consisted of ten slotted waveguide antennas built to fit commercially available Ku band LNBs. These LNBs are tuneable to either the 10.7 – 11.7 GHz or the 12.5 – 12.75 GHz satellite bands. Each array element is switched remotely and the resulting signal sampled by a spectrum analyser and stored. The transmitter was built in the 10.7 – 11.7 GHz band as this is relatively quiet (in the radio sense) in northern Australia.

The array was mounted on the Lucinda (North Queensland, Australia) Bulk Sugar Terminal jetty. This jetty extends 6.7 km out to sea giving a receiver station less subject to changes in duct structure from land influences. The transmitter was mounted on a scaffold mast at a height of 6m AMSL. The transmit system was located at the James Cook University research station on nearby Orpheus Island. Tidal differences of about +/- 1 metre in transmitter height were taken into account in the simulations.

Each RF element was calibrated against all others using a single source and the entire system was then calibrated to a standard atmosphere path loss profile.

5.5.4   Results

The spar buoy was positioned 500 metres north of the jetty, into the prevailing wind to avoid temperature and turbulence errors from the jetty structure. Data from the spar buoy was collected and analysed resulting in duct height verses time graphs, as shown below in Figures 5.13, 5.14 and 5.16. A log-linear evaporation duct model was assumed and the model duct height parameter was estimated by minimising the sum of squares between measured refractivities and model refractivities.

The data was filtered through a 5-minute window to remove rapid or anomalous changes in the readings. However the graphs still show considerable change, but the predominant duct height is readily identified in these figures.
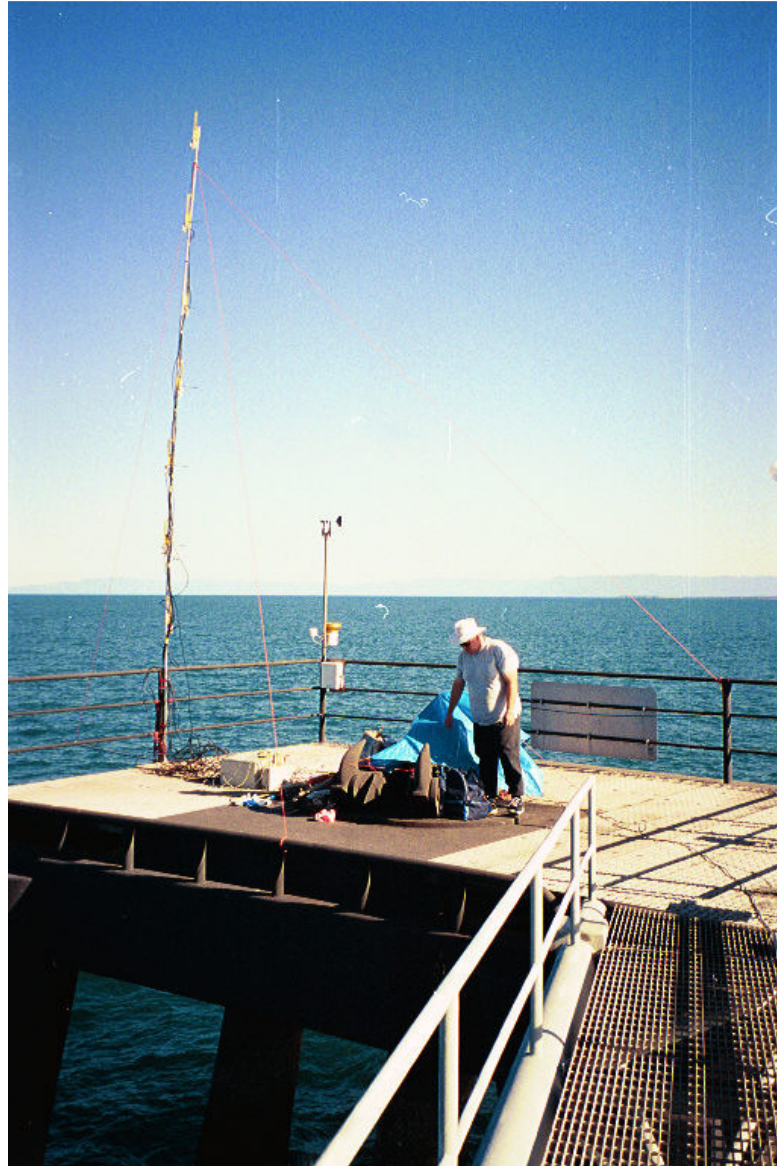
Figure 5.12: Ten-element array and weather station on jetty

Using the duct data, a time was selected and the associated RF data for that time was analysed. The RF data was averaged over a 5-minute period to remove rapid fluctuations probably due to near field reflections. The RF data was calibrated and the TERPEM standard atmosphere path loss simulation was used to calibrate path loss prediction models with measured and simulated results. While the array and associated switch equipment was carefully calibrated a variable change of about +/- 1 dB was noted through the switch box. This has been incorporated as error bars in subsequent graphs. This data and commentary is presented below.
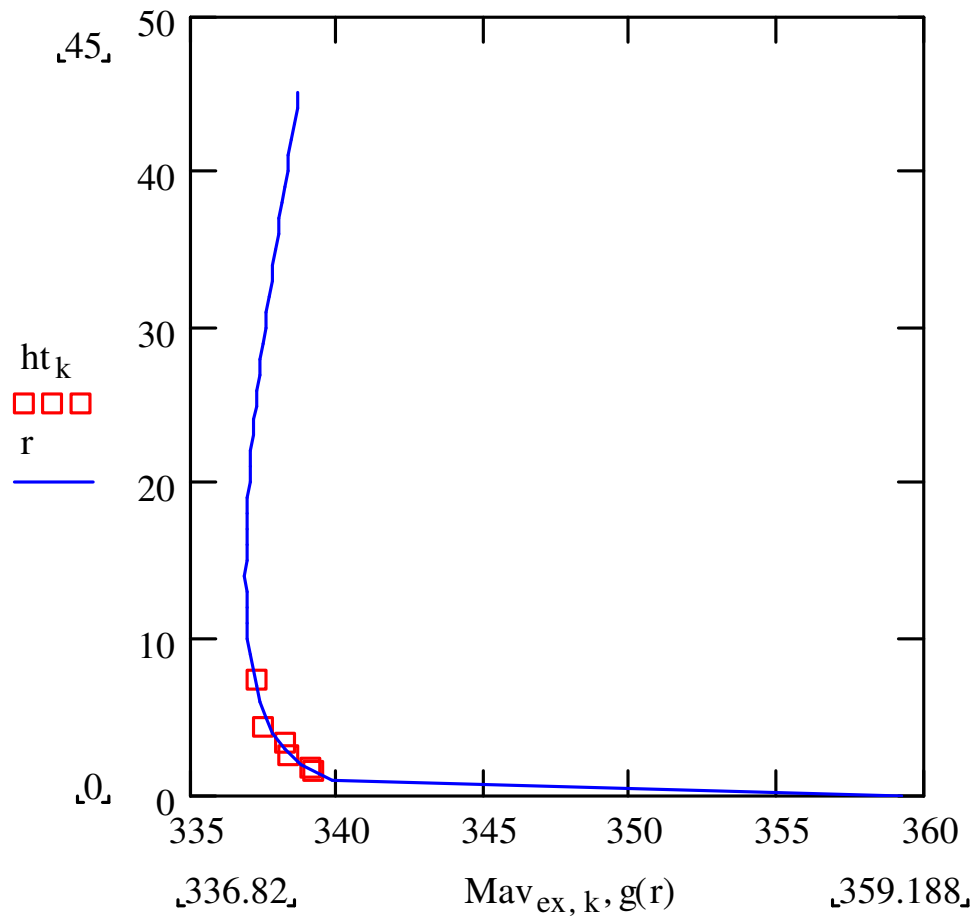
Figure 5.13: Evaporation duct, sampled data curve fit. Mav is average modified refractivity, M.
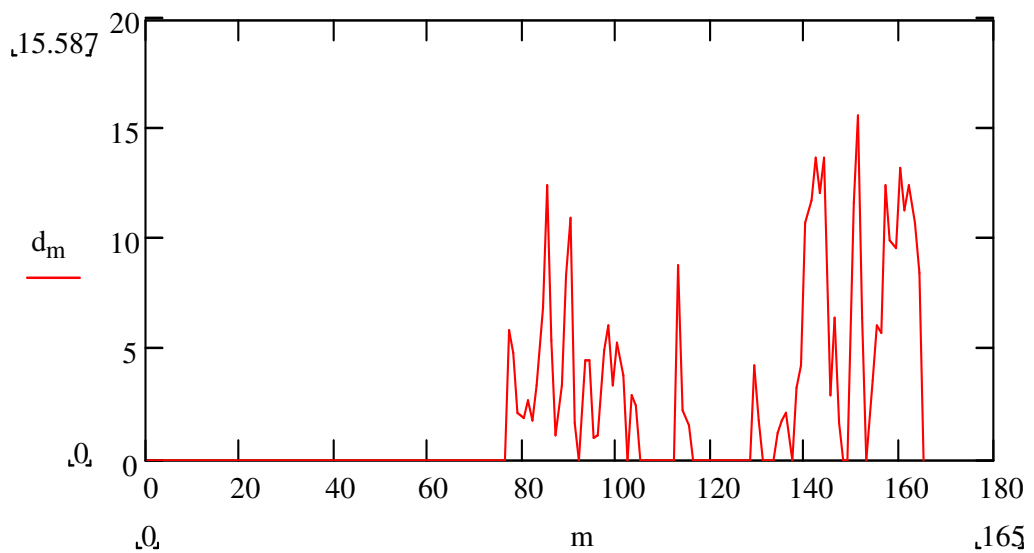
Figure 5.14: Duct heights as measured from the Spar-Buoy 14 May 10:25 – 13:10 (x-axis is minutes, y-axis is metres). Buoy starts recording at approximately 11:50 am EST.

Figure 5.14 shows duct heights measured at the beginning of the trial. Duct heights taken at these times are not accurate as the curve fit solution as used by us does not work accurately for ducts below about 10 metres as the dN/dh measured is subject to 'noise' from the errors inherent in the measurements. In addition the curve may not behave in the log linear manner described by Babin [39], further work with higher buoy masts would be required to resolve this but to build a larger spar buoy was beyond our budget.

The duct heights in Figure 5.14 should only be interpreted as giving a general indication of a low duct being present. Approximate wind speed and direction data was also obtained for conditions at the time from the Lucinda Automatic Weather Station, which are sufficient to support the ducting phenomena observed.

Wind speed from 11:00 – 14:00 EST was light and variable with a relative humidity of about 60%. Between 12:00 (95 minute mark) and 14:00 the wind picked up although it remained somewhat variable and gusty.

With little or no wind, or light wind gusts combined with the cooler sea surface temperatures, typical for the month of May, we would expect the formation of a small evaporation duct, with an average duct height of around 5 metres, based on results from previous measurement campaigns. This is what we see in Figure 5.14. The variability in the duct height estimates is quite large and can be partially explained by the gusty wind conditions observed on the day. On the other hand, a low height evaporation duct profile shows little variation in refractivity for the first few metres above mean sea level, and in fact the random errors in the individual buoy refractivity measurements may be greater than the overall trend in refractivity due to small changes in heat and humidity. Thus, both systematic and random errors in temperature and humidity may lead to some spurious duct height estimates associated with the curve fitting routine. In the case of low or rapidly varying ducts a major factor in the large dispersion of these duct height results is likely to be due to ill-conditioned curve fitting although in strong ducts this error reduces considerably as shown in Figure 5.13.

Thus in Figure 5.14 the duct appears unstable because the curve fitting technique contributes toward erroneous estimates, although we do see an average trend toward a low duct height being present.

Looking at Figure 5.15 we see a comparison of the measured path loss in the array and three simulations using the TERPEM software package. The 2.5 m simulated duct aligns almost exactly with the observed path loss and would indicate that at the time of the RF measurements a 2.5 m duct existed for a large percentage of the path.

By 16:00 EST (5 minute mark in Fig 5.16) the wind had picked up considerably being recorded at 22 kph. As expected [44] a strong and stable duct has formed as evident in the data of Figure 5.16.
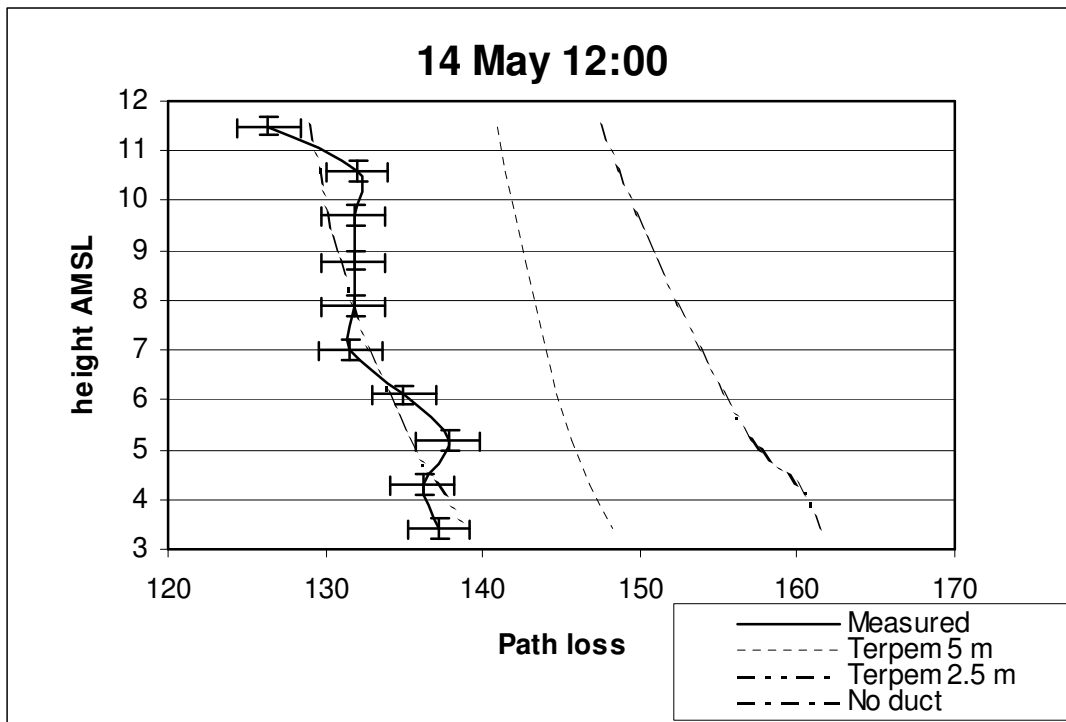
Figure 5.15: Comparison of measured path loss and TERPEM simulations for various duct heights on 14 May 2001.
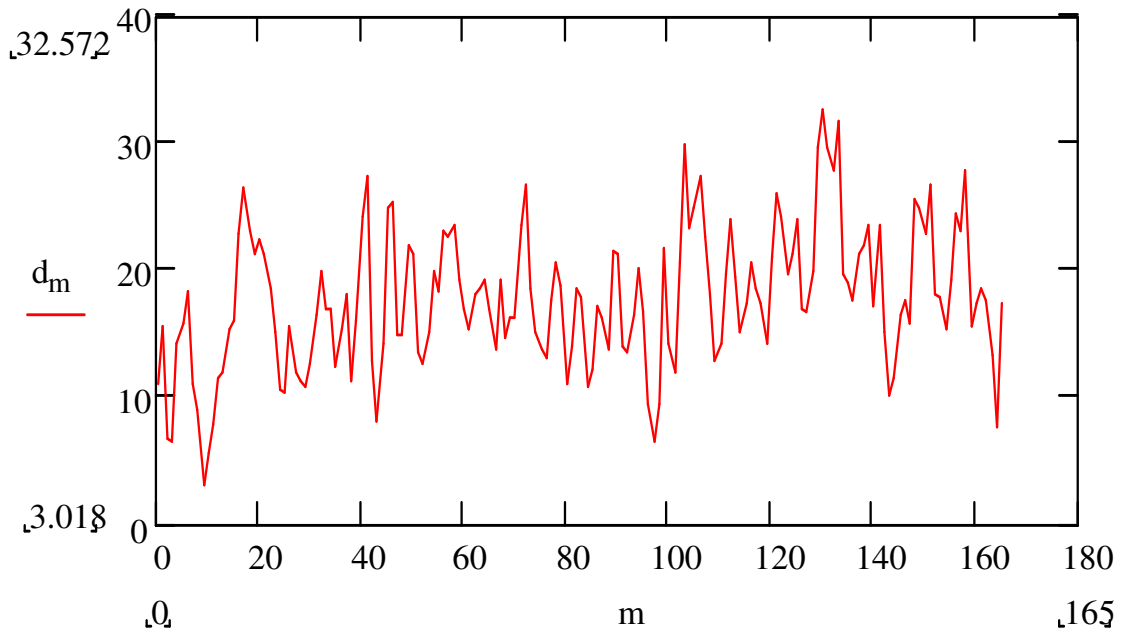
Figure 5.16: Duct heights as measured from the Spar-Buoy 14 May 2001 15:55 – 18:40.

At 17:00 (65 minute mark) an average duct height of around 15 metres was measured. This height is used to generate a TERPEM path loss simulation and these values are compared with measured RF signal levels, the results of which can be seen in Figure 5.17.

The measured results are very similar to the simulations except at low antenna heights where path losses exceed simulated losses by 2 dB with the actual predicted heights for maximum power differing by only 2 metres. This may be within the calibration error of the receive array as the array is affected by wind, however the lowest elements are held more firmly than the top elements and this difference can be seen in many other result sets, so we assume the difference is real and, as yet, unexplained. The irregularity in the measured data at 9.8 metres is a calibration error.

While these and other results are heartening, without angle of arrival information we cannot perform a secondary check on the estimated refractivity profile obtained from the spar measurements. However, with angle of arrival data, one could conceivably find a refractivity profile, so that when it is used in a ray trace, it best re-produces the measured angles of arrival.
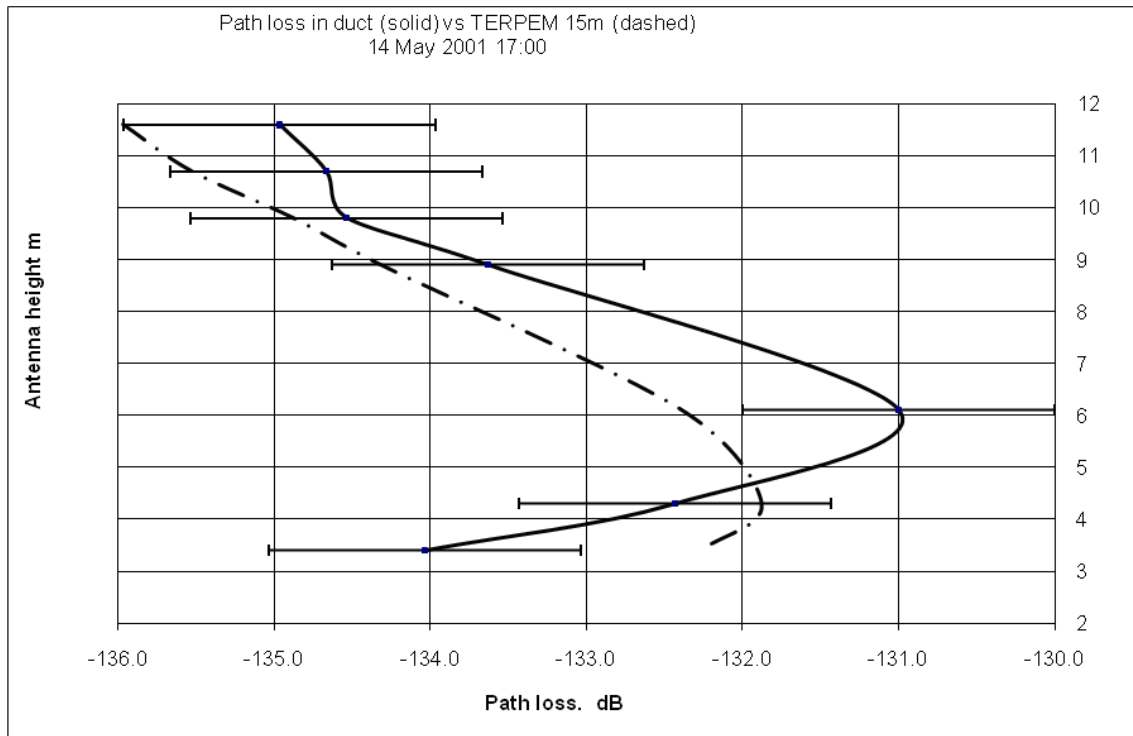
Figure 5.17: Comparison of measured values and TERPEM 15 metre duct simulation.
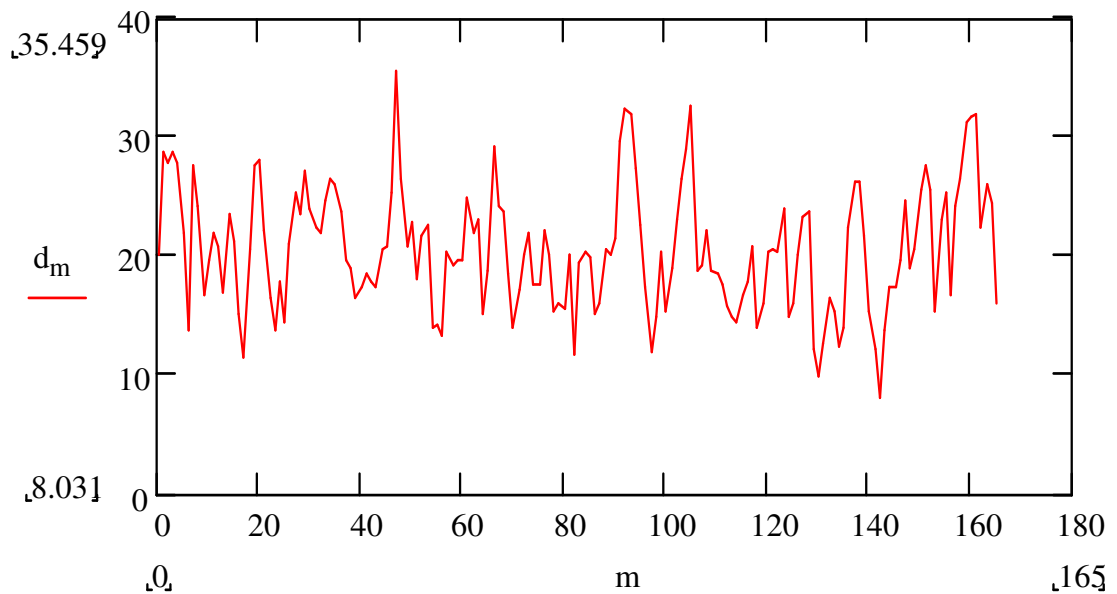
Figure 5.18: Duct heights as measured from the Spar-Buoy 14 May 2001 18:45 – 21:30.

By 20:00 (75 minute mark in Fig 5.19) the wind was about 15 kph and a strong and stable duct had formed at about 18 - 20 metres, see Figure 5.19. At exactly 20:00 the duct appears to be at around 18 metres.
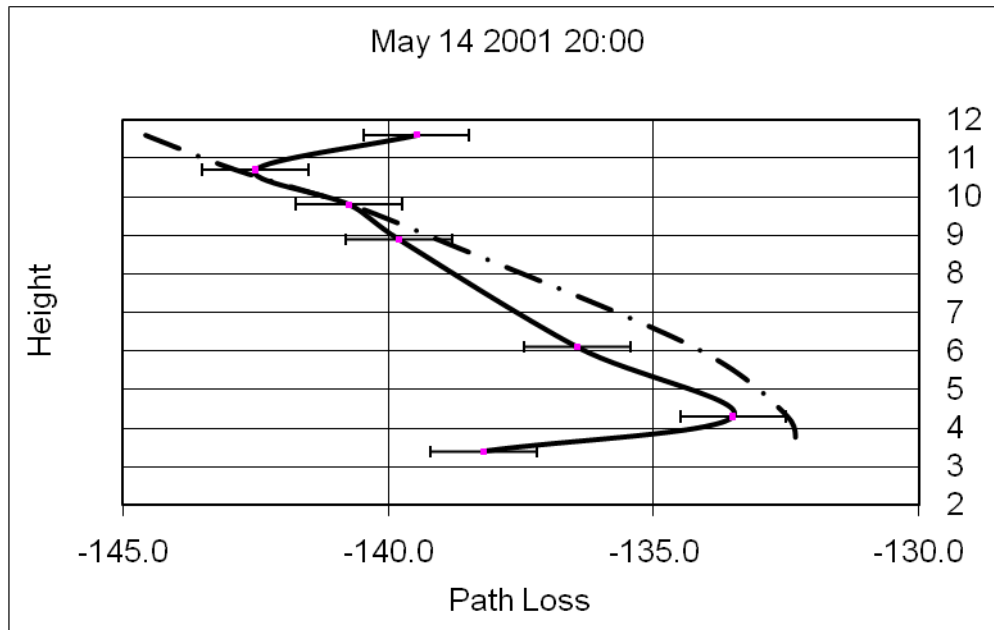
Figure 5.19: Comparison of measured values and TERPEM 18 meter duct simulation.

TERPEM was used to generate a simulated path loss for an 18 metre evaporation duct and this curve was compared to the actual received values. This comparison is evident in Figure 5.19. Again we see an unexplained difference in path loss at lower antenna heights and some difference (about 5dB) at the top of the mast. The difference in reading from the top antenna was most likely due to mast bending resulting in antenna pointing errors.

5.5.5 Duct heights in the littoral

In Chapter 4 I gave an indication of duct height expectation in the region of interest. In analysing the May 2001 data we concluded that our findings reinforce the trends measured in earlier experiments. I therefore republish Figure 4.2 showing an analysis of evaporation duct height occurrence. Furthermore, the May 2001 data can be prepared for inclusion into the SG3 data banks on evaporation ducts.

In Figure 4.2 (represented) the duct height statistics in the tropical littoral is shown as the centre (at the top or bottom of the graph) dotted curve. These heights were determined from instrumented buoy data. We can combine both this, measured RF and simulated RF to determine that a duct will form over tropical littoral oceans in nearly all circumstances where there is some wind.

5.5.6 *Implications for ITU-R studies and some concluding remarks*

ITU-R Recommendations P-452 and P-453 give us vital propagation information needed when undertaking sharing studies between existing and proposed services. A recent example is in the 13.74 – 14 GHz band where terrestrial satellite services wished to expand in a band heavily used by maritime and defence radars.

While the path models AREPS and TERPEM lead to accurate generalised path loss predictions within the evaporation duct, the actual occurrence of the duct may be underestimated in the tropical littoral zone. A comparison with Figure 4.2 (reproduced below) shows that ducts which may affect propagation occur for up to 90% of the time. This suggests more care is needed than suggested by the predictions.
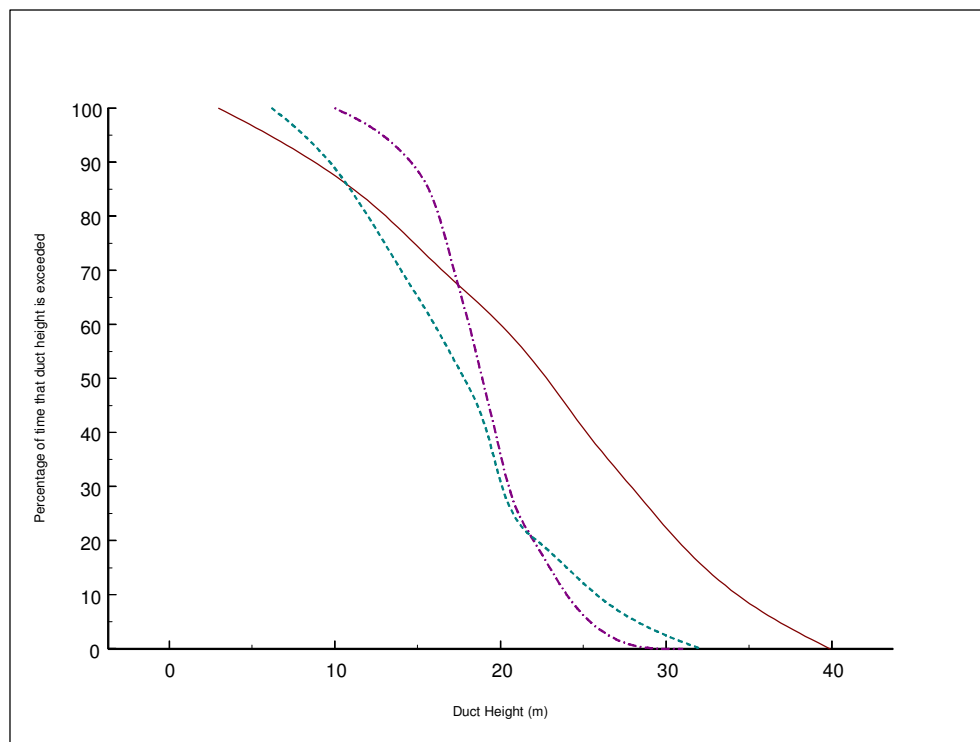
Figure 4.2: Distribution of measured duct heights. (Represented from Chapter 4)

Many sharing studies look at both long and short-term interference effects and in many cases short-term interference can exceed the long term by many dB. If a factor in the difference between long and short-term interference is underestimated or omitted the results of the study could be invalid resulting in unacceptable interference to the existing service. In this case it is possible that the occurrence of ducts in some areas, particularly the tropical littoral, may be underestimated using the traditional models.

Studies presented above indicate that a duct is present for up to 90% of the time in the tropical littoral, ongoing data analysis supports this proposition. In the case of sharing studies therefore it is recommended that where a difference between long and short-term interference is critical the presence of a duct should be assumed. It is not as easy to assume an actual duct height as this depends on numerous meteorological parameters. However looking at Figure 4.2 it can be seen for the tropical littoral a value of between 15 and 20 metres is probably best. It is suggested therefore that if an interferer and victim receiver are both located below 20 metres, ducts at 15, 20 and 25 metres should be assumed and appropriate sharing studies undertaken.

This work has also shown that the propagation simulation program, TERPEM, is accurate in modelling propagation in the presence of a duct in the tropical littoral zone and can be used, combined with measured radio data, to gain an insight into duct formation. As a result of this research I suggest that any studies carried out using ITU-R Rec. P-452 be validated using this or similar packages.

In the case of ITU-R sharing studies, it has been shown that confidence in the likelihood of almost permanent ducts, during clear-air conditions, in the tropical littoral is growing and that it would be prudent to assume a duct is always present in this region when conducting studies to protect sensitive receivers.

5.6   References

[35] Paulus, R. A., "Practical Application of an Evaporation Duct Model". Radio Science, Vol 20, No 4. 1985.

[36] Jeske, H. "State and Limts of Prediction Methods of Radar Wave propagation Conditions over the Sea." Modern Topics in Microwave Propagation and Air-Sea Interaction. D. Reidel Publishing Boston MA. 1973.

[37] Musson-Gennon, L. Gauthier, S. Bruth, E. "A Simple method to Determine Evaporation Duct Height in the Sea Surface Boundary Layer." Radio Science, Vol 27 No 5 1992.

[38] Battaglia, M.R., "Modelling the radar evaporative duct", RANRL Technical Note 3/85, Department of Defence, Defence Science and Technology Organisation, Weapons Systems Research Laboratory, RAN Research Laboratory, Australia, 1985.

[39] Babin. S. M. "A New Model of the Oceanic Evaporation Duct and its Comparison with Current Models". PhD Thesis. University of Maryland (USA) 1996.

[40] Dockery, G.D. and Kuttler, J.R., "An Improved Impedance-Boundary Algorithm for Fourier Split-step solutions of the Parabolic Wave Equation", IEEE Transactions on Antennas and Propagation, vol. 44 (12), pp. 1592-1599, 1996.

[41] Miller, A. R., Brown, R. W and Vegh, E., "New Derivation for the Rough-Surface Reflection Coefficient and for the Distribution of Sea-Wave Elevations", IEEE Proceedings, Vol. 131, pp. 114-116, April 1984.

[42] Barrios, A.E., "Parabolic Equation Modelling in Horizontally Inhomogeneous Environments", IEEE Transactions on Antennas and Propagation, Vol. 40 No 7, July 1992.

[43] TERPEM User Guide, Signal Science Limited, 20 Alexander Close, Abingdon, Oxon, OX14 1XA, UK.

[44] Kulessa, A. and Hermann, J., "Atmospheric Turbulence and the evaporative Duct", DSTO Electronics & Surveillance Laboratories, Edinburgh, South Australia, November 2000, limited release report.

Chapter 6

Some observations of over the horizon microwave radio propagation inside the tropical maritime evaporation duct in North Queensland, Australia

In this chapter, I present the results of our longest and most conclusive radio-path experimental campaign. The first section examines expected propagation results over a long path using local ducting knowledge and makes observations from these results.

The second section explores some unexpected anomalous propagation over a long path using the evaporation duct as a transmission media, examines these results and makes some observations on potential causes based on conditions in the area at the time. This last section forms the basis of later chapters.

Four research conference papers originated from the work presented in this Chapter.

6.1 Introduction

It has been shown in previous chapters that an evaporation duct forms over oceans due to rapidly changing humidity profiles immediately above the sea's surface.

Evaporation ducts can trap propagating waves leading to increased radar ranges or an increase in interference from remote transmitters. There can be advantages to this, especially when designing over water 'duplex' microwave systems or using the duct as a transport mechanism. The disadvantages though are also many such as anomalous radar returns or interference.

Previous chapters have established the average height of the duct and diurnal changes in the duct in various climatic conditions and seasons. Various models are available to determine duct height [45] and we draw on these. Propagation at 10.6 GHz and 11.7 GHz over a 20 km path has been extensively measured during this research resulting in a good understanding of propagation over a short path within the duct. This chapter describes an experiment over a very long over-the-horizon path of 72.2 km at 10.7 GHz using a very low transmit antenna height (4 metres) and a receiving array ranging from 3.6 metres AMSL to 11.7 metres AMSL mounted on a platform 7 km out to sea.

This experiment was conducted over the period 8 to 13 July 2001.

In Section 6.2 of this chapter I present some results which support the hypothesis proposed in this research. In Section 6.3 I present some different results for which we do not have a full explanation but are able to postulate causes based on local knowledge of the radio and meteorological environment.

In both cases an analysis of received signal strength along with general weather conditions is presented. Finally conclusions are drawn for the implications and applications of anomalous propagation within the evaporation duct, that is, the presence of an evaporation duct will carry a signal over a long distance and that the available PRM models are capable of predicting this when presented with reasonably accurate weather information.

6.2   Normal ducting events

By normal ducting events, events where the theory of ducting and measured signals levels corresponds within the bound of uncertainty inherent with our measurements are inferred.

6.2.1   The path

The radio path was established from Toolakeah Beach, 20 km north of Townsville, Queensland, to the Bulk Sugar Terminal jetty at Lucinda, North of Ingham. The jetty extends 7 km out to sea and provided an excellent platform for this research.

The overall path length was 72.2 km. The transmitter was positioned on the sand dunes at Toolakeah Beach with an effective transmitter height of 4 metre AMSL. The transmitter consisted of a 20 mW YIG source tuned to 10.6 GHz and a 0.6 metre 26-dBi parabolic antenna for a total transmit power of 36 dBm EIRP allowing 3 dB loss for off bore site, feed and feeder loses.

The receiver was positioned at the end of the Bulk Sugar Terminal jetty at Lucinda. The receiver consisted of an array of receivers each having a 16 dBi slotted guide antenna and a 55 dB LNC via a cable and switching assembly with 2 dB inherent loss (average). These were connected to a switching matrix from which the signal was sampled at approximately 60-second intervals for each array element. Antenna heights were recorded AMSL at a 1.5m tide on Monday 9 July, 12:00.

Figure 6.1 shows the path diagram and associated earth bulge for a k=4/3 standard atmosphere. From this figure, it can be seen that the path is not free space and that earth bulge is significant. The diffraction path for this system had a calculated 215 dB loss while the free space equivalent is 150.2 dB yielding a received signal of approximately -110 dBm for the spherical diffraction path or –40 dBm if the path were line of sight.

The noise floor of the test equipment was approximately –100 dBm. These figures also allow for measured losses in the feeder and switch matrix. Other variable losses are represented where needed as error bars.

In Figure 6.1, the blue curve represents the sea surface; the straight brown line represents straight path and the curved (lower) brown line the first Fresnel zone.

It is important to note that significant differences in losses due to sea state that have not been fully quantified were observed. This and all other calculations assume a smooth sea surface.
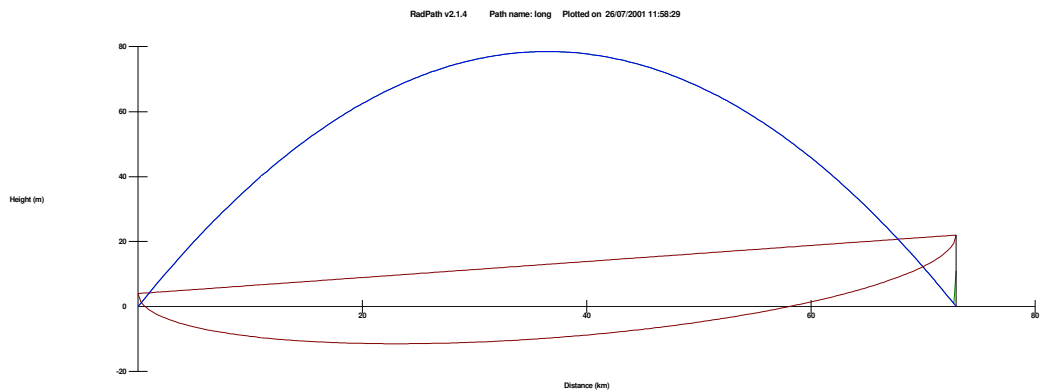
Figure 6.1: Path showing k =4/3 bulge and Fresnel zone
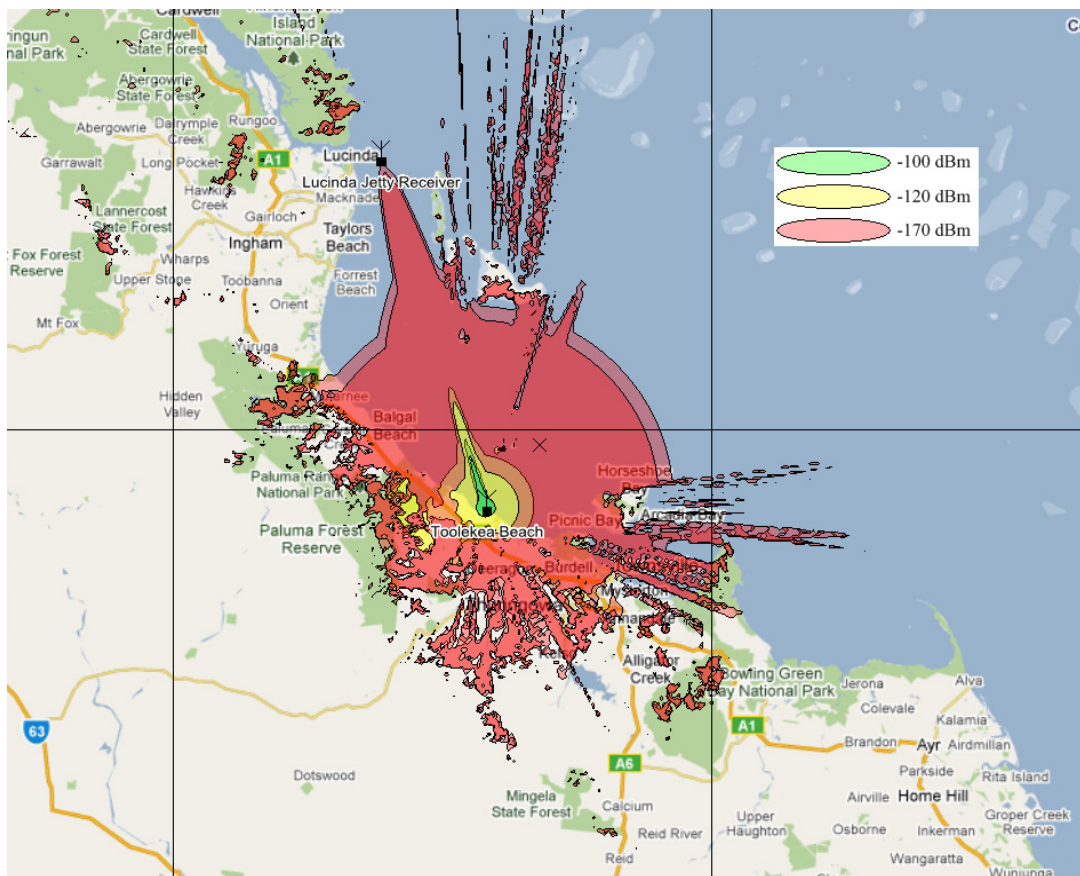
Figure 6.2: A power profile for a standard atmosphere.

Figure 6.2 shows the power profile for the long path. Each colour represents the power that would be received at that point. This profile was derived using a program called 'WRAP' utilising the ITU-R P.562 propagation recommendation, a 4/3 Earth radius and a Digital Elevation Model (DEM) resolution of 754 metres. The transmit antenna gain was set at 26 dBi giving a received power of -171.5dBm at 4 metres and -170 dBm at 10 metres. These powers would not normally be sufficient to sustain a communications link.

6.2.2 The weather

The weather for the entire experiment was fine with average daytime temperatures of 25 degrees Celsius and night-time temperatures around 16 degrees Celsius. Sea surface temperature was measured at Lucinda for the day at an average of 24.2 degrees Celsius. Humidity varied from around 54% during the day to 73% at night. Wind speeds varied during the day up to 24 kph measured at the Toolakeah Beach end of the path.

Weather in this area is quite complex. To the south, Townsville is in a rain shadow caused by an escarpment and remnant hills; immediately to the north of Lucinda is Hinchinbrook Island, a very high mountainous island which in itself generates weather; about half the path could be considered as next to dry tropics with the other half being seaward of wet tropics.

The seas over which the path lay are shallow and warm with many islands nearby. The islands break up a predominant easterly wind and under certain circumstances this allows sea and land breezes to dominate. Wind measurements used in this campaign were derived from the Townsville AWS as those from Lucinda were found to be erroneous due to the placement of the anemometer behind a sugar-loading shed. Some discrepancy in winds at one end of the path and the other is expected and this is best outlined in [46].

The author acknowledges now that weather measurements were a weakness in our overall research as we were reliant on an inaccurate Bureau of Meteorology automated measuring station and some very basic hand held and commercial units of our own.

However the achieved accuracy is similar to that available to technicians in the field and was in any case constrained by budget.

6.2.3   Signal in a duct

A microwave signal propagating in a duct is trapped and thus can only spread in the horizontal direction. The duct tends to act as an angular filter due to the differences in refractivity and Snell's law, thus angles greater than about 0.5 degrees will not be reflected from the duct and this energy will be lost. Because of the geometry of ducting high ducts will therefore only support a small number of modes (one or two for ducts greater than 30 metres) while low ducts may support many modes.

The ability of a duct to filter energy impacting on it at greater than about 0.5 degrees means that we expect any energy reflected from a rough sea surface at these angles to also be lost but that some may be reflected at lower angles producing spurious modes. This topic is expanded upon in Chapter 8.

It is anticipated that this would be seen in rapid scintillations of the received signal power, however we also expect longer period scintillation from normal atmospheric focusing and defocusing events and so it is not possible to separate these variations using a simple amplitude array, for this we need a more complex array capable of discerning angles of arrival and sample intervals much shorter than those used in this research.

Our experiments measured received signal strengths over a one-week period. On four out of the seven days we noted very high signal strengths indicating the presence of a very strong duct. On other days a stronger than 'expected' (i.e. no duct signal) was noted but slightly weaker than the four strong days mentioned above. A possible explanation for these days and for observations of another 'fade' event is explained in Section 6.3.

Figure 6.3 shows the five-minute averaged received signal strengths over a 24-hour period on July 12 2001.   Sea surface temperature varied diurnally from 24.5 degrees to 25.4 degrees Celsius (NOAA and remote measurement), air temperatures from 16 – 25 degrees Celsius and relative humidity from 73% (night) to 54% (day).

The data shown in Figure 6.3 is indicative of the data received during most of the week, except for the periods where unexplained anomalies were observed. One 24 hour period was therefore chosen for further in depth examination. This section will concentrate on the diurnal behaviour of the duct as depicted in this data.

While observing the data as it was collected, I postulated that an evaporation duct was present over the entire 24 hour period. On observing data for the other days of the experiment I concluded that a duct was present for all other periods observed during this experiment. As can be seen in Figure 6.3 received signal strengths in all cases exceeded those for a spherical diffraction path and in some cases exceeded expected line of sight levels during the day when the duct was (as expected) stronger.

In order to verify this hypothesis, that this reduced path loss was the result of an evaporation duct, the Babin model [47] was used to establish the height of the evaporation duct for midnight on July 12 2011. The model, while not as accurate as other later methods [45] is adequate for this purpose and gave an estimate of 20 metres for the duct height.
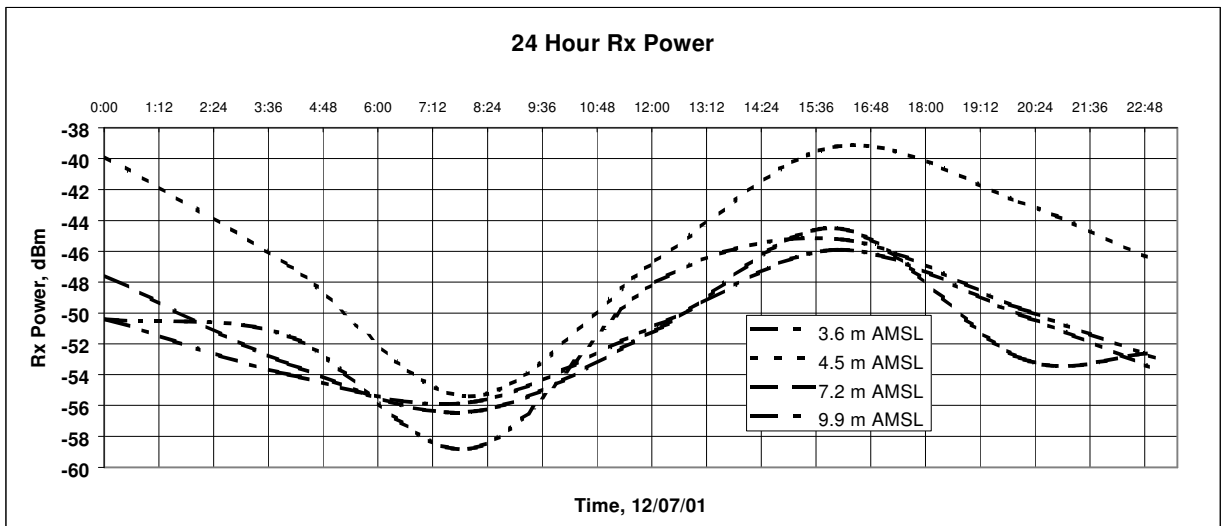
Figure 6.3: 24-hour variation in average received signal power 12 July 2001.

Figure 6.4 shows a vertical slice of the received signal strengths taken at eleven minutes past midnight. Only six elements of the ten are shown as we experienced some equipment failure during the campaign. The tide at the time of reading the slice was high (2.51 metres), thus the 4.5 metre AMSL height shown needs to be adjusted down, the actual height ASL was at the time 3.5 metres.

Figure 6.5 shows a TERPEM plot for a 20-metre duct at a distance of 72.5 km. All other TERPEM settings match the physical characteristics of the link.

Although the TERPEM plot is smooth, a very good correlation exists between the measured path losses and the predicted. The height of the maximum is very close to predicted and the overall received power well within experimental tolerances. Without the deployment of our complex micro-meteorological measuring equipment these measurements give confidence that a duct of the order of 20 metres was present at midnight on 11 July 2001 and confidence in the ability of software such as TERPEM and AREPS to predict such anomalies given duct height or meteorological data.
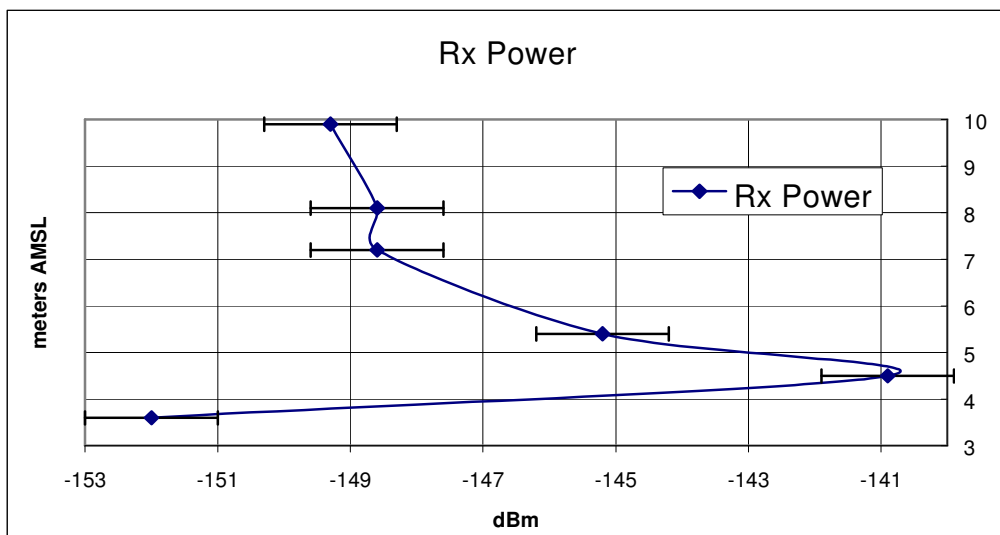
Figure 6.4: Vertical 'slice' at 00:11 12 July 2001
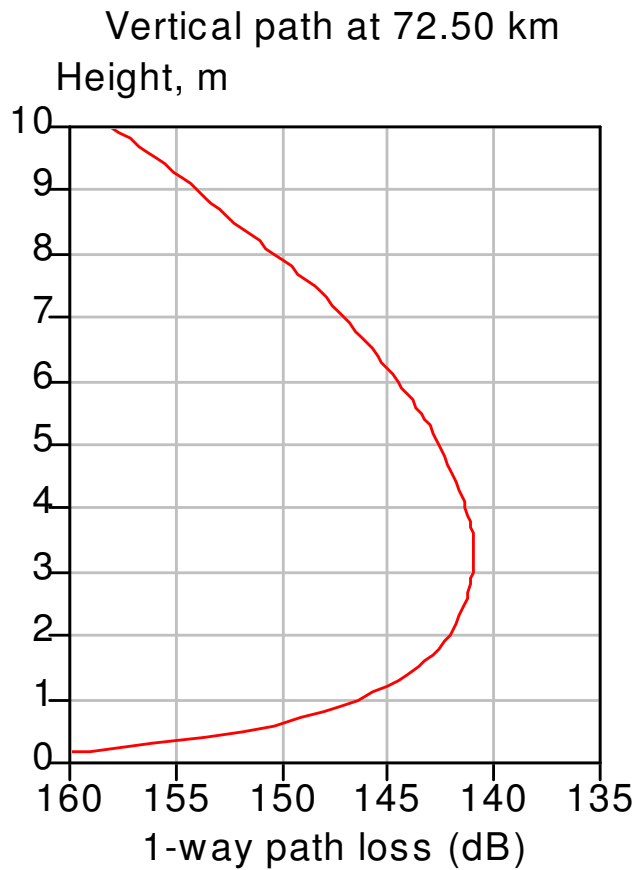
Figure 6.5: TERPEM Path Loss Simulation. 20 Metre duct at 72 km.

The problem of course is that such data is not readily available and hard to take from on board a vessel due to local effects. A radio method of determining duct height would therefore be a valuable tool in a number of applications including duct prediction, anomaly cancellation and perhaps even atmospheric parameter measurement.

6.2.4 Ducted signal over time

Over warm tropical waters, in the absence of any meso-scale winds, we expect a land breeze to dominate in the early morning and then as the land heats in the morning drop back to a sea breeze [46]. On the 12th of July 2001 the dominant gradient or synoptic wind was an East Nor-Easter (ENE) at 10 – 15 kph. Thus as the land breeze developed it competed with the gradient wind to produce a calm. With no wind the supersaturated air needed to form a duct cannot mix above a metre or so and thus the duct collapses.

Figure 6.6 shows a time period on the morning of the 12th where the duct is assumed to have collapsed due to the reducing signal strengths and the differences in received signal strengths between elements. The reader should note that a curve fitting technique from the Excel program was used to create the solid lines rather than a 5 minute averaging window used in Figure 6.3 resulting in some small differences. Comparing this collapse to the wind strengths shown in Figure 6.7 we again see a strong correlation supporting this proposition.

Table 6.1 shows wind directions for the period. It can be seen from this and an interpretation of local conditions from [46] that before the calm event the land breeze predominates. As the land breeze dies down the vector sum of the winds shifts south and then East South-Easterly (ESE) as the land warms under the morning sun. From eight o'clock onwards wind strength increases from which we would expect mixing and duct formation. Returning to Figure 6.3 again a strong correlation between wind speed and signal strength can be seen, which supports the proposition that the duct collapsed and reformed in the presence of dominant winds and the land/sea breeze combination.
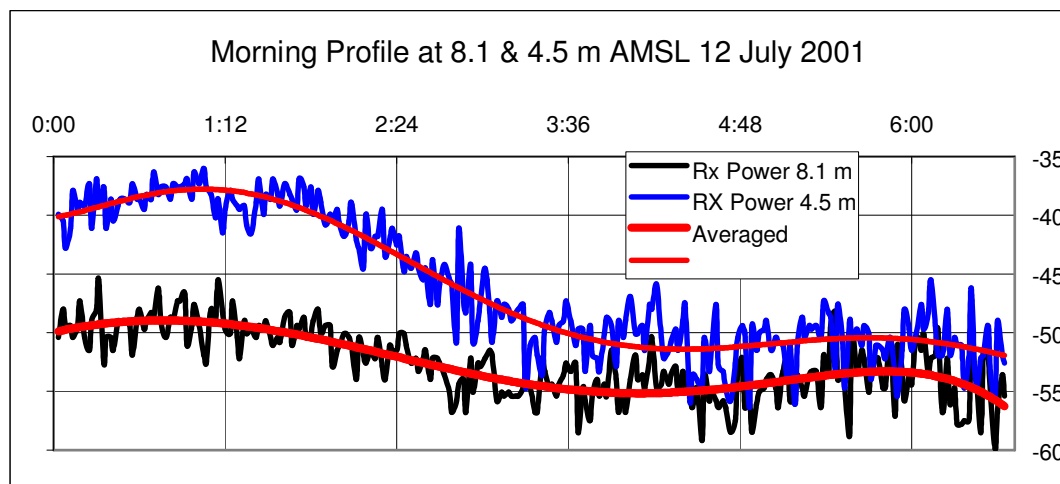
Figure 6.6: Midnight to 06:30 12 July 2001.
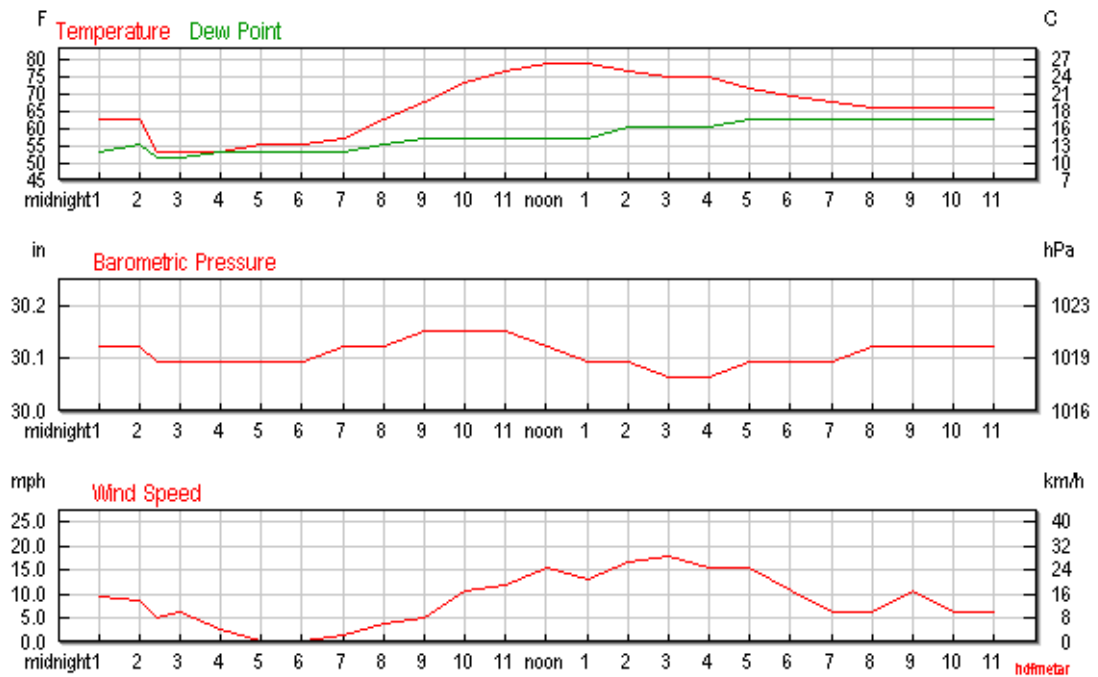
Figure 6.7: Wind Speeds, pressure and temperature for 12 July [BoM AWS Lucinda].

Table 6.1: Wind Directions for 12 July [BoM Lucinda AWS].

Time	00	01	02	03	04	05	06	07	08	09	10	11
W Speed	13	15	13	7	9	4	0	0	6	7	17	18
W Dirn	ESE	ESE	SE	SSE	W	W	Calm	Calm	S	S	ESE	ESE

Time	12	13	14	15	16	17	18	19	20	21	22	23
W Speed	24	20	26	28	24	24	17	9	9	17	9	9
W Dirn	ENE	NE	NE	ENE	ENE	E	E	E	SE	E	SE	SSE

6.2.5 Conclusions

In this section some experimental results along with weather statistics for a long range experiment were presented. Excellent correlation between observed events, radio and ducting theory were found. Hence it can be deduced that PEM models such as TERPEM are excellent tools for predicting general propagation inside the evaporation duct provided accurate duct heights are known.

It can also be concluded that a duct can hold up a radio path well over what would be considered normal in a standard atmosphere. This obviously has implication for path

design from both usable signal and interference perspectives. These concepts are further explored in subsequent chapters.

6.3 Some anomalous and as yet unexplained events

6.3.1 Introduction

In Section 6.2 a series of results that agreed extremely well with current thinking on propagation within the evaporation duct and duct formation was presented. In this section an investigation of two events not fully explained by the theory of ducting as we understand it thus far is presented. However, using local knowledge and a good basis in the behaviour of radio in the presence of a stratified atmospheric it is felt that our explanations of these phenomena are plausible. Those results for a double trapping atmosphere presented later in the chapter seem to agree very well with the models despite good weather data not being available at the time.

6.3.2 Collapsing duct in good wind

It has previously been shown that normally it could be expected that when a fair wind is present a duct will be sustained once developed. On 13 July 2001 some data that suggests this cannot be relied upon were recorded. Figure 6.8 shows signal strength, averaged over a five minute window, from all working elements of the array between 17:00 and about 18:15.

A decreasing signal strength, which we normally associate with a duct that is collapsing or spatially breaking up, can be seen. In this case however the spread of signal strengths remains relatively the same as compared to say Figure 6.6 in Section 6.2. The relationship between each element is also reasonably stable. It is possible to theorise then that the duct did not collapse either in height or over an area (breaking up) and so the reduction in signal must be attributed to another cause.

Looking more closely at one set of data taken at 4.5 metres AMSL in Figure 6.6 it can be seen that the signal drops to almost the expected weak duct levels shown in Figure 6.1 of Section 6.2. Now on 12 July when similar signal strengths were received calm

winds were recorded and thus the duct was collapsing. On 13 July during the event recorded in Figures 6.8 and 6.9 wind speeds of 17 – 24 kph were recorded with the wind backing from ENE through East to ESE. We would expect a wind of 17 – 24 kph to be strong enough to sustain a duct.
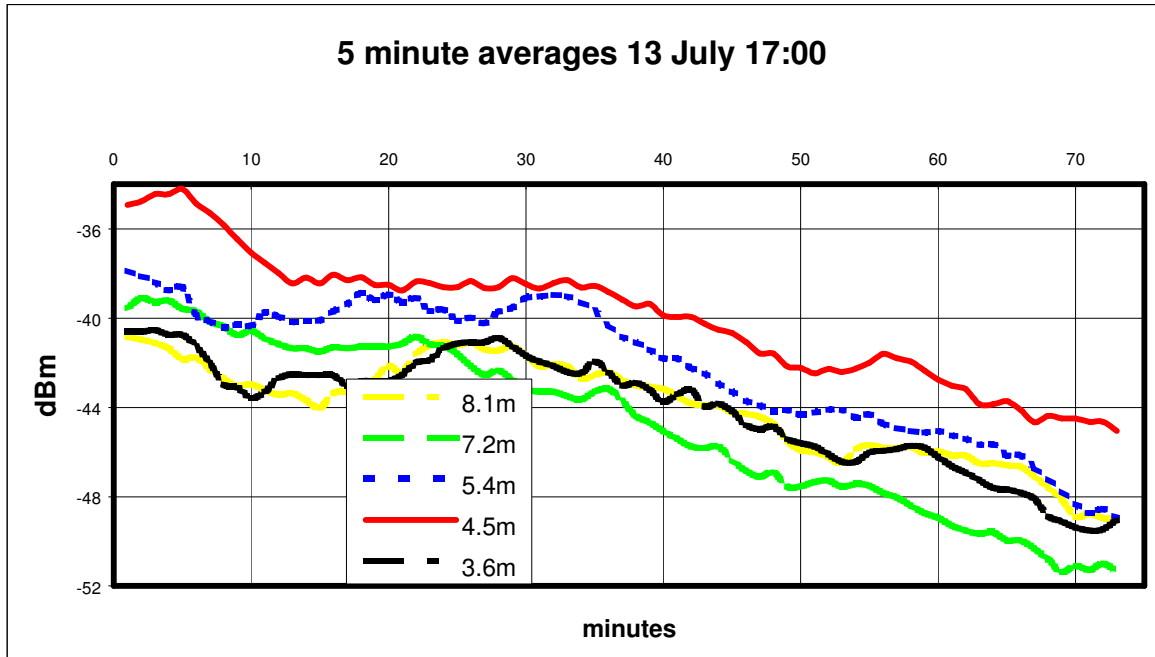
Figure 6.8: 5 minute average received signal strength at height for 17:00 – 18:00 on July 13 2001.
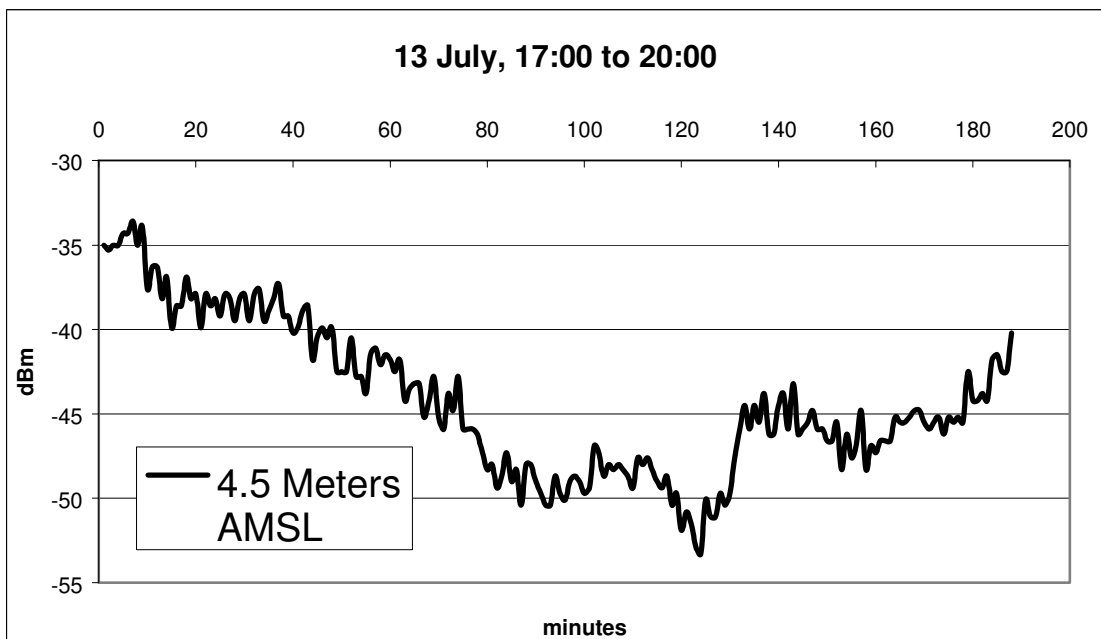
Figure 6.9: Received signal strength at 4.5 metres on 13 July.
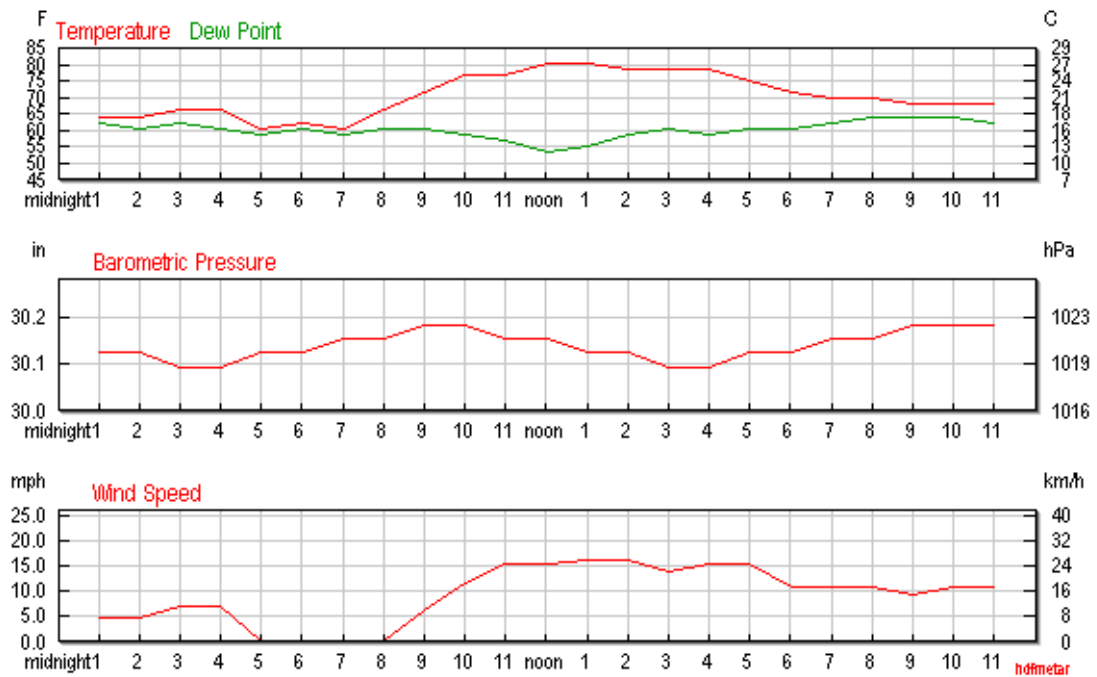
Figure 6.10: Weather for Townsville 13 July 2001 [BoM Lucinda AWS]

Looking at Figure 6.10, which are the weather observations for Townsville (some 50 km from the center of the path), three significant events can be identified. At noon the dew (relative humidity) point drops as temperature increases, but then increases sharply without a comparable decrease in temperature between noon and about 5 pm. At 4 pm the temperature begins to decrease more rapidly that would normally be expected and between 2 and 5 pm the barometric pressure drops. Shortly after this the wind speed drops and changes direction, shown in Table 6.2.

Although not forecast and although we have no other meteorological data for the period, we assume that a weak low-pressure trough crossed the path at about 5 pm local time causing the wind to decrease in strength and back from an East Nor Easterly to an Easterly (which is likely to be the vector sum of the geostrophic wind and the sea breeze). But why did this affect the duct so markedly?

Table 6.2: Wind directions for 13 July 2001.

Time	14:00	15:00	16:00	17:00	18:00	19:00	20:00
Wind Dirn	ENE	ENE	ENE	ENE	ENE	Easterly	ESE
Speed kph	26	22	24	24	17	17	17

Figure 6.11: Experimental Area

If we look at Figure 6.11, one explanation seems plausible. The Palm Group of Islands will block a wind coming from the ENE so prior to about 5 pm much of the path would have been in the lee of the islands and thus over relatively calm seas. (The transmit site lies just below the extent of the map).   This may have caused the duct to collapse over an area mid path. While ducts would most likely be present at either end of the path we would predict significant signal loss through this discontinuity. No work has been carried out on coupling between ducts, or into ducts from landward. The latter may be useful to system designers.

A South Easterly wind however would expose most of the path to unshielded wind thus increasing the chop. A duct acting as an angular filter is discussed briefly in Chapter 8, where it is postulated that the duct only propagates energy impinging on it at angles of less than 0.5 degrees; that above 0.5 degrees passes from the duct. In addition, in the case of a choppy sea, much energy could be expected to be dispersed but general propagation within the duct to remain the same. This would explain the relationship between the elements and the reducing signal strength during the event. I discuss the duct acting as an angular filter from the theoretical perspective briefly in Chapter 7; however this is beyond the scope of the goal of this project.

As yet however there is no other proven explanation for these observations but it is hoped that ongoing research into ducts may one day provide more solid answers.

6.3.3   Formation of a transient evaporation ducting event

This section overviews a transient ducting event experienced during one day of our experimental campaign. The topic is touched on here and explained in more depth in the next chapter.

On 10 July received signal strengths indicated no evaporation duct was present for much of the day. This is supported by no significant wind over most of the day except for a few hours around 3 pm. Figure 6.12 shows the observations for Townsville on that day.
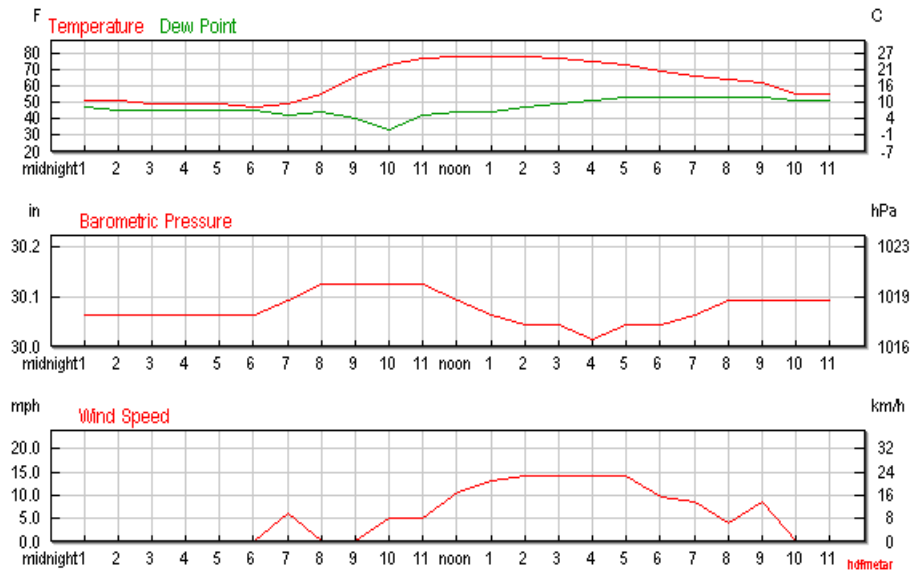
Figure 6.12: Weather for Townsville 10 July 2001 [48]

Figure 6.13 shows the received signal strengths from 2:00 PM on that day. We assume, but without solid evidence, that an advection duct had formed in the area. Figure 6.14 shows a photograph taken on 11 July. Above the island in the background (Palm Island) smoke can be seen forming a layer. This could indicate the presence of an advection duct and explain the stable, but higher than expected (in a no-duct situation) signal strengths observed for most of 10 July.

One time period of interest is noted between about 3 pm and 4 pm. At that time signal strengths increase significantly for about 30 minutes and then drop to below the daily average swinging rapidly between a high and a low for about 30 minutes thereafter. During the period of signal enhancement significant differences between the signal from the two array elements are also noticeable indicating some form of multipath mode has most likely been established.

Looking at the weather for that period we find that the wind had reached a maximum speed of about 22 kph, but at the time of the fade event, had changed direction to the North by about 30 degrees. No precipitation was observed or recorded however a significant and sudden drop in barometric pressure at the time could indicate the passage of a small front or trough.
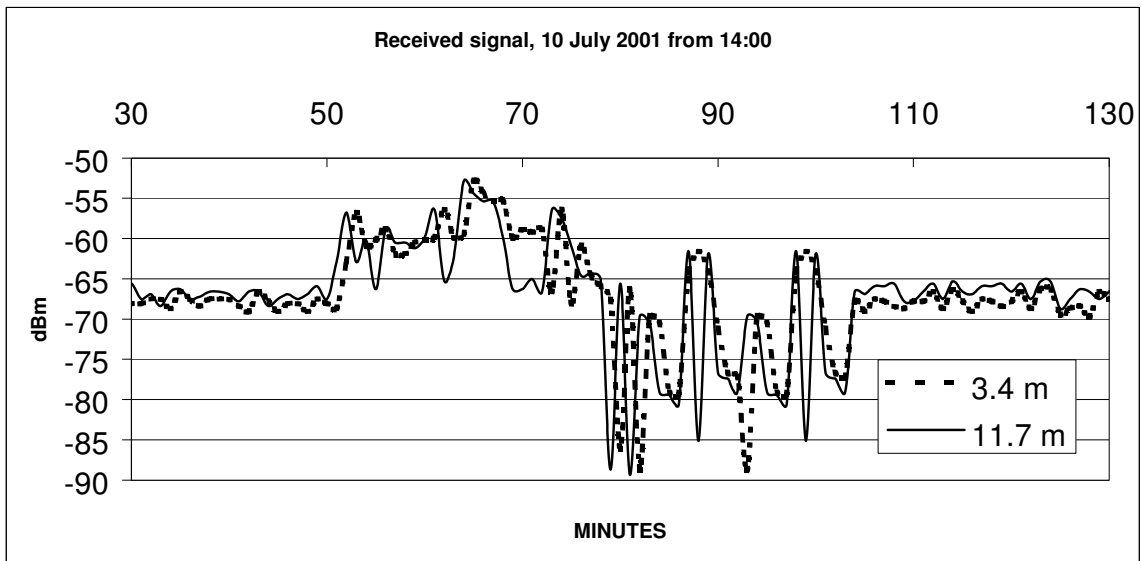
Figure 6.13: A fade event on 10 July 2001.

The only available barometric charts do not show any frontal passage or nearby troughs however the sudden drop in barometric pressure suggests a trough did indeed pass over the path. (N.B, this is relative to the high pressure weather system predominating on the day).

Wind-speed started increasing at about midday and this would normally trigger the formation of a duct soon afterwards. In this case however no activity that could be attributed to evaporation ducting was observed until 3 pm and it was very short lived (only 2 hours).

Looking at Table 6.3 we see the wind changed direction between about 2 and 5 pm again indicating the passage of a meteorological event such as a trough. This corresponds with the drop in barometric pressure. Allowing for the fact that the observation station was 50 km from the centre of the 73 km path, the time difference between the weather observations and the fade event can be explained.

Table 6.3: Wind directions for 10 July 2001.

Time	12:00	13:00	14:00	15:00	16:00	17:00	18:00
Wind Dirn	ENE	ENE	ENE	NE	NE	ENE	NE
Speed kph	16.7	20.4	22.2	22.2	22.2	22.2	14.8

Figure 6.14: The receiver array with Palm Island and smoke in the background on 10 July.

Looking again at Figure 6.13 we can see that the signal fluctuates deeply and rapidly and a significant difference can be seen between the two elements, which are about seven metres apart. This suggest strong multipath. If we assume an advection duct was present as previously argued, then the formation of a high (around 20 metres) evaporation duct over some or the entire path some time after midday could produce a good single mode multipath for the signal reflected from the higher advection duct. As to why a duct would form and disperse so quickly on such a day we as yet have no explanation, however the event and wind measurements do correlate very well leading us to believe that this is what actually occurred.

The path showed good received signal strength, far greater than that predicted by the diffraction model. Received signal strengths were overall in agreement with those predicted by the AREPS program using the parabolic equation model (PEM). Superimposed over the average signal were large fluctuations of the order of 10 dB.

Figure 6.15 shows the received signal for a two-hour period on 14 July 2001. Second order polynomial trend lines have been incorporated to show the slow fading response of the duct. These changes are of the order of change measured in the duct during the 1999 measurement campaign. The previously mentioned rapid changes in signal

strength are evident which are possibly caused by the interaction of the propagating wave with a rough sea surface.

Figure 6.16 shows the five-minute averaged received signal strengths over a 24-hour period on July 12 2001. Sea surface temperature varied diurnally from 24.5 degrees to 25.4 degrees (NOAA), temperatures from 16 – 25 degrees Celsius and relative humidity from 73% (night) to 54% (day).
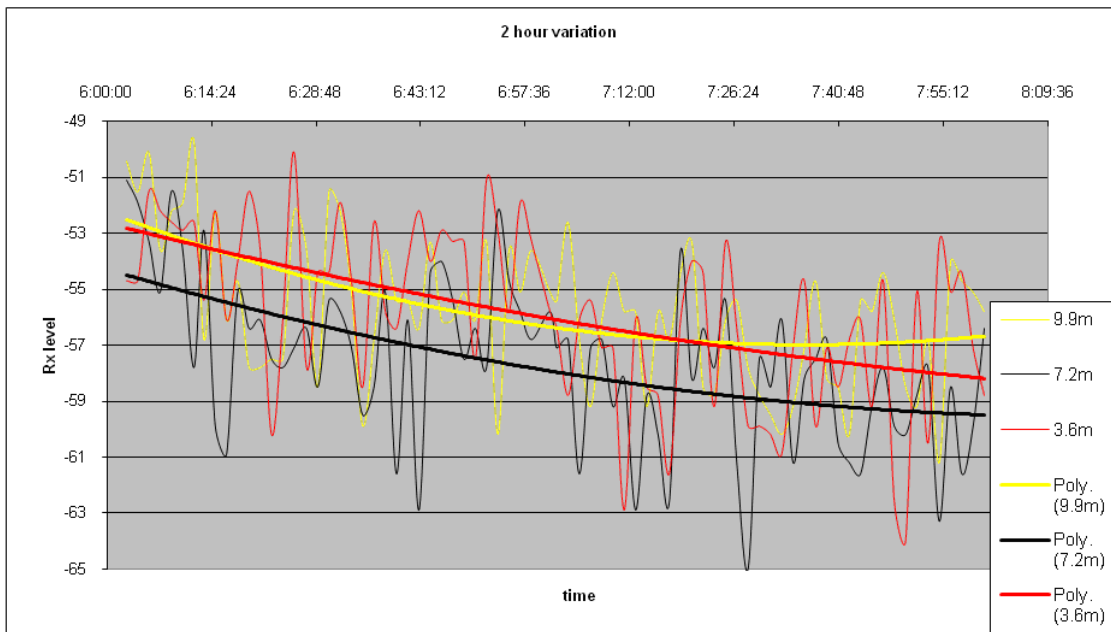
Figure 6.15: Two hour variations in received signal strength.
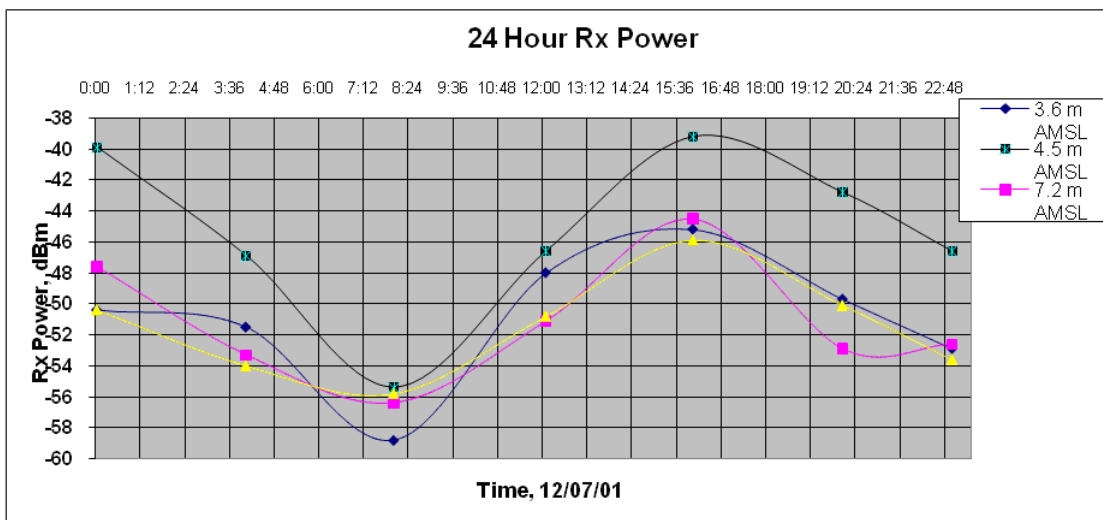
Figure 6.16: 24-hour variation in average received signal power.
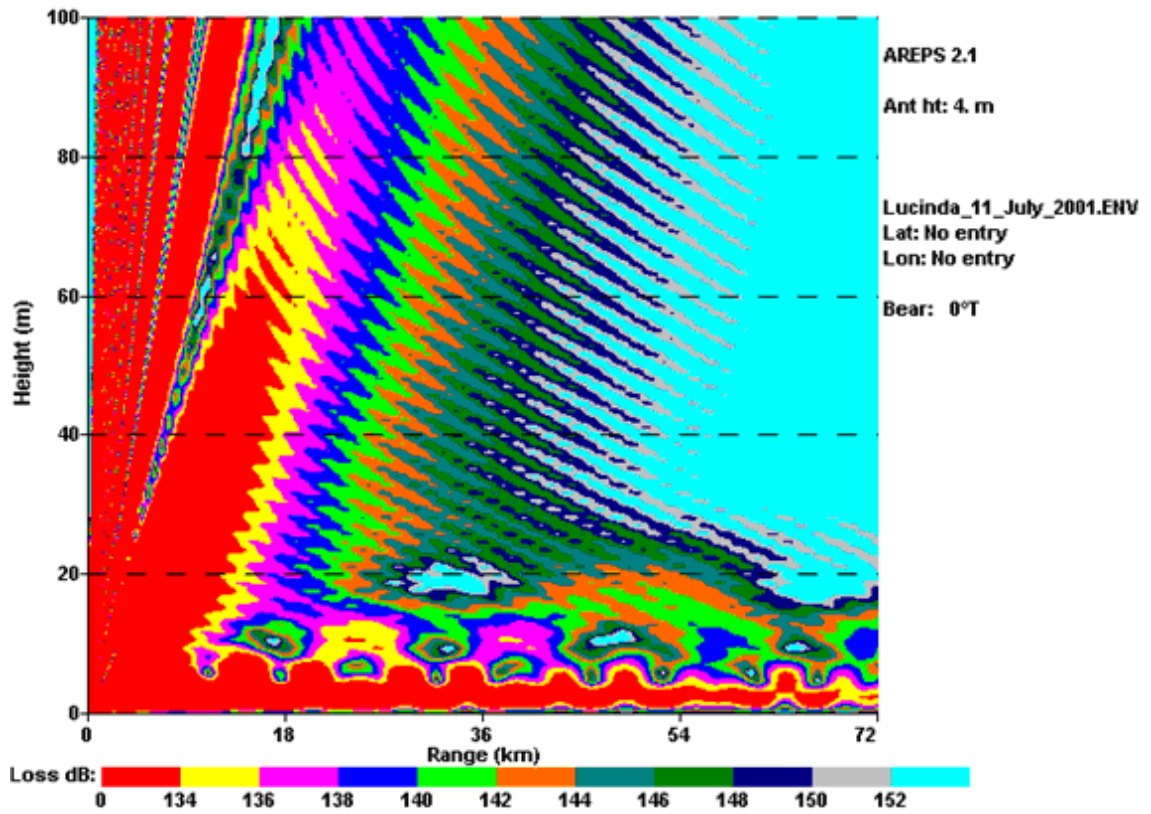
Figure 6.17: 11 July 2001 Afternoon Profile
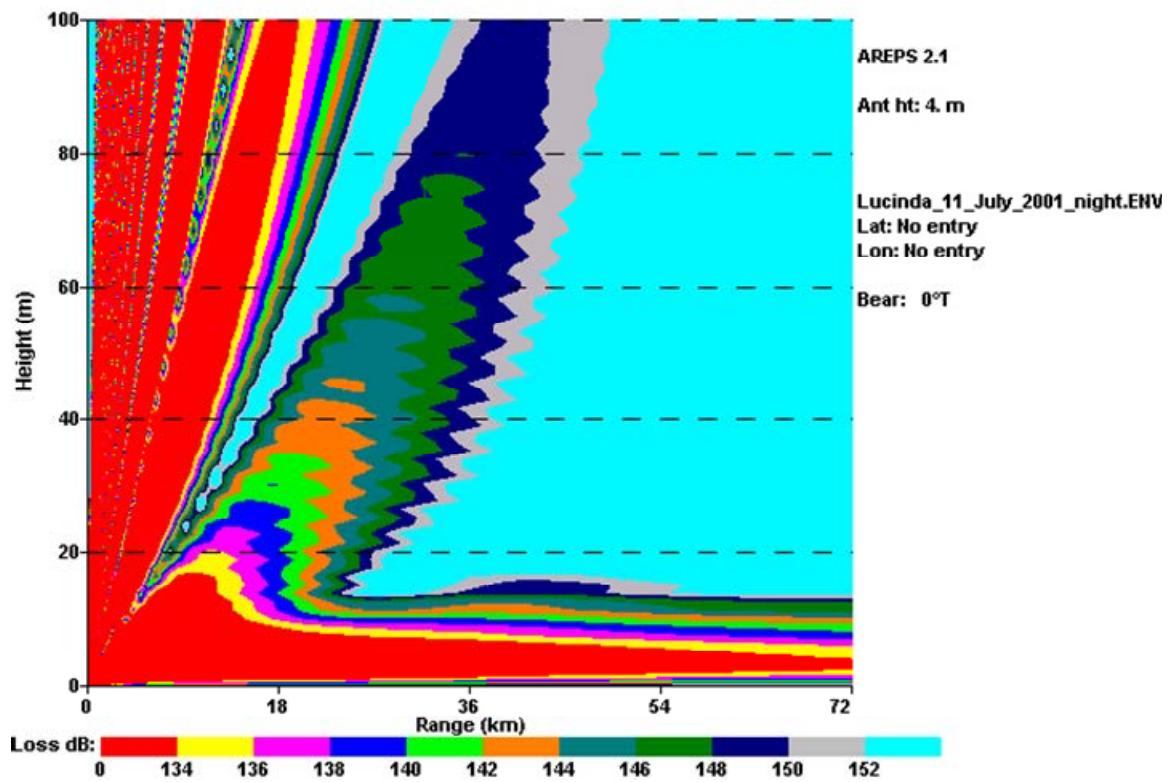
Figure 6.18: 11 July 2001 Late Evening Profile

Using temperatures and humidity taken on the day, AREPS calculated a duct height of 29 metres and gave the complex propagation loss diagram seen in Figure 6.17 At night, AREPS calculated a duct height of around 10 metres; the path loss as calculated by AREPS for this situation is depicted in 6.18.

Figures 6.19 and 6.20 show the vertical path loss profile at 72 km as calculated by AREPS.
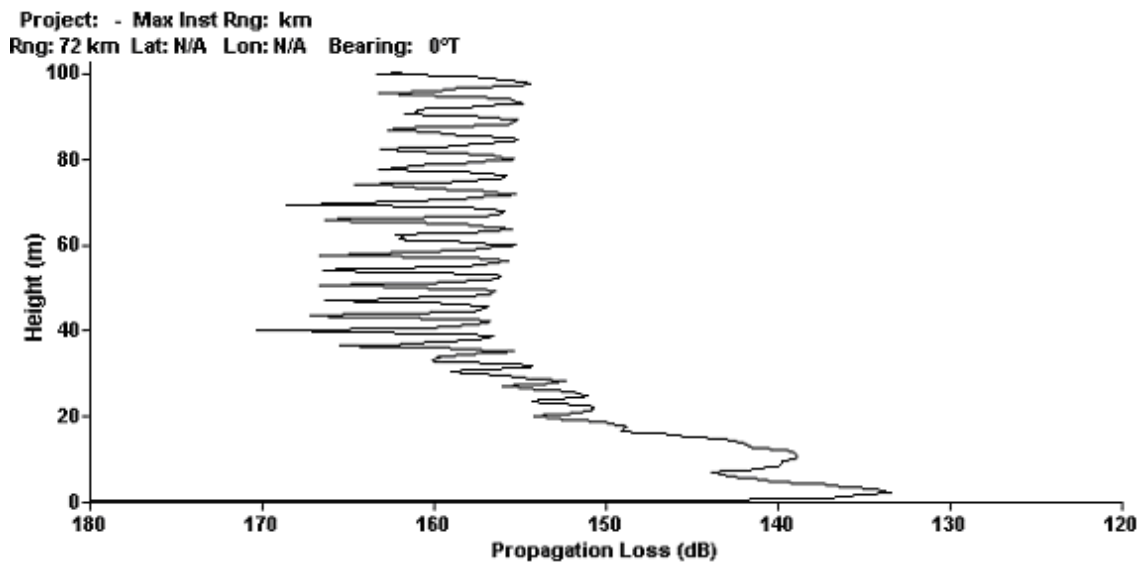
Figure 6.19: Afternoon loss vs. height from AREPS.
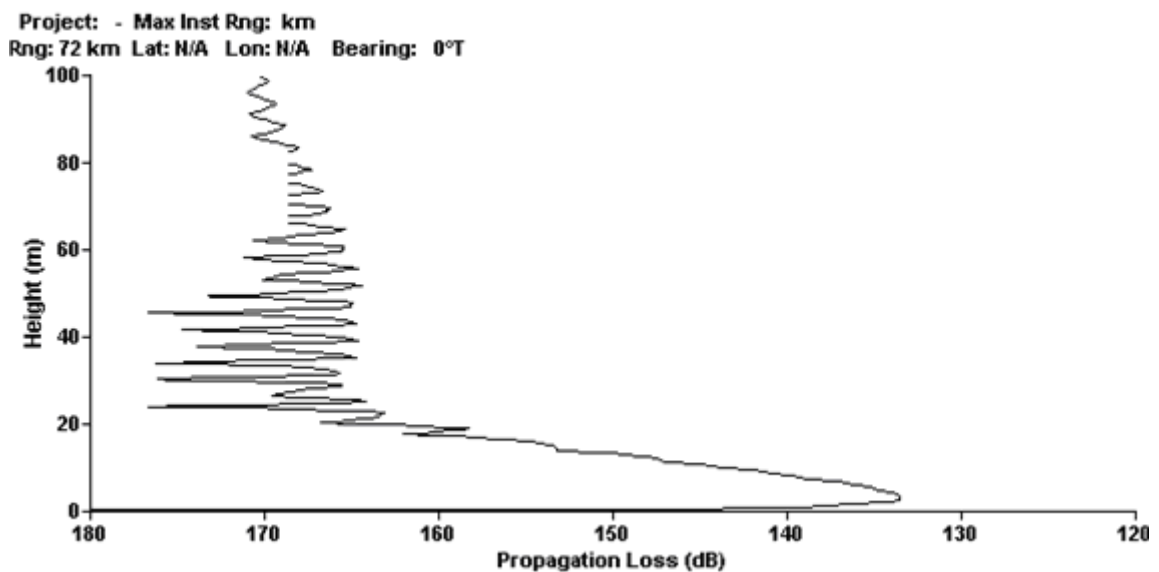
Figure 6.20: Loss vs. height, late evening, from AREPS.

The above profiles measure propagation loss over a 100-metre height. Our array could only measure up to 11.7 metres. In Figures 6.21 and 6.22 below the AREPS data is adjusted for the measurement system and imposed over the signal strength measured in the array.
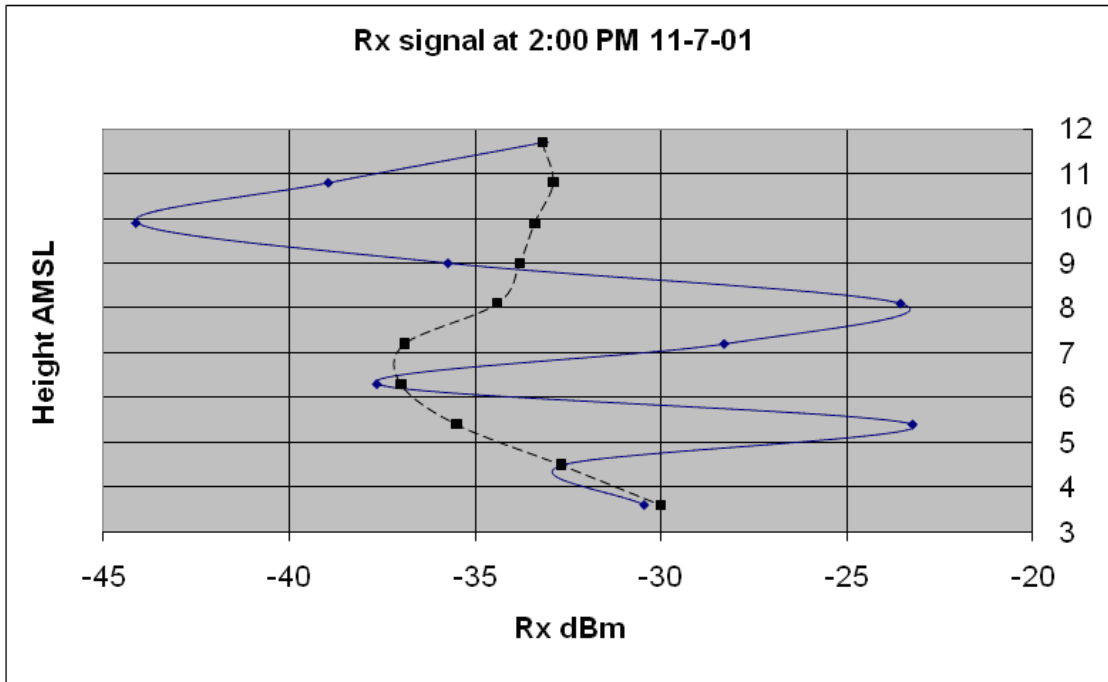
Figure 6.21: 2:00 PM measured signal (solid line) with AREPS simulation (broken line)
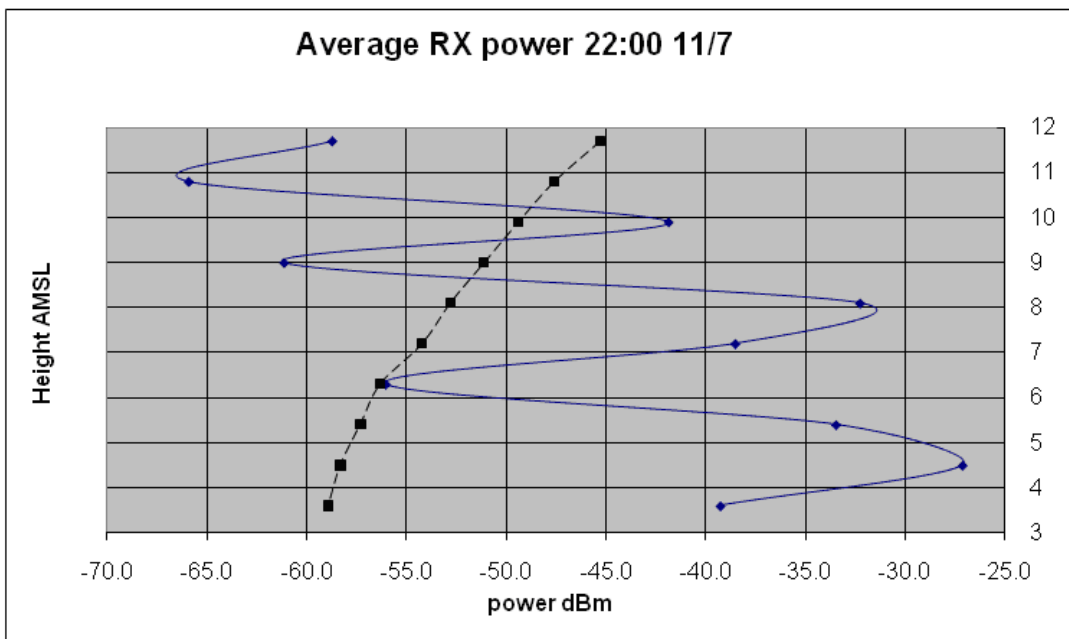
Figure 6.22: Measured signal (solid line) with AREPS simulation (broken line), late evening.
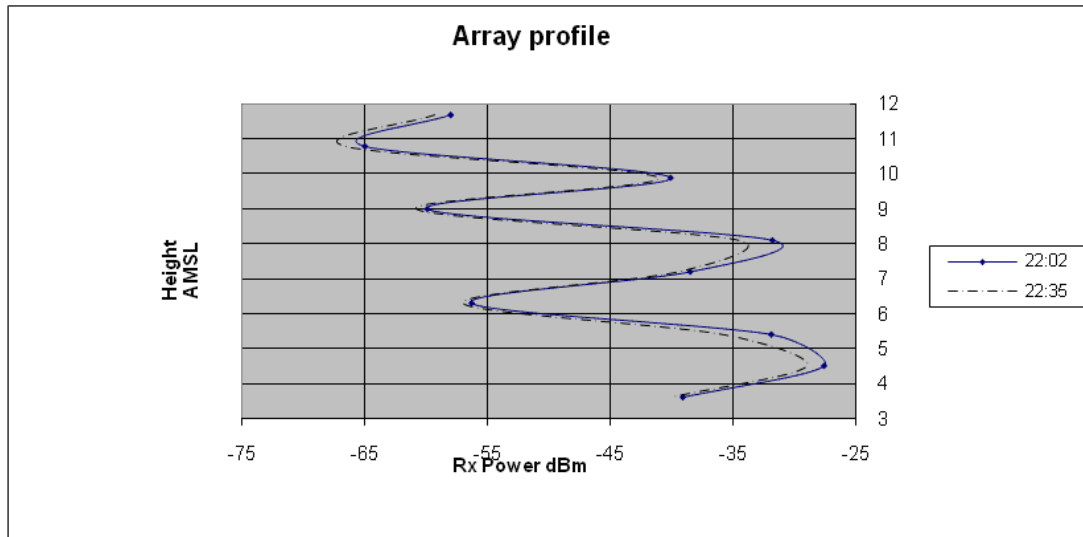
Figure 6.23: Two sets of measurements, 30 minutes apart.

It is obvious from the two figures above that the received signal strengths are of the same order as those predicted by AREPS. This information then, along with previous measurements taken in the area, indicates the presence of the evaporation duct over the full 24-hour period. This result in itself is significant for the planners of coastal microwave systems and the users and operators of microwave radar. What can also be seen though is that the AREPS predictions at that level are smooth whereas the actual measurements show considerable fluctuation over height.

Figure 6.23 below shows very good correlation between two sets of five-minute averages taken 30 minutes apart on the evening of measurement. This removes the possibility of the level fluctuations over height being a temporal anomaly.

If these effects are not caused by the system but are not predicted by the AREPS program the question can be asked, what causes them?

In Figure 6.24 a series of duct height measurements taken in the same area in 1999 by the research team can be seen. The series shown was taken over a 100-minute period in the early afternoon using a series of atmospheric sensors on a tall spar-buoy anchored near Lucinda. The duct height can be seen to increase after midday, which is expected as the sea breeze intensifies, from 10 metres to nearly 25 metres in the space of an hour. These two duct heights correspond approximately to those simulated above. More rapid

duct height fluctuations can also be seen with an amplitude of about 3 metres with a period of around ten minutes. A possible cause for these is local variation in wind speed. These are likely to cause variation in signal strength over this period however the readings in Figure 6.23 show little evidence of this. It would appear then that these differences in signal strength are caused by a relatively stationary effect.

Looking for a causal effect for the semi-stationary interference pattern seen in the above readings we noted a fire on a nearby island. The smoke rose to about 250 metres and then spread indicating the possibility of coastal advection and thus the formation of an advection duct. In the photograph shown as Figure 6.14 above, the receiver array can be seen with Palm Island in the background. The smoke from this fire can be seen to the right of Palm Island. The smoke layering is obvious and strongly stratified suggesting a temperature inversion at that height. Using the height of Palm Island as a reference this layer is estimated to be around 250 metres.
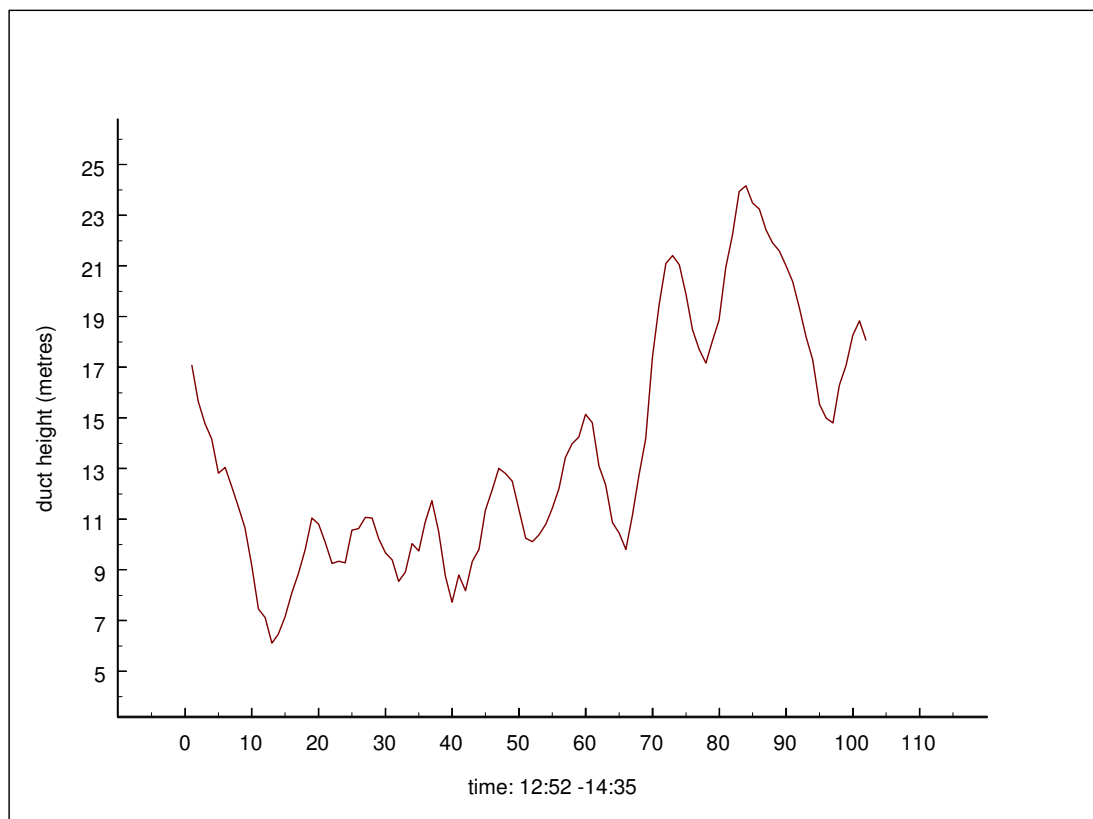
Figure 6.24: Duct height variation with time, July 1999.

Another AREPS environment profile was built using previously measured results for near surface atmospheric values and creating a trapping layer at around 250 metres. The results can be seen in Figures 6.25 and 6.26 below.

Comparing Figure 6.25 with its cousin, Figure 6.19, we see that the more complex, 'double trapping' atmosphere creates a more complex received signal strength in the first few metres of the atmosphere where our measurements were taken. Figure 6.25 is an approximation using the path losses above and the link budgets from the measurement system. While this is not an exact replication of the measured data, the similarity with the received levels in Figure 6.19 is obvious. Given that, in the absence of soundings, the upper air structure was 'guestimated' from visual observations this similarity is remarkable and points to the influence of complex atmospheric influences in such long paths.

For completion Figure 6.27 shows the transmitter mounted at Professor Peter Arlett's beach house on Toolakea Beach north of Townsville.
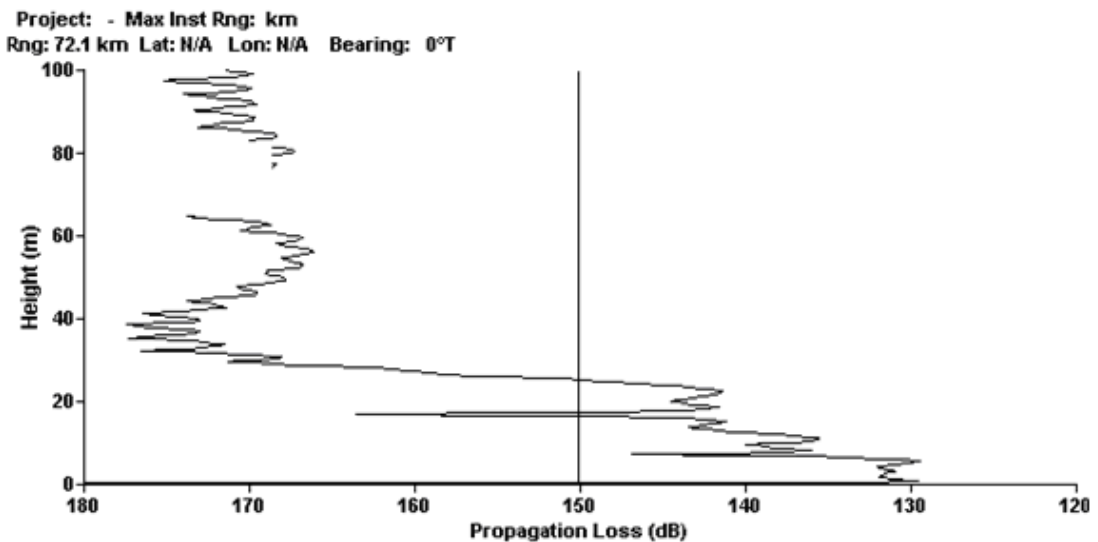
Figure 6.25: AREPS prediction for the simulated atmosphere.
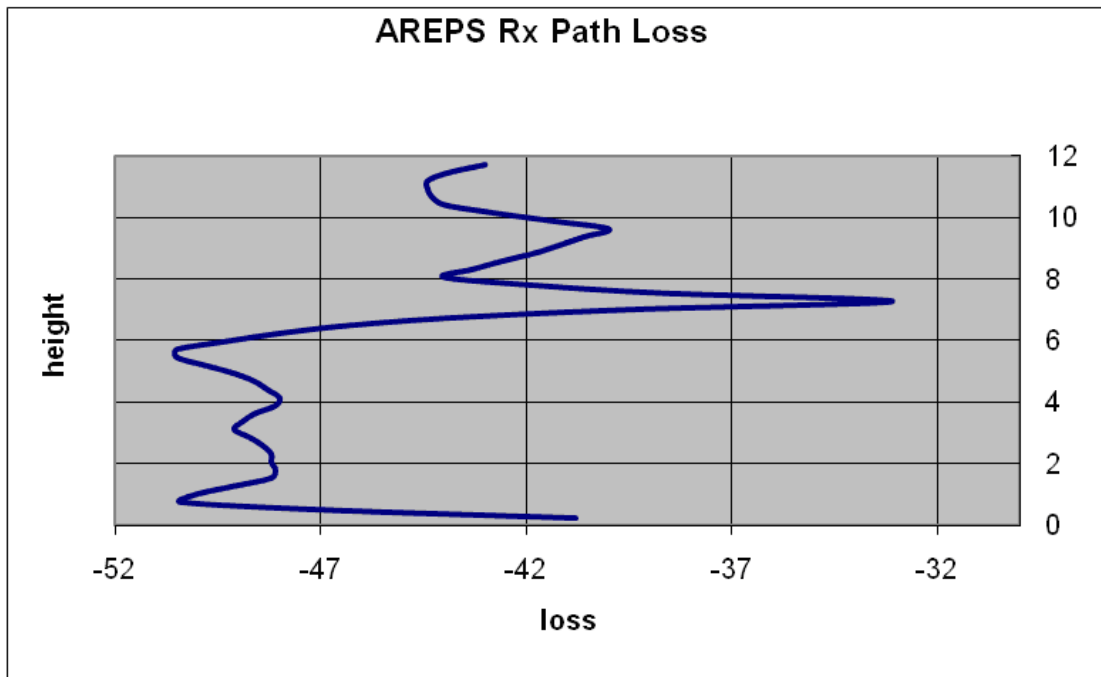
Figure 6.26: AREPS received signal simulation using simulated 'double trapping' atmosphere.

Figure 6.27: Transmitter at Toolakea Beach.

6.4 Conclusions

In this chapter I have presented the findings from a long distance propagation experiment inside the evaporation duct at 10.7 GHz. The ability to hold such a strong signal over 72.2 kilometres has indicated both potential uses and dangers of the evaporation duct in tropical regions. From one 24 hour measurement period which is indicative of a week of experimental data, it can be seen that the duct is capable of holding a communications link up with a C/N of at least 10 dB while a duct is present over the path. However based on our results on duct formation shown in Figure 4.2 such a link would only be useful for store and forward communications as the duct is an unreliable propagation mechanism in real time.

The ability to hold open a communications link, or look beyond the horizon with radar also indicates a downfall of the evaporation duct. Traditional Australian microwave design uses Radiocommunications Assignment and Licensing Instruction FX-3 (Fixed Service) (RALI FX3) [49] as the design criteria. RALI FX3 does not cater for ducting of this strength. Individual systems designed to this standard could potentially suffer interference from each other in coastal regions even if many kilometres apart.

During the experiment a complex fade event was measured over the link. It has been shown that there are good reasons to conclude that this is caused by a double trapping atmosphere; the evaporation duct combined with an advection duct around 250 metres. Comparisons between measured and simulated data favour this hypothesis.

6.5 References and papers

6.5.1 Published papers

The following papers were published as a result of this research:

Kerans, A.J. and Woods, G.S., "Comparison of Microwave Propagation Models and Evaporation duct Height Estimation Techniques with Actual Near Water Atmospheric and Radio Data Taken in North Queensland, Australia in May, 2001", 2nd Student Conference on Research and Development (SCOReD 2002), Shah Alam, Malaysia, 16-17 July 2002.

Kerans, A.J., Woods, G.S. and Kulessa, A.S., "Microwave Propagation within a Tropical Maritime Evaporation Duct, a Comparison of Measured Data and Simulations" ClimDiff, Fortaleza, 17-19 November 2003.

Kerans, A.J. and Woods, G.S., "Observations of anomalous over the horizon microwave radio propagation inside the tropical maritime evaporation duct in North Queensland, Australia. Part One: normal ducting events", URSI Commission F, Triennium Open Symposium, Cairns, Queensland, Australia, 1-4 June 2004.

Kerans, A.J. and Woods, G.S., "Observations of anomalous over the horizon microwave radio propagation inside the tropical maritime evaporation duct in North Queensland, Australia. Part Two: some anomalous and as yet unexplained events", URSI Commission F, Triennium Open Symposium, Cairns, Queensland, Australia, 1-4 June 2004.

6.5.2   References

[45] Ivanov, V. K., Shalyapin, V. N. & Levadnyi, Y. V., "Determination of the evaporation duct height from standard meteorological data", Izvestiya Atmospheric and Oceanic Physics, Vol. 43, No 1, pp 36-44, October 2007.

[46] Harvey, A., "Real Time Monitoring and Short-Term Forecasting of Maritime Weather", James Cook University Masters' Thesis, March 2001.

[47] Babin, S. M., Young, G.S. and Carton, J.A., "A new model of the oceanic evaporation duct", Journal of Applied Meteorology, Vol. 36, No. 3, pp 193-204, March 1997.

[48] www.wunderground.com archives.

[49] Australian Communications and Media Authority, Radiocommunications Assignment and Licensing Instruction FX-3 (Fixed Service) See http://www.acma.gov.au/WEB/STANDARD/pc=PC_2708 (constantly upgraded).

Chapter 7

The evaporation duct as an angular filter

Some simple observations about the duct acting as an angular filter are made in this chapter. With the benefit of a decade of research in the field of propagation inside the tropical evaporation duct, these conclusions are obvious to the author of this Thesis; however they may not be as obvious to the designer or operator of a radio system.

The postulation also opens up a potential interesting field of research and some initial suggestions on method are also included.

Chapter 1 Introduction and Thesis format	
Chapter 2 Microwave propagation, measurement and simulation	
Chapter 3 Radio-meteorology and the tropical littoral zone under study	
Chapter 4 Meteorological measurement and prediction techniques	
Chapter 5 Propagation simulation in a duct using TERPEM and AREPS and observations supporting the accuracy of these models	
Chapter 6 Some observations of over the horizon microwave radio propagation inside the tropical maritime evaporation duct in North Queensland, Australia	**Chapter 7** The evaporation duct as an angular filter
Chapter 8 Short range propagation experiments,	**Chapter 11** A theoretical design for long range over ocean microwave links using the tropical evaporation duct / **Annex 1** Informing the Military Community
Chapter 9 Methods for extracting angle of arrival	**Annex 2** Implications for designers of fixed services utilising over water paths
Chapter 10 Mathematical methods for measuring angle of arrival in over ocean	
	Chapter 12 Research and Thesis conclusions

7.1 Introduction

This Chapter briefly introduces the concept of the duct acting as an angular filter. This is presented theoretically only, because while the implications possibly have a profound effect as discussed in Chapter 6, the actual physical verification and measurement of the effect is beyond the scope of this research.

Nonetheless the concept is presented here and further thought is encouraged by suggesting a simple experimental methodology that may help both verify and quantify the effect.

The basic, and somewhat obvious, postulate is that if an oceanic evaporation duct will only reflect energy incident at 0.5 degrees or less then it is a simple angular low pass filter in the direction of a receiver in the duct.

With a smooth sea and a 'tight' beam antenna then most of the energy transmitted into the duct could be expected to propagate towards the receiver. However we have shown that ducts rely on wind to both establish and sustain. Thus when a duct is present the sea surface will most likely not be mirror like, there will be specular reflection, depending upon the sea state a significant amount of scattered energy will be lost through the duct.

This means that radar metrology of the sea state may be missing some vital angular information which could affect its accuracy.

We will briefly explore the theory, implications and a simple design which may be able to verify and quantify this.

7.2 Some basic refractive theory relative to this research

Angles incident on a receiver that are reflected from a duct can be calculated using Snell's law. Since v_z (phase velocity in the z direction) is the same for incident and reflected waves with v_{x1} (phase velocity in the x direction) being the same magnitude

with opposite direction, the angle of incidence onto the duct will equal the angle of reflection towards the receiver.

Figure 7.1 shows a diagram of Snell's law as it relates to ducting. This figure will be referred to throughout this chapter. This figure shows a characterised duct on the left (dashed line) and a very simplified model of a stratified layer (solid line) which shows how ΔM is derived. On the right is a diagram of incident, reflected and transmitted waves on the duct where '1' is the incident ray, '2' the transmitted ray, '3' the reflected ray and '4' is the direct ray. Region 1 is below the duct, Region 2 the 'standard' atmosphere above it. The effective height of the duct is the reflective atmospheric boundary. This is shown and discussed as a plane for simplicity whereas it is actually a thick layer. The author hopes this simple illustration helps conceptualise propagation in the duct.
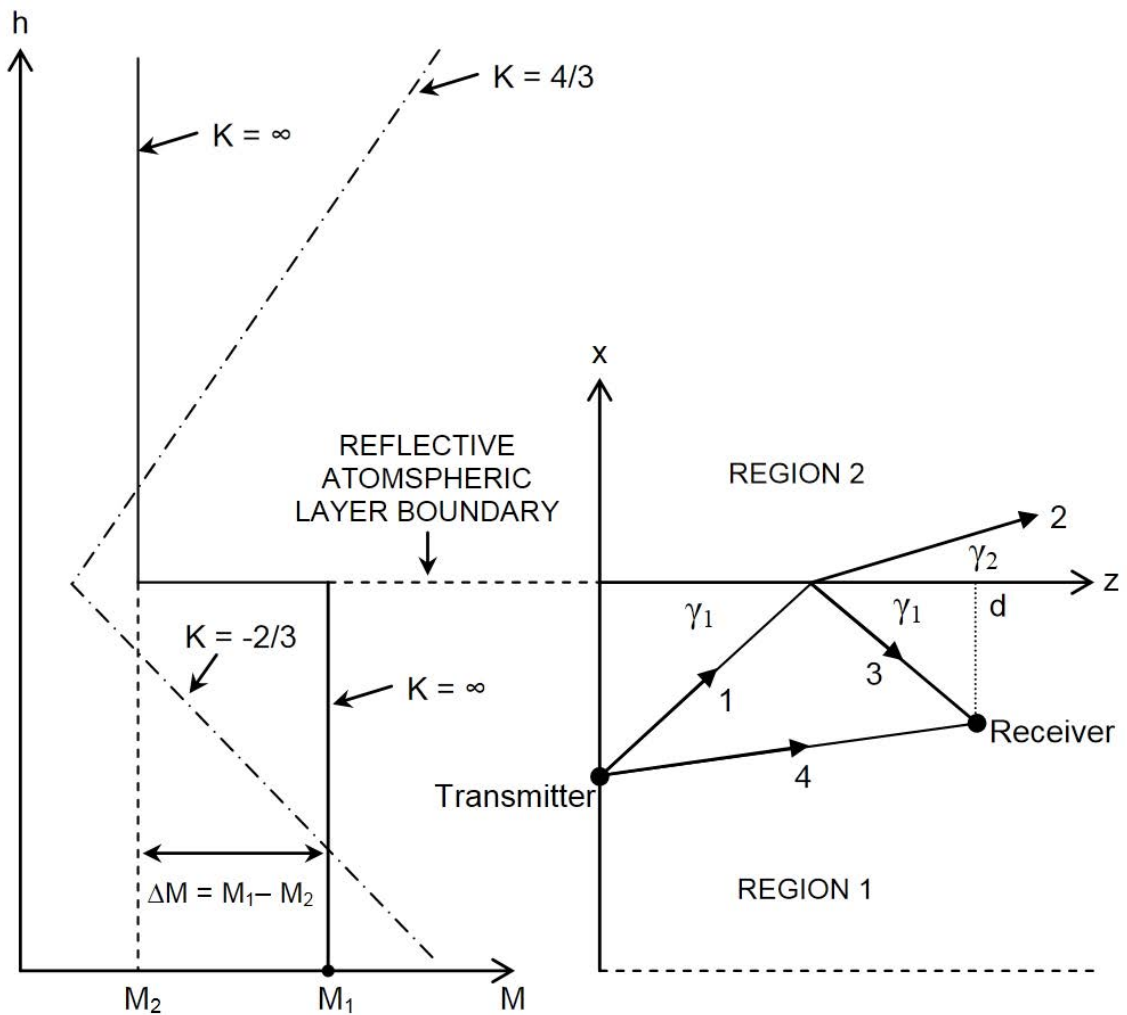
Figure 7.1: Snell's law, reflection inside a duct. Adapted from [15].

The duct varies with time as we have shown, but very slowly, thus reflections from a duct can therefore be assumed specular at any instant in time even though there may be some element of diffuse scattering involved over time intervals longer than a few seconds. Specular reflection is the 'mirror like' reflection of radio waves, where a single incoming ray will have a single outgoing ray.

Ducts will not be 'mirror like' over time intervals greater than a second. We have shown in previous chapters that they vary with time and distance, see Figure 5.18 for example. Thus over long time periods reflection from them will in reality be diffuse. Diffuse reflection means that from a single incident ray many separate rays will form following reflection. Our arrays took up to ten seconds to capture a 'slice' of the wavefront travelling from the transmitter, over this time the duct would have behaved in a diffuse manner introducing yet another uncertainty in our measurements.

Measurement of atmospheric parameters to determine the level of diffuse scattering is almost impossible so the specular assumption must be made for simplicity. Forward wave reflection from the sea's surface is highly diffuse, but it not a highly researched topic, for this brief Chapter the author drew extensively on a text by Long [50].

From Snell's law we find:

$$\frac{Cos\,\gamma_1}{Cos\,\gamma_2} = \frac{k_2}{k_1} = \frac{m_2}{m_1} = \frac{v_1}{v_2}$$

(7.1)

Where ε is the dielectric constant ≈ 1, $k_1 = \sqrt{\varepsilon_1}\,k_0 = 2\pi/\lambda_1$ and $k_2 = \sqrt{\varepsilon_2}\,k_0 = 2\pi/\lambda_2$ are the propagation constants in regions 1 and 2 in Figure 7.1. Since $\varepsilon_1 \approx \varepsilon_2 \approx \varepsilon_0$ then $k_1 \approx k_2 \approx k_0$ and $\lambda_1 \approx \lambda_2 \approx \lambda_0$.

Recall from equation 2.11 that $M = (m - 1)10^6$ (M units).

From our measurements over warm tropical oceans in far north Queensland Australia discussed in Chapter 4, we determine that the approximate values of M at the boundary are $M_1 = 330$ and $M_2 = 300$. Converting to m values we have $m_1 = 1.00033$ and $m_2 =$

1.00030 which are both approximately equal to 1. We can therefore simplify Snell's law to obtain:

$$Sin\,\gamma_0 \approx \sqrt{2(m_1 - m_2)} = \sqrt{2\Delta M.10^{-6}} \approx \gamma_0$$

(7.2)

Where γ_0 is the cut-off angle below which no energy is transmitted, known as the critical or Brewster angle. This is the lower limit for γ_1 when $\gamma_2 = 0$. From Snell's law we know $\gamma_1 > \gamma_2$ when the incident ray arrives from the less dense medium.

30 modified refractivity (M) units is assessed to be the maximum value of ΔM seen in these measurements. From Equation 7.2 this equates to an angle of arrival of 0.44 degrees. The average angle of incidence on the wave reflected from the duct is assumed from measurement of duct height to be 0.2 degrees. The derivation of these duct heights is covered in Chapter 4. What this tells us is that any ray incident on a duct at an angle greater than approximately 0.44 degrees will be totally transmitted. In many cases the change in M through the height of the duct will be less than 30 M-units, as discussed in Chapter 4.

Energy incident at exactly γ_0 would in theory propagate along the duct. This is known as an evanescent wave [15], however in the opinion of the author duct irregularities in time, distance and height would mean this wave would be very quickly either transmitted or refracted and can thus be ignored.

Thus only energy reflected at less that approximately 0.44 degrees would propagate forward towards the receiver. The actual loss incurred in this process is complex and beyond the scope of this research but in the case of a microwave transmitter would be a function of the antenna beam width, the duct height and the path length.

Energy propagated in the duct would be maximum in a flat sea; however there would then be no wind and thus no duct. Where wind is present energy will only reflect at below 0.44 degrees for elements of each wave in the illuminated zone at an angle where incidence plus reflection results in a wave front at less than 0.44 degrees without

obstruction by wave-tops. In moderate winds, waves tend to 'white cap' which may also reduce the reflected energy inside the duct.

The sea surface is complex being made up of numerous separate wave patterns caused by wind, swell and reflections. Figure 7.2 from [51] shows this complexity including an exaggerated cross section. The exaggerated cross section may help in visualising a ray striking the surface from a very small angle. Very little of the surface is parallel to the horizontal thus very little reflection will occur at angles less than 0.5 degrees.

From the discussion above it has been established that radio waves will only propagate forward if the total angle of transmission and reflection is less than 0.44 degrees from the horizon (in reality the plane of the duct). Looking at Figure 7.1, the area of the surface of the wave that will reflect forward with an angle between 0 degrees and 0.44 degrees is that part of the surface at or near parallel with the horizontal. On any but a smooth surface experienced in 'dead calm' conditions this area will be quite small between 6% for approximately 12 dB loss or 1% or less, for a loss of 20 dB or more.

This is indeed a complex field, but data in Chapter 6 of Long [50] suggests that in a sea caused by a 10 knot wind, sufficient to sustain a duct, reflection loss from an incident wave would be greater than 20 dB and should not be sensitive to polarisation.

As shown later in Chapter 10 this knowledge is needed in the design of any radio array capable of resolving multiple incoming rays reflected from either the duct or the sea's surface. The maximum angle also means the duct acts as an angular filter to the diffuse reflections from the sea resulting in near specular transmission of any rays striking the array from above.
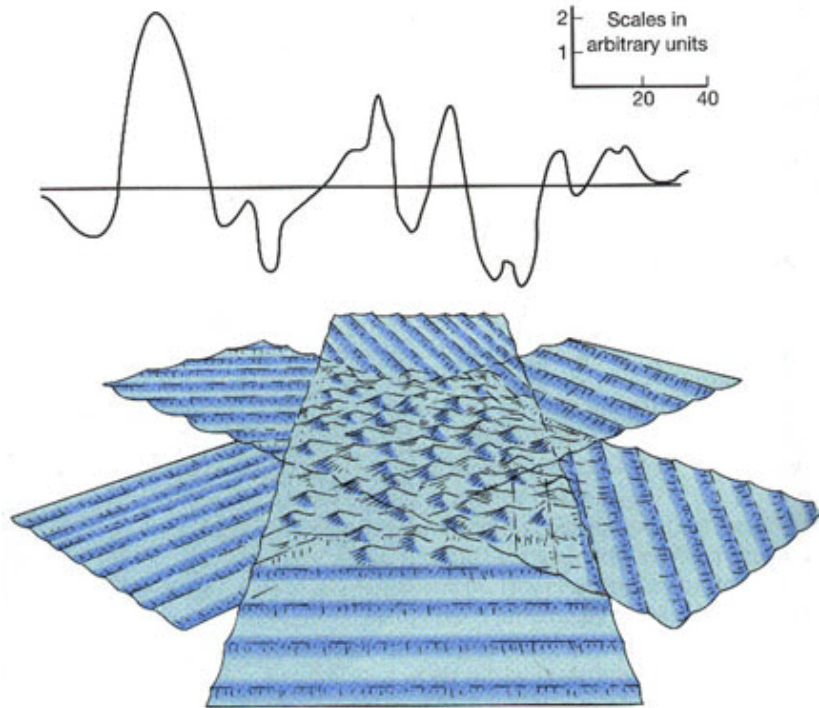
The ocean waves that we observe are a complex of many different
sets of waves of different wave lengths, periods and heights.

Figure 7.2: Complex Ocean Waves [51].

7.3 Transmission coefficients and Fresnel formulas

To solve reflection in the duct we must meet the boundary conditions for
electromagnetic fields at the duct reflecting surface. Specifically:

$$E_{y1} = E_{y2} \tag{7.3}$$

for the E field and

$$H_{z1} = H_{z2} \tag{7.4}$$

for the H field.

Expanding E_{y1} and E_{y2} we have [15, pp 24 – 31]:

$$\frac{B}{A} = \frac{1 - \dfrac{k_{x2}}{k_{x1}}}{1 + \dfrac{k_{x2}}{k_{x1}}} = r_H$$

$$\tag{7.5}$$

where k is a vector representing a plane wave travelling in positive x and z directions and r_H is the voltage reflection coefficient for H-Pol waves, and

$$\frac{C}{A} = \frac{2}{1 + \frac{k_{x2}}{k_{x1}}} = t_H = 1 + r_H \tag{7.6}$$

where t_H is the transmission coefficient for H-Pol waves. A represents the incident wave, B the reflected and C the refracted wave, and

$$\frac{k_{x2}}{k_{x1}} = \frac{k_2 Sin\gamma_2}{k_1 Sin\gamma_1} = \sqrt{1 - \left(\frac{Sin\gamma_0}{Sin\gamma_1}\right)^2} \tag{7.7}$$

The direction of r_H is opposite that of t_H when $r_H = 1$, i.e. total internal reflection within the duct then t_H is 0. Also of note is that the reflection coefficients for both V-Pol and H-Pol waves are identical except around the Brewster angle [50]. Much reflection over long paths takes place at or near the Brewster angle and so for this reason our systems were designed to only measure H-Pol waves.

Since in our study the incident wave originates in the denser air within the duct, and because we are mainly studying total internal reflection within the duct, it is useful to derive simplified expressions for the Fresnel formulas for the angles of interest (that is below about 0.44 degrees).

When the transmitter is placed inside the duct ΔM is positive and:

$$Sin^2\gamma_0 = 2\Delta M.10^6 \approx \gamma^2_0 << 1 \tag{7.8}$$

When $0 \le \gamma_1 \le \gamma_0$: $\qquad r_H = r_V = e^{j\left(-\pi + 2\arcsin\frac{\gamma_1}{\gamma_0}\right)}$ $\qquad\qquad$ (7.9)

This is total internal reflection and all the energy striking the ducts upper reflective surface is reflected back towards the sea or array. In this case the reflection coefficient is 1 and the phase varies between -π and 0 depending on the angle of incidence.

When $\gamma_0 \leq \gamma_1 << \pi/4$:

$$r_H = r_V = \frac{1 - \sqrt{1 - \left(\frac{\gamma_0}{\gamma_1}\right)^2}}{1 + \sqrt{1 - \left(\frac{\gamma_0}{\gamma_1}\right)^2}}$$

(7.10)

When $\gamma_1 >> \gamma_0$:

$$r_H = \frac{\gamma_0^2}{4} \frac{1}{Sin^2\gamma_1}$$

(7.11)

and

$$r_V = \frac{\gamma_0^2}{4} \left(\frac{1}{Tan^2\gamma_1} - 1\right)$$

(7.12)

While not used in this study, equation (7.12) is included for interest as the angle where $r_V = 0$ is called the Brewster angle and is found to be $\pi/4$.

When $\gamma_0 << \gamma_1 << \pi/4$:

$$r_H = r_V = \left(\frac{\gamma_0}{2\gamma_1}\right)^2$$

(7.13)

These formulae give us some idea of the amount of energy reflected within the duct depending on the angle of incidence. It is restated here that these formulae apply only to a perfectly stratified layer. As is shown later in this Thesis, this cannot exist in an actual duct because of local variations in wind speed and sea surface temperature, however this is a reasonable assumption in any theoretical study.

A simple illustration of this theory is shown in Figure 7.3. Note angles are necessarily exaggerated to illustrate the concept.

In the previous chapter a long distance experiment was discussed during which path losses as low as free space were observed. This suggests that very little energy is lost through the duct in situations similar to those experienced during this experiment.

An explanation for this is the relatively narrow beamwidths for parabolic antennae, approximately 2.5 degrees for a 3 dB beamwidth for the antenna used in the experiment.

This directs or focuses the energy into the duct and depending on the angle, up to the critical angle, this energy is refracted back towards the centre forming the direct ray. Thus energy within the +/- 0.44 beam would propagate directly as the main beam (see Figure 2.6). Energy propagating upwards at angles greater than 0.44 degrees would leave the duct at the duct height (for a 20 metre duct this would be approximately 265 metres from the transmitter) and energy propagating downward at greater than 0.44 degrees would reflect diffusely with some leaving and some remaining in the duct. But the majority of energy would propagate within the duct supporting the conclusions of Chapter 6.
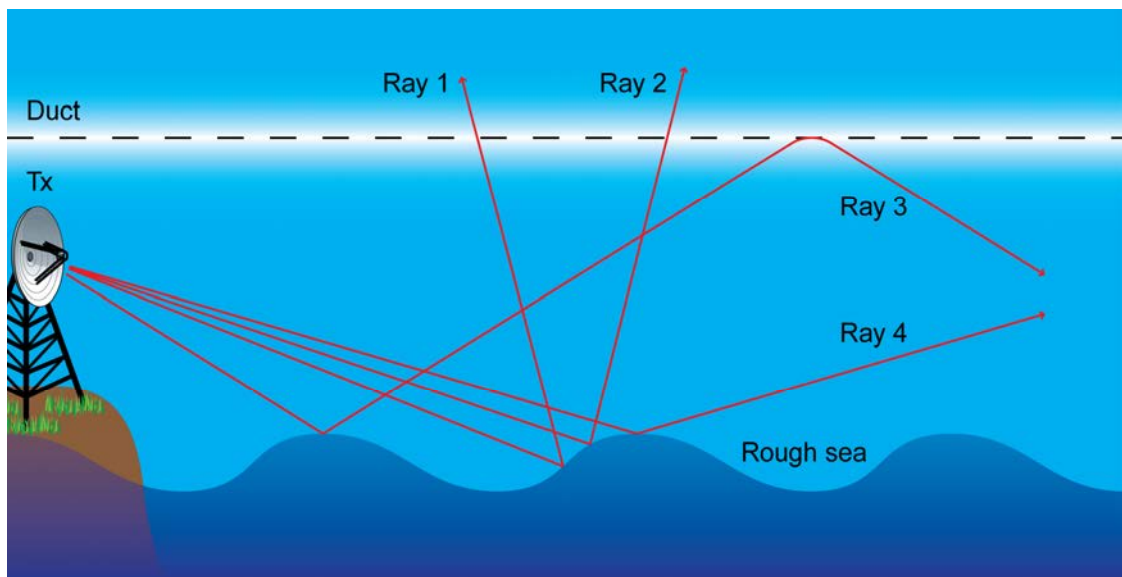
Figure 7.3: Angular propagation in the duct.

7.4   Suggested method for measuring angular spectrum in and outside of the duct

Our large array appears capable of resolving angle of arrival (AoA), however due to its design it is limited to plus or minus 0.5 degrees. In order to prove the duct acts as an angular filter and to establish how much energy is retained and how much is lost we should be able to look at all possible angles into the receiver both in and above the duct.

In addition we do not need to resolve the actual angles of arrival, a distribution would suffice. Thus a correlation of a known series or code would be sufficient to give us a reasonable understanding of the spread of AoA at a receiver.

In [52] the authors discuss correlating a received GPS signal in order to monitor sea waves. Their process is readily adaptable to measuring an AoA distribution both within and above a known duct.

An experimental system derives from the components of the very large array is shown in Figure 7.4. By transmitting the GPS code at 10.7 GHz and then comparing it with another received at the far end a correlation curve showing AoA spread should be achievable. The antenna would be mounted at two heights (or more as the experiment suggested) so as to measure AoA both within and above the duct.
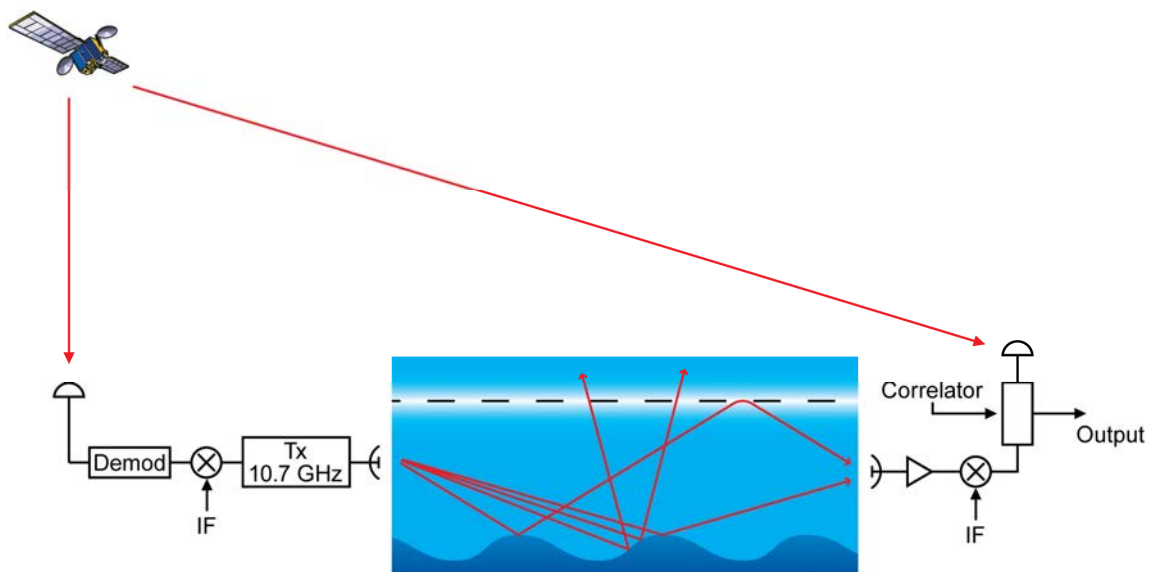
Figure 7.4: Suggested AoA experiment.

7.5   Conclusions

In this brief chapter I have discussed how the duct most likely acts as an angular filter. This has implications for radar measurement of sea state as some information may not be available to a receiver depending on antenna height.

7.6 References

[50] Long, M.W., "Radar Reflectivity of Land and Sea", Artech House, 2001.

[51]   The Department of Geology at the University of Puerto Rico at Mayagüez, "Waves", last viewed 31 March 2011, http://geology.uprm.edu/MorelockSite/morelockonline/2-waves.htm).

[52] Jian Cui et al, "Wave remote sensing by GPS", IEEE Oceans '10, May 2010.

Chapter 8

Short range propagation experiments, conclusions and results

In this chapter, a series of short range propagation experiments between the jetty at Lucinda and Orpheus Island are examined. The experiment was used to further validate PEM models and to assess our duct height estimation technique. The results are used to inform other chapters.

```
┌─────────────────────────────────────────────────────────────────────┐
│                    ┌───────────────────────────────┐                │
│                    │         Chapter 1             │                │
│                    │  Introduction and Thesis format│                │
│                    └───────────────────────────────┘                │
│                                  │                                  │
│                    ┌───────────────────────────────┐                │
│                    │         Chapter 2             │                │
│                    │ Microwave propagation, measurement and simulation│               │
│                    └───────────────────────────────┘                │
│                                  │                                  │
│                    ┌───────────────────────────────┐                │
│                    │         Chapter 3             │                │
│                    │ Radio-meteorology and the tropical littoral zone under study│          │
│                    └───────────────────────────────┘                │
│                                  │                                  │
│                    ┌───────────────────────────────┐                │
│                    │         Chapter 4             │                │
│                    │ Meteorological measurement and prediction techniques│             │
│                    └───────────────────────────────┘                │
│                                  │                                  │
│                    ┌───────────────────────────────┐                │
│                    │         Chapter 5             │                │
│                    │ Propagation simulation in a duct using TERPEM and AREPS│        │
│                    │ and observations supporting the accuracy of these models│      │
│                    └───────────────────────────────┘                │
│                                  │                                  │
│                    ┌───────────────────────────────┐                │
│                    │         Chapter 6             │                │
│                    │ Some observations of over the horizon microwave radio│         │
│                    │ propagation inside the tropical maritime evaporation duct in│  │
│                    │ North Queensland, Australia   │                │
│                    └───────────────────────────────┘                │
└─────────────────────────────────────────────────────────────────────┘
```

Chapter 1
Introduction and Thesis format

Chapter 2
Microwave propagation, measurement and simulation

Chapter 3
Radio-meteorology and the tropical littoral zone under study

Chapter 4
Meteorological measurement and prediction techniques

Chapter 5
Propagation simulation in a duct using TERPEM and AREPS and observations supporting the accuracy of these models

Chapter 6
Some observations of over the horizon microwave radio propagation inside the tropical maritime evaporation duct in North Queensland, Australia

Chapter 7
The evaporation duct as an angular filter

Chapter 8
Short range propagation experiments, conclusions and results

Chapter 9
Methods for extracting angle of arrival and duct heights

Chapter 11
A theoretical design for long range over ocean microwave links using the tropical evaporation duct

Annex 1
Informing the Military Community

Chapter 10
Mathematical methods for measuring angle of arrival in over ocean propagation experiments

Annex 2
Implications for designers of fixed services utilising over water paths

Chapter 12
Research and Thesis conclusions

8.1   Introduction

During these short range experiments a vertical profile of received signal strength from a crystal locked transmitter at 10.7 GHz 18.2 kilometres away, propagating on an over water path inside the tropical evaporation duct, were collected. The received signal was collected with a ten element array made up of 21dBi horn antennas and LNBs as described in Section 8.3.

The path of 18.2 km was chosen for a number of reasons. Firstly a short range was needed so that we could be assured of a usable signal that would be relatively immune from other anomalies as described in Chapter 6.

In addition the path needed to be as 'over sea' as possible to remove the unknown effect of the land. The availability of both the Lucinda sugar loading jetty and the James Cook University, Orpheus Island Research Station (OIRS) made this location ideal. A number of short experiments were conducted between 1999 and 2008.

In addition a number of measurements of near ocean atmospheric measurements were taken and from these the height of the evaporation duct inferred. These measurements were compared to duct height calculations using TERPEM, which are based on the 'bulk parameter' method of calculating duct height.

Instrumented floating buoys are used to measure the atmospheric parameters of temperature, humidity and atmospheric pressure. In addition to the radiocommunications measurements we use these experiments to verify the accuracy of duct height prediction in certain wind speeds.

The collected data was compared to a simulated field using the TERPEM parabolic equation based propagation software [53].

This Chapter describes a short range experiment used to compare PEM models with known duct heights and received signal strengths. In this campaign a radio array deployed along with the spar buoy were used to determine path losses and actual duct height.

A large amount of data was collected and examined to form the conclusions presented in this chapter. .

Other short range experiments were also performed, but without the benefit of the spar buoy to give a derived duct height these campaigns were not as useful for comparison with the PEM models as those where we had direct duct height measurements.

8.2   May 2001 duct height estimation experiment

As can be seen from the duct height estimation, both the path and the duct vary rapidly, so for clarity single representative samples will be explored

We know that he evaporation duct traps radio emissions. This can be beneficial if extended range is sought, but if a radar detector is above the duct an obstacle, or even an incoming missile, may not be detected.

In this five day experiment studies of the evaporation duct were carried out in order to classify the duct in the tropical zone. Duct height measurements were taken during the entire period of the experiment although only results for the period of the radio experiments are analysed further. This will enable corrections to be made to the design of various radio systems, including ship borne radars based on the use of commercially available prediction packages, TERPEM and AREPS as described in previous chapters.

In some cases temperature and humidity were measured at 6 heights above the sea; one measurement of atmospheric pressure was taken. From these values the atmospheric refractivity known as the M factor were calculated and a curve was fitted to give equivalent duct height as outlined in Chapter 4.

In Figure 8.1 the duct height is plotted with time. The thick line represents a polynomial curve fit giving approximate smoothed duct height over the diurnal cycle. The rapid variations are considered to be the effects of micro changes in local temperature and humidity and possibly some pressure changes due to wind gusts. These may also represent actual changes in the duct although no rapid fluctuation in our RF transmissions were found to support this.
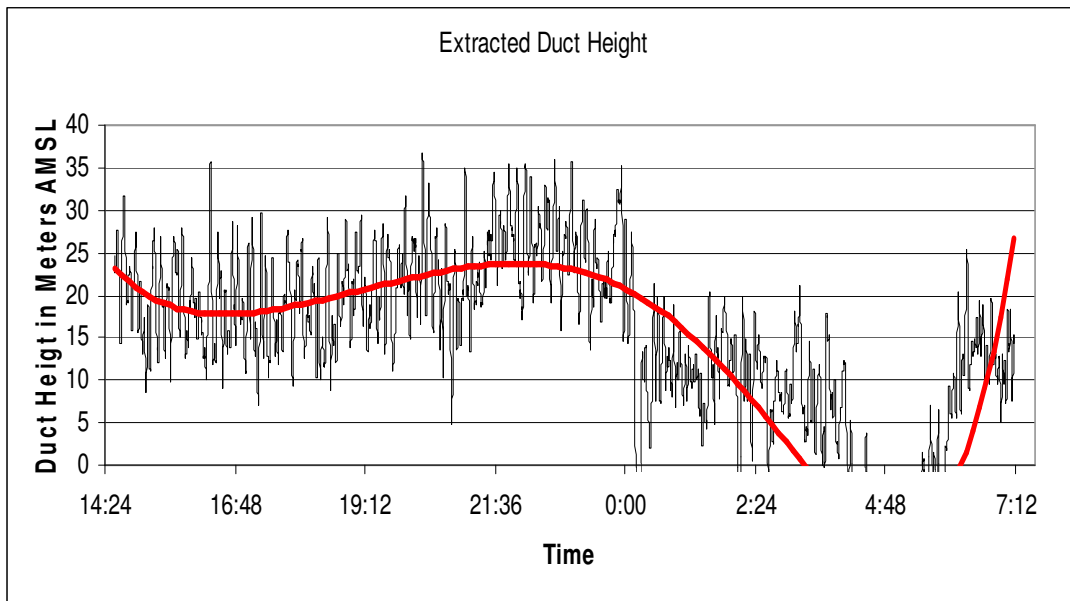
Figure 8.1: Duct heights for 14:24 – 07:12 on 14 and 15 May 2001

Examining this curve we see duct heights that fit well within the expectations.

Looking at the curve for 17:00 hours on 14 May we see a duct height of approximately 18 metres.

8.3   May 2001 array measurements

A ten-element array was used to sample the signal over a vertical profile ranging from 3.4 metres to 11.5 metres above sea level. The array consists of ten 21 dBi horn antennas, each with a commercial Ku band LNB, a switch box and control system. Measurement was taken via a spectrum analyser.

In this case the receivers were mounted on a rigid structure to reduce error from defocusing due to mast bending observed in Chapter 6. The array was calibrated through the switch to reduce errors.

The array was mounted at the end of a 6 km long Bulk Sugar Terminal jetty at Lucinda in Queensland. A photograph of the array can be seen in Figure 8.3 where the first use of the horn antennas is evident.

The transmitter was 18.4 km away on Orpheus Island at the James Cook University research station. The path was entirely over water.

Figure 8.2 shows the path, the lower red line is represented in this experiment. The upper red line represented an experiment where unfortunately the solar panels powering our transmitter were stolen by a passing yachtsman.

The array was used to measure a vertical profile, which was calibrated using figures on pages 141 and 142 and compared with various PEM propagation software packages. In this chapter we compare some measured results using TERPEM. The outputs for TERPEM for the ducting environment measured are presented in Figures 8.4 and 8.5.
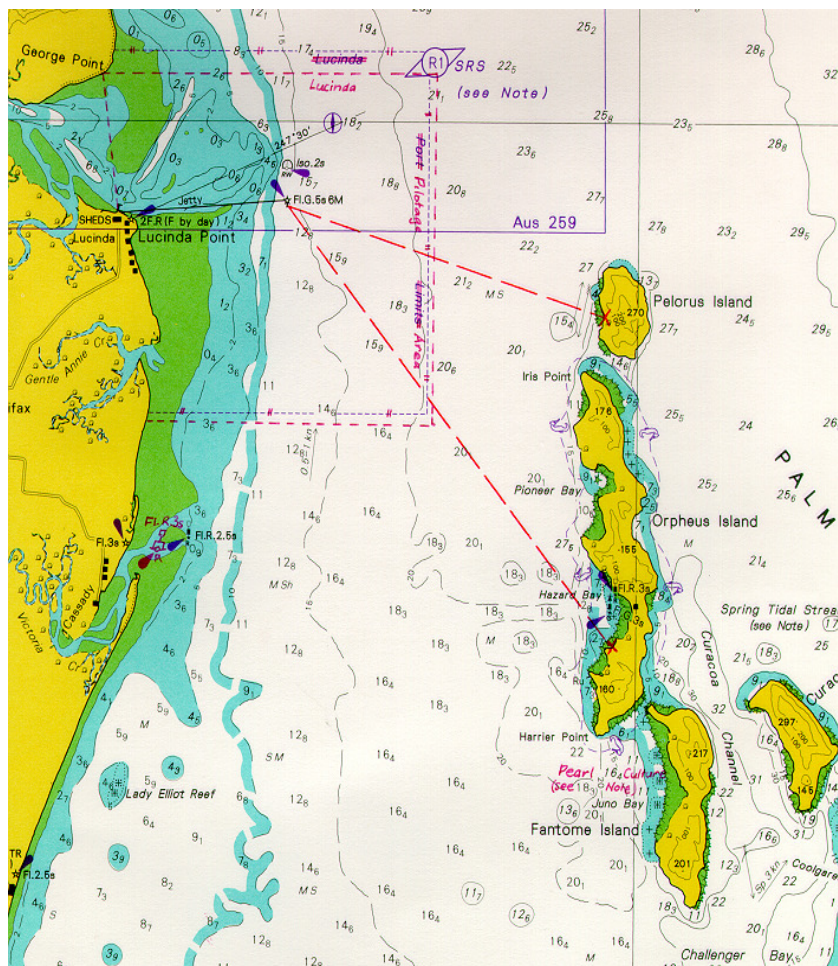
Figure 8.2: The experimental path.

Figure 8.3: The receiver array.

Figure 8.4 shows path loss over distance and height as simulated using TERPEM. A vertical slice of the profile is shown in Figure 8.5 for the duct and distance of this experiment. This profile can then be compared with a slice taken by the array to verify the simulation package's accuracy and applicability which is overlayed.
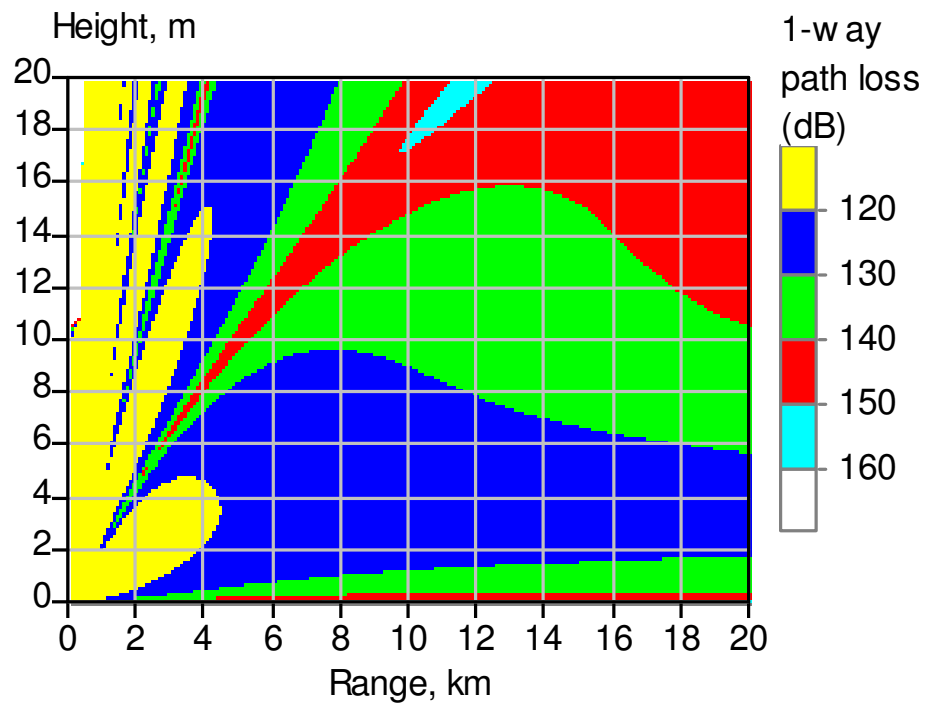
Figure 8.4: TERPEM plot for 18m duct.

The dashed line in Figure 8.5 is a TERPEM vertical slice at 18.4 km which simulates the path under test. Wind speed for this measurement was 20.4 kph (6.7 m/s), temperature was 26.0 degrees with a relative atmospheric humidity of 57% measured at the BoM Lucinda AWS at 17:00.

The solid line in Figure 8.5 is the received signal strengths for the array. This represents an average of five signal measurements taken over approximately one minute. These are calibrated for error and to show path loss as outlined below.
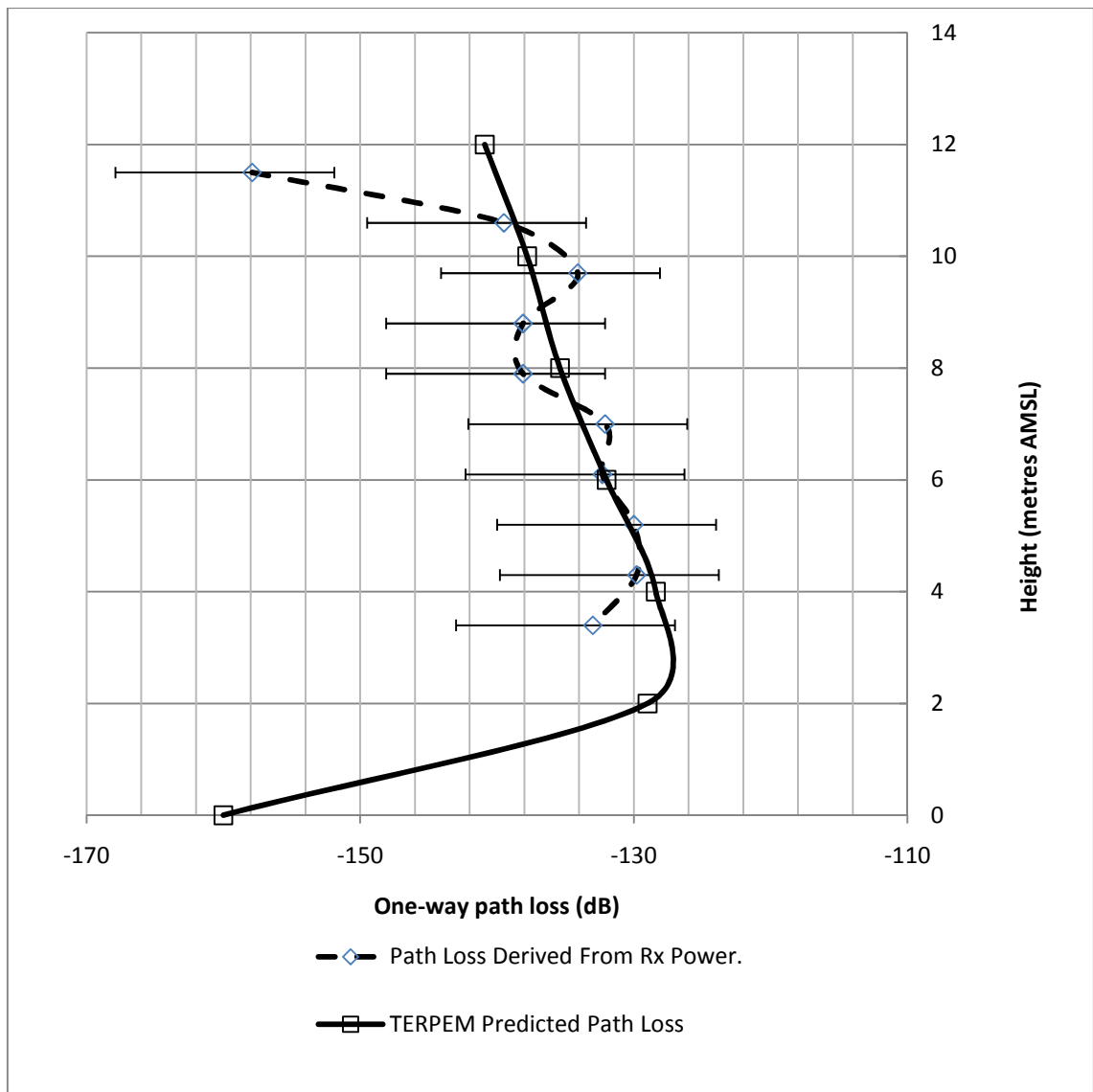
Figure 8.5: Received signal strengths.

Looking at Figure 8.5 we can see that the predicted vertical profile is evident in both the measured data and the simulation. To calibrate the two curves we take the sensor at 3.4 metres. From Figure 8.5 this represents a path loss of 127.5 dB.

Path loss can be calculated from the measured data by:

$$L_P = P_R - G_T - G_R - G_{LNB} - P_T + L_S \qquad (8.1)$$

Where P_R is the received power,

G_T is the transmit antenna gain, 32 dBi; Possible pointing and focussing errors +0/- 3dB

G_R is the receive antenna gain, 21 dBi; Possible pointing error +/-0.1 dB

G_{LNB} is the low noise amplifier (LNA) gain, 50 dB; Drift error +/-3 dB
(Drift)

P_T is the transmit power, 20 dBm; +/- 2 dB (measured over time in shade and
sunlight)

and L_S are system losses 10.1 dB. (Measured)

The total estimated and measured errors for this system are +6dB and -10 dB (i.e. between 6 and -10 dB). Other possible uncertainty includes scatter from rough sea, losses (or gains) through non-homogeneous duct and losses due to propagation through aerosols. These cannot be specified and are thus ignored however a general appreciation of temporal variation (over a timescale longer than reflections from choppy seas) can be had from Figure 8.7.

The uncertainties associated with the transmit end would exhibit throughout the receive array, that is <5dB. While care was taken with both focussing and 'panning' (aiming a parabolic dish) these errors would still be evident. The author is experienced at aligning microwave systems and feels -3 dB would be a reasonably accurate estimate for all of these uncertainties.

The other uncertainties are independent of each other. At the receive end the horn antennas used had quite wide main beams and were vertically aligned with each other. Thus pointing error here would be predominantly a 'panning' issue with minimal difference between elements. The LNBs however were subject to different sun/shade combinations and had shown up to -3 dB drift in gain with an average of -1 dB during calibration.

A final uncertainty is that caused by the difference between AMSL and actual sea height with tide. With a buoy the duct will always be determined above actual surface height, while the array is fixed. This means that over the measurement period there would have been a difference of 1m between predicted and actual duct height if the prediction were accurate.

Should further combined buoy and radio experiments be conducted this uncertainty could be used by measuring and using actual sea level at each sampling time.

At 3.4 metres the received signal is – 20.1dBm equating to a path loss of –133.0 dB, compared to the predicted -128.0 dB, and taking into account uncertainties. These uncertainties are dominantly negative in the range of -4dB 'average uncertainty' and ignoring antenna number 10, this is considered to be a good match.

Other pictorial representations of modelled verses actual receive levels are shown in previous chapters. However to properly classify the PEM models where we have known duct heights we represent the mean error for each of 10 received signal strength verses predicted path loss for 15:00 – 19:00 on 14 May when the duct was reasonable stable.

An obvious anomaly is with element 10. Given this is the same LNB as used in previous experiments where a lower than expected signal strength was noted it is possible that LNB 10 was faulty. The antenna used for element 10 was different for the two experiments removing any possibility of a faulty antenna casting. Thus LNB 10 was faulty and was discarded in later experiments.

Errors for the gain of the receive antennas could also explain some of the differences although each of the horns used in this case was calibrated with a main beam difference of only +-/0.1dB. These errors could be reduced via more careful calibration.

However from these measurements and taking errors into account we can still conclude that TERPEM gives a very good representation of expected low-level path loss in the typical dry season weather conditions predominant at the time of measurement.

8.4   July 2001 Experiments

A second propagation experiment was conducted in July 2001, in this case to test the accuracy of the AREPS PEM software. During this campaign we were unable to arrange for a crane to launch the spar buoy, and so the experiment was conducted

without actual duct height estimations. AREPS contains a function which will estimate duct height using bulk atmospheric measurements which are input by the user. The duct height was determined from within the AREPS program using bulk weather parameters derived from the Lucinda AWS and our own commercial weather station.

Following the May expedition and prior to the July experiments all of our LNBs were retested. and had concluded that two were unstable. Thus only 8 receivers were used in the July experiment. In addition the actual transmitter was much more carefully calibrated to remove as much uncertainly as possible and each receive element was calibrated against a known power source before being placed on the tower.

During this experiment we recorded around 10 hours of measurements on 11 and 12 July. Selected series and interpretations are presented here.

Figure 8.6 shows the results of one hour of typical averaged receive power versus the AREPS simulation. This measurement is from 22:00 – 23:00 on 11 July. This is presented to highlight the possible errors inherent in selecting a particular time to compare a received power with a simulation.

The temperature at 22:00 was 18 Degrees Celsius, Humidity was measured at 73% with a 13 kph (3.6 m/s) wind from the South East. Barometric pressure was 1021 hPa. It was partly cloudy, but night-time conditions.

Using weather data input from the BoM Lucinda AWS, AREPS predicted a stable duct at 18m. As these conditions remained relatively stable throughout the hour (measured at the Lucinda AWS) except for the wind shifting to the East South East and strengthening to 15 kph (4.1 m/s) by 23:00, there is no reason to believe the duct would have fluctuated significantly in that time.
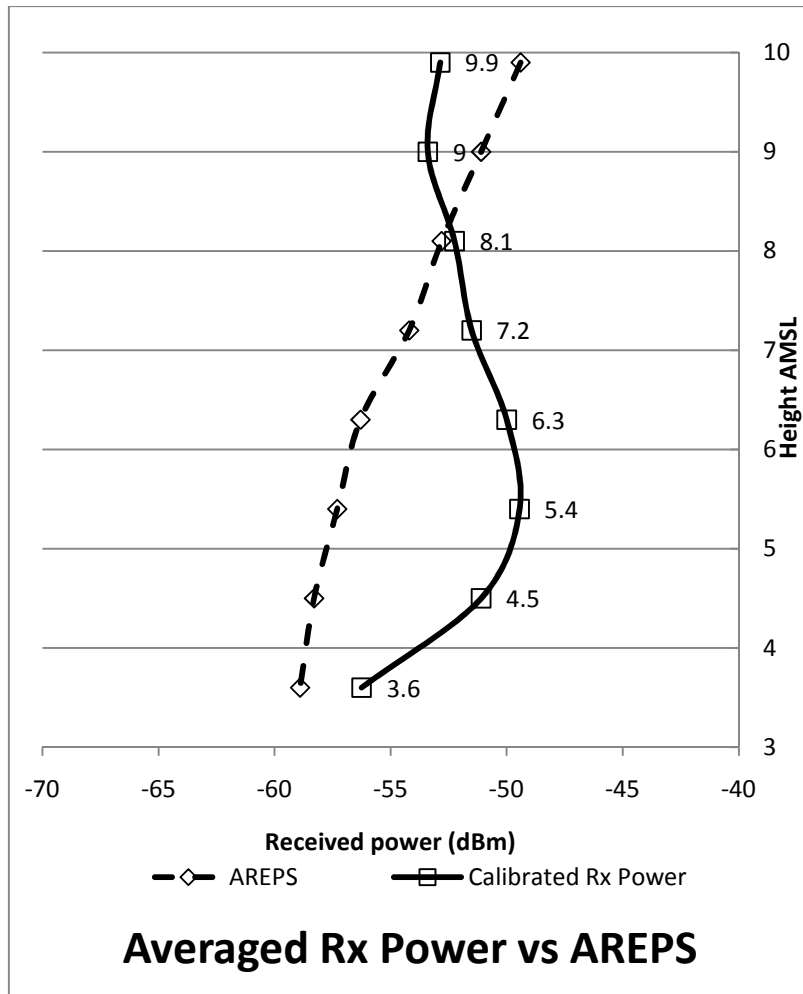
Figure 8.6: One hour averaged signal vs AREPS simulation 22:00 Hrs 11 July 2001.
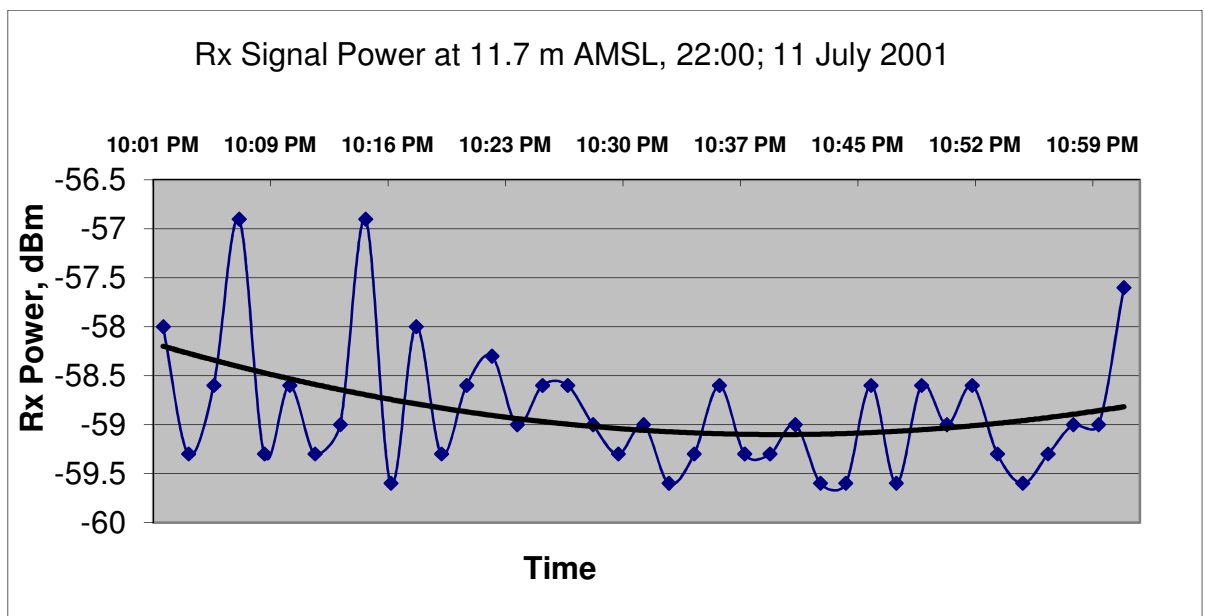
Figure 8.7: Actual Rx Power levels for 22:00 – 23:00 on 11 July 2001.

Figure 8.7 shows the fluctuation in actual received power levels from a separate (un-calibrated) receiver at a height of 11.7 m. The data set from this receiver is not included in the averaged figures in Figure 8.6 but serves to separately show the temporal variation in received signal strength measured at 2 minute intervals. Thus this variation would be due to slow moving events such as the passage of an ocean swell or variation in the duct height and strength along the path. Of note is an approximately 2.5 dB variation over a reasonably short period.

To resolve fast moving events, such as that caused by reflection from ripples and chop would require a much faster sampling rate.

Figure 8.8 shows a snapshot comparison at 14:00 hours on the 11th of July 2001. The AREPS simulation is the broken line, the received power is the solid line. In this illustration the fluctuations of up to 20 dB caused by the abovementioned events are readily observable. Of note the wind at this time was measured by us at 26 kph (7.2 m/s) and the sea was observed to be choppy with white capped waves exceeding about 1.5m (eye observation only).
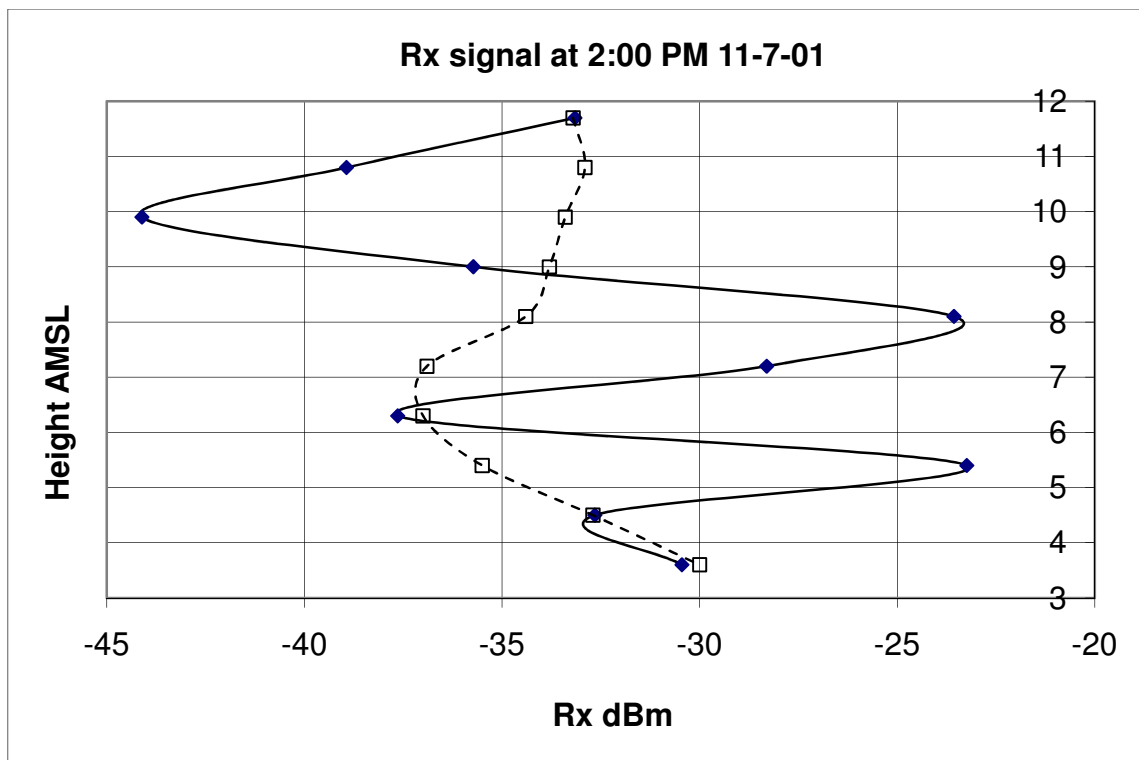
Figure 8.8: A 'snapshot' comparison at 14:00 Hours on 11 July 2001.

From Figures 8.6 and 8.8, and taking into account uncertainties in calibration, deployment and those inherent in averaging a fluctuating signal, the author feels that AREPS gave a good approximation of both received signal strength and thus logically duct height, in the absence of other duct height estimations.

8.5   Duct height and wind speed

An evaporation duct is in essence the difference in refractive index caused by saturation of the air just above the sea. This varies with height, but is also dependent on wind speed for mixing. If there is no wind the duct has been shown to collapse very quickly [54].

Measurements undertaken by the research team have shown a clear link between duct height and horizontal wind speed.

An acceptable approximate of this dependence is given by Kulessa and Hermann in [54] and is:

$$d(u) \approx \frac{d \max}{1 + d \max DA^2 / u^2} \qquad (8.2)$$

where d is the duct height, d max is the 'peak height' the duct reaches, u is wind speed and D and A are constants related to duct height dependence on atmospheric and water temperatures and humidity, these parameters are referred to as 'bulk parameters'. Sea surface temperatures on the day were 26° Celsius, measured from the NOAA satellite.

This equation has two solutions, but only one is stable within the bounds of measured wind speeds. Using realistic inputs to calculate D and A this equation yields a duct height of approximately 17 metres for the measured conditions and is within expected error given the gustiness of the sea breeze on the day.

These findings agree well with the duct heights derived from spa buoy data shown in Figure 8.1.

8.6   Conclusions

This series short range of experiments presented above have shown that the radio data, simulations, spa buoy calculations and duct height vs. wind speed theories agree very well in practice. Provided either bulk parameters or wind speed are known a duct height can be estimated and from this one of the PEM packages will give a very good understanding of general RF behaviour in the duct.

Thus all of these tools, PEM models and duct height estimation techniques, have been shown in this case to be reliable for general estimation of radio-wave propagation inside the duct and for estimating duct height with an accuracy suitable for design and operation of RF systems.

8.7   References

[53] Levy, M., "Parabolic Equation Methods for Electromagnetic Wave propagation", IEE Press, 2000, ISBN 085296 764 0.

[54] Kulessa, A. S., Heron, M. L. and Woods, G. S., "Temporal variations in evaporation duct heights", Proceedings of Workshop on Radio Science 1997 (WARS 97), National Committee for Radio Science, Australian Academy of Science, pp. 165-170, 1997.

Chapter 9

Methods for extracting angle of arrival and duct heights

In this chapter the design of the equipment used to gather our radio propagation data is discussed and we look at a cost effective 16 element array that was designed by the author and installed by the team. One research publication resulted from this work.

Chapter 1 Introduction and Thesis format	
Chapter 2 Microwave propagation, measurement and simulation	
Chapter 3 Radio-meteorology and the tropical littoral zone under study	
Chapter 4 Meteorological measurement and prediction techniques	
Chapter 5 Propagation simulation in a duct using TERPEM and AREPS and observations supporting the accuracy of these models	
Chapter 6 Some observations of over the horizon microwave radio propagation inside the tropical maritime evaporation duct in North Queensland, Australia	
	Chapter 7 The evaporation duct as an angular filter
Chapter 8 Short range propagation experiments, conclusions and results	
Chapter 9 Methods for extracting angle of arrival and duct heights	**Annex 1** Informing the Military Community
Chapter 10 Mathematical methods for measuring angle of arrival in over ocean propagation experiments	**Chapter 11** A theoretical design for long range over ocean microwave links using the tropical evaporation duct
	Annex 2 Implications for designers of fixed services utilising over water paths
Chapter 12 Research and Thesis conclusions	

9.1 Smaller arrays up to ten elements

Simple arrays were used for the short and long distance measurements in this project as described previously. Initially these were constructed from slotted waveguide antennas with a gain of 12 dB. Mounted vertically they served as a good horizontally polarised receiver array for a series of measurements.

In this arrangement each array module was connected to a commercial Ku band LNB and the signal, at about 900 MHz, was sampled via a simple sensor connected to a switch box controlled with software.

Figure 9.1: Ten element array using slotted guides and guyed pole.

Figure 9.2: Ten element array using horns and rigid structure.

The slotted guide array is shown in Figure 9.1. It was mounted at the end of Lucinda Bulk Sugar Terminal jetty on a simple pole. As can be seen in the photo the system was subject to weight and wind load bending which cause some minor received signal strength errors in our measurements.

To overcome this, the short range experiments were carried out using the same LNBs connected to the horns manufactured for the large array, these were mounted to a rigid frame eliminating the defocusing caused by mast bending. This system can be seen in Figure 9.2.

In both cases the same measurements and switch matrix was used to collect signal strengths.

Calibration was carried out prior to installation using a far field transmitter. Each LNB unit and associated cable and connector was numbered and calibrated throughout the measurement range. This calibration was rechecked after installation using a simple leaky source connected to a transmitter thus yielding the relative differences through the entire switch matrix for verification.

9.2 The large 16 element array

Evaporation above warm tropical oceans causes a significant change in the refractive index of atmosphere immediately above the sea surface. This localised change in the refractivity gradient causes ducts, regions where RF energy becomes partially or fully trapped. Temperature inversions, which are caused by advection or subsidence, at higher elevations, also cause ducts, which result in the partial trapping of signals. Enhancements in signal amplitudes in some regions are offset by depletions elsewhere colloquially referred to as "radio holes" [55]. One method of locating these holes in real time would be via a-priori knowledge of AoA into a ship borne array.

This chapter presents the theory design and construction details for an 11 GHz array constructed and deployed on Orpheus Island and reviews other equipment used by the group to determine duct heights. The array consists of an 11 GHz transmitter; capable of being Frequency Modulated (FM) and a 16 element horn array receiver. The transmitter is typically placed below the radio horizon (at 5 metres) transmitting over a warm tropical ocean, at Lucinda 100 km north of Townsville, Queensland Australia. The receiver array will be situated on Orpheus Island, 18.5 km distant.

Previous work on AoA measurement in ducts [56] has relied on expensive arrays using phase matched waveguide and injection coupled low noise amplifiers (LNAs). It was thought this complexity was necessary to obtain the phase accuracy required to calculate angles of arrival with the required precision of 0.1 of a degree.
Not only is this technique expensive requiring custom made LNAs and a wave-guided local oscillator signal, in the Australian environment the extremes of temperature between full sun and shade would cause uneven heating of the waveguide runs and thus introduce additional phase error.

Due to funding constraints we were unable to afford the expense of a fully phase locked array. To continue the work beyond simple amplitude profiles, the author needed to come up with a concept for an array that could be built for under $5,000 and use as far as possible commercial off the shelf products. This chapter describes the array concept, which has been constructed and tested. The analysis of the results obtained during a campaign in October 2007 is beyond the scope of this research.

Inexpensive commercial LNAs are available in the satellite broadcast bands between 10.7 and 11.7 GHz. A number of these LNAs were purchased and found to operate adequately at 10.2 GHz outside of the terrestrial fixed link bands. This is important to avoid interference to fixed links and interference from fixed links causing errors in our experiments.

To match these LNAs we constructed sixteen 21 dBi horn antennas. These too were constructed by the author with economy in mind. The antennas were sand cast out of aluminium and the transitions to the LNAs filed by hand. Powder coated and fitted with a plastic radome to prevent moisture ingress to the LNAs, each antenna cost around AUD$50. In such a design the main problem lies in accurately compensating for phase drift in the 15 free running LNAs. This cannot be done by measuring the incoming signal as the duct causes phase changes and it is these which we must measure.

In front of the array at a known and accurately measured distance we place a second transmitter operating at a known frequency separation from the distant transmitter. This system serves as a single local oscillator for the entire array.

This second crystal locked source, 2 MHz above the measured source at 10.5 GHz, transmitted into the front of each horn over a surveyed path. The stability of the sources is important but not vital, as only a phase comparison is done not an absolute measurement. The sources are spaced closely at 2 MHz so that a good margin above the Nyquist sampling rate can be maintained using an inexpensive 'PICOLAB' analogue to digital (A to D) converter sampling at 50 MHz.

This arrangement gave two signals into the sampling system which are altered equally by the test array. The phase and amplitude errors, detected in this way, can then be

corrected for the signal under test and from this the phase and amplitude of the signals and thus the angles of arrival derived. This process is depicted below in Figure 9.3 and the completed down-converter and phase box shown in Figure 9.4.

9.2.1 Characterising duct behaviour

The effective duct height is the most important parameter to be determined; from it the refractivity profile can be inferred. Atmospheric measurements were made using environmental measuring equipment depicted in Figure 5.12. This equipment measures temperature, pressure and humidity along with wind speed and sea surface temperature.
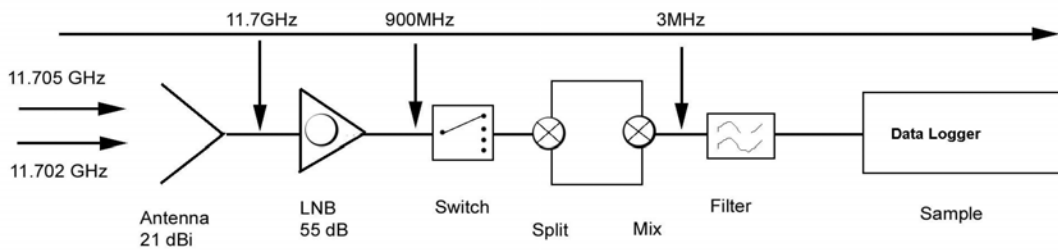
Figure 9.3: Down-conversion Process.
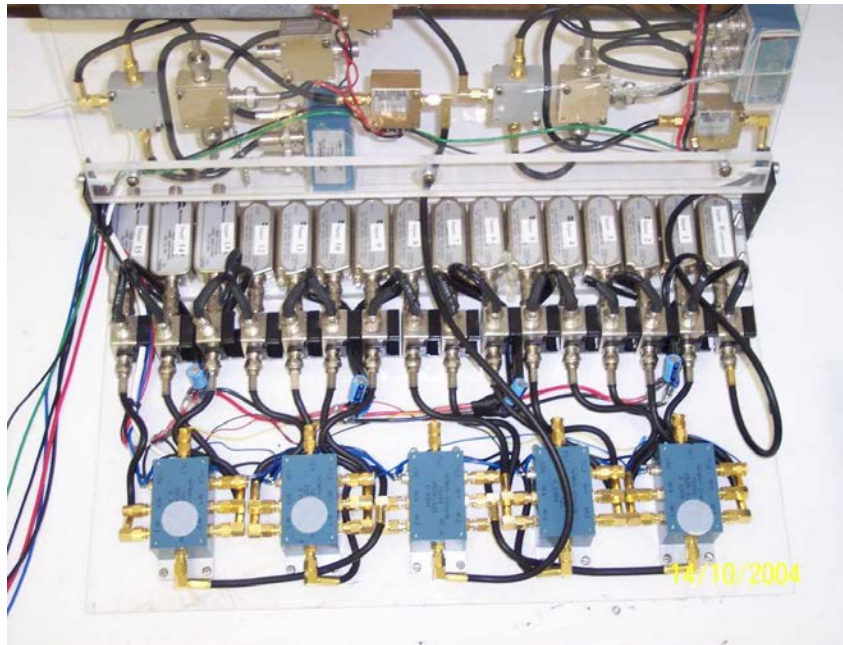
Figure 9.4: The down-converter built in hardware.

The equipment produced good results [57], but is bulky and for stable readings must be deployed away from any large structure such as a ship.

A prime application of ducting knowledge is to ships at sea and the effect on radar. Clearly atmospheric bulk measurements are not practical in the operational environment. Another method of detecting duct parameters is through a receiver array detecting a signal from another ship or a fixed station. The received power levels could then be compared with those calculated using the PEM. As previously described a number of programs are available to simulate the PEM such as AREPS [58] and TERPEM [59].

AoA for signals propagating in a low duct, such as characterised by the oceanic evaporation duct, can be expected to arrive at a receiver over a range of +/-0.5 degrees. The duct can be characterised if these angles of arrival and amplitude variations with height are known. In order to measure complex amplitude and from it infer AoA, a large array is needed.

Previous AoA experiments have been carried out by Webster Et Al [60]. The array used in these studies was purpose built using locked local oscillators and all feeder runs were waveguide. This array, with substantial waveguide hardware, would be bulky and difficult to fit to a small ship or tower. In addition the construction of a similar array for this project was estimated to cost in excess of AUD$250,000. Our research was funded by a small Australian Research Council grant of only AUD$18,000. Another method had to be found!

The author's complex array design, once constructed consisted of 16 elements spaced at 0.9 metres operating at a frequency of around 11 GHz using commercially available parts from the domestic Ku band satellite market. With the data collected from this arrangement it is hoped to be able to measure angle of arrival to within 0.05 degrees using an improved Fourier process. More accurate measurements are likely using more complex measurement processes such as Maximum Likelihood Estimation (MLE). The system has been designed in such a way that the data can be collected and the software modified as more accurate data is needed.
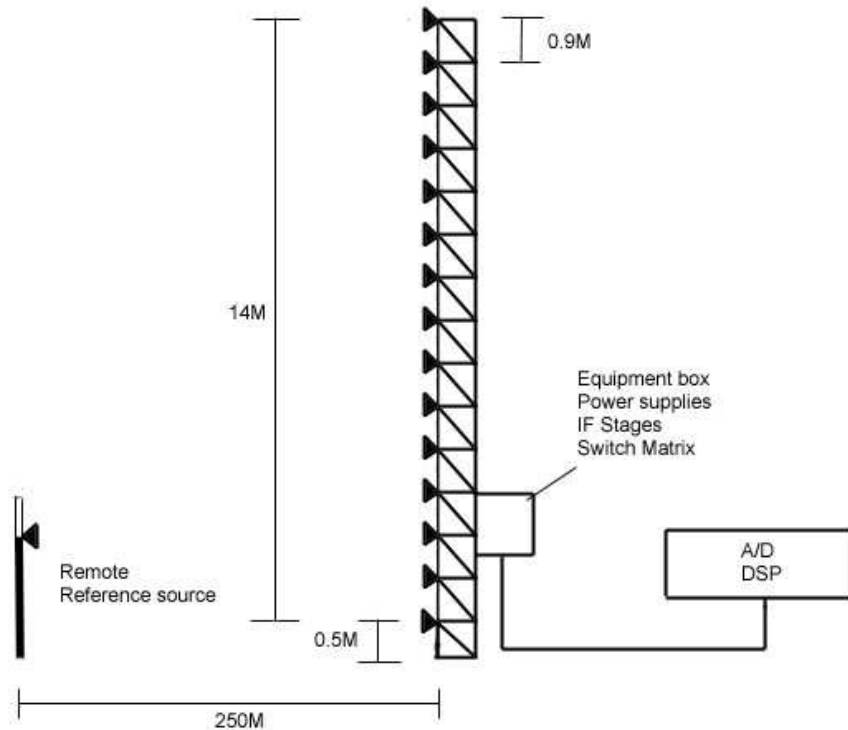
Figure 9.5: Schematic of the installed array.

9.2.2   A description of the array

A schematic diagram of the array is shown in Figure 9.5 with a diagram of how the whole radio and meteorology experiment was installed in Figure 9.6. The array consists of fifteen 12 dBi gain horn antennas, spaced at 33 wavelengths; this spacing was chosen to avoid aliasing. At 11 GHz the wavelength is 2.7 cm, so each antenna is spaced at approximately 90 cm for a total array height of about 14 metres.

Each of the horn antennas is sand-cast aluminium, costing less than AUD$50 each when powder coated. A photo of a horn antenna under test is shown in Figure 9.7. The gain and pattern of each horn was measured and calibrated, but each was found to be remarkably accurate for such a primitive manufacturing technique. Each horn connects to a commercial LNB delivering 51 dB of front-end gain and down-converting to

900 MHz. Each LNB cost AUD$100. The local oscillator of each LNB is free running. That is the LNBs are not frequency or phase locked together in any way. Phase and frequency locking would have rendered a more accurate solution but would have been cost prohibitive.

Instead, a second signal 3 MHz separate from the measured signal was transmitted from a source 250 metres distant. This provides a second signal free of significant propagation distortions. The composite received signal is down-converted in the LNBs, split and then mixed together. Following filtration a 3 MHz signal containing all the required amplitude and phase information is obtained and sampled in the A/D converter.
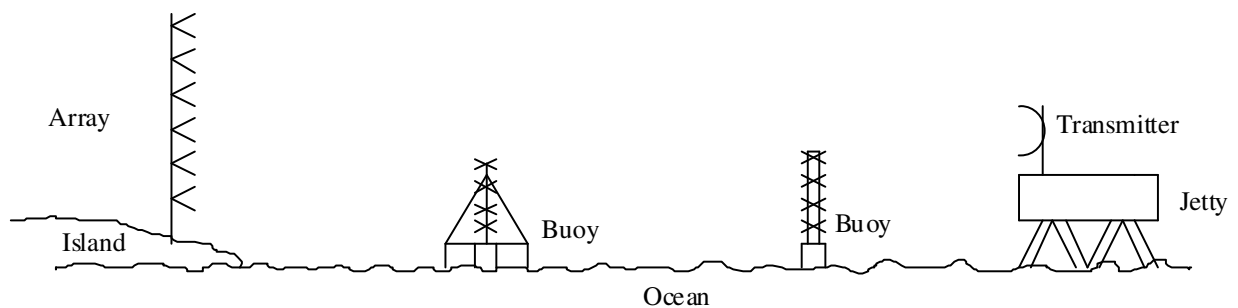
Figure 9.6: The installed large array experiment.
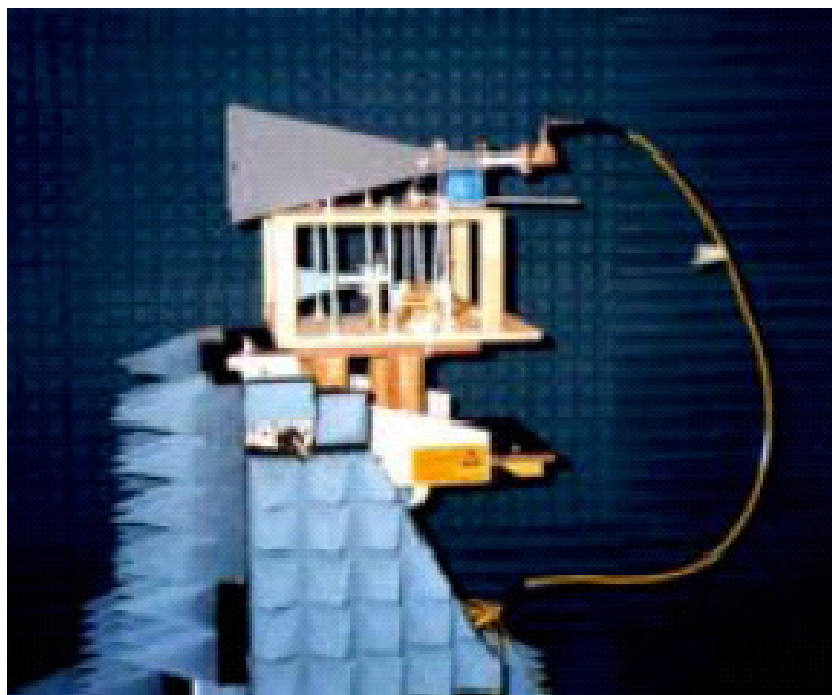
Figure 9.7: 21 dBi sand cast horns, AUD$50 each (2000).

The split mix arrangements are carried out in simple hardware, it would also be possible to sample a down-converted signal and carry out this process in software.

A number of obvious sources of error will remain present, such as changes in the propagation path of the local oscillator, producing both phase and amplitude errors. In [60] the authors state *'Simulated tests were run in which phase errors were deliberately introduced for the low amplitude signals the results showed that such errors had little effect on the derived values of AoA'* (for the Fourier method of AoA derivation).

With such a heartening discovery in mind, we set out to learn as much as possible about amplitude and phase errors in the reference signal, such as those caused by rain, reflection from the sea surface and localised atmospheric disturbances. We will take these into account where possible, but accept those beyond our control as errors in the overall system.

A signal propagating within a duct can be expected to contain a number of wave fronts associated with various modes of propagation. These modes are analogous to those in an optical fibre. Since total refraction within a duct is unlikely and since refraction is dependent upon angle of incidence, the number of modes is inversely proportional to duct height. For ducts at between 10 and 15 metres a number of modes can be expected with varying signal strengths. Reflection from sea surface clutter will also become a part of the received signal and the effect of sea state is being independently studied. The wave front impinging upon the array is therefore quite complex.

The signal, once obtained using the hardware described, above is processed within a P.C. where AoA and complex amplitude over height can be calculated. From these measurements we hope to eventually be able to accurately characterise duct height and strength through comparisons with simulations, models and meso-scale meteorological modelling of the atmosphere around Lucinda.

9.2.3 Signal processing and final output

Since the system is essentially a digital radio, its software can be changed to meet emerging needs or to gain further improvement in measurement accuracy. Initially a

Fourier based AoA detection method will be used similar to that used by Webster in [60], accuracies of around 0.05 degrees are expected. A more complex methodology is also possible and will be developed once the antenna is deployed. Based upon the known signal characteristics and estimated angles of arrival, the MLE method is expected to deliver AoA accuracies within 0.01 degrees. This AoA data will enable a ray-tracing program to accurately predict the average height of the duct. Signals not corresponding to this average height would then represent differences in the duct height and give some idea of duct structure with range.

Complex amplitude signals will also be calculated by the system. These along with the known range can be used to verify the accuracy of various propagation models based upon the PEM.

9.2.4 The transmitter

The transmitter used a system called a 'penny feed', a simple waveguide and splash back reflector feeding a 28 dBi parabolic antenna. Figures 9.8 shows the transmitter being installed on the Lucinda jetty, the penny feed is visible in this picture. Figure 9.9 is the installed transmitter. Fabrication of a penny feed is simple and contained in many texts and on the Internet.

The actual transmitter is housed in the cabinet visible in figure 9.9 and the system is powered from the jetty power system (not shown).

Figure 9.8: Transmitter showing penny feed.

Figure 9.9: Transmitter installed on jetty.

9.2.5 Engineering considerations

Figure 9.11 shows the installed array. Orpheus Island is a remote island in the Palm Island group. It has limited resources and all materials and machinery have to be brought via a small landing craft onto the beach.

The foundations for the tower and guy ropes were dug by hand, but had to be substantial to resist potential cyclones. This meant a 1.5 metre square concrete block, dug and mixed by hand, and four 0.7m square blocks. A considerable feat for two men; (Mr Erik Lensson and the author).

The array, weighing about 215 kg, was erected lying down and pulled into position manually using ropes as shown in Figure 9.10. During this process safety was the paramount concern (as it should be for all research programs). 25 years of combined radio installation experience with 'Telecom Australia' (Becker and the author) aided us in this process. Once erect the tower was held in place by four double guy systems.

Lightning is also an issue in the tropics, on the top of the array a lightning arrester can be seen and this was connected via a 20mm earthing cable to an extensive earthing mesh.

Power to the array was 240V drawn from nearby accommodation blocks. For safety this power was buried to a depth of 600mm and shielded. Despite this the power was later damaged by building works.

This array was tested and found to work and a large amount of combined radio and associated meteorological data was collected in October 2007. While this Thesis marks the end of my formal association with this project I hope this data is useful to others in the future.

Finally, and this section seems appropriate, I would like to say thank you to the installation team. Two weeks of hot and thirsty work installing a working prototype of a very large array for measuring angle of arrival in a duct.

The installation team are pictured and named in Figure 9.12.

Figure 9.10: Raising the array by hand. The white building at the centre of the photo is the end of the jetty 18.6 km distant.

Figure 9.11: The large array installed on Orpheus Island.

Figure 9.12: The array installation team (From left to right: Erik Lensson (JCU), the author (JCU), John 'Boris' Becker (JCU), Adrian Whichello (UC))

9.3   Conclusions

This chapter has presented the design of one of our experimental tools, a 16-element array for the measurement of AoA inside the tropical evaporation duct. The entire array was constructed for less than $15,000. From the lessons learned in the construction of the array and the processes derived for AoA calculation we hope to be able to design a simple ship portable device capable of predicting duct height at sea and perhaps taking other measurements useful to determine the moisture content of the atmosphere at the time.

A significant amount of data was collected from this array along with meteorological data from deployed buoys in October 2007 and I hope this will serve to keep future students engaged for some time to come.

9.4 References and papers

9.4.1 Papers

The following papers were published as a result of this research:

Kerans, A.J., Kulessa, A.S., and Woods, G.S., "Estimation of angle of arrival using amplitude measurements across an array", Eighth Australian Symposium on Antennas Sydney, 12-13 February 2003, Session 6.

9.4.2 Seminar

A presentation was made to the CSIRO workshop on antennas in Epping in February 2004:

Kerans, A.J. (JCU), Becker, J. (JCU), Lensson, E. (JCU), and Whichello, A. (UC), "Construction of a large array on Orpheus Island"

9.4.3 References

[55] Anderson, K. D., "Radar Detection of Low-Altitude Targets in a Maritime Environment", IEEE Transactions on Antennas and Propagation, Vol. 43, No 6, June 1995.

[56] Hermann, J., Kulessa, A. et al., "Impact of elevated atmospheric structures upon radio-refractivity and propagation", Workshop on the Applications of Radio Science 2002 (WARS-02), Sydney, Australia, February 2002.

[57] Kerans, A.J., Kulessa, A.S., Hermann, J. and Woods, G. S., "Evaporation Duct Statistics Around Australia and the West Pacific", AP2000 Millennium Conference on Antennas & Propagation, Davos – Switzerland, 9-14 April 2000.

[58] Advanced Refractive Effects Prediction System (AREPS) US Navy SPARWAR, www.sunspot.navy.mil

[59] Levy, M., "Parabolic Equation Methods for Electromagnetic Wave propagation", IEE Press, 2000, ISBN 085296 764 0.

[60] Webster, A. and Scott. A, "Angles of Arrival and Tropospheric Multipath Microwave Propagation", IEEE Trans on Antennas and Propagation, AP-35 No 1, January 1987.

Chapter 10

Mathematical methods for measuring angle of arrival in over ocean propagation experiments

In this chapter, the mathematical theory behind extracting AoA information from the large array is discussed. Three conference papers were published as a result of this research.
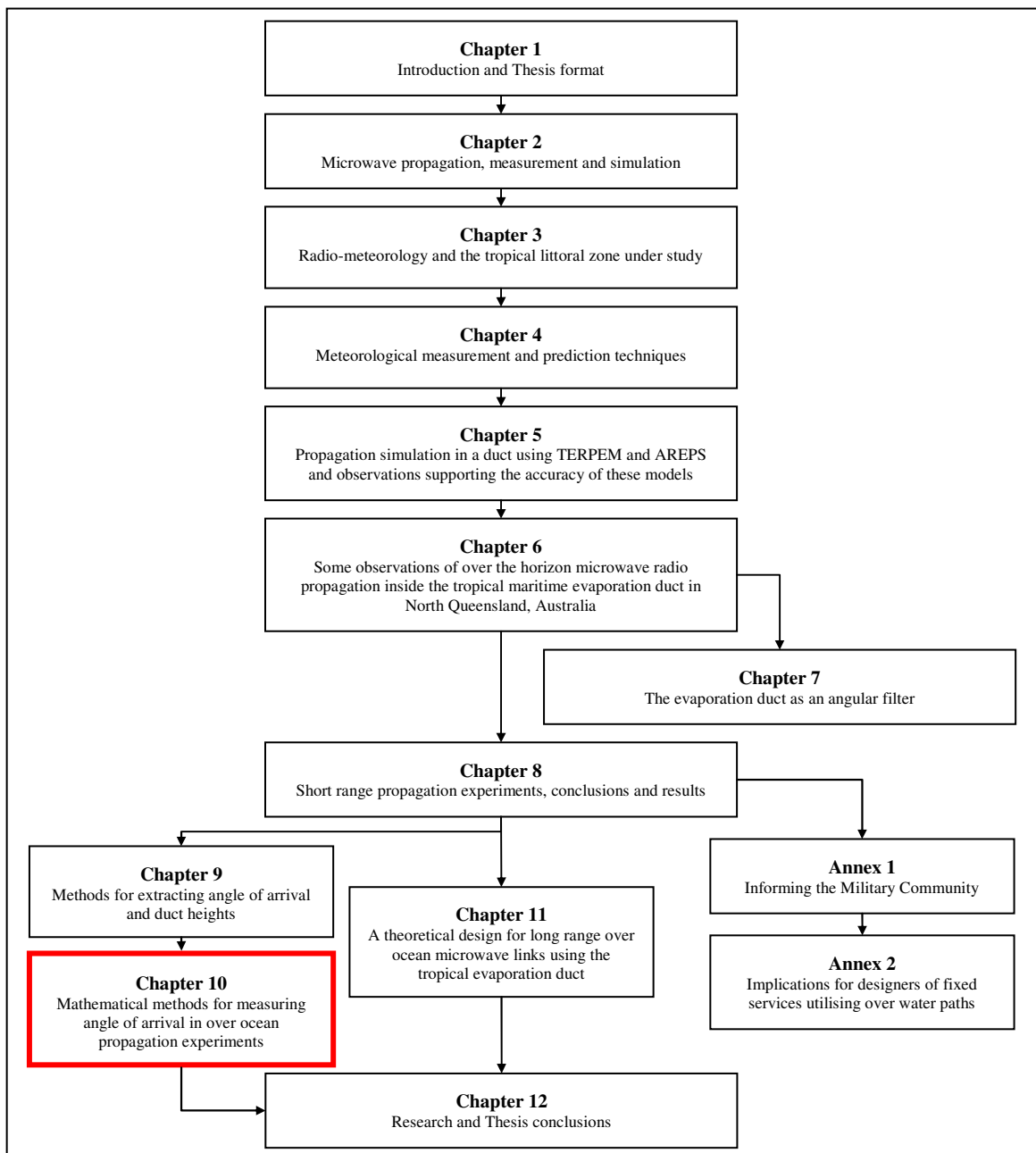
10.1   Introduction

As we have discovered in our experiments to date radio propagation experiments are a useful tool when verifying propagation models and identifying anomalies in a practical link. This chapter details a physical and mathematical method to determine amplitude profiles and angle of arrival in an over-ocean propagation experiment. A new technique for measuring the phase of radio signals received by incoherent detectors is described.

Frequency drift and offsets arising because the different receivers are incoherent are compensated for by way of a common reference signal injected into each channel. The relative phases of the unknown signals are obtained by processing the down-converted and digitised waveforms. A novel technique based on an adaptive, discrete-time quadrature delay estimator (QDE) algorithm is used for this purpose. This algorithm is insensitive to variations in the amplitudes of the input signals, and does not require an accurate prior estimate of the frequency of the input sinusoids. This approach is shown to be an accurate, low cost alternative to conventional vector measurement techniques when used with large antenna arrays and is therefore well suited to fixed link, AoA measurements.

10.2   Methodology

The ability to measure the arrival direction of a radio wave can be useful in various radio engineering applications. Finding the direction to an opposing force from intercepting radio transmissions from radar or communication equipment is clearly a handy tactic in military situations. Measuring the directions at which signals arrive in a mobile radio environment is also of interest to studies involving smart antennas [61], mobile radio propagation modelling [62] and location based servicing [63]. Long term, AoA measurements have also been employed to determine the multipath environment experienced in fixed terrestrial radio links [64].

In this application, the AoA measurements provide information on the reflectivity of the earth and the vertical structure of the atmosphere. However, to date, very little work has been reported on angle of arrival measurements in the maritime environment. Over-ocean amplitude profile measurements have been taken by numerous researchers [65],

[66] but no long-term AoA measurements have ever been reported. This is despite the fact that this region should provide interesting results from the point of view that atmospheric structures like the evaporation duct are very common in this environment.

A fundamental requirement in all AoA measurement systems is equipment with which to measure the direction of arrival of the incident radio signal. Two types of measurement system are commonly employed. One approach uses a simple amplitude measurement at the receiver. In this technique, the radiation pattern of the receiving antenna(s) provides the required angular discrimination [67]. Better directional resolution is usually possible by performing a vector measurement (both amplitude and phase) at the receiver. In this case, a multi-element antenna array is commonly used at the receiver in order to detect multiple signals with different receive angles simultaneously. Different receiver array configurations are possible [68].

The focus of this chapter is AoA measurement techniques suitable for use on the fixed, over-ocean, radio links used in our experiments. In this situation, a large array using vertically stacked elements is best suited to separating the tightly grouped elevation angles at which rays are normally received. Conventional vector measurement systems for this situation usually use a microwave frequency Local Oscillator (LO) signal that is distributed to mixers attached to each antenna in the receiver array. Each signal is therefore synchronously detected for later amplitude and phase measurement at a lower Intermediate Frequency (IF). A problem with this measurement system though, is the cost and complexity of the electronics needed to ensure signal coherence. The magnitude of the problem is only fully appreciated when it is considered that a practical receiver array may utilise 10-20 elements spread over a vertical height of 20 metres or more [69].

This chapter describes a new, vector measurement technique suitable for use with our large receiver arrays used in our AoA measurements. In this method, signals received on each element of the array are down-converted to an IF frequency using separate, low cost, Low Noise Converters (LNCs). Offsets and drift in the different LNC's are compensated for using a reference signal that is externally injected into the array. The IF signals are digitised and processed to determine the received signal amplitude profile and AoA readings. The processing technique employed is based on a novel quadrature

phase detection technique which, besides giving excellent accuracy, is also insensitive to variations in the amplitudes of the input signals. This approach also does not require an accurate prior estimate of the frequency of the input sinusoids. The theoretical basis for this technique and some practical measurements are reported.

10.3   Angle of arrival measurement technique

The usual AoA measurement technique employed for microwave terrestrial links consists of a vertical array of uniformly spaced antennas. Consider a linear array of N elements aligned along the z-axis as shown in Figure 10.1. If the incoming wave is composed of M rays, each with a distinct AoA θ_i, the vector signal received at each antenna may be written as

$$r(z) = a(z).e^{j\phi(z)} = \sum_{i=1}^{M} a_i.e^{j\phi_i} \tag{10.1}$$

where a_i are the amplitudes and ϕ_i the phases of the M components making up the incoming wave. The values a(z) and $\phi(z)$ are the total amplitude and phase respectively, resulting from the vector addition of all M incoming rays.

The amplitudes of each of the incident rays are assumed to be constant over the length of the array L, but the phase term ϕ, depends on the relative position along the array. Measuring phase with respect to the antenna at position z=0, the phase of a particular ray will be related to the AoA of the same ray by,

$$\phi_i = \frac{2\pi\, z \sin\theta_i}{\lambda} \tag{10.2}$$

where λ is the wavelength and θ_i the AoA of the i-th ray.
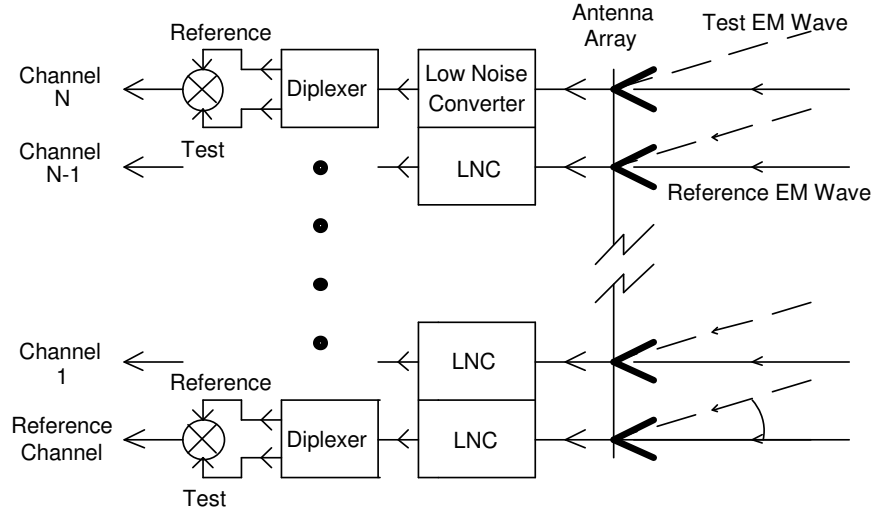
Figure 10.1: M-channel AoA receiver array.

The AoA spectrum can be obtained from the Fourier transform of the complex amplitudes r(z), measured along the array, that is

$$R(\gamma) = \int_{-L/2}^{L/2} r(z).e^{-j2\pi\gamma z} \ dz \qquad (10.3)$$

where L is the length of the array and γ is the Fourier transform variable.

Since the arrival angles θ_i are distinct, (10.2) shows that each ray produces a phase term with a unique rate of change with z. The function described by (10.1) is therefore analogous to a time varying signal composed of a sum of M sinusoidal terms, each with a different frequency. Using this analogy, the angle of arrival spectrum described by (10.3) will produce a spectrum with peaks at points corresponding to

$$\gamma_{peak} = \sum_{i=1}^{M} \frac{\sin\theta_i}{\lambda} \qquad (10.4)$$

Equation (10.4) shows the AoA of the different rays, θ_i, can be found from calculating the location of the spectral peaks, γ_{peak}. In any real measurement system the theory described previously is influenced by the practical constraint of having only a finite number of noisy samples of the function r(z). In this case, aliasing and windowing

effects will restrict the practical limits on range and resolution obtainable in the AoA measurements [64]. However, these effects are not further studied in this research.

From an implementation perspective, the only measurement needed to build an AoA sensor is the ability to measure the vector amplitudes of the signals received at the various antennas making up the array. That is, sample the value of r(z) = a(z) ∠ϕ(z) in (10.1). Practically, there can be some problems in making these measurements though. The spread in the AoA values to be measured on a typically radio link are normally very small (often <1°) and therefore precise raw measurements are important. Another problem is that the number and physical spacing of the antennas used in a typical array makes conventional vector measurement electronics expensive to build. The standard technique for making vector measurements at high frequency, synchronous detection, relies on mixing of the incoming signals with a common LO signal [69]. The low frequency output from the mixer contains the required amplitude and phase information of the incoming RF signal. Unfortunately, this scheme may be expensive to implement. The discrete mixers attached to each antenna in the array can be a large cost. The cost of the high frequency cabling needed to distribute the common LO signal to each of the antennas, is also a significant expense that needs to be considered. Finally, another potential problem with this approach is phase errors due to uncalibrated phase changes in the LO signals applied to the different mixers caused by heating and cooling of the high frequency cables and the electronics.

To overcome the high cost and potential problems of conventional vector measurement schemes when applied to an AoA measurement system using a large array, the authors have developed a new technique for this application. In this technique, antennas in the AoA array are attached to separate, low cost, LNC converter modules. Normally this type of measurement system would not be suitable for measuring phase since the LNC outputs are incoherent. This problem is overcome in the new technique by injecting a reference radio signal into the front of the array as shown in Figure 9.5. The injected reference signal has a slightly different frequency to the test signal. The signal captured by an element of the array situated at z = z_n can therefore be written as,

$$V_{RF}(z_n) = a(z_n)\cos(\omega_t t + \phi(z_n)) + \cos(\omega_r t + \varphi) \tag{10.5}$$

where $a(z_n)$, $\phi(z_n)$ are the time varying magnitude and phase terms representing the sum of the individual rays propagating via different paths from the other end of the radio link at a frequency ω_t, while φ and ω_r are the phase and frequency of the injected reference signal. If the reference signal is employed, a conventional, incoherent LNC can be used at each antenna element. The signal at each element after down-conversion is given by:

$$V_{IF}(z_n) = \frac{a(z_n)}{2}\cos\{(\omega_t - \omega_L)t + \phi(z_n) - \varepsilon_L(t)\} + \frac{1}{2}\cos\{(\omega_r - \omega_L)t + \varphi - \varepsilon_L(t)\} \qquad (10.6)$$

where ω_L is the LO frequency of the LNC attached to the antenna element at $z = z_n$ and $\varepsilon_L(t)$ is the LO phase.

Remembering the LO frequency and phase will vary with time, both effects are accommodated in (10.6) by writing the LO phase as a time varying parameter, $\varepsilon_L(t)$. It should be noted though that these terms cancel in the mixing process described below and therefore do not influence the accuracy of the overall measurement. One approach to making the necessary measurement is to split the signals using a diplexer and mix the reference and test signal in each channel, as shown in Figure. 10.1. The output of this mixing process (after filtering) is a difference signal with a phase equal to the difference between the test and reference signals, given as:

$$V_e(z_n) = \frac{a(z_n)}{8}\cos\{(\omega_t - \omega_r)t + \phi(z_n) - \varphi\} \qquad (10.7)$$

The immediate objective is to find a(z_n) and ϕ(z_n). These values are samples of the general amplitude and phase variation over the length of the array, r(z) = a(z) $\angle\phi$(z). Hence, once the amplitude and phase is measured at each element in the array, the AoA can be found using the method described in equations (10.1)-(10.4).

Equation (10.7) shows that the output obtained in each channel is a sinusoidal signal with a constant, yet unknown frequency corresponding to the difference in frequency between the incoming test and reference signals, and amplitude proportional to the size

of the incident test signal. The required magnitude term, $a(z_n)$, can therefore be found by determining the amplitude of this signal. The proposed method of doing this in this case is to sample the signal and then find its root mean squared amplitude. Finally, the measurement of the phase term in (10.7) reduces to a problem of determining the relative phase difference between this output at $z = z_n$ and a reference antenna output (typically the output at $z = 0$), which has an output given by:

$$V_r(z) = \frac{a(0)}{8}\cos\{(\omega_t - \omega_r)t + \phi(0) - \varphi\}$$
(10.8)

Measuring the phases of the signals produced in this type of system presents some problems though. Firstly, the frequencies of the signals to be measured may not be known exactly as standard sources like a YIG or a DRO will not be frequency locked. Furthermore, the measurement frequency will fluctuate with time as the various sources heat and cool. In the array built for this project, the difference signals will be centred at about 5 MHz but it is estimated that the actual frequencies may drift by up to a 100 kHz about this centre frequency. Secondly, the received signal magnitudes will vary as the individual rays with different angles of incidence sum at the antenna input. The phase detector therefore needs to adapt to these changing conditions. Finally, the measurement needs to be performed quickly if we wish to measure phases over the full length of the array at a rate sufficient to monitor short-term variations in the atmospheric conditions.

The phase estimation problem can be formulated by the need to determine the phase between two versions of the signal, $x(t)$, in the presence of measurement noise, $n(t)$. In a discrete-time sampled data system, with sampling period T, the estimation problem becomes one of determining an estimate of the true delay using the measured samples, $x_1(kT)$ and $x_2(kT)$, of the signals $x_1(t)$ and $x_2(t)$. For simplicity and without loss of generality, we normalize the sampling period (i.e. let $T = 1$), which results in the sampled signals as given by:

$$
\begin{aligned}
x_1(k) &= A_1\cos(2\pi f_0 k) + n_1(k) \\
x_2(k) &= A_2\cos(2\pi f_0 k + \phi) + n_2(k)
\end{aligned}
$$
(10.9)

The problem is to estimate the phase ϕ from the current and past samples of $x_1(k)$ and $x_2(k)$. A common processing technique to find this phase is based on a quadrature phase detector [70]. In this approach it is first necessary to generate quadrature reference signals. If the input frequency is known, the quadrature-phase signal can be generated from the in-phase signal by a simple delay [70]. In this application though, the input frequency is not accurately known, and the quadrature-phase signal must be generated from the in-phase signal, $x_1(k)$ using the Hilbert transform [71]. That is;

$$
\begin{aligned}
x_{1I}(k) &= x_1(k) = A_1 \cos(2\pi f_0 k) + n_1(k) \\
x_{1Q}(k) &= \mathcal{H}[x_1(k)] = A_1 \sin(2\pi f_0 k) + n_3(k)
\end{aligned}
\tag{10.11}
$$

where H [ ] is the Hilbert transform operator.

The input signal $x_2(k)$ from (10.9) is then multiplied by $x_{1I}(k)$ and $x_{1Q}(k)$ to generate the modulated terms $Qm_1(k)$ and $Qm_2(k)$. Finally, once we low-pass filter these outputs, the phase term is obtained as in:

$$
\phi = \tan^{-1}\left[\frac{LPF[Qm_2(kT)]}{LPF[Qm_1(kT)]}\right] \approx \tan^{-1}\left[\frac{\sin \phi}{\cos \phi}\right]
\tag{10.12}
$$

10.4 Measurement results

To test the performance of the new incoherent AoA measurement technique, the system shown in Figure 10.2 was assembled based upon the initial array design in Chapter 8. The signals detected on each antenna in the receiver array are amplified and frequency down-shifted using commercial LNCs. Each LNC has a separate internal oscillator so the received signals will be incoherent in this system. To synchronise the received signals so phase delay measurements can be performed, a reference source is injected along with the test signal into the front of the receiver array. Two, 10mW DRO sources at 10.728 GHz and 10.73 GHz are used as the test and reference sources in this case. After a second stage of down-conversion, the received signals are finally digitized and sent to a PC for storage and analysis. The signals were sampled at a rate of 50 MS/s using an 8-bit converter.

The AoA system built was primarily designed for testing indoors, rather than as a fully-fledged AoA measurement sensor and as such only incorporates a simple two-element receiver array. The test system was also different to the proposed AoA sensor in that the "split and mix" operations were not implemented in hardware but were done off-line by processing the digitized signals. In a practical implementation, this type of approach might have speed or memory storage limitations but this design was adequate to demonstrate the principle.

To simulate variations in the AoA of the test signal, the position of the 10.728 GHz test source was varied linearly in 25mm steps. At each position, the raw data sequences were stored on the PC where they were later processed. The data was processed using MatLab and the procedure described above to determine the time delay difference in the tests signals measured in the two array channels. The measured delay (in units of the sample period) versus position is graphed in Figure 10.3. Using only two elements in the receiver means it will only be possible to measure the AoA of a single incident ray. Receiving more than one signal, as is highly likely in the indoor environment used for this experiment, will perturb the expected delay reading. The measurements seen in Figure 10.3 therefore appear to be reasonable. The response is essentially linear but with some perturbations about the predicted straight line. This type of response is characteristic of a dominant direct ray and a smaller reflected signal.
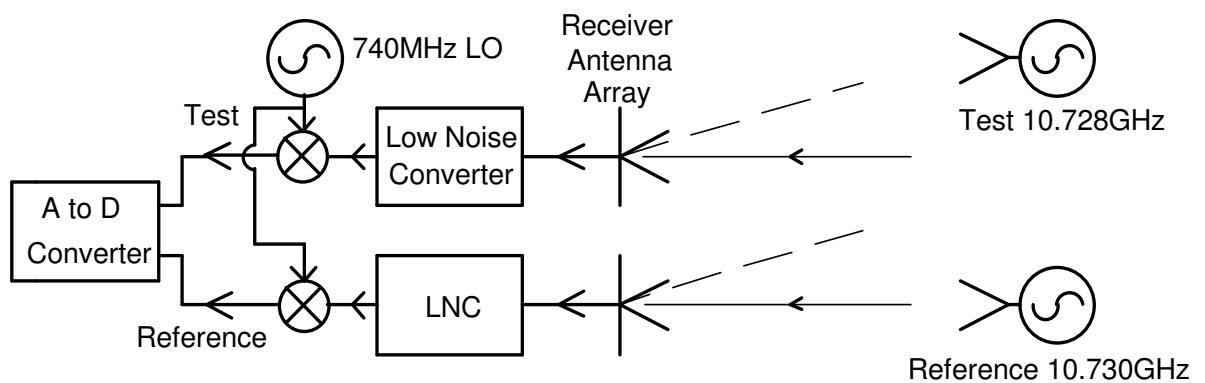
Figure 10.2: Two element AoA measurement system used in testing.

Delay versus Position
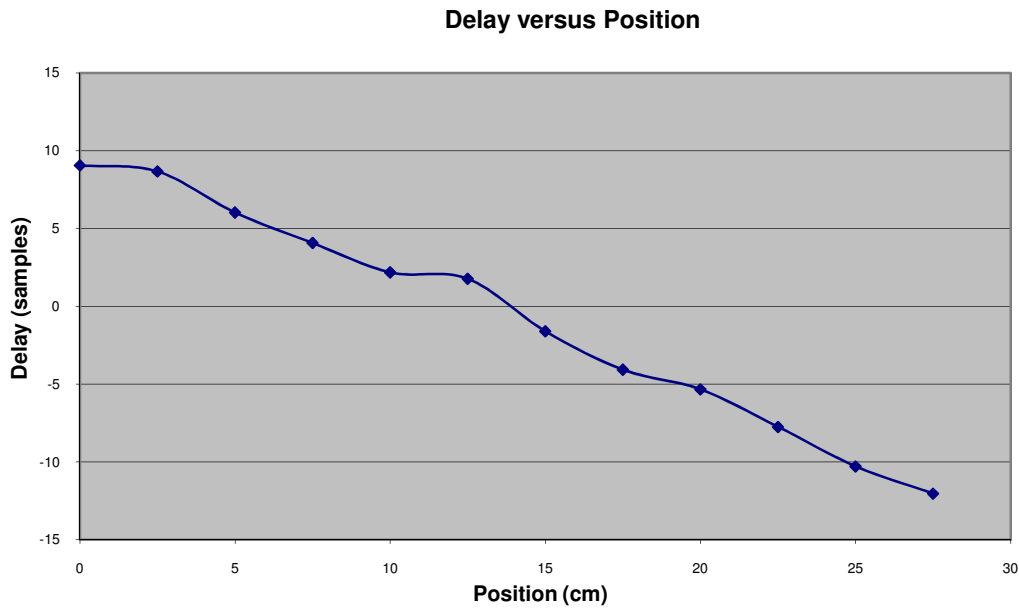
Figure 10.3: Phase delay versus position of test antenna.

A typical spectrum analyser view of the signals received on the two channels of the array is shown in Figure 10.4. Note that the signal received at each of the antennas contains two major frequency components. The two components correspond to the reference and test signal, respectively. The two signals are cantered at different frequencies though because the two channels use separate incoherent receivers. Other smaller spurious components can also be seen in this figure. These spurious signals could cause problems if other broadband phase detection techniques were employed.

Finally the next photograph, Figure 10.5, shows a spectrum analyser plot of a signal received using the large array on Orpheus Island. A strong 3 MHz signal was received with phase information intact using a local oscillator 250 metres from the receive array and a measured source 18.7 km away on the Lucinda jetty.

Data was collected from this array during a campaign in October 2007. This data was analysed using the MATLAB program previously described, however the results were inconclusive as the angle of arrival spread exceeded 2 degrees and individual angles of arrival within this range could not be identified. We have previously shown that at least for the signal refracted from above a limit of >0.5 degrees is expected. Further work is required to develop the MATLAB program and filters to properly asses this data. This work is beyond the scope of this Thesis.
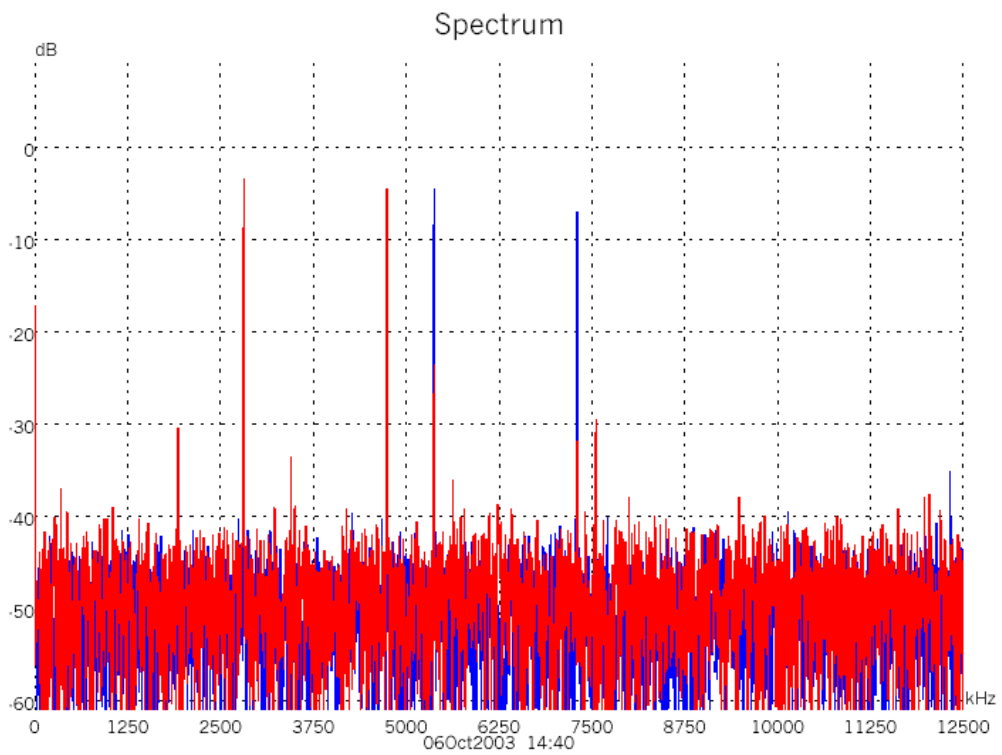
Figure 10.4: Typical spectrum of signals received on 2 channels of the AoA array.

Figure 10.5: The first received 'split and mix' signal.

10.5 Conclusion

This chapter has outlined the theory behind our new angle of arrival measurement technique which was designed to support our over-ocean propagation studies. The advantage of this approach was that common "off-the-self", incoherent receivers could be employed in the receiver array to reduce costs while still providing very good accuracy. The various channels in the receiver are synchronised by injecting a reference signal into each of the receiver elements. A new technique for processing the received signal to determine the phase delay was also described. This approach was based on a Quadrature Phase Detector technique using the Hilbert transform to generate the quadrature reference component. This approach was attractive in this situation as the frequency of the detected signals does not need to be known accurately and it was therefore possible to accommodate frequency drift with the transmitter and receiver equipment. Laboratory measurements using a two-element receiver array were presented to demonstrate this approach. Results consistent with an indoor propagation path were recorded giving confidence in the proposed techniques. A 10.7 GHz AoA receiver which uses a 16-element array and this measurement technique for over ocean propagation studies was built and deployed on Orpheus Island in 2002.

10.6 References and papers

10.6.1 Papers

The following papers were published as a result of the research outlined in this chapter:

Woods, G.S., Maskell, D.L. and **Kerans, A.J.**, "New angle of arrival measurement technique for over ocean propagation studies", Ninth International Conference on Communication Systems, ICCS 2004, Singapore, 6-9 September 2004.

Woods, G. S., **Kerans, A.J.** and Maskell, D.L., "Simulated Angle of arrival Measurements for an Over Ocean Microwave Radio Link", URSI Commission F, Triennium Open Symposium, Cairns, Queensland, Australia, 1-4 June 2004.

Maskell, D.L., Woods, G.S. and **Kerans, A.J.**, "A Hardware Efficient Implementation of an Adaptive Subsample Delay Estimator", ISCAS 2004, Vancouver, Canada, May 2004.

10.6.2 References

[61] Paulraj, A. and Papadias, C., "Space-time processing for wireless communications" IEEE Signal Processing Magazine, pp. 49-83, November 1997.

[62] De Jong, Y. and Herben, M., "High-resolution angle-of arrival measurement of mobile radio channel", IEEE Transactions on Antennas and Propagation, Vol. AP-47, No.11, pp. 1677-1687, November 1999.

[63] Rappaport, T., Reed, J. and Woerner, B., "Position location using wireless communications on highways of the future", IEEE Communications Magazine, pp. 33-41, October 1996.

[64] Webster, A. and Merritt, T., "Multipath angles-of-arrival on a terrestrial microwave link", IEEE Transactions on Communications, Vol. 38, No.1, pp. 25-30, January 1990.

[65] Kulessa, A.S., Woods, G.S., Piper, B. and Heron, M.L., "Line of Sight EM Propagation Experiment at 10.25GHz in the Tropical Ocean Evaporation Duct", IEE Proceedings on Microwaves, Antennas and Propagation, Vol. 145, No 1, February 1998.

[66] Hitney, H.V., Richter, J.H., Pappert, R.A., Anderson, K.D. and Baumgartner, G.B., "Tropospheric radio propagation assessment", Proceedings of the IEEE, Vol. 73, No. 2, pp. 265-283, February 1985.

[67] Ikegami, F. and Yoshida, S., "Analysis of multipath propagation structure in urban mobile radio environments" IEEE Transactions on Antennas and Propagation, Vol. AP-28, pp. 531-537, July 1980.

[68] Ellingson, S., "Design and evaluation of a novel antenna array for azimuthal angle of arrival measurement", IEEE Transactions on Antennas and Propagation, Vol. AP-49, No. 6, pp. 971-979, June 2001.

[69] Webster, A. and Scott, A., "Angles-of-arrival and tropospheric multipath microwave propagation", IEEE Transactions on Antennas and Propagation, Vol. AP-35, No.1, pp. 94-99, January 1987.

[70] Maskell, D.L. and Woods, G.S., "The discrete-time quadrature subsample estimation of delay", IEEE Transactions on Instrumentation and Measurement, Vol. 51, pp. 133-137, February, 2002.

[71] Hussain, Z.M. and Boashash, B., "Hilbert transformer and time delay: Statistical comparison in the presence of Gaussian noise", IEEE Transactions on Signal Processing, Vol. 50, pp. 501-508, March, 2002.

Chapter 11

A theoretical design for long range over ocean microwave links using the tropical evaporation duct

In this chapter, I build on the work presented in previous chapters and also outlined in Annex 2. From this I present a design for a microwave path inside the evaporation duct. One research paper was published as a result of this research.
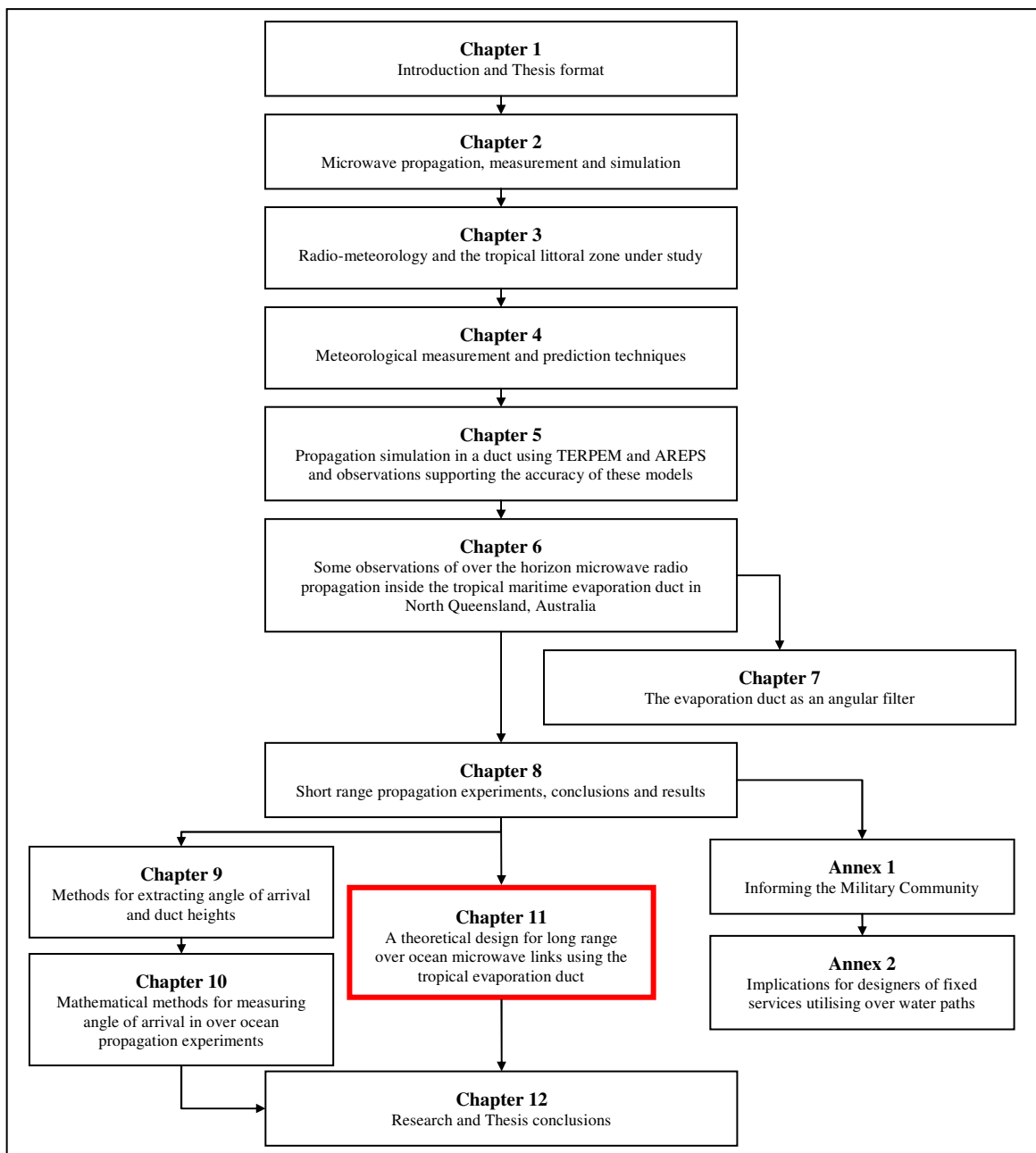
11.1   Introduction

In previous chapters I outlined how measurement and simulation of the evaporation duct over warm tropical waters in the Australian littoral zone have shown that an oceanic duct is present for a significant part of each day over the full year. This duct is capable of maintaining signals over paths of up to 100 km with a predicted reliability exceeding 50%.

These sorts of availabilities would not support continuous high data rate low error communications, they may however be viable for low data rate or non time critical communications or provide backup for satellite systems to platforms such as oil rigs.

Such systems could be used for store and forward transmission of non-time critical data. In order to maximise the availability of such systems careful link planning is necessary. Such a link could be used to transmit store and forward non time critical data between platforms at sea or from sea to land and vice versa. This chapter draws from ten years of previous research and systems link design experience in order to provide what I believe is the first published comprehensive theoretical methodology for planning a link using the duct as a communications channel and this is then compared to a link established on the Great Barrier Reef by James Cook University.

11.2   Meteorology

In order to use the duct to support a communications channel we first need to have an idea of its height and its persistence. In Chapter 4 our extensive campaign of measurements was discussed, this campaign resulted in the diagram shown in Figure 4.2.

From this diagram it is possible to gain a good understanding of duct heights and the percentage of time they are prevalent and from this deduct the potential reliability of any path which uses the duct as a transport mechanism for this particular area of research. Other similar research is available for many areas, but the similarity between the temperate and tropical evaporation duct probability gives comfort that in most places some kind of duct will be present.

In Figure 4.2 the solid curve is for the equatorial West Pacific in February, the purple, dashes and dots curve is for the Coral Sea in May and the pale blue, dashed curve is for the coastal region around Lucinda, Queensland in October. From this data it has been established that the upper extent of ducts was 40 metres and a duct height of 20 metres was exceeded for approximately 50% of the time. Using this data and given the variability of duct heights we will use a height of 20 metres as our design height.

One final piece of information not clear in Figure 4.2 is that the reliability of the measuring equipment decreased with duct height. Ducts of around 10 metres and below are difficult to measure and are unstable, thus from this data we can establish that a reliable duct is only available for 90% of the time.

Other factors affecting the reliability of the path are duct strength, which is a function of atmospheric bulk parameters [72], wind and rain as a duct collapses in light winds or in heavy rain.

11.3   Frequency selection for microwave transmission within the duct

Propagation in the duct is frequency dependant. Measurements have confirmed that available PEM based models, AREPS and TERPEM, are sufficiently accurate to determine bulk effects of ducts. These can therefore be used to determine the best available bands in which to deploy the link.

The first task is to select a frequency band that is most resilient to varying duct height. From Figure 11.1 we can see that the lowest path losses are available from 3 GHz to about 6 GHz depicted by the deeper red section, however these ideal path losses are only available in a duct range of between 25 and 40 metres, or from Figure 11.1 a theoretical maximum availability of only 10 – 15%.
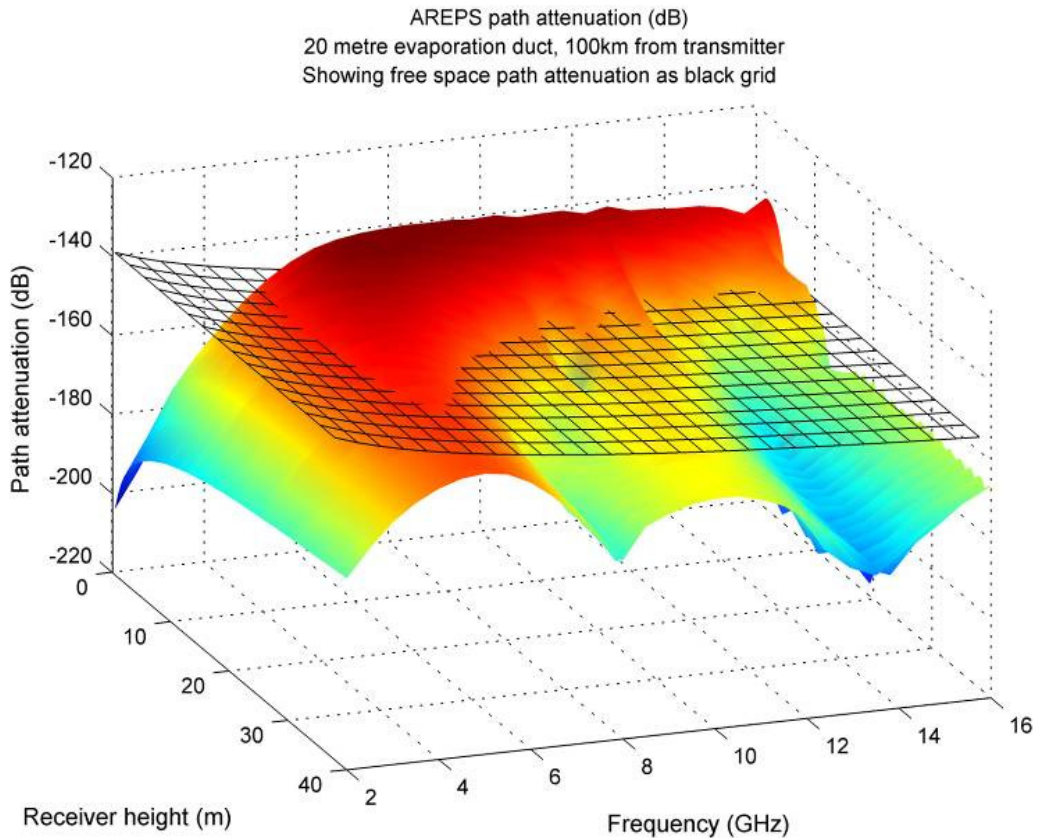
Figure 11.1: A collated AREPS simulation of path loss against frequency and receiver height.

Looking again at Figure 11.1 it is clear that some signal strength must be sacrificed to maximise availability and using the -140 dB contour we can see that a band at around 8 GHz will sustain a path loss of -140 dB or better over a duct height range of 15 to 40 metres for a theoretical availability of 80%. Gain however can be derived from antennas and controlled via power, so a range of between 5 GHz and 11 GHz would seem to be viable. This would allow the use of two 'Class Licensed' [73] point-to-point bands in Australia.

11.4   System frequency and antenna height design

To operate using the lower path losses inside the duct both transmitter and receiver must be inside the duct. The ideal height of each (which will be the same) can also be derived using another interpretation of collated AREPS plots for a given range.

AREPS path attenuation (dB)
5 metre evaporation duct, 75km from transmitter
Showing free space attenuation as black grid
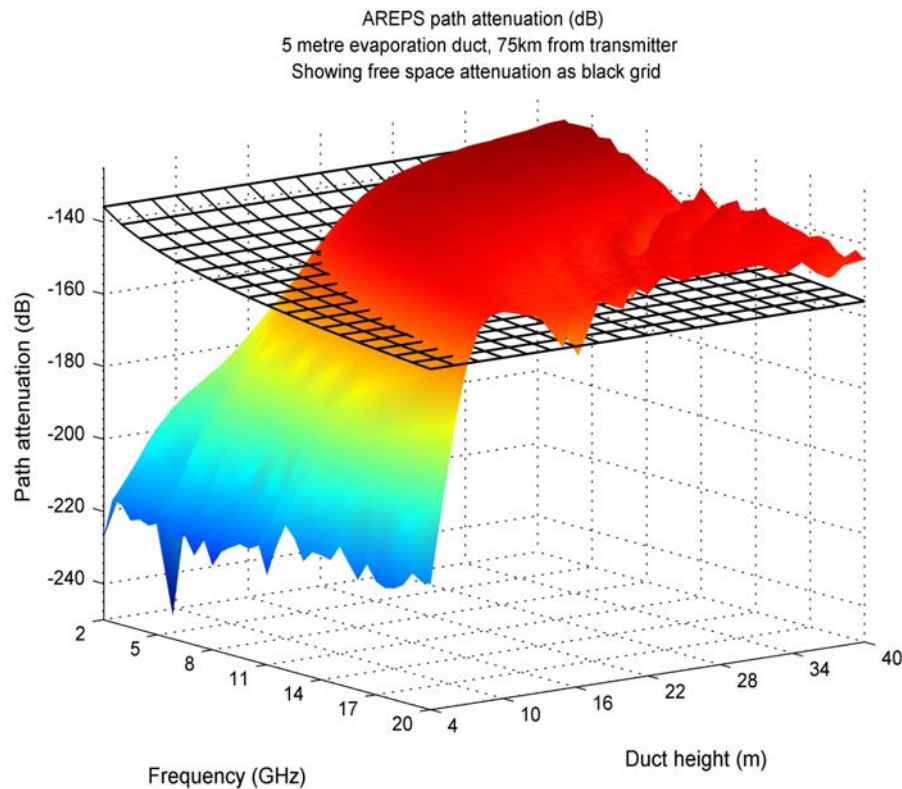
Figure 11.2: Collated AREPS simulation showing ideal antenna heights vs. frequency.

It can be seen in Figure 11.2 that at 75 km a band around 6 GHz gives the best available antenna height range. This is important because for systems deployed at sea tidal ranges can vary up to seven metres and systems must generally be deployed above maximum wave height. At 10 GHz a height of 5 metres is important while at 5.8 GHz a range of between 5 and 20 metres is available.

Figure 11.3 shows an actual measurement compared to a TERPEM simulation for a 76 km path in a measured 15 m duct. We can see that the strongest signal was received at about 6 metres AMSL which strongly supports the receiver height suggested by the simulation in Figure 11.2.

So our ideal design would be at 5.8 GHz (a 'free' class licensed band) with both transmit and receive antennas at around 7 metres AMSL. However to use 10.7 GHz we could design the system with both antennas at 5 – 6 metres AMSL with the maximum gain permitted by the class licence. Alternatively a licensed system in 6 GHz could use additional power to overcome fade.
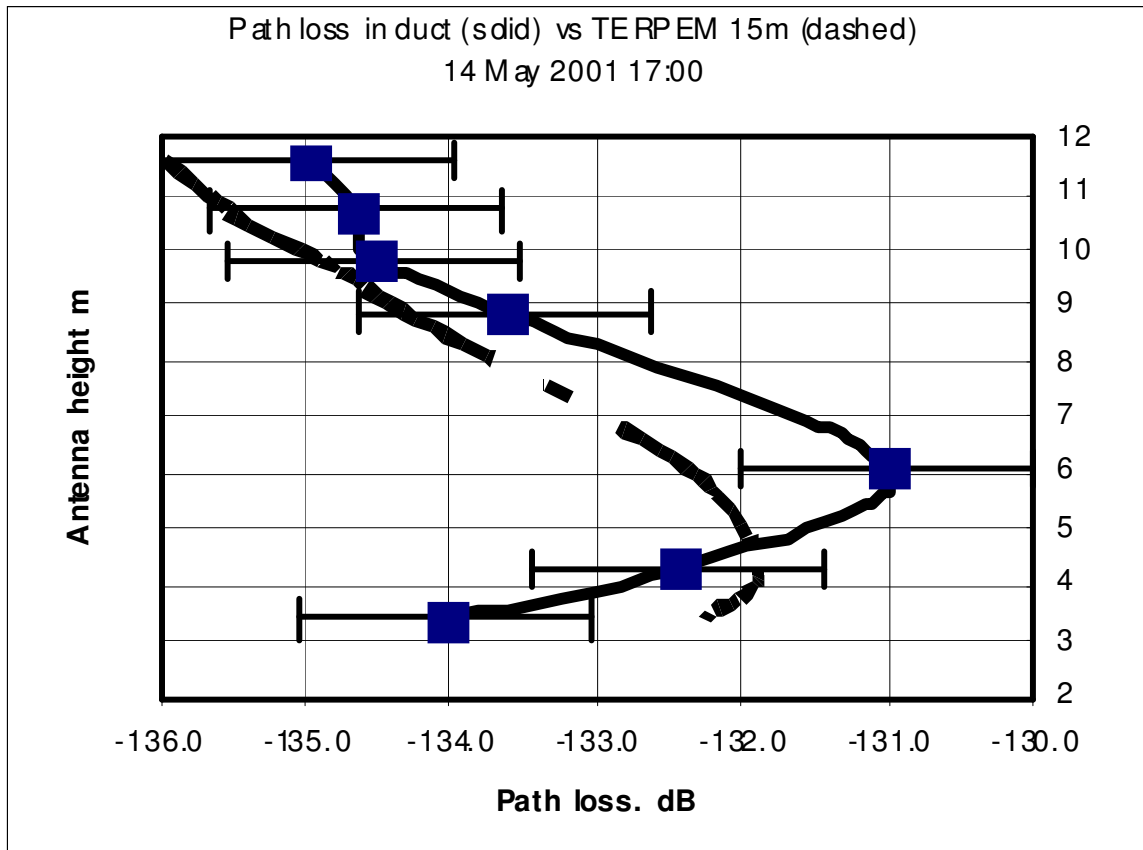
Figure 11.3: An actual measurement over a 76 km path at 10.7 GHz.

11.5   Critique of an actual system

In a separate but related project to our research James Cook University constructed an actual high capacity microwave link from Davies Reef on the Great Barrier Reef to the Australian Institute of Marine Science (AIMS) on Cape Cleveland near Townsville. This system is reported in [74].

The system operated over a 78 km path at a frequency of 10.6 GHz, very similar to our long range experiment reported above. The paper reports that similar findings to those described in previous chapters with a theoretical ideal height for the antennas of 5 metres although I disagree with the paper in that it suggests 10.7 GHz is 'ideal' where I find the lowest loss band for this situation to be 8 GHz. Due to mounting constraints both the transmit and receive antennae were installed at an average of 7 metres AMSL.
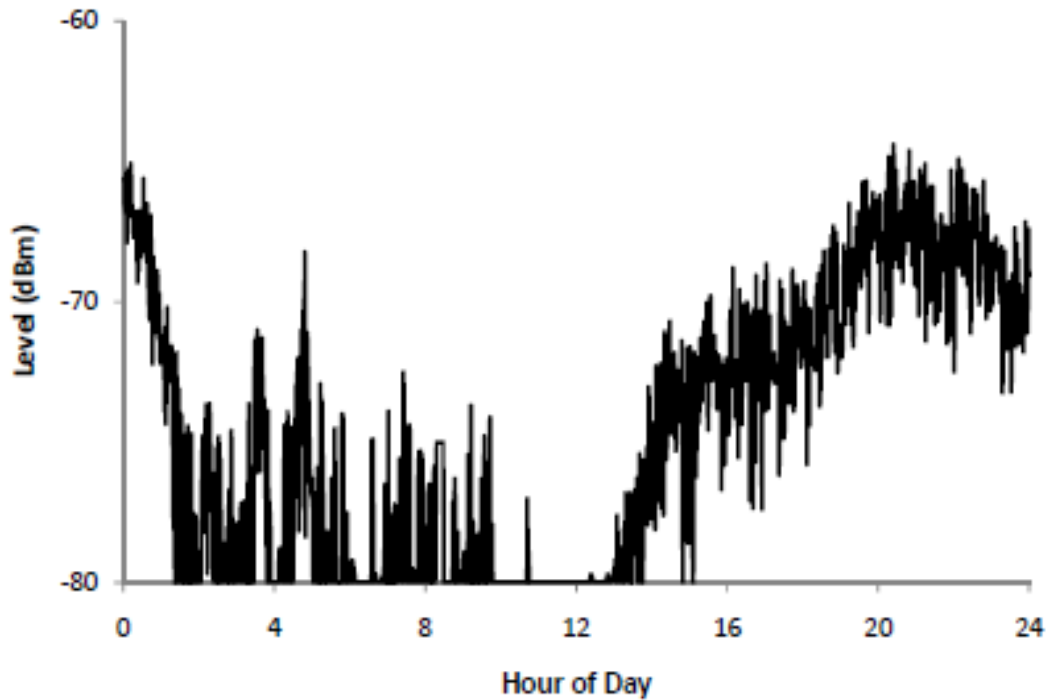
Figure 11.4: Received signal level for 6 August 2007 for the Davies Reef link.

Figure 11.4 shows the received signal level for this system on one day of the trial. As expected from our research the signal level, corresponding to a collapsed or weak duct, is very low in the early morning. However counter-intuitively the signal remains low until about 13:00 hours when we would expect the duct to have become established at between 5 and 25 metres depending on wind conditions.

Supporting this, our long path experiment showed the lowest receive powers shortly after sunrise (as expected) with a peak at around 15:30 at a 4.5 metre antenna height. A 24 hour period of our experiment is shown in Figure 11.5. Of note is that while our transmit arrangement was similar, our receive antennae were only 12 dBi slotted guide systems compared with high gain parabola in the Davies link. This represents a significant difference in overall gain.

Of interest a low tide of 1.0 metres occurred at about 09:45 on 6 August 2007. This would mean the antennae at both end would have been a minimum of 8 metres AMSL at that time. With the tide rising to a high of 2.5 metres at 17:00 the effective height of the antennae would have dropped to 6.5 metres, approaching ideal. It would be possible

to suggest that this is indicated as a causal factor in the signal strengths, but this is inconclusive.

In addition Figure 11.1 indicates that signal strength over a long path drops significantly in any duct at or below about 15 metres. From Figure 11.1 this represents about 30% of the time for this region.

Overall our research suggests that an additional path loss of between 5 and 10 dB per antenna will be encountered at an effective antenna height of 8 metres. This can be seen in Figure 11.5 or simulated using AREPS.

A close examination of the plots in Figure 11.2 would also suggest that at the calculated optimal frequency of about 8 GHz an additional 5 dB of 'duct gain' would be available bringing the overall path loss down by 20 dB except where no duct existed.

While it is not possible to derive the actual received powers from Figure 11.4 for the morning of 6 August 2007 it is obvious that an additional 20 dB of signal would have made a significant difference for most if not all of that day in terms of availability.
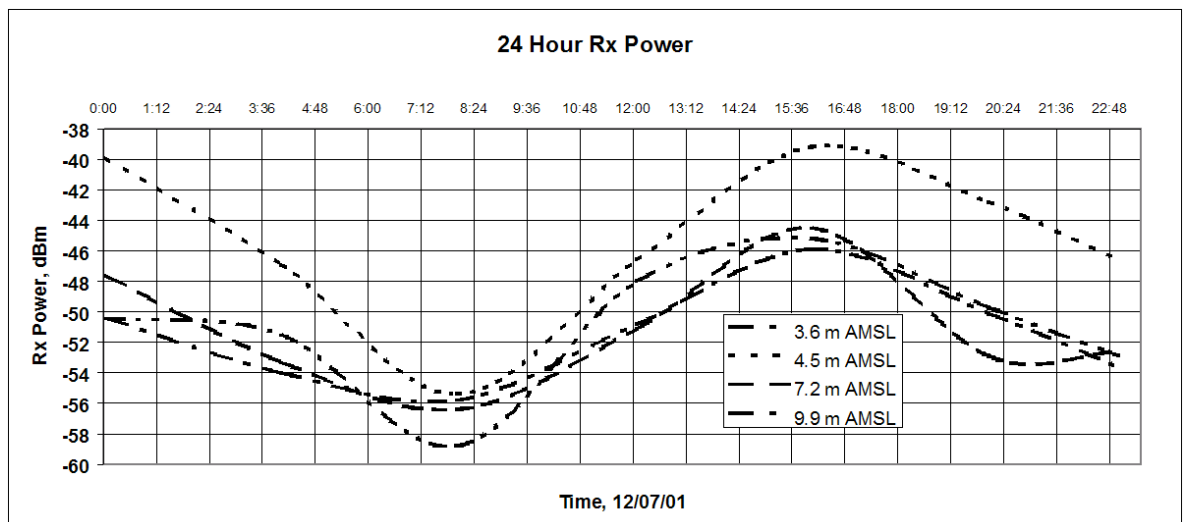
Figure 11.5: A 24 hours snapshot of the authors' long range experiment.

11.6   Conclusions

This chapter has shown that the tropical evaporation duct is capable of sustaining a high data rate microwave link over ranges of up to 80 km with an availability of up to 80%. This would be useful for data which is not time critical that can be transmitted at varying speeds on a store and forward basis.

We have concluded though that the design of such systems is critical given the physical factors at play and have discussed this in terms of another trial experiment that, while not in our view a perfect design, proved highly successful.

11.7   References and papers

11.7.1 Papers

The following paper was published as a result of the research presented in this chapter:

Kerans, A.J., Kulessa, A.S., Woods, G.S. and Clark, A.J., "A theoretical design for long range over ocean microwave links using the tropical evaporation duct", IEEE Oceans'10, Sydney, Australia, 24–27 May 2010.

11.7.2 References

[72]   http://www.acma.gov.au/WEB/STANDARD/pc=PC_1612

[73]   Babin, S. M., Young, G.S. and Carton, J.A., "A new model of the oceanic evaporation duct", Journal of Applied Meteorology, Vol. 36, No. 3, pp 193-204, March 1997.

[74]   Woods, G.S., Ruxton, A., Huddlestong-Holmes, C. and Gigan, G., "High Capacity, Long Range, Over Ocean Microwave Link using the Evaporation Duct", IEEE Journal of Oceanic Engineering, Vol. 34, No. 3, pp. 323-330, August 2009.

Chapter 12

Research and Thesis conclusions

Chapter 1
Introduction and Thesis format

Chapter 2
Microwave propagation, measurement and simulation

Chapter 3
Radio-meteorology and the tropical littoral zone under study

Chapter 4
Meteorological measurement and prediction techniques

Chapter 5
Propagation simulation in a duct using TERPEM and AREPS and observations supporting the accuracy of these models

Chapter 6
Some observations of over the horizon microwave radio propagation inside the tropical maritime evaporation duct in North Queensland, Australia

Chapter 7
The evaporation duct as an angular filter

Chapter 8
Short range propagation experiments, conclusions and results

Chapter 9
Methods for extracting angle of arrival and duct heights

Chapter 11
A theoretical design for long range over ocean microwave links using the tropical evaporation duct

Annex 1
Informing the Military Community

Chapter 10
Mathematical methods for measuring angle of arrival in over ocean propagation experiments

Annex 2
Implications for designers of fixed services utilising over water paths

Chapter 12
Research and Thesis conclusions

This work, both in comparing the output of some existing computer-based models with actual propagation experiments and in actually conducting a range of propagation experiments together with the work on duct height and predominance has significantly increased the body of knowledge in evaporation ducts, propagation within them and the design of systems to alleviate or even use their unique properties.

12.1   Research conclusions

There are many uncertainties inherent in a measurement system as complex as the one used in this research. For the meteorology were minimised uncertainties in our spar buoys through careful calibration, however the use of these buoys introduced uncertainties of their own. When measuring ducts with heights in excess of 30 metres, a buoy with sensors only up to six metres means a curve fitting process must be used to derive duct height. While these methods were trialled against other models and against actual radio data errors in the range of 2 metres were possible in this process.

The radio measurements were also subject to significant uncertainty. Again careful calibration was used, but simple pointing and focussing errors introduced uncertainties in the range of 5 dB. The measurements themselves were conducted over time intervals of up to a minute, in this time the duct can change markedly under normal atmospheric processes, again introducing uncertainties we were unable to fully determine.

The most rewarding element is that the goals of this research, within the constraints of these errors and uncertainties, were met. Numerous complex experiments involving the deployment of heavy equipment were conducted. During these campaigns we were reliant on many people, boats, cranes and even basic hand tools. Each radio experiment involved the design and construction of new equipment all in an outdoor highly corrosive maritime environment.

Finally the design and construction of our large array involved both novel techniques in the laboratory and novel techniques in erecting such a large structure with only people and hand tools on a remote barrier reef island.

Returning to the original research questions posed at the beginning of this Thesis and repeated for clarity. Below is an attempt by the author of this Thesis to answer each and reference them to this body of work:

Question 1: Are the available PEM models (AREPS and TERPEM) useful in predicting evaporation ducts in the Australian tropical littoral and if so, with what caveats?

In my view yes, but only for general wide area evaporation duct prediction and simulation. Such models cannot exactly predict the radio environment in the absence of pico scale meteorological information. It has also been shown that duct height over large areas does not correlate well meaning propagation inside the duct would be more complex than predicted by modelling. In addition mid and upper layer atmospheric layering also has an effect, particularly over long paths, such that even the general simulations may prove inadequate for short periods of time.

The findings presented in Chapter 5, the findings for long range experiments in Chapter 6 and short range experiments outlined in Chapter 8 support this conclusion.

Question 2: With what prevalence do evaporation ducts exist in the tropical littoral?

Meteorological measurements carried out early in the project have shown the prevalence of ducts in the tropical littoral and southern Australian temporal seas. This is best displayed by reviewing the major output of that work from Chapter 4, the prevalence curve shown below in Figure 12.1. The figure shows the percentage of time that a given duct height is exceeded as a function of duct height for three different regions. The solid curve is for the equatorial West Pacific in February, the purple, dashes and dots curve is for the Coral Sea in May and the pale blue, dashed curve is for the coastal region around Lucinda, Queensland in October.

It has been shown in this Thesis that evaporation ducts can be expected for significant parts of a year and, except in conditions of strong rain or no wind, would be experienced for a significant part of each day.

Question 3: **Could a plot of receive signal strengths verses height from an RF system be used to determine if an evaporation duct is present?**

This is an interesting question; the answer is of course yes. Given a number of measurements at different heights and similar known duct profiles at that range a lookup table system could establish the presence of a duct and its approximate height. The more complex the data or lookup table the more accurate the system would be.
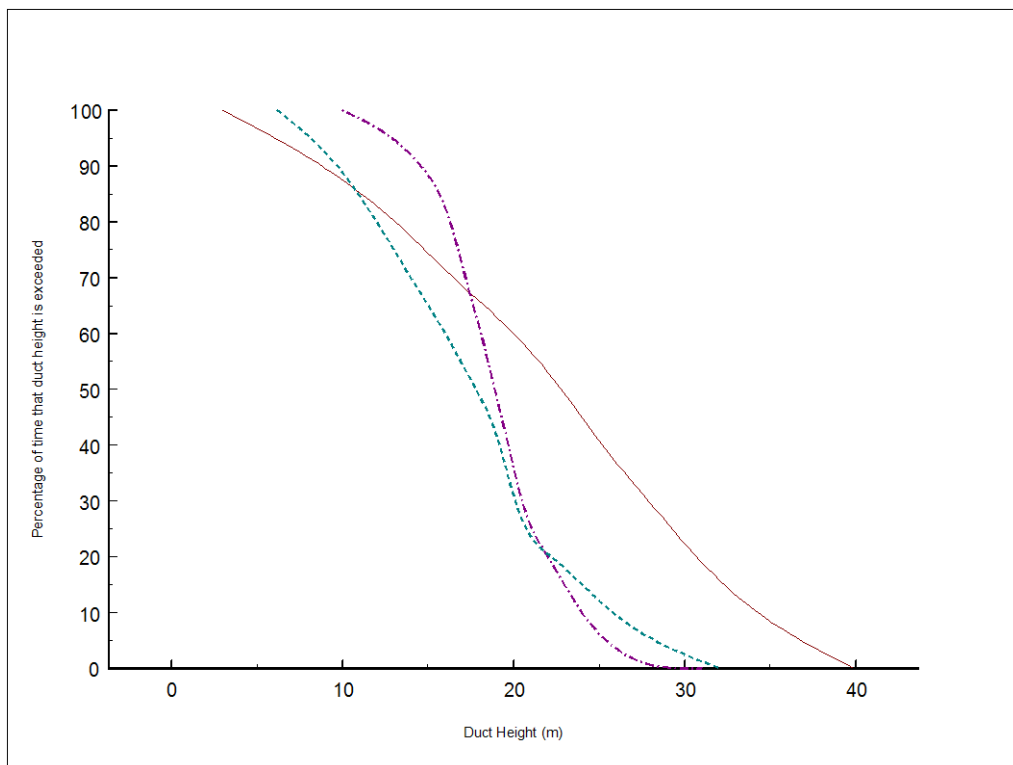
Figure 12.1: Duct height statistics for the North Eastern Australian littoral.

Our experiments have shown that a lookup table using actual RF measurements would work, however our system appeared to contain calibration errors in the range of 5 dB which would provide more accuracy if rectified.

While a more accurate system would produce more accurate results the bulk parameter models used in the PEM software are only valid if their input parameters are accurate. These may vary over both distance and time and will naturally introduce more error into such a system.

What is interesting however is a comment made at Oceans'10 by Professor Mal Heron (ex of JCU Physics). If a duct height is known along with some other basic meteorological measurements then many other meteorological measurements could be derived, perhaps giving accurate information on sea and atmospheric conditions in that area.

Question 4: What effects of evaporation ducting are important to radio designers?

In this Thesis I have shown that evaporation ducts are an important consideration for both designers and operators. For designers they present an opportunity to establish a store and forward microwave link over long ranges over oceans. Such systems may be able to support the data requirements of remote reef sensors, oil rigs or perhaps in certain circumstances enable remote intelligence gathering.

However designers must also take into account the negative effects of ducts, these have been shown to range from radar anomalous returns and black holes, to high power interference from unwanted transmitters many kilometres distant.

Designer of over ocean systems should take these factors into account when calculating unwanted signal strength, fade and perhaps even diversity antenna positioning (inside or above the duct).

Question 5: Can the evaporation duct be used to support the transmission of useful data or for any other useful purpose?

The author believes that the evaporation duct is a viable transport medium for store and forward non-real time data. Research that has been carried out and documented in this Thesis has shown that availabilities of between 20% and 80% could be expected on most days, however the number of days a duct would not be present each year is as yet unknown, thus our answer is inconclusive.

An unanswered question in this body of work is that of the angle of arrival spectrum due to ducts. We have collected some data from the 16 element array and have spar buoy data from the path between. It is my hope that this data will be analysed by another student in the near future and I would be delighted to assist in this endeavour.

12.2   Final Conclusion

The research for this project has taken a decade, however in that time many new things have been learned and much data collected that may in the future reveal more secrets about tropical evaporation ducts.

Research and learning from this project have been shared with the Military, the international research community, the International Telecommunication Union, systems designers of radio systems and my employer, the Australian Communications and Media Authority.

Research on the topic of propagation within evaporation ducts is far from finalised. The PEM models studied continued to evolve as does the ability to take more accurate and ubiquitous meteorological measurements expands at a fantastic rate along with the computing power needed to analyse this mass of data.

I have learned much from this project and I hope others will benefit from the work presented too. In particular I have realised that with such fascinating research often the journey is more important than the destination.

Finally while standing on a deserted beach in far north Queensland in June 2010, I observed an island, Green Island, slowly emerge from over the horizon. Ducts of course affect the optical as well as the radio spectrum, eventually in mid morning as the duct developed the island was clear above the horizon.

So it is true, provided you have a sea breeze to mix the evaporative moisture in the lower atmosphere and change the refractive index sufficiently, on a fine day you can see (almost) forever.

Annex 1

Informing the Military Community

In this Annex, I discuss anomalous propagation within the evaporation duct from a military perspective using the information gathered during the research to give this group of mariners some insight into the effect ducting may have on their operations.

One research journal paper was published as a result of this work.
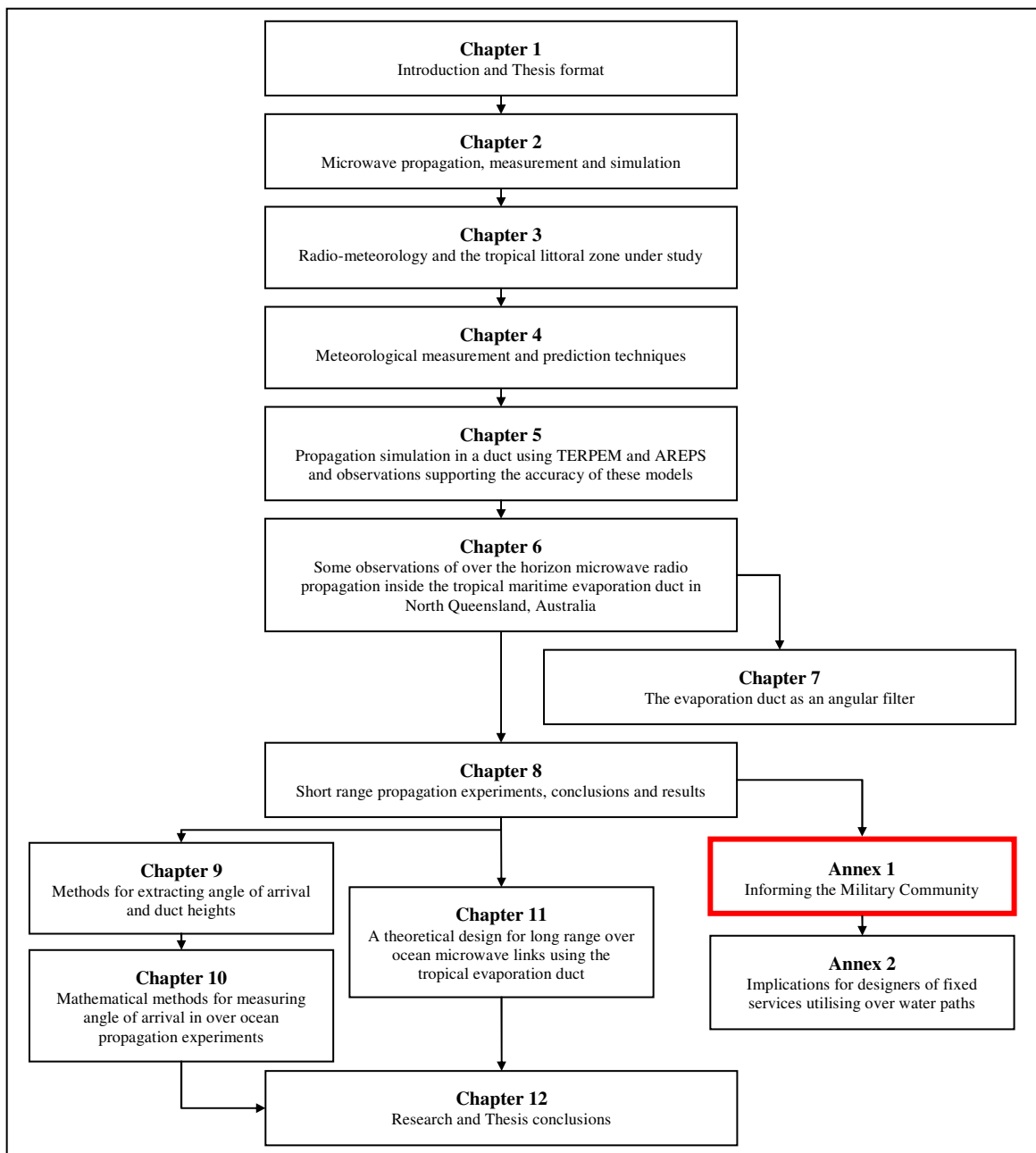
A1.1 Introduction

Previous chapters have demonstrated how the radio refractive index of the atmosphere is governed by the combination of atmospheric temperature, pressure and humidity. Over oceans, humidity gradients can cause an effect known as the evaporation duct. Such a duct has the property of trapping radio waves between the sea surface and the top of the duct, which can result in extended range or radio black spots. The amount of channeling is dependent on the carrier frequency, the duct structure and various transmitter and receiver properties including antenna tilt and height above sea level. Knowledge of the duct and how it will effect propagation is therefore of some importance to people using or designing maritime radio equipment for use in maritime and littoral environments. It allows designers to overcome disadvantages while making use of the advantages of extended range.

A1.2 Ducting for Naval Commanders

Numerous works over the past two decades have noted incidences of reduced or extended radar detection ranges and extended radio link ranges over water, for example in [75]. These changes in detection or propagation range are usually associated with surface based evaporation ducts.

In [75] Anderson notes that there have been numerous incidences where maximum radar detection ranges of low-altitude targets over the ocean are less than expected. This appears to be in stark contrast to reports from the Darwin N.T (Australia) area where radars have detected 'thunderstorms' which later turn out to be the hills of East Timor.

The reduced ranges Anderson reports on are caused by the radar holes discussed in previous chapters. Of more serious concern today is the fact that these holes can be simulated very close to the sea surface, the existence of such holes in a real maritime environments would be sufficient to cloak an incoming missile or hostile small craft. Research over the past decade, including our own, has shown that low grazing angle microwave radio propagation at low elevations over oceans will usually encounter an atmospheric refractive index gradient which will give rise to anomalous propagation or,

ducting. The research presented in this Thesis has shown this phenomenon to be particularly prevalent over warm tropical waters in the tropical littoral zone around the northern Australian coastal region and can be expected in most areas of the Asia Pacific region where Australian military forces deploy.

Surface based ducting over oceans is referred to as the evaporation duct. The duct traps radio waves propagating at low angles, below about 0.5 degrees to the horizontal, and is therefore important in maritime radar and communications applications.

Ducting can result in enhanced or degraded propagation including:

- radar/radio 'black holes'
- interference beyond the ranges and occurrences predicted in ITU models
- extended range radar tracking and signals interception.

A thorough understanding of ducting will therefore assist naval commanders understand information presented by radar systems as well as overcoming or taking countermeasures to reduce the adverse affects of radar black holes. Additionally ELINT or SIGINT operations can benefit from a better understanding of the propagation mechanisms to make the reception of such signals easier and in some cases safer. From a civilian and military perspective this Annex shows that further work is required on the ITU interference prediction recommendation contained in ITU-R Rec. P-452 and that considerable care should be taken when studying sharing between radars and other systems over or near warm tropical oceans.

Figures A1.1 and A1.2 show a simulation of propagation inside a 29 metre duct (day) and a 10 meter duct (night) using a program developed by the US Navy called AREPS [76]. AREPS allows a user to study the effect of ducting when duct heights are known or where only bulk parameters are know. Our work has so far shown that this and models like it, based on a method known as the parabolic equation method (PEM) are accurate enough to give warning of anomalous propagation conditions.
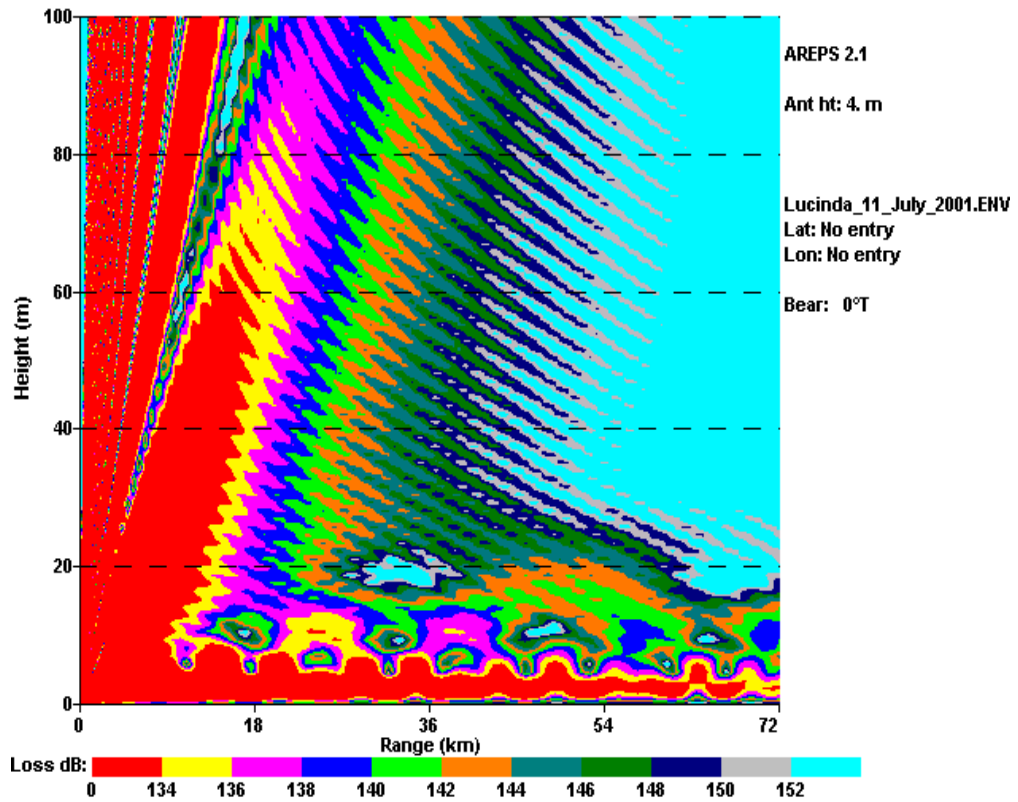
Figure A1.1: Propagation inside a 29 Metre Duct.
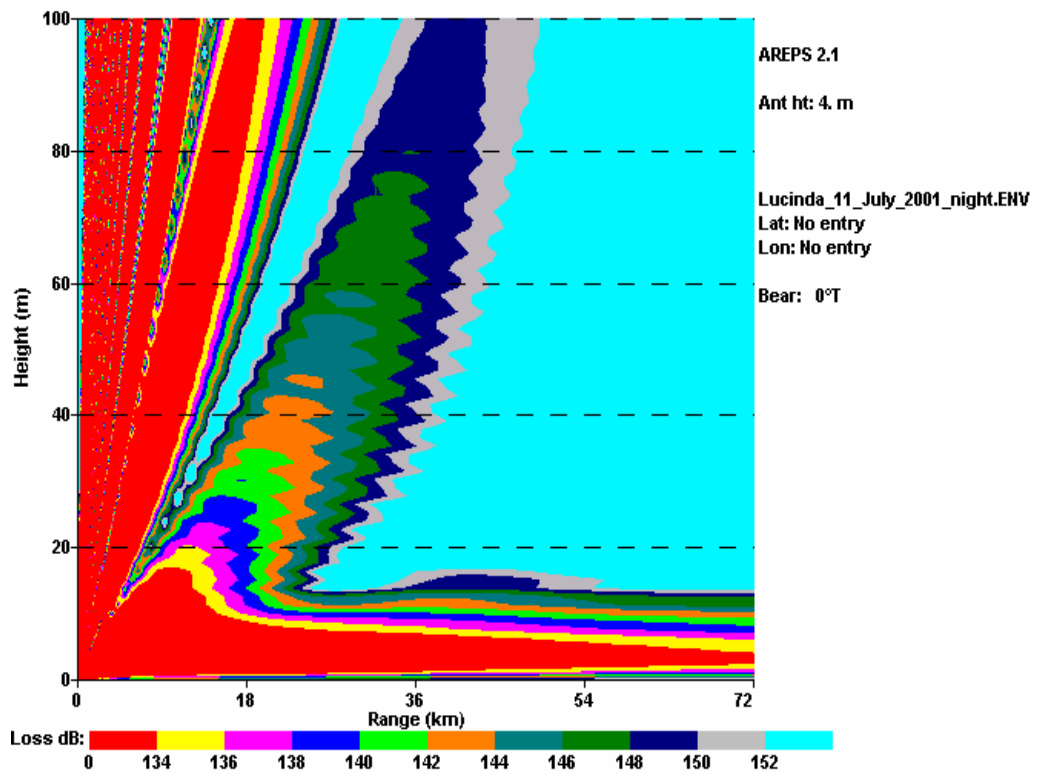
Figure A1.2: Propagation inside a 10 Metre Duct.

Of particular note in both figures are the extended range of propagation, seen most clearly in Figure A1.2, and propagation 'black holes' shown clearly in Figure A1.1 as lighter round areas in close to the transmitter at a height of about ten metres. A target in one of these areas, such as an incoming missile or hostile small vessel, would have a high probability of remaining undetected by radar systems. Wind speed affects duct height and reflection from the sea surface.

The propagation shown in Figures A1.1 and A1.2 are for light wind and do not take into account sea roughness. It can be theoretically shown using programs such as AREPS and TERPEM [77] that the incidence of 'black holes' reduces with a rough sea. We are yet to physically confirm this through experiment and it is likely that experimental systems needed to confirm this would be very complex. A resolution of this issue is possibly more likely via a reporting mechanism for 'disappearing targets' at sea.

A duct acts as an angular filter, only radio waves propagation at an angle below about 0.5 degrees are trapped in the duct, so as sea surface roughness increases with wind speed energy can be lost from within the duct and propagate above it.

Received signal strengths for the long distance experiment from 4 elements of a ten element array over a 24 hour period are shown in Chapter 6. These signal powers have been calibrated for system errors. Of interest is the strongest signal, received at the second lowest element at 4.5 m AMSL.

A strong link between diurnal variations in the sea-land breeze system, air temperatures and duct height and strength has been suggested in [78] and is supported in the literature. This behavior is evident in the diurnal variation of received signal strength across the array.

The powers discussed in Chapter 6 are the result of a path loss in the range 140 to 160 dB and are of a sufficient level to cause interference to the input of a radar system.

A1.3 ITU studies affecting maritime radar systems and the *Phalanx* close in defence system

Phalanx is a fast-reaction, rapid-fire 20-millimetre gun system capable of providing Naval ships with a "last-chance" defence against anti-ship missiles and littoral warfare threats that have penetrated other fleet defences. *Phalanx* automatically detects, tracks and engages anti-air warfare threats such as anti-ship missiles and aircraft and an emerging new littoral warfare threat, armed small craft. This new threat includes small, high-speed surface craft, small terrorist aircraft, helicopters and surface mines. *Phalanx* accomplishes these engagements via an advanced search and track radar system operating between 13 and 14 GHz integrated with a stabilized, forward looking infra-red (FLIR) detector. This integrated FLIR provides *Phalanx* with a unique multi-spectral detect and track capability for littoral warfare threats and dramatically improves the existing anti-air warfare capability. *Phalanx* is the only deployed close-in weapon system capable of autonomously performing its own search, detect, evaluation, track, engage and kill assessment functions. *Phalanx* also can be integrated into existing Combat Systems to provide additional sensor and fire-control capability [79].

Phalanx shares much of its frequency band with the fixed satellite service (FSS). In this band the FSS transmits from the Earth (uplink) and could, if many terminals were operated around the coast, cause considerable interference to Phalanx systems. When the FSS first sought entry into the band the ITU undertook studies to ensure compatibility with radar terminals. The studies resulted in the current constraint on FSS use of the band to earth stations with antennas no smaller than 4.5 m in diameter had been imposed with a view to limiting the number of FSS earth stations likely to be deployed, and thus limiting the interference to radar terminals.

The ITU assessed interference into radiolocation systems in terms of a decrease in probability of detection, which leads to a decrease in radar range and/or target tracking ability. Taking into account these factors, the ITU has concluded that the appropriate criterion to ensure the protection of maritime and land mobile radars would be a Interference/Noise ratio of –6 dB, corresponding to an interference power level of -133 dBW in a bandwidth of 10 MHz at the receive output flange of a radar antenna.

A proposed sharing criterion to satisfy the above radiolocation protection level for FSS Earth stations with a diameter less than 4.5 m, would be a single entry interfering power flux density (pfd) level of: **for maritime radar**: X dB(W/(m$^2 \cdot$ 10 MHz)) not to be exceeded for more than Y% of the time produced at 36 m above sea level at the normal baseline (low water mark) as defined in UN Convention on the Law Of the Sea [80].

However, problems occur when we use Rec P-452 to calculate the percentage of time interference will be present. Using calculations in the Recommendation, duct incidence is 24%, while we have measured it exceeding 90% in most cases. In the opinion of the team, for the tropical littoral zone within latitude 25 of the equator it should be assumed that ducts will always be present. While this is slightly conservative it would ensure the continued viability of the *Phalanx* system and ensure the incidence of interference was not underestimated.
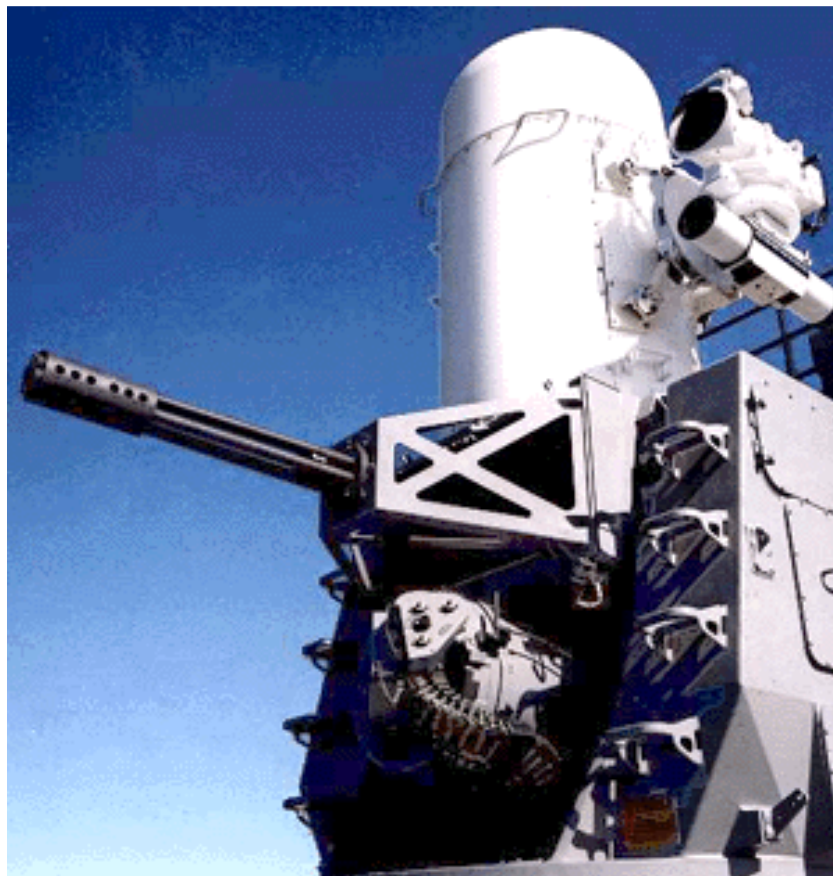
Figure A1.3: *Phalanx* on the deck of decommissioned USS Missouri (Author).

Also of note is the baseline of 36 metres mentioned in the report. While this was intended to provide protection for units mounted high on an aircraft carrier's structure it again does not take into account ducting.

Referring again to Figure 2.5 in Chapter 2, the scenario of the 36 metre radar receiver is depicted by the tall tower in the centre of the duct, above the duct. From this we see that increased height does not mean increased signal strength in the duct. It is possible therefore that if actual measurements were made both the interfering signal strength and incidence from low mounted coastal FSS would be significantly underestimated as only the scattered signal would be seen.

In Figure 4.2 in Chapter 4 we see the incidence of ducts higher than 36 metres is between about 5% and 25% (the latter figure of interest as it is what Rec P-452 predicts). So, in the tropical littoral, we believe that again, the incidence of interference to *Phalanx* systems mounted on smaller vessels, such as the Australian Navy's Anzac Class Frigate, will be significantly underestimated.

A1.4 General radar issues

Anomalous propagation in ducts can increase or reduce radar range depending on the mix of radar height, target height and duct height. Anecdotal evidence told to the author suggests that distant storms have been mistaken for nearby islands, ships at a distant pulse repetition factor (PRF) range have been 'avoided' by violent manoeuvre and some targets, including missiles, have been seen with the naked eye but missed by radar.

Much of this is not recorded or published, but some is. In [81] Eli Brookner reports on radar reception anomalies during fog events (stratified layers):

"Periodically through the year, an Atlantic coast vessel traffic control radar, located near the entrance to Delaware Bay, observes a reduction in detection range from 37 km to 17 km. Sometimes ships can be seen visually from the radar tower before they can be observed on the radar screen."

This would be of concern to any mariner operating in busy sea lanes, but especially to the military commander operating in a hostile area. Thus it is imperative commanders

and radar operators at least understand which conditions lead to ducting or other forms of anomalous propagation and adjust their operations accordingly.

A1.5   Conclusions and future work

It is evident from these and other studies that [75] Naval Commanders need to be at least aware of the effects of propagation inside the evaporation duct and how they affect radar and other signals systems operating above 1 GHz.

The viability of Phalanx radar systems and any other microwave radar system operated in the band 13.75 – 14 GHz is under threat because the ITU Recommendations used in sharing studies under-estimate the prevalence of ducts in the tropical littoral. A significant amount of work is needed on propagation over tropical oceans which can be fed back to update ITU Recommendations. The currently available information is inadequate to properly study sharing between the FSS and radar where the interfering wave propagates over oceans.

A1.6   References and papers

A1.6.1 Papers

The following paper was published as a result of this work:

Kerans, A.J., Kulessa, A.S., Woods, G.S., French, G. and Hermann, J., "Implication of Anomalous Propagation in the Evaporation Duct for Radars at X and Ku Band", Journal of Battlefield Technology, Volume 6, Number 3, pp. 25-29, November 2003.

A1.6.2 References

[75] Andersen, K.D., "Radar Detection of Low-Altitude Targets in a Maritime Environment", IEEE Transactions on Antennas and Propagation, Vol. 3, No. 6, June 1995.

[76] SPAWAR Advanced Refractive Effects Prediction System (AREPS) program, www.sunspot.spawar.navy.mil

[77] Levy, M., "Parabolic Equation Methods for Electromagnetic Wave propagation", IEE Press, 2000, ISBN 085296 764 0.

[78] Kulessa, A. S., Heron, M. L. and Woods, G. S., "Temporal variations in evaporation duct heights", Proceedings of Workshop on Radio Science 1997 (WARS 97), National Committee for Radio Science, Australian Academy of Science, pp165-170, 1997.

[79] http://www.chinfo.navy.mil/navpalib/factfile/weapons/wep-phal.html

[80] ITU-R CPM Report 2002, www.itu.int

[81] Brookner, E., "Radar performance during propagation fades in the Mid-Atlantic region", IEEE Transactions on Antennas and Propagation, Vol. 46, No. 7, July 1998.

Annex 2

Implications for designers of fixed services utilising over water paths

The theory and research behind our final paper in terms of its implications for fixed link designers where an over-water path is present is highlighted in this Annex.

```
┌─────────────────────────────────────────────────────────────────────┐
│                        Chapter 1                                     │
│                 Introduction and Thesis format                       │
│                            ↓                                         │
│                        Chapter 2                                     │
│         Microwave propagation, measurement and simulation            │
│                            ↓                                         │
│                        Chapter 3                                     │
│      Radio-meteorology and the tropical littoral zone under study    │
│                            ↓                                         │
│                        Chapter 4                                     │
│         Meteorological measurement and prediction techniques         │
│                            ↓                                         │
│                        Chapter 5                                     │
│    Propagation simulation in a duct using TERPEM and AREPS           │
│      and observations supporting the accuracy of these models        │
│                            ↓                                         │
│                        Chapter 6                                     │
│    Some observations of over the horizon microwave radio             │
│   propagation inside the tropical maritime evaporation duct in       │
│                North Queensland, Australia                           │
│                                                                     │
│                        Chapter 7                                     │
│              The evaporation duct as an angular filter                │
│                                                                     │
│                        Chapter 8                                     │
│    Short range propagation experiments, conclusions and results      │
│                                                                     │
│   Chapter 9              Chapter 11           Annex 1                │
│ Methods for extracting   A theoretical design  Informing the         │
│ angle of arrival         for long range over   Military Community    │
│ and duct heights         ocean microwave links                       │
│                          using the tropical     Annex 2             │
│   Chapter 10             evaporation duct        Implications for     │
│ Mathematical methods                             designers of fixed   │
│ for measuring                                    services utilising   │
│ angle of arrival in                              over water paths     │
│ over ocean                                                           │
│ propagation experiments                                              │
│                        Chapter 12                                    │
│              Research and Thesis conclusions                         │
└─────────────────────────────────────────────────────────────────────┘
```

A2.1 Introduction

In 1965 the Australian Postmaster-Generals' (PMG) Telecommunications Planning and Research Division released Research Report No. 6004, 'Tasmania (Stanley) to King Island Radio Propagation Measurements" by G. F. Jenkinson. The report related to work carried out between June 1962 and April 1964. The title is fully reproduced as the text is unavailable as a reference.

The antennae were about 12 dBi YAGIs one mounted at 390 feet (119 metres) AMSL, and the other 460 feet AMSL (140 metres). (The reader should now glance at Figure A2.1 for a second).

The abstract stated: *"As a guide in the design of a radio telephone system linking King Island and Tasmania, 450 Mc/s propagation measurements were made [and] results showed that this path would not provide a satisfactory service due to low median received signals and very deep fading".*

The report goes on to try to identify the source of the problem, from small intermediate islands, or perhaps equipment faults. The report finally leaves the question unanswered saying:

"For a continuous period of 6 ½ days the signal was below the receiver threshold for approximately 90% of the time and below -45 dBFS virtually all of the time.

Due to generally poor signal strengths a more detailed analysis is not at present justified".

Our work in the Gulf of St. Vincent (a similar temperate location) suggests a duct of about 20 metres would be present for around 75% of the time extending as high as 40m on occasion. At 450 MHz from high towers this would effectively represent another form of reflective obstruction along the whole path and could perhaps refract the signal away from the receiver for 'period of up to 6 ½ days".

In 1967 the PMG again sent Mr Jenkinson, this time armed with an aeroplane, radiosondes and equipment to measure refractive index and discovered high level inversion layers but because of restrictions due to height was unable to establish ducts below about 100 feet (35 metres). His work is recorded in PMG Report 6258, 5 October 1967. (One day I will put all of these on a website). Thus began the Australian fixed link communities' interest in ducting.

Recently as part of my work as Engineer in Charge of Spectrum Planning for the Australia Government I was asked by a Marshall Islands engineer why his short path microwave fixed link over an enclosed island lagoon experienced deep fade. I told him about ducts, but without a good knowledge of his particular system could not offer further assistance.

A2.2 A hypothetical design

Now let us design a hypothetical link between Orpheus and Lucinda.

A short haul system is required between Lucinda and Orpheus Island, some 19 km across the sea. To reduce reflection fading a high tower is used on Orpheus while a short tower is used at Lucinda. To achieve the required availability a flat fade margin of 50 dB is required for this path. The Lucinda receiver operates at 10.75 GHz. Both antennae are 28 dBi with 250 mW transmitters. Feeder losses are ignored for the purposes of this exercise.

A search is carried out to find other potential sources of interference. A low power GSM base station feeder link is found 72.2 km to the south. The transmitter, also at 10.75 GHz, is mounted at 5 metres. Antenna discrimination reduces the energy transmitted towards the design receiver by 27 dB for a total power of 40 dBm. The receiver also has antenna discrimination, with only 16 dBi gain in the direction of the unwanted transmitter. The unwanted link has a power given by:

$P_{UW} = P_T - L_P + G_R$
Where P_T = 40 dBm, L_P = 215 dB (Cylindrical loss model),
G_R = 16 dBi.
P_{UW} = -159 dBm.

The wanted link budget can be calculated in the same way to yield a wanted signal of -80 dBm to the input of the receiver, combining this with the required C/I this allows an unwanted signal power of –140 dBm. This gives a margin of 19 dB and, ignoring rain fade, the link closes.

A2.3 Interference scenarios based on Lucinda measurements

Microwave radio systems design techniques rely on propagation information provided in ITU Recommendation ITU-R P-530. The derived information can then be used in the link design using ITU-R F.1093. In Australia Communications and Media Authority (ACMA) RALI FX3 defines requirements for frequency coordination based mainly on these two ITU documents. The 'quick' design, while not meeting all the requirements of ITU-R F.1098 does meet the requirements of RALI FX3.   Flat fade margins (FFM) are incorporated to ensure the systems meet the performance requirements outlined in ITU-T[2] G.821 and G.826 in a fading environment, thus interference above the FFM threshold cannot be tolerated.

A long path duct propagation experiment at 10.6 GHz was carried out in July 2001 between Toolakeah Beach and Lucinda. Details of this experiment are covered in Chapter 6.

The signals measured during this experiment were on average 60 - 100 dB higher than those predicted by simple cylindrical propagation models. Powers into the input of the victim receiver are in the order of –100 dBm, giving a C/I of 20 dB and in some cases, little or no FFM. Such a system would not meet any ITU-T availability criteria.

An even worse case is possible where the wanted transmitter is above the duct and both the victim receiver and unwanted transmitter are wholly within the duct. This situation is depicted in Figure A2.1 which is reproduced from Chapter 2 for clarity.

---

[2] International Telecommunications Union, Telecommunication Standardisation Sector.
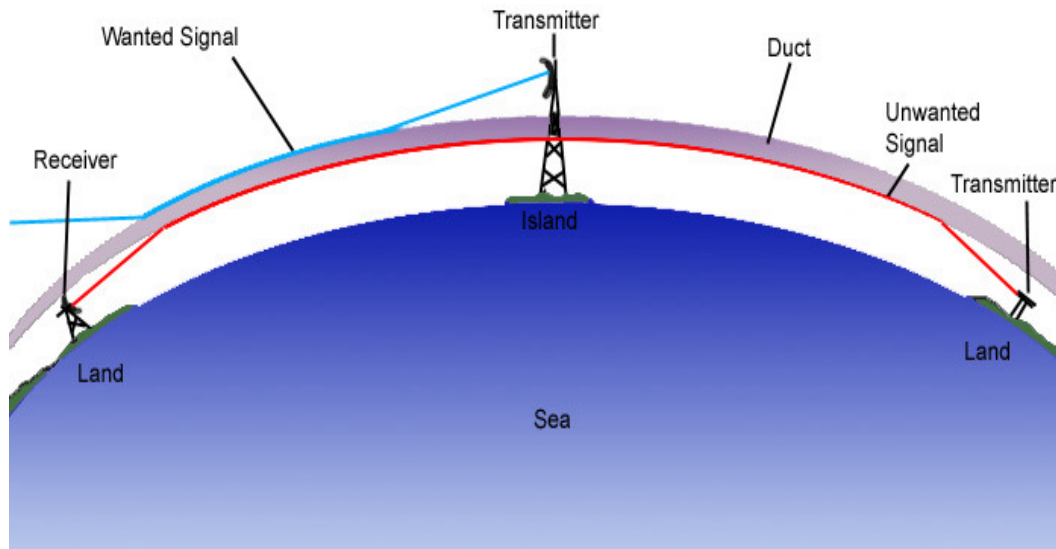
Figure A2.1: The evaporation duct interference scenario for a terrestrial radio link (Reproduced from Chapter 2).

It is common practice on over water paths to use a low high antenna pair so as to move any multipath reflections out of the antenna main beam. When this is done the scenario in Figure A2.1 becomes possible. Here we see the wanted signal mostly deflected by the duct while the unwanted signal is trapped. This could lead to a situation where the interfering signal was stronger than the received signal even allowing for antenna discrimination.

Looking back at Figure 4.2, we see that duct height exceeds 20 metres in the Lucinda area for more than 25% of the time. This suggests the possibility of the events pictured in Figure A2.1 are highly likely in areas such as Lucinda if care is not taken with system design and coordination calculations.

A2.4 Wind and sea conditions

Figures 4.3 and 4.4 show examples of how duct height relates to wind speed. Sea state is generally also dependent on wind speed but can also be affected by wind direction; i.e. onshore or offshore and the swell. Ignoring the effects of wind direction some PEM can predict the changes due to scattering caused by rough seas. Levy in [82] has proposed the PEM model TERPEM, which takes into account Sea State. This model would also be able to take into account wind direction through changes in the 'terrain' models used so as to cater for the smooth to rough transitions caused by land shielding.

Essentially a rough sea scatters the reflected wave so that less power is coupled into the duct than into a duct of similar height but over a smoother sea. We note, however, from the examples in Figure 4.2 that for northern Australia where sea surface temperatures are greater, duct heights are sustained in low wind speed conditions. Ignoring the effects of sea swell, one can conclude that large ducts can exist over relatively calm tropical waters.

Thus losses due to sea scattering effects would be less in Northern Australian waters than in the south given the same duct height. Nevertheless an increase in sea surface scattering linked with an increase in duct height would be a mitigating factor in system design if it could be proved reliable.
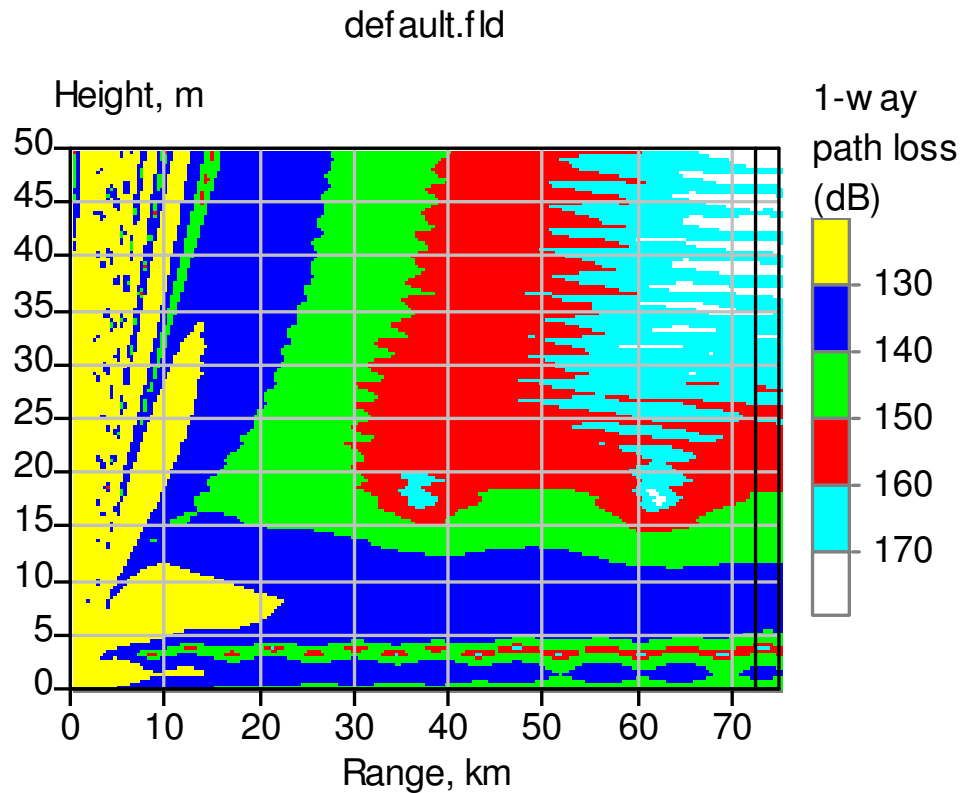
Figure A2.2: Calm sea microwave propagation through a duct at 29 metres, transmit antenna is at 5 metres.
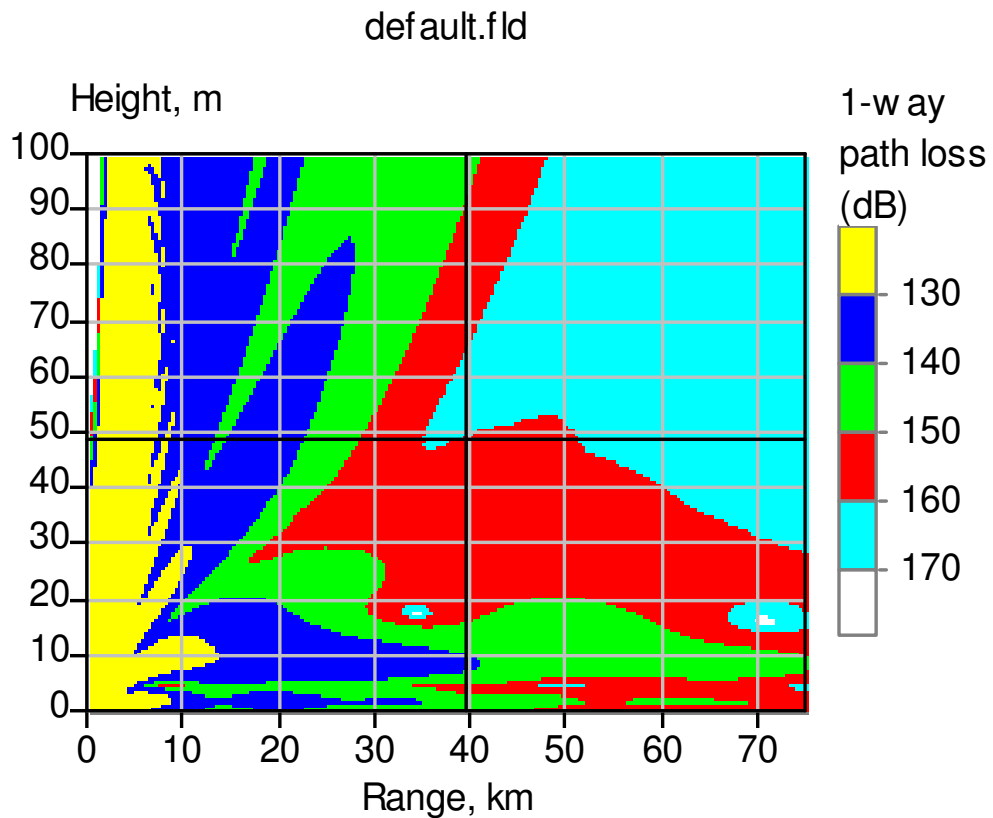
Figure A2.3: Rough Sea microwave propagation through the duct described in Figure A2.2.

Figure A2.2 shows a propagation model simulated on TERPEM for a smooth sea state. The predicted one way path loss is significantly less than predicted by a free space cylindrical diffraction model. It is also less than the signal path loss obtained in the same ducting conditions but over a rougher sea, as shown in Figure A2.3.

A2.5 Conclusions and implications for radio link path design

In coastal environments evaporation duct heights depend strongly on wind speed. When sea breezes are the dominant wind flow, duct heights can be highly variable over a 24 hour cycle. During periods when evaporation ducts are strong, extended propagation results for low elevation microwave emissions which in turn can lead to interference for fixed terrestrial radio links.

The theoretical approximation based on free space and cylindrical losses gave a received signal strength from our transmitter of around –159 dBm. The actual

measurements and those predicted by TERPEM were around –33 dBm. A link designed to operate at Lucinda based on the cylindrical predictions would fail. While these measurements are made at 10 GHz similar results are expected in most bands above 4 GHz.

In the case where the victim receiver and an interfering transmitter can both be expected to be within a duct, a PEM or other duct model should be used to calculate path losses and thus ascertain the probability of interference. In the absence of such a model the actual path losses appear within 10 dB of a free space model so this could be used as a first approximation provided some margin for error were allowed.

A2.6 References

[82] Levy, M., "Parabolic Equation Methods for Electromagnetic Wave propagation", IEE Press, 2000, ISBN 085296 764 0.

Finally I would like to thank Garth Jenkinson for copies of archival material quoted at the beginning of this Annex.